

Development and Application of

A Generalized Reynolds-stress Model of Turbulence

G.J. Reece B.A. (Hons.) M.Sc.

Thesis submitted in partial fulfilment of the requirements for
the degree of Doctor of Philosophy in the Faculty of Engineering
in the University of London, and for the Diploma of Imperial College

March 1977

ABSTRACT

Chapter 1 traces the history of Man's understanding of fluid flow from the earliest times. In Chapter 2, the problem of solving the Navier–Stokes equations is discussed, with special reference to the role of the computer. In Chapter 3, the exact equations for the Reynolds stresses are derived, and an appropriate level of closure is determined. The Reynolds-stress equations are analysed in Chapter 4, and a model derived that is suitable for finite-difference solution. The special case arising near walls is treated in Chapter 5, and the model is adapted to cater for such situations. The results obtained for two-dimensional flows are presented in Chapter 6, and extensive comparisons are drawn with existing data. In Chapter 7, a further extension of the model enables it to handle three-dimensional flows. Results are presented, and comparisons drawn with experimental data. In Chapter 8 we summarise the achievements of the model and make recommendations for future work.

We shall bring all things to rights, said my father, setting his foot upon the first step from the landing.—This Trismegistus, continued my father, drawing his leg back, and turning to my uncle Toby—was the greatest (Toby) of all earthly beings—he was the greatest king—the greatest law-giver—the greatest philosopher—and the greatest priest.....

...And engineer—said my uncle Toby—
.....In course, said my father.

STERNE, *The Life and Opinions of Tristram Shandy, Gent.*
Volume IV, Chapter XI

ACKNOWLEDGEMENTS

The work embodied in this thesis would not have been possible without the unstinted help of all the colleagues and fellow-students of heat and mass transfer I had occasion to consult. Those who will recognise their contributions include in particular Drs K. Hanjalić, W.P. Jones, A. Melling, D. Naot, C.H. Priddin, W. Rodi and D.G. Tatchell.

I should also like to thank Dr R.G. Taylor and Professor J.H. Whitelaw for agreeing to serve on my 'thesis committee': their advice and encouragement were invaluable.

Financial support for the work came from the Science Research Council, and additional support was given by the Central Electricity Generating Board: this generosity is gratefully acknowledged.

The staff of the Imperial College Computer Centre provided advice and an excellent service, without which the computational work could never have been achieved.

My greatest debt – and the one it is most pleasant to acknowledge – is, of course, to my supervisor, Dr B.E. Launder. The original inspiration, the impetus to completion, and any success in this work are all due to him. Any failures are my own contribution.

Gordon Reece

Imperial College

November 1976

CONTENTS

1. The History of Turbulence Theory	1
Table 1–1	16
Plates 1–13	18
Figure 1.1	31
References for Chapter 1	32
2. The Navier–Stokes Equations – Techniques of Solution	35
Figure 2.1	40
References for Chapter 2	41
3. The Reynolds-stress Equations	42
4. The Reynolds-stress Model	54
5. The Situation Near Rigid Boundaries	91
6. Prediction of Two-dimensional Flows	104
7. Three-dimensional Boundary-layer Flows	112
8. General Conclusions	129
Appendix A Modelling in Hydrodynamics	133
Appendix B The Solution of Equations (4.32)–(4.34)	137
Appendix C The 2–D Computer Program	142
Appendix D Listing of the 2–D Computer Program	147
Figures for Chapters 3–8	181
References for Chapters 3–8	241
Nomenclature	244

1

THE HISTORY OF TURBULENCE THEORY

1.1 The Pre-history of Turbulence

Many of the earliest civilisations were based on the proximity of rivers. Thus, for example, Neolithic cultures were to be found in the valleys of the Indus, Nile, Danube and the Tigris and Euphrates. It would therefore be surprising if close examination of such relics as we have of these civilisations did not reveal some measure of understanding of the way water flows.

Neolithic pottery is highly informative. *Plate 1** shows a Gerzean pot, now in the British Museum, which dates from before 3 200 B.C. It bears the earliest known Egyptian representation of a boat under sail. The stylised image of the sea or river foreshadows the standard hieroglyph for water



in which we see the rudiments of our letter M – *via* the Hebrew letter \aleph (*mem*: 'mayim' = water). The early Egyptians did not mince their glyphs: for example, 'woman' was ∇ and we may safely assume that any design of the predynastic period was deliberate and meaningful rather than purely decorative. *Plate 2* shows juxtaposed whorls and water-symbols, on a pot contemporary with that of *Plate 1*. The juxtaposition of these two symbols suggests an awareness of the existence of different types of fluid flow.

Definite evidence of a knowledge of vortex-type motion is provided by the cave-drawings of Tegneby in south-west Sweden. *Figure 1.1* is a sketch of these drawings, which date from the Bronze Age, which occurred in the latter half of the second millenium B.C. in that part

* The figures, plates and references for the introductory historical chapters (1 and 2) will be found immediately after the appropriate chapter, while those for the remaining chapters have been placed after Appendix D

of the world. The lower picture may well have been intended to depict a capsized boat. Our particular interest is excited by the whorls (i.e. eddies or vortices) placed below each boat.

Of course, the whorl has been evident in decoration from Megalithic times (e.g. the entrance to megalithic ruins at New Grange, Ireland, and at Tarkien in Malta). The mere appearance of whorls does not of itself confirm or even suggest any insight into the motion of fluids: in the context of illustrations of water, however, whorls must be presumed to represent eddies or vortices.

Any remaining doubt is removed when we examine *Plates 3–9*. These show details of Assyrian reliefs, mostly from the walls of the North-West Palace of Ashur-nasirpal II at Nimrud (now in the British Museum). These reliefs were executed in about 850 B.C. and show incidents in the military campaigns of Ashur-nasirpal. For the first time in history, flowing water is drawn realistically. Indeed, very few of the extant Assyrian reliefs show regular types of flow: for this, see Plate 8. This fact suggests that the Assyrians, unlike anyone else before the present century, recognized that most naturally-occurring flows are turbulent, and that turbulence is the 'natural' condition of any flow, except for very special conditions (very low Reynolds numbers).

On the evidence of *Plates 3–9*, the Assyrians seem, in a simple pragmatic fashion, to have understood the essentially irregular and random nature of turbulent flows. This is shown in particular by Plate 7a–b, where we see the flow crossing and recrossing itself in a clear attempt on the part of the artist to depict haphazardness. Judging from his representations of fish (Plate 6), we see that the sculptor idealized and smoothed out the original draughtsman's understanding of what he drew, so that we may conclude that the Assyrians saw fluids as moving at least as haphazardly as they drew them. The difficulties of working in stone will also have forced the sculptor to neglect minor details. In view of these considerations, the accuracy of the images in *Plates 3–9* is quite impressive. The attempt to show the flow in a corner in Plate 9 is especially interesting. Plate 5 suggests an awareness of the intermittency charac-

teristic of free boundaries, such as the surfaces of rivers.

The Assyrians differed from almost all their successors of the next 2 300 years in resisting the temptation to smooth out the turbulence altogether. Greek vases and Roman paintings show all moving fluids as smooth and regular. Indeed, all Greek and most Roman representations of flowing water are trivially idealized. The striking exception is found, once again, in the form of a sculpted relief. (*Plate 10*). It is no coincidence that this dates from the openly aggressive expansionist era of Roman imperial history. Sculpture was used to adorn public buildings with permanent stone representations of military triumphs. It was clearly a far greater achievement to have effected the crossing of a violent (turbulent) river than that of a sluggish (laminar) one. However, the fact remains that the representation of turbulent flow in *Plate 10* (the bottom of the helical design on Trajan's column) is separated by roughly a thousand years on either side from anything remotely approaching its realism.

Mediæval manuscript illuminations (c.g. *Plate 11*) show the beginnings of a renewed awareness of the irregularities to be found, for instance, at the foot of a waterfall. Such examples are, however, relatively rare, and do not represent any kind of generalized insight.

The same must, in the end, be said of the work of Leonardo da Vinci. *Plates 12–15* show some of Leonardo's remarkable work in drawing real fluids in motion. Leonardo's insight, albeit as deep as will ever be achieved into the appearance of turbulent flow, did not influence those who followed him. The accurate drawings were reserved for the privacy of his manuscript notebooks, and thus remained unknown until the present century. Leonardo rendered the flow visible to the naked eye by sprinkling tiny seeds into the fluid – the technique of 'seeding' the flow, still used to this day.

Ironically, perhaps, it would appear that the best understanding of real fluid flow has until recently been achieved by artists rather than scientists. Even Leonardo was essentially a professional artist but an amateur scientist.

Thus we see that an awareness of the existence of irregular flows was gained at a few isolated points in the history of civilisation, only to be lost and rediscovered after a further lapse of time. Even if we disregard Leonardo's achievement entirely, from the historical point of view, on the grounds that he concealed his discovery, we are left with what on the surface seems like a puzzle.

How was it possible for simple people like the Ancient Egyptians to observe and record a phenomenon which was ignored by almost everyone else until about 1840? This fact alone would make the phenomenon of turbulence most unusual in the history of science. But turbulence is unusual in that it is at once ubiquitous and highly complicated.

An explanation can be found in Man's overwhelming urge to simplify what he sees, even – or especially – where Nature is inherently complex. The idea of recognizing the complexity of a phenomenon and proposing an approximate explanation is relatively modern: it is a product of the present century when science, following Heisenberg, Popper and Goedel, was finally forced to accept its own essential fallibility. In effect, the demand for 'scientific truth', implying as it did the coincidence of two conflicting ideals, required the justification of scientific assumptions and conjectures in terms of their absolute truth. Not only did this mean that there could be only one answer to any question (e.g. Euclidean geometry precluded the possibility of non-Euclidean explanations of the same phenomena; Newtonian mechanics prevented scientists from accepting relativistic models until the evidence was overwhelming) but it meant that inexplicable deviations from theory had to be dismissed as spurious or ignored altogether.

This last appears to have been the case for turbulence. The phenomenon was (and still is) resistant to a simple causal explanation in terms of a closed system of second-order differential equations. Scientists preferred to ignore it altogether until about 1860.

1.2 The Nineteenth Century

Though scientists ignored turbulence, engineers like **Poncelet** and **Saint-Venant** investigated turbulent flow in considerable detail, but without bothering to explain it, let alone understand it. The crucial first observations of the transition from laminar to turbulent flow were made by **Hagen** [1839] and independently by **Poiseuille** [1840]. These were the first explicit observations of a phenomenon that was seen implicitly by **Girard** [1816], who noted in the course of a series of experiments on the effect of temperature on the flow in narrow pipes that

“On peut ajouter que le mouvement devient plus difficilement linéaire dans un tuyau de conduite que dans un petit tube.”

(page 332).

The first systematic investigation of the mathematical basis of turbulence was that of **Boussinesq**. His first work in this field was published in 1868. However, it is to his 680-page *Essai sur la théorie des eaux courantes*, submitted to the Academie des Sciences in 1872, and published in 1877, that we owe the first thorough, detailed attempt to explain the phenomenon of turbulence.

In the first ten lines of the Essay, Boussinesq gives a very clear account of the problem, recognizing that there are two distinct modes of fluid flow, one in which velocities vary continuously from point to point, and one in which there may be large differences between the velocities of adjacent particles – this last misconception stemming from Boussinesq’s conviction that turbulence was a molecular phenomenon. He further asserts that turbulence is associated particularly with the presence of walls, and adduces evidence that the no-slip condition holds.

Boussinesq’s essay is remembered primarily for his introduction of an *eddy viscosity*, ϵ , recognized by him as being an analogue of the laminar viscosity, which it dwarfed in magnitude. He stated that the exchange coefficient ϵ was a function of the flow rather than a property of the fluid. He saw it as a function of the boundary conditions, of a length-scale, and of fluid properties such as density. In this way, Boussinesq opened the door to turbulence modelling.

One innovation due to Boussinesq with which he has not been credited by previous authors, e.g. Rouse & Ince [1957], is the suggestion that the actual velocity of a turbulent flow at any point could be written as the sum of a mean value and a fluctuating component (Boussinesq's 'agitation'). As Rouse and Ince [1957], page 209] attribute this innovation to Reynolds in 1894, it is worth quoting the relevant passage from Boussinesq's Essay, written in 1872:

"La quantité ξ_1 exprimerait évidemment la vitesse relative d'écartement des deux molécules, si les vitesses vraies u_1, v_1, w_1 , qui s'observent aux divers points, se trouvaient toutes diminuées à chaque instant de leurs valeurs moyennes locales respectives u, v, w , ou si, en d'autres termes, tout mouvement général de translation cessait, mais que l'agitation, représentée par les excès $u_1 - u, v_1 - v, w_1 - w$, restât en chaque point ce qu'elle y est en effet: cet agitation d'agitation sur place, sans mouvement progressif, pourrait d'ailleurs se réaliser effectivement sous l'action de forces convenablement choisies: il n'est nullement incompatible avec l'incompressibilité supposée du fluide, car $u_1 - u, v_1 - v, w_1 - w$, substitués à u, v, w dans la condition linéaire de continuité, y satisfont par le fait même que u_1, v_1, w_1 et, par suite, u, v, w la vérifient."

From this passage it is clear that Boussinesq had considered very carefully the implications for continuity of his assumptions. He was also entirely aware of the possibility of turbulence without mean motion relative to the walls, and he introduced the time-averaging concept which is generally attributed to Reynolds. He maintained that the turbulent motion occurred at the molecular level, whereas we now know that it involves entities of a size several orders of magnitude greater than that of the molecules (see, e.g., Hinze [1959], page 7). As errors go, however, this was a fairly useful one: not only did it enable Boussinesq to visualize the flow in terms which he could understand, but it pointed the analogy with molecular motion which, as we shall see, enabled Prandtl to provide the first useful explicit formulation of ϵ . It was the lack of such an explicit expression for the exchange coefficient that made Boussinesq's hypothesis of limited immediate practical value.

Reynolds' publication in 1883 of his now-famous experiments set in train a succession of similar attempts, dedicated to the determination of the *criterion* (the critical Reynolds number) at which the transition to turbulent flow occurred. Inconclusive results showed that there was, in fact, no single universal Reynolds number at which this happened. The search then switched to one for 'upper' and 'lower' critical Reynolds numbers: the first a maximum for laminar flow, and the second a minimum value for turbulent flow. By definition, the latter had to exist, as all flows, whether laminar or turbulent, have zero as the lower bound for their Reynolds number. The search for an upper critical Reynolds number was finally called off after laminar flows had been observed at Reynolds numbers of 40 000 by Ekman [1911]. The inference drawn by Schiller [1925] was that the transition from laminar to turbulent flow was dependent on the initial disturbance. The high-Reynolds-number laminar flows were difficult to achieve and maintain: they were unstable. Thus laminar flow could be contrived at Reynolds numbers for which turbulence was the norm, but the slightest disturbance would cause the flow to revert to its natural turbulent condition. The fact that the reverse effect had never been observed demonstrated that turbulence was the general state of affairs, except at very low Reynolds numbers, at which any turbulence will be damped by the laminar viscosity and die away.

In his 1895 paper, Reynolds re-examined the Navier–Stokes equations in an attempt to derive the criterion analytically. By considering the motion of fluids as composed of the (mean) motion of their centres of gravity together with a superimposed (fluctuating) motion relative to the centre of gravity, Reynolds deduced that the presence of turbulence could be attributed to the existence of non-zero quantities \overline{uv} , $\overline{v^2}$, ... (the nine *Reynolds stresses*).

1.3 The Twentieth Century

Considerable disquiet was felt at the very end of the nineteenth century at what was regarded as an unacceptable degree of discrepancy between theory and experiment. Rayleigh identified the problem in the following terms [1892]:

"It is possible that, after all, the investigation in which viscosity is ignored altogether is inapplicable to the limiting case of a viscous fluid when the viscosity is small. There is more to be said for this view than would at first be supposed. In the calculated motion there is a finite slip at the walls, and this is inconsistent with even the smallest viscosity. And further, there are kindred problems relating to the behaviour of a viscous fluid in contact with fixed walls for which it can actually be proved (†) that certain features of the motion which could not enter into the solutions were the viscosity ignored from the first are nevertheless independent of the magnitude of the viscosity, and therefore not to be eliminated by supposing the viscosity to be infinitely small..... Considerations such as these raise doubts as to the interpretation of much that has been written on the subject of the motion of inviscid fluids in the neighbourhood of solid obstacles."

† Rayleigh [1883]

In the following year [1893] Rayleigh published the first solutions of the Navier–Stokes equations that relied on none of the customary simplifications – one-dimensionality, very slow motion in which the term $(u \cdot \text{grad})u$ could be neglected, or very-high-speed motion, in which it was thought that the viscosity could be ignored.

It was, however, not for another ten years that a satisfactory generalized treatment of the equations was provided for the problem of the flow near walls. Prandtl [1904] systematically re-examined the equations to determine just which terms could be ignored from the outset, and which ones, despite their apparent irrelevance, had to be retained. In his paper, presented to the Third International Congress of Mathematicians, Prandtl developed the entire theory of the boundary-layer, which has been, and remains, the single most powerful tool for the simplification of the general Navier–Stokes equations.

An intuitive understanding of the physical process had been obtained independently by Lanchester, whose ideas were to prove

most useful to Prandtl in developing the applications of his theory. It is perhaps striking that these two men, with their common dislike for the intricacies of mathematics, should have seen their way through what was essentially a mathematical problem. In a sense, the difficulties had been spurious, in that they had been introduced as a consequence of the slovenly use of mathematical techniques. Once Rayleigh had pointed out that the processes of taking the limit and of solving the equations were not commutative, the mathematical barrier to an understanding of the equations was removed. In a rare moment of candour, Prandtl described the Navier–Stokes equations as *unangenehm* ('unpleasant'), and it was probably his dislike of mathematical complexity that gave Prandtl the extra incentive to simplify the equations once for all – a task in which all others had failed.

A more detailed understanding of the physical nature of turbulent flow was achieved in 1911 by Stanton, who provided the first velocity 'profiles'. These were obtained for rough- and smooth-walled pipes, and agree perfectly with more recent measurements, for example those of Laufer [1951]. By keeping the Reynolds number Ud/ν constant, but varying U (the mean inlet-velocity) and d (the pipe-diameter) in inverse ratio, Stanton showed conclusively that the velocity profile was determined in every detail by the Reynolds number.

In the context of his vorticity-transport theory [1915], in which he treated vorticity as a transferable quantity, Taylor introduced the concept of a *mixing-length*. In 1925 Prandtl made use of this idea in a rather different form to take up the challenge left by Boussinesq: the formulation of an explicit expression for the exchange coefficient ϵ . Prandtl used the equation of mean motion which showed that the term in question was $\epsilon \partial U / \partial y = -\rho \overline{uv}$. He argued that u and v were both of order $\ell \partial U / \partial y$ and thus transformed the problem into one of providing a formula for ℓ , which was (Prandtl [1927]):

"a length which may be interpreted as the diameter of the masses of fluid which move as a whole and also as the path traversed by those masses relative to the rest of the fluid before they lose their individuality again by mixing with the turbulent fluid by which they are surrounded....."*

* The German phrase *aber auch* might have been rendered more helpfully as 'or alternatively'.

The length ℓ , which we shall now call the mixing-length[†], bears a definite relationship to the mean free path in the kinetic theory of gases. In the latter, the transference of momentum due to molecular motion is discussed in a way similar to our present account of the transference of momentum by the large-scale ("macroscopic") motion of whole masses of fluid."

Thus, as we said on page 6 (above), Prandtl made use of Boussinesq's analogy with molecular motion, but recognized that it was no more than an analogy. In effect, his proposal meant that the exchange coefficient ϵ , an essentially positive quantity, could be expressed as

$$\epsilon \equiv \mu_{\text{turbulent}} \equiv \rho \ell^2 |\partial U / \partial y|$$

1.3.1 Further measurements: turbulent quantities

The equipment available for flow-measurement at the turn of the present century was exclusively of the mechanical high-inertia slow-response type. It was incapable of measuring small quantities fluctuating (typically) 5 000 times per second. With the development of the hot-wire anemometer this picture changed. According to Pannell [1924], the first hot-wire measurements were made in England by Shakespeare in 1902. However, it was not until the theory (of the cooling of thin cylinders in a stream of air) had been improved by King [1914] that the first measurement of turbulent fluctuating quantities could be undertaken. King foresaw the application of his work in this field when he wrote [1916]:

"An important point...is its property of giving a consistent measure of turbulent velocity."

The first measurements were in fact made by Burgers in 1926, who showed oscillograms of the fluctuating quantities and indicated how to measure correlations between them. Dryden and Kuethe

[†] In fact, the translators used the term *path of mixing*, representing the German term *Mischungsweg* which was still being used by Taylor in 1935 in the absence of a acceptable English translation.

[1929] solved the problem of eliminating the phase-shift introduced by the thermal inertia of the wire. Their paper was followed by the work of Reichardt [1933], who published remarkably accurate measurements of the autocorrelation $\overline{v^2}$ in a plane channel. In the following year Wattendorf & Kuethe published similar measurements, to be followed in 1936 by the publication of further measurements, ostensibly on the same channel, of the values of $\overline{v^2}$. The latter measurements, performed by Sadron, displayed what we now know to be the correct shape, but showed a ratio of $\overline{v^2}$ to $\overline{u^2}$ of about 1.5 to 1, instead of the correct ratio of roughly 1 to 4 near the wall. It is only fair to record that Wattendorf acknowledged this possibility explicitly; we must presume problems of calibration. The meticulous work of Reichardt, published in 1938, eliminated this error. Reichardt's work, covering the same correlations, was to form the empirical basis of Prandtl's 1945 model in which the turbulent kinetic energy k , where

$$k \equiv \frac{1}{2} (\overline{u^2} + \overline{v^2} + \overline{w^2}),$$

was made the subject of a transport equation. The failure of any of these workers to make separate measurements of the correlation $\overline{w^2}$ was to handicap theoreticians for a further twenty years. Wieghardt based his 1945 calculations on the assumption that $\overline{v^2}$ and $\overline{w^2}$ were equal, which they are not, in general.

1.3.2 The emergence of a mathematical theory of turbulence

The growing corpus of experimental information on the detailed structure of turbulent flows served, *inter alia*, to emphasize a basic defect in the existing theory. As all the explanations of turbulent phenomena were essentially ostensive, they were inherently unlikely to be susceptible to indefinite generalization. A heuristic theory was required, preferably mathematical, and ideally starting from the equations of motion.

The first steps in this direction had been taken by Reynolds in 1894, when he had derived the equations of mean motion, which highlighted the rôle of the turbulent correlations $\overline{u_i u_j}$. Reynolds in fact went much further than this. To obtain information about

the 'criterion' for transition from laminar to turbulent flow (or *vice-versa*) Reynolds had considered the integral over the flow domain of the turbulence energy. He isolated the dissipative and productive terms, and thus derived, in effect, the integral of the turbulence energy equation. This approach, which could have been most fruitful, was to remain a mathematical curio.

The technique that was in fact destined to lead to a better mathematical understanding of turbulence was that of statistical analysis. In a stream of fundamental publications, culminating in 1935 with the four papers *Statistical Theory of Turbulence* Taylor laid the basis of subsequent theoretical work. The particular need was for a theory of how the quantities $\overline{u_i u_j}$ were transported. Boussinesq's eddy-viscosity hypothesis, albeit most useful once it had been given life by Prandtl, could really only cope with one such quantity, and measurements showed that in general this was not likely to be a viable assumption. In the second of his 1935 papers, Taylor introduced the valuable notion of *isotropic turbulence*, an idealization which simplified the problem to the point where it could be treated mathematically.

In 1938 von Kármán & Howarth derived the first theory of the transport of turbulence correlations. Their theory, though in principle restricted to the isotropic case, revealed most of the problems, including that of closure, and suggested paths to a solution. They introduced the technique of tensor notation, which made their theory and that of Taylor much simpler to express and easier to use. von Kármán, anticipating this publication, had [1937] introduced the idea of a *turbulence-energy balance*. In effect, he took Reynolds' integral form (above), and differentiated it to obtain a local form, for a 'control volume' rather than for the whole flow. This meant introducing the concept of the *diffusion* of the energy, which von Kármán saw as related to the adjacent coexistence of different levels of turbulence energy. He therefore proposed that this term should be modelled in terms of the gradient of the energy:

$$\text{Diffusion} \sim \frac{d}{dx_2} (\kappa u_2' \frac{dk}{dx_2})$$

Prandtl foreshadowed the model he was to publish in 1945 in his address to the 1938 Congress of Applied Mechanics, where he was searching for a better formulation for the characteristic velocity of turbulent motion. The direction in which he was looking is clear from the fact that he introduced Reichardt's measurements of turbulence correlations. Prandtl's 1945 proposal, by providing an equation for the turbulence energy k , obviated the need to argue that u and v were both proportional to $\ell \partial U / \partial y$; this quantity represented a characteristic velocity of turbulence, and could therefore be replaced by the quantity $k^{1/2}$. This gave

$$\mu_{\text{turbulent}} \propto \rho k^{1/2} \ell$$

which, however, still required a separate specification for ℓ .

Prandtl's essentially pragmatic approach had meanwhile been overtaken by the work of others. Kolmogorov [1942] had published what was, in effect, the first proposal for a multi-equation model of turbulence. He derived from phenomenological considerations equations governing the behaviour of two independent properties of the flow. Prandtl, by choosing the length-scale as one of these properties, avoided a second differential equation. Kolmogorov proposed a second equation to generate a characteristic frequency of the turbulent motion. Later workers (see Launder & Spalding [1972], p. 18) were in fact to propose differential equations for ℓ , among other variables; Prandtl implicitly preferred to retain an algebraic formulation of ℓ .

In 1945, Chou showed that it was not necessary to rely so heavily on phenomenological considerations. Chou's paper contains the first definitive treatment of the Reynolds-stress equations, and hence implicitly of the equation for the turbulent kinetic energy. He deduced the exact equations analytically, and derived the equations governing the transport of the triple-velocity correlations $\overline{u_i u_j u_k}$, which occur in the equations for the Reynolds stresses. Chou proposed to effect closure of the equations by assuming the two-point correlations to be Gaussian, and hence deducing formulae for the quadruple-velocity correlations in the equations for the triple-velocity correlations. Thus he

proposed a closure of the equations of turbulence involving

3 equations of mean motion

1 equation of vorticity decay (removing the need for the separate specification of a length-scale)

6 equations for the Reynolds stresses

10 equations for triple-velocity-correlations

1 equation of continuity

Chou dealt rigorously also with the most difficult term in the Reynolds-stress equations, that involving the pressure fluctuations. Though Chou's proposals were both extravagant and (in respect of the neglect of the quadruple-velocity correlations) somewhat arbitrary, his analytical approach anticipated the lines along which much subsequent work was to proceed. Once the general equations of Reynolds-stress-transport were available, the problem of turbulence could be seen as that of their closure.

This, then, was the position in 1945. The history of the work since that time is best dealt with in the context of a more detailed analysis of the individual terms in the Reynolds-stress equations, i.e. in Chapter 4 below.

1.4 Summary

In retrospect, we can see that in spite of an unusually slow start, the understanding of turbulent flow was destined to follow the usual path of historical evolution. There are generally, in the history of a science, three discernible phases: the first, that of the *experimental* recognition of a phenomenon, and its detailed investigation; the second, where the observations are gathered into a *phenomenological* theory, and the third, where a reappraisal of the theory generates a *mathematical* model. Like all such divisions, these phases are somewhat ill-defined. It is generally quite misleading to think of them as strictly consecutive. They may overlap, or appear in the 'wrong'

order — as for example when Dirac predicted the existence of ‘holes’ from the equations of quantum mechanics and saw his prediction verified by observation. *

Ideally, the derivation of a mathematical theory should proceed from the governing equations alone, but in practice the derivation is often guided by a foreknowledge of the physical results. This remains the case for turbulence theory, where all practical theories for the solution of physical problems require an admixture of simplifying phenomenological arguments, if only to short-circuit what would otherwise still be tremendously difficult and time-consuming tasks. One example of this is the use of the von Kármán [1930] ‘log law’ for the mean velocity in a well-defined region near walls. To insist on solving the full Navier–Stokes equations for this region is (in most cases) quite unnecessary. The boundary-layer approximation, though only an approximation, is sufficiently accurate for most of the purposes for which it was designed.

All these considerations become entirely academic in the absence of the basic technology which enables accurate observations to be made in the first place. To illustrate this, and to summarize the achievements described in this Chapter, we provide a chronological Table of the work done up to 1945.

* This should not be confused with Popper’s requirement that a scientific theory *must* be capable of making predictions: we are concerned with wholly novel phenomena, not routine predictions.

TABLE 1-1

<i>Date</i>	<i>Technique Used</i>	<i>Measurements or Observations</i>	<i>Phenomenological Theory</i>	<i>Mathematical Theory</i>
1000 BC	Visual observation	Eddies occur		
0		Eddies overturn boats		
1000 AD		Rivers are turbulent		
1500		Waterfalls Weirs, etc.		
1600		Viscosity exists		
1700	Pitot tube	No slip at walls	Ad hoc formulae	Inviscid theory
1800				

1800				Navier's equations Stokes' theory
1850		Transition observed Effects of viscosity at walls Search for criterion	Boussinesq's eddy-viscosity	Reynolds' equations
1900		Boundary-layers	Prandtl's theory of boundary-layers	Prandtl's equations
1910		Accurate mean- velocities		
1920	Hot-wire anemo- meter		Vorticity-transfer	Statistical theory
		Turbulent fluctuations	Momentum-transfer	
1930	Correction for phase-lag	Correlations	Universal profile (log-law)	Isotropic theory
			Energy-balance	
1940			Kolmogorov's equations	
1945			Prandtl's theory	Reynolds-stress equations

The Understanding of Fluid Flow

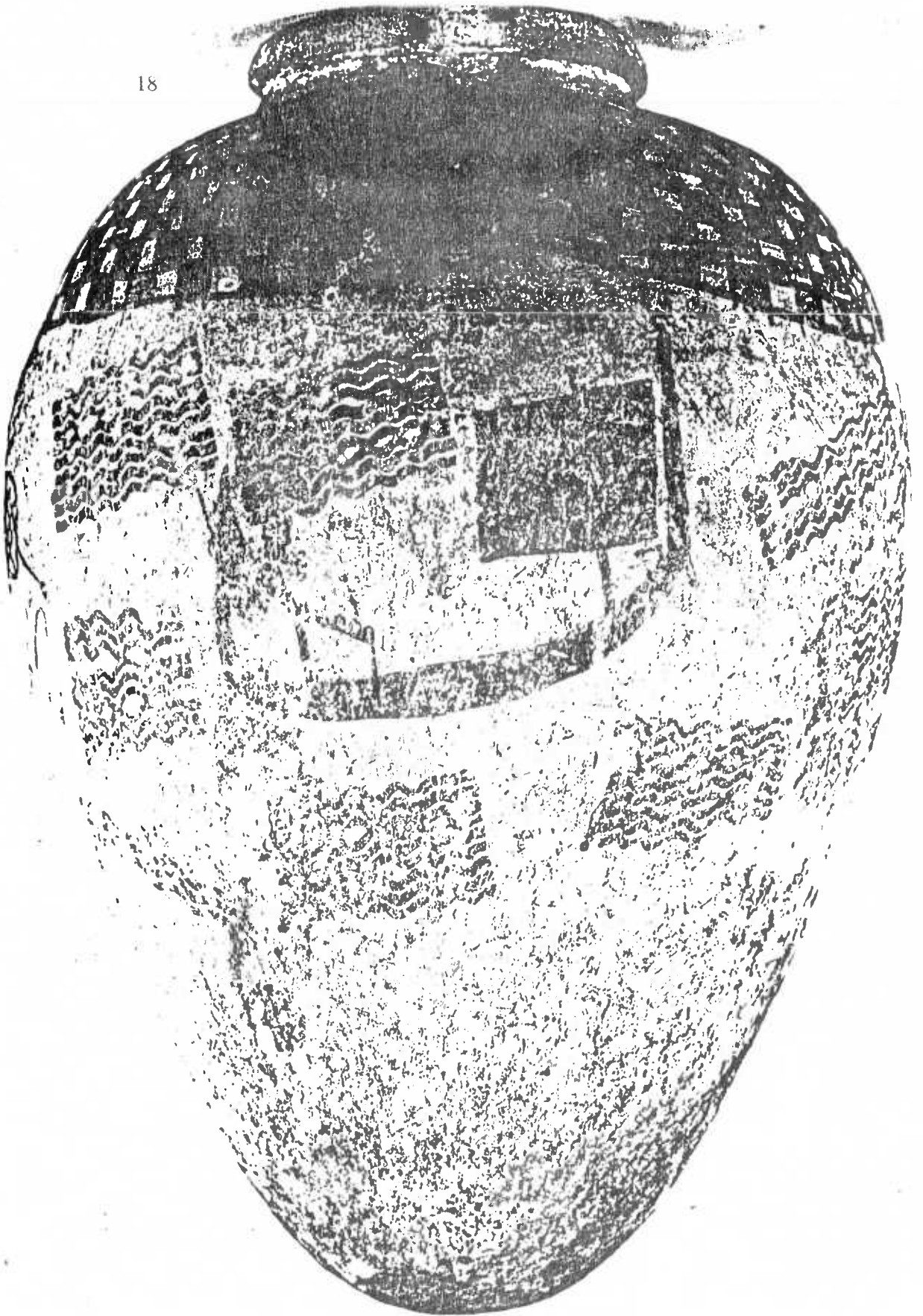


Plate 1. Gerzean Pot (courtesy British Museum)



Plate 2. Naqada II Pot (courtesy British Museum)

124541, 124513, 124515

20

King Ashurnasirpal leads his chariotry in crossing a river by boat.

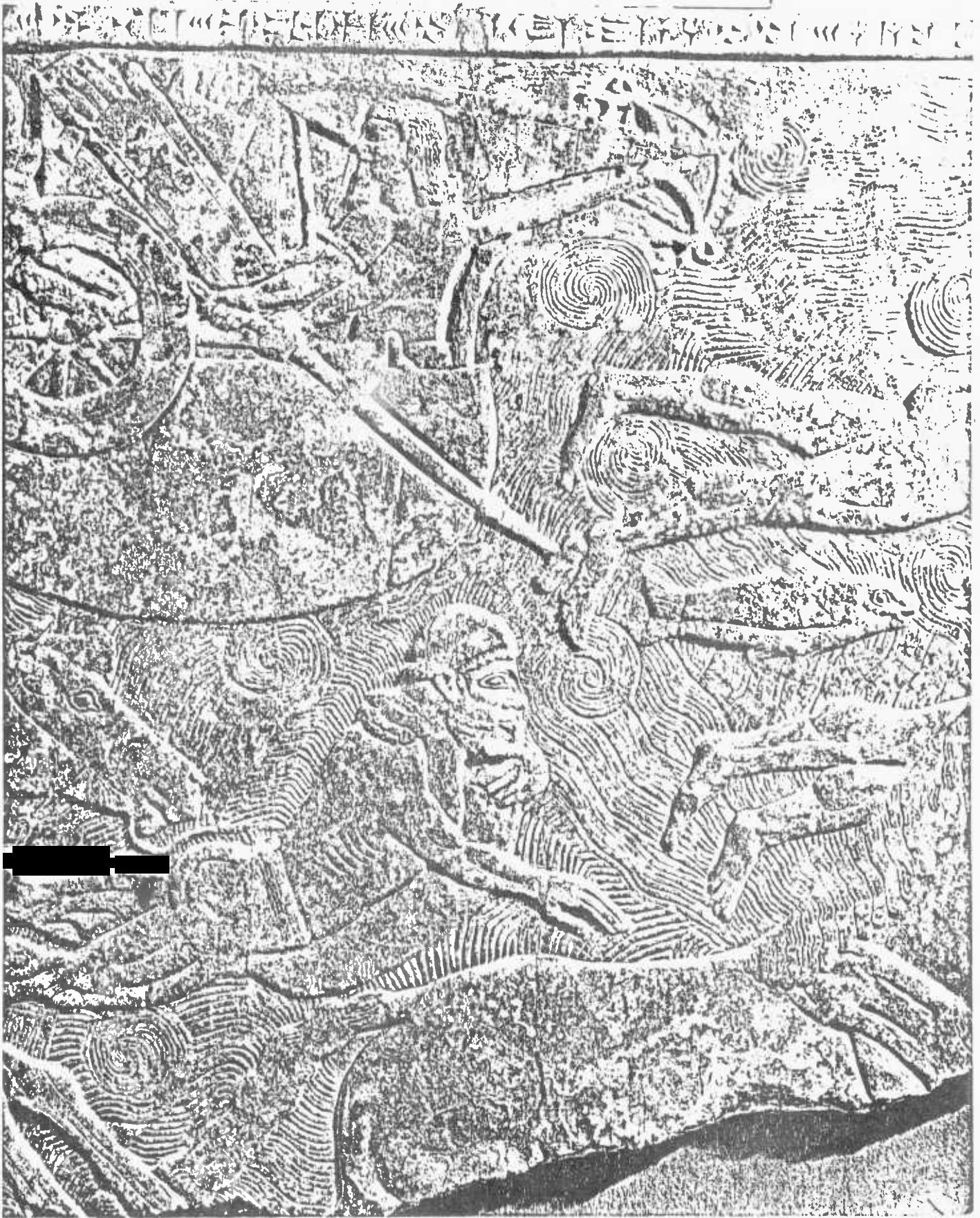


Plate 3. Assyrian Wall Relief

(courtesy British Museum)

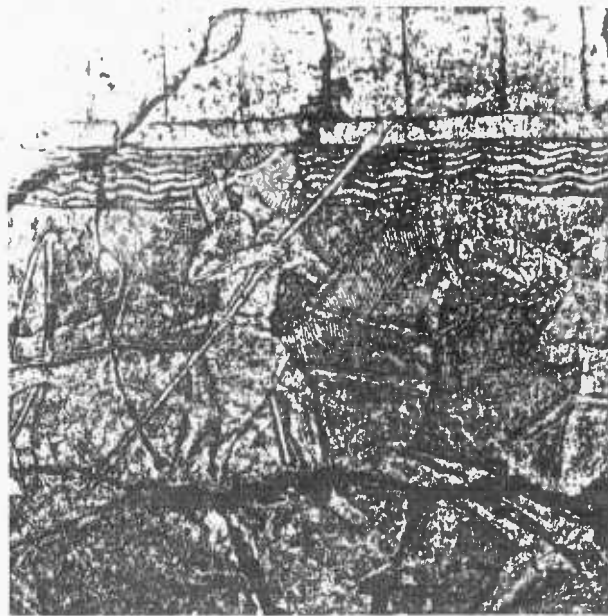


Plate 4. Assyrian Wall Relief (courtesy British Museum)

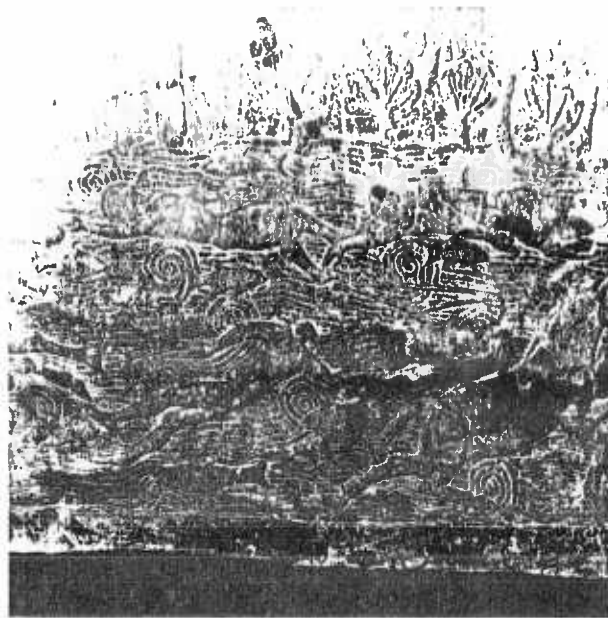


Plate 5 Assyrian Wall Relief (courtesy British Museum)

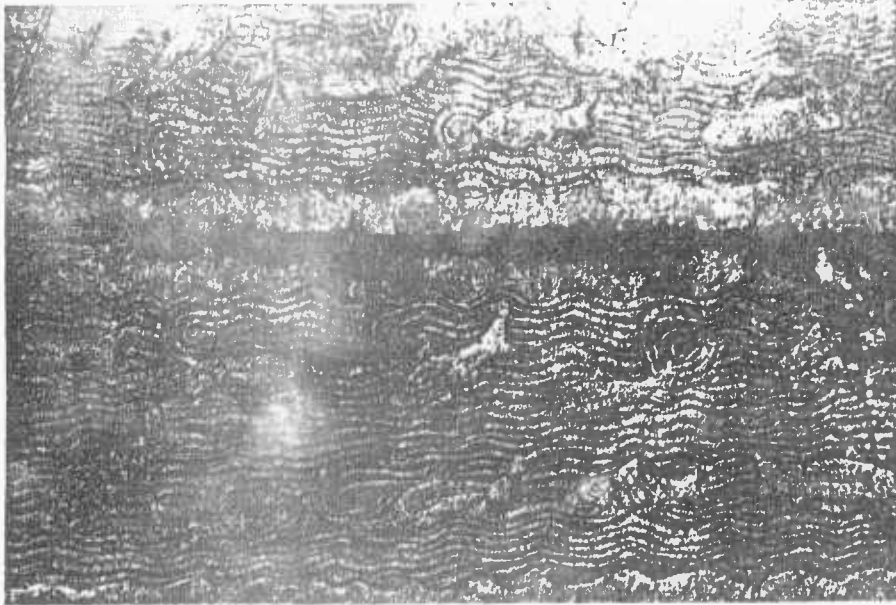


Plate 6. Assyrian Wall Relief (courtesy British Museum)

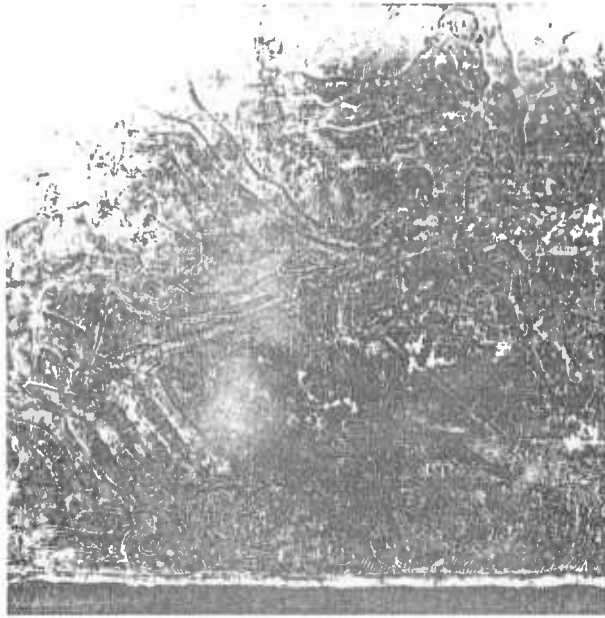


Plate 7a Assyrian Wall Relief (courtesy British Museum)



Plate 7b Detail of Plate 7a

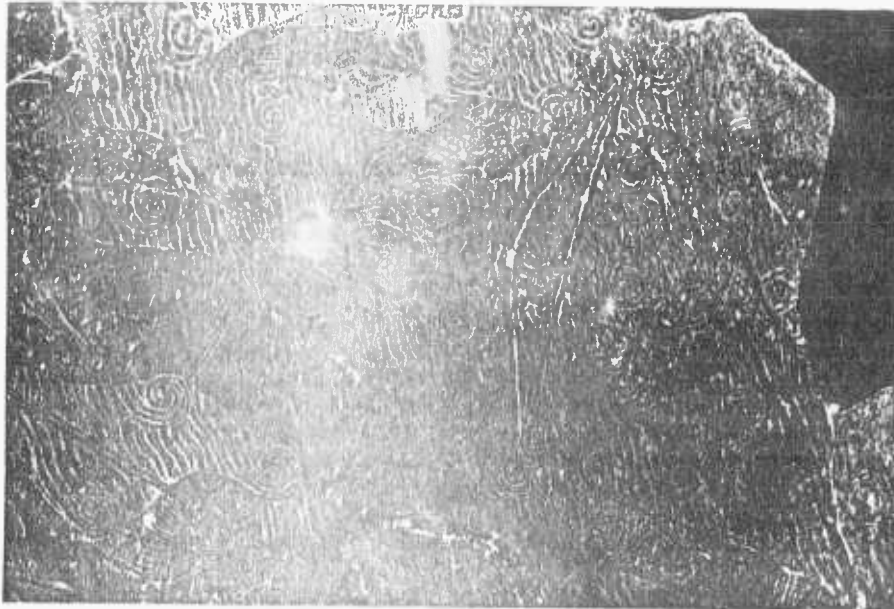


Plate 8 Assyrian wall relief (courtesy British Museum)



Plate 9 Assyrian wall relief (courtesy British Museum)

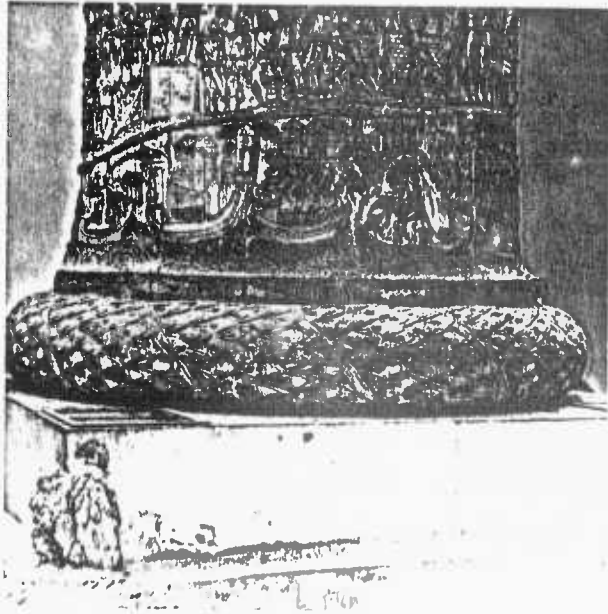


Plate 10. Trajan's Column (detail of foot)



Plate 11. From 'Sir T. Mandevile's Travels', by courtesy of the British Museum.

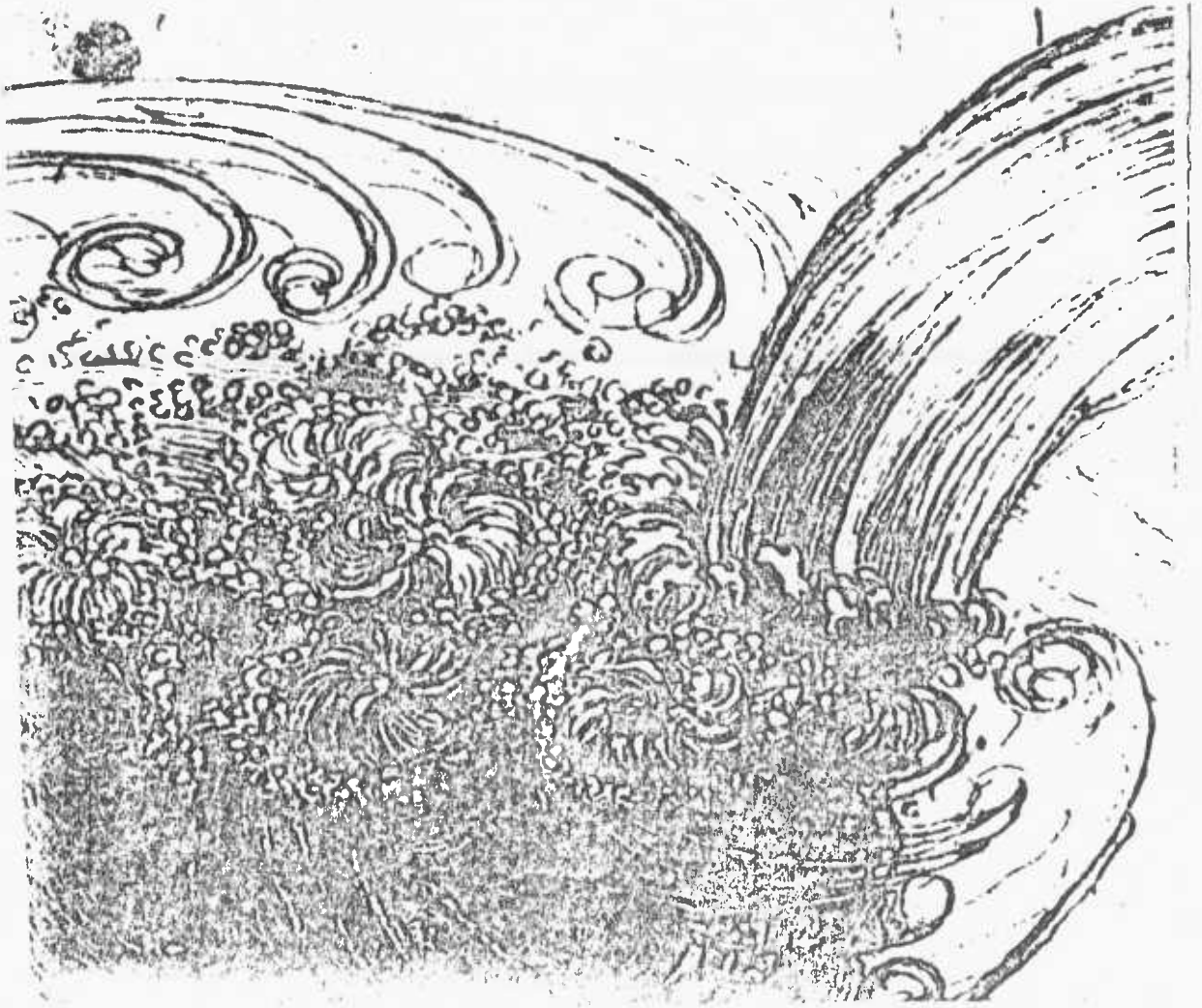


Plate 12. Drawing by Leonardo (courtesy Royal Library, Windsor)

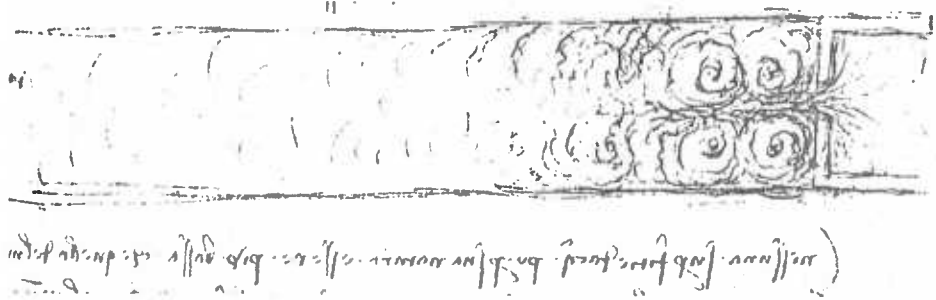


Plate 13. Drawing by Leonardo (courtesy Royal Library, Windsor)

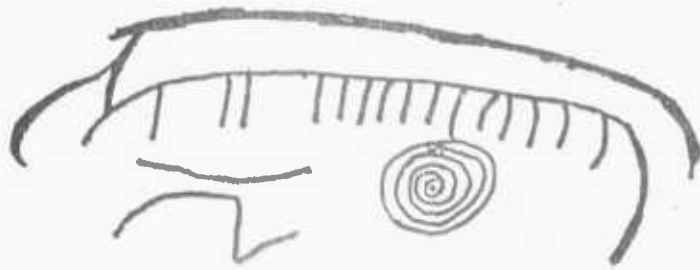
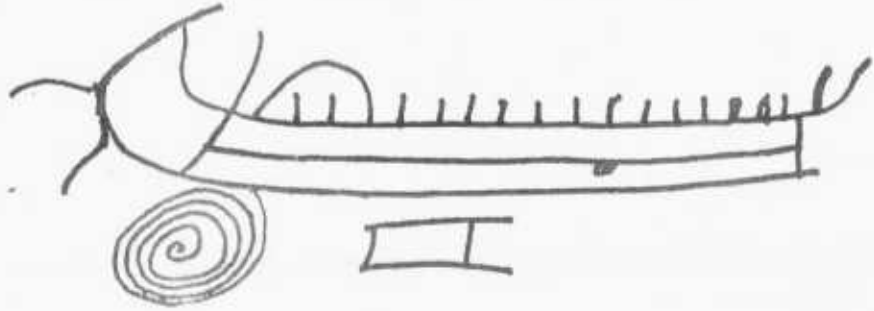


FIGURE 1.1 Bronze-age drawings, carved in rock in caves at Tegneby, Bohuslän, Sweden; *circa* 1200 B.C.

References to Chapter 1

1. Boussinesq, J., *Mémoire sur l'influence des frottements dans les mouvements réguliers des fluides*, J. de math. pures et appl. 13, p. 377 [1868]
2. Boussinesq, J., *Essai sur la théorie des eaux courantes*, Mém. Acad. Sci., 23, 1–680 [1877]
3. Burgers, J.M., *Experiments on the fluctuations of the velocity in a current of air*, Proc. Roy. Acad. Amsterdam, 29, 547–558 [1926]
4. Chou, P.Y., *On velocity correlations and the solutions of the equations of turbulent fluctuation*, Quarterly Appl. Math., 3, 38–54 [1945]
5. Dryden, H.L. & A.M. Kuethe, *Effect of turbulence in wind-tunnel measurements*, NACA Report No. 342 [1929]
6. Du Buat, *Principes d'hydraulique, vérifiés par un grand nombre d'expériences faites par ordre du Gouvernement*, 2nd edition, Paris [1779]
7. Ekman, V.W., *On the change from steady to turbulent flow in liquids*, Arkiv math. astr. fys. 6, No. 12 [1911]
8. Euler, L., *Principes généraux du mouvement des fluides*, Hist. de l'Acad. de Berlin [1755]
9. Euler, L., *De principiis motus fluidorum*, Novi Comm. Acad. Petrop. [1759]
10. Girard, P.S., *Mémoire sur le mouvement des fluides dans les tubes capillaires et l'influence de la température sur ce mouvement*, Mém. de la classe sci. math. et phys. de l'Inst. de France 1813–1815 (*sic*), 249–380 [1816]
11. Hagen, G., *Ueber die Bewegung des Wassers in engen Roehren*, Pogg. Ann., 46, 423–442 [1839]
12. Hinze, J.O., *Turbulence*, McGraw–Hill, New York [1959]
13. Karman, T. von, *Mechanical Similarity and Turbulence*, Nachr. Ges. Wiss. Goettingen, 58–76 [1930]
14. Karman, T. von, *The fundamentals of the statistical theory of turbulence*, J. Aero. Sci., 4, 131–138 [1937]
15. Karman, T. von, & L. Howarth, *On the statistical theory of isotropic turbulence*, Proc. Roy. Soc. A, 164, 192–215 [1938]
16. King, L.V., *On the convection of heat from small cylinders in a stream of fluid: determination of the convection constants of small platinum wires with applications to hot-wire anemometry*, Phil. Trans. Roy. Soc. A, 214, 373–432 [1914]

17. King, L.V., *The linear hot-wire anemometer and its applications in technical physics*, J. Franklin Inst., 181, 1–25 [1916]
18. Kolmogorov, A.N., *The local structure of turbulence in an incompressible fluid for very large Reynolds number*, C.R.Acad. Sci. U.R.S.S., 30, 301–5 [1941]
19. Kolmogorov, A.N., *Equations of turbulent motion of an incompressible fluid*, Izvestiya Akademiya Nauk S.S.S.R., ser. fiz, 6, 56–58 [1942]
Translated into English by D.B. Spalding as Imperial College Mech. Eng. ON/6
20. Lanchester, F.W., *Aerodynamics*, Archibald Constable & Co., London [1907]
21. Laufer, J., *Investigation of turbulent flow in a two-dimensional channel*, NACA Report 1053 [1951]
22. Launder, B.E. & D.B. Spalding, *Lectures in Mathematical Models of Turbulence*, Academic Press, London [1972]
23. Leonardo da Vinci, *drawings in the collection of the Royal Library at Windsor [c. 1507]*
24. Navier, C.L.M.H., *On the laws of motion of fluids taking into consideration the adhesion of the molecules*, Ann. chim. phys. 19, 234–245 [1821]
25. Pannell, J.R., (ed. R.A. Frazer), *The Measurement of Fluid Velocity and Pressure*, Edward Arnold, London [1924]
26. Pitot, H. de, *Description d'une machine pour mesurer la vitesse des eaux courantes et le sillage des vaisseaux*, Hist. de l'Acad. des Sciences [1732]
27. Poiseuille, J., *Recherches experimentelles sur le mouvement des liquides dans les tubes de très petits diamètres*, Comptes Rendus, 11, 951 & 1041, 12, 112 [1840]
28. Prandtl, L., *Ueber Fluessigkeitsbewegung bei sehr kleiner Reibung*, Proceedings of the Third International Congress of Mathematicians, 484–491 [1904]
29. Prandtl, L., *Bericht ueber Untersuchungen zur ausgebildeten Turbulenz*, Z.a.M.M., 5, 136–139 [1925]
30. Prandtl, L. in Ewald, P.P., T. Pöschl & L. Prandtl, *Physics of Solids and Fluids*, Blackie and Sons, London [1930]
Translated by J. Dougall and W.M. Deans from articles in the 11th Edition of Muller-Pouillet's Lehrbuch der Physik
31. Prandtl, L., *Beitrag zum Turbulenzsymposium*, Proceedings of the Fifth International Congress of Applied Mechanics 340–346 [1938]

32. Prandtl, L., *mit einem ergaenzenden Zusatz von K. Wieghardt, Ueber ein neues Formelsystem fuer die ausgebildete Turbulenz*, Abh. Akad. d. Wiss. Goettingen, 6–19 [1945]
33. Rayleigh, J.W.Strutt 3rd Baron, *On the circulation of air in Kundt's tubes, and on some allied acoustical problems*, Phil. Trans. Roy. Soc., 175, 1–21, [1883]
34. Rayleigh, *On the question of the stability of the flow of fluids*, Phil. Mag., 34, 59–70 [1892]
35. Rayleigh, *On the flow of viscous liquids, especially in two dimensions*, Phil. Mag., 36, 354–372 [1893]
36. Reichardt, H., *Die quadratischen Mittelwerte der Laengschwankungen in der turbulenten Kanalstroemung*, Z.a.M.M., 13, 177–180 [1933]
37. Reichardt, H., *Messungen turbulenter Schwankungen*, Die Naturwiss., 24/5, 404–8 [1938]
38. Reynolds, O., *An experimental investigation of the circumstances which determine whether the motion of water shall be direct or sinuous, and of the law of resistance in parallel channels*, Phil. Trans. Roy. Soc. A, 175, 935– [1883]
39. Reynolds, O., *On the dynamical theory of incompressible viscous fluids and the determination of the criterion*, Phil. Trans. Roy. Soc. A, 186, 123– [1894]
40. Rouse, H. & S. Ince, *History of Hydraulics*, Iowa Institute of Hydraulic Research, 1957; reissued Dover Books 1963.
41. Schiller, L., *Das Turbulenzproblem und verwandte Fragen*, Phys. Z., 26, 566–595 [1925]
42. Stanton, T.E., *The mechanical viscosity of fluids*, Proc. Roy. Soc. A, 85, 366–376 [1911]
43. Stokes, G.G., *On the theories of the internal friction of fluids in motion, and of the equilibrium and motion of elastic solids*, Trans. Camb. Phil. Soc., 8 [1845]
44. Taylor, G.I., *Eddy Motion in the atmosphere*, Phil. Trans. Roy. Soc. A, 215, 1–26 [1915]
- 45a–45d Taylor, G.I., *Statistical theory of turbulence I–IV*, Proc. Roy. Soc. A, 151, 421–444, 444–454, 455–464, 465–478
46. Wattendorf, F.L. & A.M.Kuethel, *Investigations of turbulent flow by means of the hot-wire anemometer*, Physics, 5, 153–164 [1934]
47. Wattendorf, F.L., *Investigations of velocity fluctuations in a turbulent flow*, J. Aero. Sci., 3, 200–202 [1936]

2

THE NAVIER-STOKES EQUATIONS – TECHNIQUES OF SOLUTION

2.1 The Navier-Stokes Equations

As we saw in §1, the Navier-Stokes equations have been accepted since the time of Boussinesq (1877) as governing the flow of fluids, both laminar and turbulent. From time to time doubts have been expressed as to their relevance to turbulent flow. The doubts – and our reasons for dismissing them – were summarized by Agostini and Bass in 1950 as follows:

“The most natural idea, the only one which actually produces concrete results, consists in using the Navier equations. To what extent are they applicable to turbulence? The turbulent motion is always a macroscopic motion with respect to a finer-scale motion, and, at the limit, with respect to the molecular disturbance. Therefore it is reasonable to believe that it satisfies the equations of the mechanics of fluids.....Solutions of the Navier equations are known only for simple conditions which are far from resembling turbulence. In other words, while conceding their validity, we practically (sic) do not know how to solve them.”

The situation has not altered radically since 1950. The equations are still impossible to solve analytically in general. Indeed the very existence and uniqueness of a solution of a degenerate case has been

shown only in the present decade. (For a review of the situation, see Temam [1976]). The existence of solutions of the general case can be inferred from the two facts that:

- (a) *the equations govern a physical flow;*
- (b) *the flow is well-defined and appears to yield consistent measurements.*

However, this argument is far from a proof of the existence of a solution, and it does nothing to confirm the uniqueness of such a solution. The fact that we may observe laminar-type flow under conditions that would normally generate turbulent flow (see page 7 above) might suggest, on the surface, that uniqueness did not even hold. However, the problem is slightly different and in a sense more fundamental: it is a question of the closedness of the physical system considered. Thus, as we have seen, in the search for a single criterion for the transition from laminar to turbulent flow, one initial condition was ignored which turned out to be crucial in determining the quantity sought: the initial disturbance due to the injected dye.

2.2 The rôle of numerical procedures

There are, of course, many simple well-defined problems that cannot be solved analytically. For example, consider the displacement of a membrane stretched over an irregular-shaped frame, or (the same problem, same equation, same boundary conditions) the laminar fully-developed flow in a duct of the same shape. In this case, equation (Laplace's equation) for certain boundary conditions; e.g. Boussinesq derived the solution for the fully-developed laminar flow in a square duct in 1868. However, the standard general method of solution in such a case is to use finite-difference techniques and a high-speed digital computer to perform what, until twenty-five years ago, would have been inconceivably tedious calculations. In this way we obtain the "exact solution" to any desired degree of accuracy of a given physical problem. The solution we obtain is, strictly speaking, the approximate solution of a set of discretized algebraic equations. These equations represent the exact differential equation, which in turn must be regarded as an acceptable rather than precise model of the original physical situation. For example, the hyperbolic functions that describe the laminar flow in a square-sectioned

duct take no account of inevitable non-uniformities of properties of the fluid nor of minute irregularities in the desired squareness of the duct.

2.2.1 *The computer*

The situation for the Navier–Stokes equations in the general case is not, however, so straightforward. If we were simply to tackle them head-on, we should find our present-day computers incapable of solving them over more than an uninterestingly minute region of space. Bradshaw estimated in 1971 (*private communication*) that to produce meaningful solutions over the smallest volume of genuine interest (say a 100-millimetre cube) would take several million years on current machines. A more recent estimate is that of Kwak, Reynolds & Ferziger [1975]. In presenting the results of their attempts to solve the three-dimensional time-dependent problem, they observe that the mesh-size must be smaller than the Kolmogorov microscale $(\nu^3/\epsilon)^{1/4}$ to resolve the smallest scales of turbulence. This would demand storage of the order 10^7 words: several orders of magnitude more than is currently available. The full simulation must therefore remain unattainable in the foreseeable future, except at very low Reynolds numbers.

The situation is summarized in *Figure 2* which plots, very roughly, the speed of computers against time in years. (The data are drawn from various manufacturers' specifications). It is worth noting that the *speed* of computers has not been increasing particularly quickly; it is the reliability, measured as a 'mean-time between failures', that has shown a dramatic improvement. The m.t.b.f. is now at least three orders of magnitude greater than the time taken to apply any of the models of turbulence considered below. *Figure 2* shows that on present indications we can not hope to achieve anything by a direct attack on the Navier-Stokes equations in our lifetime. Indeed if present international political and economic trends continue, lack of investment will delay any further major advances in computer

technology.* On the other hand, it is perhaps worth pausing for a moment to note just how far we have progressed in the twenty-five years since Charney, Fjörtoft and von Neumann [1950] published the first computer-based solutions of hydrodynamic equations. They used ENIAC to solve the barotropic vorticity equation, producing about 50,000 punched cards in the course of each of four forecasts of the weather. Undaunted, they predicted that:

"... one has reason to hope that Richardson's dream [1922] of advancing the computation faster than the weather may soon be realized, at least for a two-dimensional model".

2.2.2 Modelling turbulence

In solving the Navier-Stokes equations, we take a slightly round-about approach, treating the equations themselves with as much general physical insight as necessary to

- (i) *eliminate in appropriate circumstances those effects that are of no significance,*
- (ii) *select those terms in the equations that can be represented in a simpler form.*

This has, as we have seen, been the traditional approach to the solution of the problem. Thus, for example, Prandtl performed the simplification (i) when he produced the boundary-layer forms of the equations [1904]. He acted in the spirit of (ii) when he replaced the previously intractable term \overline{uv} in the Reynolds equations by a mixing-length formula [1925] (see page 9 above). Together, (i) and (ii) form the theoretical basis of *turbulence modelling*.

We do not, however, regard the technique of 'turbulence modelling' as a makeshift procedure. As we have already suggested (page above) the only novel feature implied by the use of approximate techniques is the fact that we can use them openly, acknowledging the techniques (but not necessarily the results) as approximate. We shall justify the approximations made in each case; we shall not try

*Moreover, it appears that even the benefits of transistor technology suffer from diminishing returns. The design problems associated with large-scale integration, as compared with discrete components, must now be 'traded off' against the advantages of reduced size. An overriding limitation, which places a premium on compactness, is the finite velocity of the signals (less than 3×10^8 m s⁻¹). All the advances in speed since 1970 have come through improved design and none represents a basic technological advance: for example, the use of parallel rather than simultaneous operation of processing units, as in ILLIAC IV (1971).

to justify them as exact representations. The task of pruning the Navier-Stokes equations of their physically insignificant terms will always be of value as there will continue to be an optimum balance between detail and speed of calculation for any given problem. Even when we have computers 10^9 times as fast as current machines it will be neither sensible or economical to solve, say, the boundary-layer flow on a flat plate by using the blockbusting head-on approach – any more than we should wish to solve a global input-output model of the economy before deciding whether to buy a new pair of socks.

In Appendix A we describe one possible approach (Birkhoff [1960]) to the problem of determining a rigorous set of criteria for the proper formulation of a mathematical model.

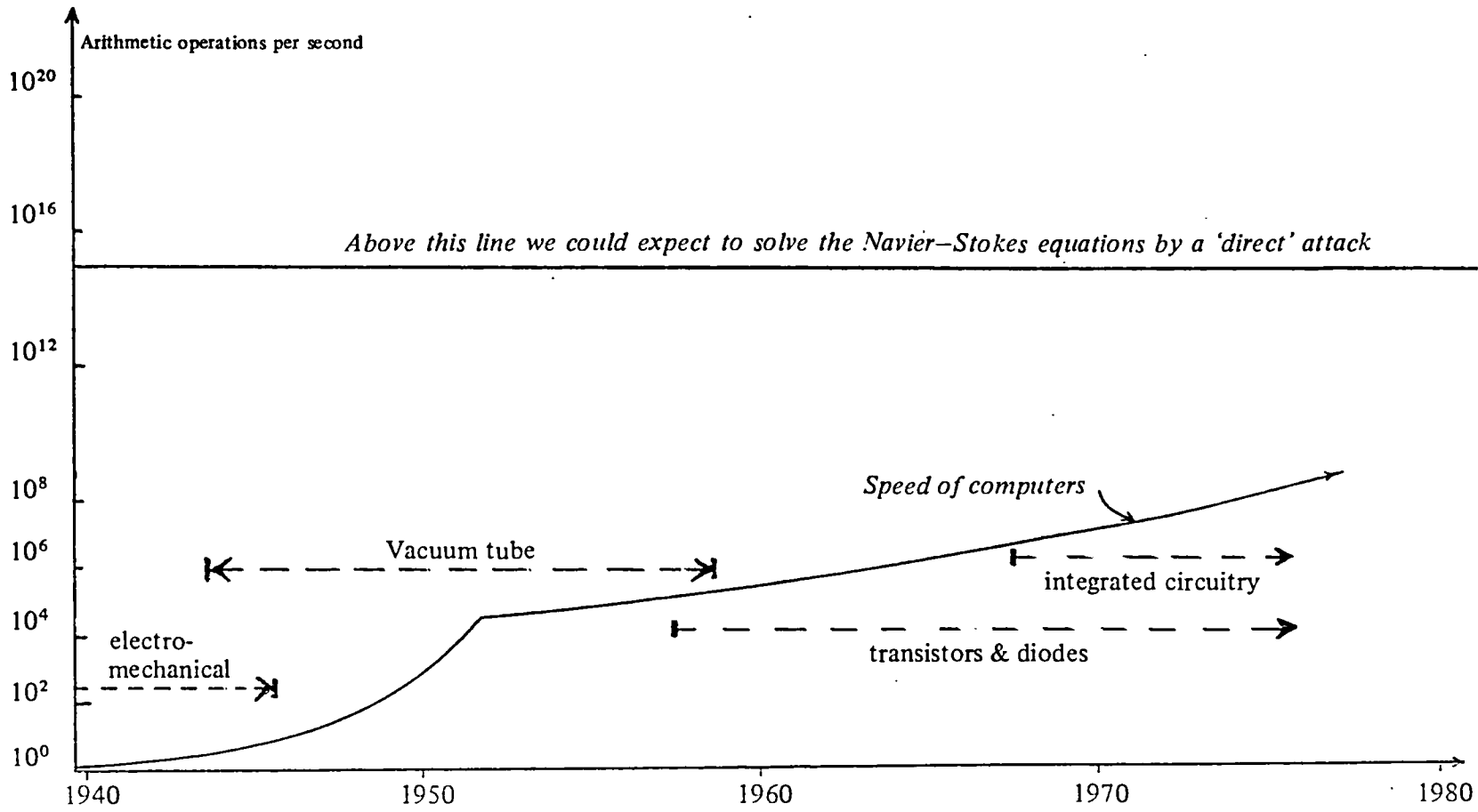


FIGURE 2.1 The speed of computers 1944-

References for Chapter 2

1. Agostini, L. & Bass, J., *Les theories de la turbulence*, Pub. Sci. Tech. du Min. de l'Air, No. 237; *The theories of turbulence*, NACA TM 1377 [1950]
2. Birkhoff, G., *Hydrodynamics, A study in logic, fact and similitude*, Princeton U.P. [1960]
3. Boussinesq, J., *Memoire sur l'influence des frottements dans les mouvements reguliers des fluides*, J. de math pures et appl. 13, p.377 [1868]
4. Boussinesq, J., *Essai sur la theorie des eaux courantes*, Mem. Acad. Sci., 23, 1–680 [1877]
5. Charney, J.G., Fjortoft, R., & von Neumann, J., *Numerical integration of the barotropic vorticity equation*, Tellus, 2, iv [1950]
6. Kwak, D., Reynolds, W.C., & Ferziger, J.H., *Three-dimensional time-dependent computation of turbulent flow*, NASA NGR-05-020-622 Report No. TF-5 [1975]
7. Prandtl, L., *Ueber Fluessigkeitsbewegung bei sehr kleiner Reibung*, Proc. III Int. Cong. Math. [1904]
8. Prandtl, L., *Bericht ueber Untersuchungen zur ausgebildeten Turbulenz*, Z.a.M.M., 5 [1925]
9. Richardson, L.F., *Weather prediction by numerical process*, Cambridge U.P. [1922]
10. Temam, R., *Navier–Stokes equations*, North Holland, Amsterdam [1976]

3

THE REYNOLDS – STRESS EQUATIONS

3.1 The Basic Equations

The Navier–Stokes equations for a Newtonian fluid of uniform viscosity and density are:

$$\frac{\partial U_i}{\partial t} + \frac{\partial}{\partial x_j} (U_i U_j) = - \frac{1}{\rho} \frac{\partial P}{\partial x_i} + \nu \nabla^2 U_i \quad (3.1)$$

where t is time, ρ the density of the fluid, the kinematic viscosity, and U_i the velocity component of the fluid in the direction x_i . We have also the equation of continuity

$$\nabla \cdot U = \frac{\partial \rho}{\partial t} = 0$$

or

$$\frac{\partial U_i}{\partial x_i} = 0 \quad (3.2)$$

where we use the Einstein summation convention in the following form: *repeated Latin indices imply summation; repeated Greek indices do not*. We shall continue to use this convention without further reference.

Applying (3.2) we can derive the standard (incompressible) form of equation (3.1):

$$\frac{\partial U_i}{\partial t} + U_j \frac{\partial U_i}{\partial x_j} = - \frac{1}{\rho} \frac{\partial P}{\partial x_i} + \nu \nabla^2 U_i \quad (3.1)'$$

3.1.1 Turbulence

We next follow Boussinesq (see 1.2 above) in writing the dependent variables U_i and P as in each case the sum of a "mean" part, \bar{U}_i and \bar{P} , and a "fluctuating" part u_i and p . The overbars denote the operation of taking the mean over a suitable period of time, which must clearly be greater than the time-scale of the slowest fluctuations but not so large as to permit the turbulence to decay appreciably. This operation involves an integration with respect to time alone and will thus commute with any differential operation involving only space co-ordinates: for brevity we shall apply this fact without further reference in what follows.

As the fluctuating quantities have zero mean, we may easily show that equation (3.1)' becomes

$$\frac{\partial \bar{U}_i}{\partial t} + \frac{\partial}{\partial x_j} (\bar{U}_i \bar{U}_j + \overline{u_i u_j}) = -\frac{1}{\rho} \frac{\partial \bar{P}}{\partial x_i} + \nu \nabla^2 \bar{U}_i \quad (3.3)$$

whence

$$\begin{aligned} \frac{\partial \bar{U}_i}{\partial t} + \bar{U}_j \frac{\partial}{\partial x_j} \bar{U}_i &= -\frac{1}{\rho} \frac{\partial \bar{P}}{\partial x_i} + \nu \nabla^2 \bar{U}_i - \frac{\partial}{\partial x_j} \overline{u_i u_j} \\ &= -\frac{1}{\rho} \frac{\partial}{\partial x_j} \left\{ \bar{P} \delta_{ij} - \mu \frac{\partial \bar{U}_i}{\partial x_j} + \rho \overline{u_i u_j} \right\} \end{aligned} \quad (3.3)'$$

as $\bar{U}_i \partial \bar{U}_j / \partial x_j = 0$ by continuity (3.2).

The three equations (3.3)' contain the following variables:

Dependent

U_i	mean velocities
\bar{P}	mean pressure
$\overline{u_i u_j}$	"Reynolds stresses"

Independent

x_i	displacement in the \hat{i} direction
t	time

Thus we see that the Boussinesq substitution $U_i = \bar{U}_i + u_i$, followed by time-averaging of the equations leads us to the equations of turbulent motion in the form derived by Reynolds [1894]. On the right-hand side of (3.3)' we see the quantities $\overline{u_i u_j}$ arising naturally as dependent variables in the equations for the mean motion of a turbulent flow. Comparison of equations (3.3)' and equations (3.2) shows immediately that the nine quantities $\overline{u_i u_j}$ (the "Reynolds stresses") represent the sole difference between equations (3.2) (the laminar form) and equations (3.3)' (the turbulent form). The presence of turbulent fluctuations can thus be identified with the existence of non-zero quantities $\overline{u_i u_j}$: the differences between the laminar velocity 'profiles' and their turbulent counterparts can therefore be attributed to these *Reynolds stresses*.

3.2 The Reynolds stresses

The Reynolds stresses occur naturally in the equations for the mean velocities of turbulent flow. In order to solve equations (3.3)' we must obtain further information in order to eliminate the Reynolds stresses. In the laminar case, we had the three equations (3.2) together with the equation of continuity, which (in general and in principle) enable us to solve for the three velocities and the pressure.

There are several ways in which we can obtain the extra information we seek.

The simplest possibility would be to provide an algebraic formula for $\overline{u_i u_j}$ in terms of the other variables and their derivatives. This is an approach which introduces no further equations, and can thus be categorized as a zero-equation formulation. Before the advent of the high-speed digital computer, this was the only approach of general appeal. The best example of this type of 'model' is Prandtl's [1925] mixing-length model (see 1.3 above); another was von Kármán's [1930] similarity model.

The mixing-length model suffers from a number of grave disadvantages:

- (i) it was devised for, and remains largely confined to, two-dimensional boundary-layers, where a single length-scale can plausibly be assumed to characterize the flow:
- (ii) while, following Prandtl, we may reasonably assert that, in the case of a wall-flow, the length-scale is proportional to the normal distance from the wall, such a specification will clearly not carry over to such flows as those contained by two walls or none – such as channel, jet and wake flows:
- (iii) we shall in any case have to specify anew in each problem a constant of proportionality between the normal distance and the length-scale, or (in the absence of a wall) the length-scale itself.

Indeed, in view of these daunting limitations, it is a remarkable fact that the Prandtl mixing-length hypothesis has been extremely successful as a method for the prediction of a wide range of two-dimensional flows. It will continue to serve us well, not least as a yardstick for the success of new, more sophisticated treatments of equations (3.3)!

Prandtl's 1945 proposal was of a *one-equation model*. As we saw in Chapter 1 (page 13) the effect of introducing an equation for the kinetic energy of turbulence was to provide an actual characteristic velocity of turbulence ($k^{1/2}$) to replace the notional velocity $\ell dU/dy$. We do not, however, overcome the difficulties of the mixing-length model, as we must still specify a length-scale separately.

Various workers have devised and applied *two-equation* models. As early as 1942, Kolmogorov proposed a model which would have involved the solution of a kinetic-energy equation and one for the frequency characterizing the turbulent fluctuations. As the equation for the turbulent kinetic energy necessarily contains the rate of dissipation as one term, it is not surprising that most two-equation treatments have involved an equation for the dissipation.

By no means all closures at this level have been of the type described, and a full account of other forms of closure is given by Launder and Spalding [1972]. If we have an equation for the dissipation, ϵ , we may then apply the high-Reynolds-number formula linking the dissipation and a characteristic length-scale:

$$\epsilon \propto k^{3/2} / \mathcal{L}$$

We then have no further need to specify the length-scale separately, and the accuracy of our model will depend on the accuracy with which we have modelled the transport of dissipation. It will, of course, still also depend on the accuracy of the relationships proposed between the Reynolds stresses and the other quantities.

However, the fact remains that it is not the turbulent kinetic energy that appears in equation (3.3)': it is the Reynolds stress $\overline{u_i u_j}$. So long as we do not solve for the Reynolds stresses that arise in equation (3.3)', we shall remain bound to the Boussinesq eddy-viscosity type of model. In the two-dimensional case, the single boundary-layer equation has only one such stress appearing in it. Thus, in this case, the level of closure can be raised significantly by including just one further equation. This was the approach adopted by Hanjalić [1970] to the problem of the solution of a flow in which the positions of zero shear stress and of maximum velocity did not coincide. Coincidence will always follow from the eddy-viscosity model:

$$\begin{aligned} \text{If } \mu_{\text{turbulent}} \frac{\partial U}{\partial y} &= -\rho \overline{uv}, \\ \text{then } \partial U / \partial y = 0 &\quad \Rightarrow \quad \overline{uv} = 0. \end{aligned}$$

Thus any model of the eddy-viscosity type must fail for any asymmetric flow. Although Hanjalić's *three-equation* model made remarkably accurate predictions for the asymmetric boundary-layer he considered, the number of flows for which it would be both adequate and an improvement on earlier, simpler ones was limited. The success of Hanjalić's predictions suggests that a fruitful line of approach would be one which enables us to solve a whole range

of flows by similar means. This necessarily leads us to the derivation and solution of equations for all the Reynolds stresses, and that is the line we propose to follow.

As we shall see in Chapter 4, the structure of the equations for all the Reynolds stresses is of a single pattern. To provide a satisfactory model of the transport of one Reynolds stress, it is necessary to make assumptions or deductions which relate to the other stresses. Having provided a scheme for the solution of one Reynolds-stress equation, we should be most unimaginative not to investigate the possibility of modifying that scheme for the solution of all the equations. Only after such an exercise can we assess the rewards in terms of accuracy and generality against the disadvantage of the additional resources required.

As we shall see, the Reynolds-stress equations are strongly coupled. For example, in order to close his system of equations, Hanjalić was forced to make assumptions about the ratios of the normal stresses in order to solve for the shear stress in a two-dimensional boundary-layer. On closer examination of the relevant data, it would appear that for the particular type of confined flows treated by Hanjalić, the assumption of a constant ratio is not in fact valid and must eventually lead to errors in the prediction of flows where the level of anisotropy varies strongly from point to point. For this reason, we shall pay particularly close attention to flows near walls, for which the anisotropy is known to vary strongly as between the near-wall and outer (or mid-channel) regions. It will therefore be largely on our success in predicting such flows that we shall be able to judge the value of the level of closure we propose.

Over the last few years other workers have also been active in this direction, notably Naot, Shavit and Wolfshtein. Their interest has been parallel to our own to a great extent. The difference of emphasis between their work and that presented here lies mainly in our specific attention to the need for near-wall modifications to the general model. We shall compare their proposals with our own, and shall apply their published model to many of the flows we examine.

3.2.1 Equations for the $\rho \overline{u_i u_j}$

To generate further equations for the quantities $\rho \overline{u_i u_j}$ we shall have to start afresh from equations (3.1).

$$\begin{aligned} \frac{\partial}{\partial t} (\overline{U}_i + u_i) + \frac{\partial}{\partial x_j} (\overline{U}_i \overline{U}_j + u_i \overline{U}_j + u_j \overline{U}_i + u_i u_j) \\ = -\frac{1}{\rho} \frac{\partial \overline{P}}{\partial x_i} - \frac{1}{\rho} \frac{\partial p}{\partial x_i} + \nu \nabla^2 (\overline{U}_i + u_i) \end{aligned} \quad (3.4)$$

Multiplying (3.4) throughout by u_k

$$\begin{aligned} u_k \frac{\partial}{\partial t} \overline{U}_i + u_k \frac{\partial u_i}{\partial t} + u_k \frac{\partial}{\partial x_j} (\overline{U}_i \overline{U}_j + u_i \overline{U}_j + u_j \overline{U}_i + u_i u_j) \\ = -\frac{1}{\rho} u_k \frac{\partial \overline{P}}{\partial x_i} - \frac{1}{\rho} u_k \frac{\partial p}{\partial x_i} + \nu u_k \nabla^2 \overline{U}_i + \nu u_k \nabla^2 u_i \end{aligned} \quad (3.5)$$

Now, taking the mean of (3.5) and invoking continuity,

$$\begin{aligned} 0 + u_k \frac{\partial u_i}{\partial t} + u_k \frac{\partial}{\partial x_j} u_i \overline{U}_j + u_k \frac{\partial}{\partial x_j} u_j \overline{U}_i + u_k \frac{\partial}{\partial x_j} u_i u_j \\ = -\frac{1}{\rho} u_k \frac{\partial p}{\partial x_i} + \overline{\nu u_k \nabla^2 u_i} \end{aligned} \quad (3.6)$$

Expanding (3.6) by the product rule:

$$\begin{aligned} u_k \frac{\partial u_i}{\partial t} + \overline{U}_j u_k \frac{\partial u_i}{\partial x_j} + u_k u_j \frac{\partial \overline{U}_i}{\partial x_j} + u_k \frac{\partial}{\partial x_j} u_i u_j \\ = -\frac{1}{\rho} u_k \frac{\partial p}{\partial x_i} + \overline{\nu u_k \nabla^2 u_i} \end{aligned} \quad (3.7)$$

Thus

$$\begin{aligned} u_k \frac{\partial u_i}{\partial t} + \overline{U}_j u_k \frac{\partial u_i}{\partial x_j} + \frac{\partial \overline{U}_i}{\partial x_j} \overline{u_k u_j} + u_k \frac{\partial}{\partial x_j} u_i u_j \\ = -\frac{1}{\rho} u_k \frac{\partial p}{\partial x_i} + \overline{\nu u_k \nabla^2 u_i} \end{aligned} \quad (3.8)$$

whence

$$\begin{aligned} \overline{u_i \frac{\partial u_k}{\partial t}} + \overline{\bar{U}_j u_i \frac{\partial u_k}{\partial x_j}} + \overline{\frac{\partial \bar{U}_k}{\partial x_j} \overline{u_i u_j}} + \overline{u_i \frac{\partial}{\partial x_j} u_k u_j} \\ = -\frac{1}{\rho} \overline{u_i \frac{\partial p}{\partial x_k}} + \nu \overline{u_i \nabla^2 u_k} \end{aligned} \quad (3.8)'$$

Adding (3.8) to (3.8)',

$$\begin{aligned} \frac{\partial}{\partial t} \overline{u_i u_k} + \overline{\bar{U}_j \frac{\partial}{\partial x_j} u_i u_k} + \left\{ \overline{\frac{\partial \bar{U}_i}{\partial x_j} u_k u_j} + \overline{\frac{\partial \bar{U}_k}{\partial x_j} u_i u_j} \right\} + \frac{\partial}{\partial x_j} \overline{u_i u_j u_k} \\ = -\frac{1}{\rho} \left\{ \overline{u_i \frac{\partial p}{\partial x_k}} + \overline{u_k \frac{\partial p}{\partial x_i}} \right\} + \nu \overline{(u_k \nabla^2 u_i + u_i \nabla^2 u_k)} \end{aligned} \quad (3.9)$$

the right-hand side of which is equal to

$$\begin{aligned} -\frac{1}{\rho} \left\{ \overline{\frac{\partial}{\partial x_k} p u_i} + \overline{\frac{\partial}{\partial x_k} p u_k} \right\} + \frac{1}{\rho} p \left\{ \overline{\frac{\partial u_i}{\partial x_k}} + \overline{\frac{\partial u_k}{\partial x_i}} \right\} \\ + \nu \overline{(u_k \nabla^2 u_i + u_i \nabla^2 u_k)} \end{aligned} \quad (3.10)$$

Now

$$\begin{aligned} \overline{u_k \nabla^2 u_i + u_i \nabla^2 u_k} \\ = \overline{u_k \frac{\partial}{\partial x_m} \left(\frac{\partial u_i}{\partial x_m} \right) + u_i \frac{\partial}{\partial x_m} \left(\frac{\partial u_k}{\partial x_m} \right)} \\ = \frac{\partial}{\partial x_m} \left(\overline{u_k \frac{\partial u_i}{\partial x_m}} \right) - \overline{\frac{\partial u_k}{\partial x_m} \frac{\partial u_i}{\partial x_m}} + \frac{\partial}{\partial x_m} \left(\overline{u_i \frac{\partial u_k}{\partial x_m}} \right) - \overline{\frac{\partial u_k}{\partial x_m} \frac{\partial u_i}{\partial x_m}} \\ = \frac{\partial^2}{\partial x_j^2} \overline{u_i u_k} - 2 \overline{\frac{\partial u_k}{\partial x_m} \frac{\partial u_i}{\partial x_m}} \end{aligned} \quad (3.11)$$

Thus, finally, substituting from (3.10) and (3.11) into (3.9),

$$\begin{aligned}
 & \left\{ \frac{\partial}{\partial t} + \bar{U}_k \frac{\partial}{\partial x_k} \right\} (\overline{u_i u_j}) = - \left\{ \overline{u_j u_k} \frac{\partial \bar{U}_i}{\partial x_k} + \overline{u_i u_k} \frac{\partial \bar{U}_j}{\partial x_k} \right\} \\
 & - 2\nu \overline{\frac{\partial u_i}{\partial x_k} \frac{\partial u_j}{\partial x_k}} + \frac{p}{\rho} \left\{ \frac{\partial u_i}{\partial x_j} + \frac{\partial u_j}{\partial x_i} \right\} - \frac{1}{\rho} \left\{ \frac{\partial}{\partial x_j} (p u_i) + \frac{\partial}{\partial x_i} (p u_j) \right\} \\
 & - \frac{\partial}{\partial x_k} \left\{ \overline{u_i u_j u_k} - \nu \frac{\partial}{\partial x_k} \overline{u_i u_j} \right\} \tag{3.12}
 \end{aligned}$$

3.3 The problem of closure

The equations (3.12) are known as the *Reynolds-stress equations*. If they were in fact simply equations for and involving the Reynolds stresses, our problem would be more or less solved. However, Table 3-1 will indicate the dependent variables that arise in the combined system of equations (3.3)' and (3.12).

As we see from Table 3-1, the result would seem to be that, far from "closing" the system of equations (3.3) by providing us with an expression or equation for $\overline{u_i u_j}$ we have succeeded in further "opening-up" the equations. As we substitute for the unknown terms in our earlier equations we seem to be gathering more and more unknown terms in our new equations.

It is immediately clear that if we proceed in the same manner (e.g. next producing an equation for the $\overline{u_i u_j u_k}$ by a similar method to that of Section 3.3) we shall never reach a truly "closed" situation in which all the variables can be determined from the equations thus derived. In other words we shall always have more variables than equations. Things cannot really be otherwise, for our equations are essentially inbred: apart from equations (3.3)' and the continuity equation we have introduced no new stock of information.

TABLE 3-1

A list of the dependent variables arising in the complete system of equations (3.3)', (3.12) & (3.2)

<i>Variable</i>	<i>Equation</i>	<i>Derived from</i>
\bar{U}_i	3.3 3.3' 3.12	3.2 3.3'
$\frac{\partial \bar{P}}{\partial x_j}$	3.3'	3.3 3.3'
$\overline{u_i u_j}$	3.3' 3.12	3.12
$\frac{\partial u_i}{\partial x_k} \frac{\partial u_j}{\partial x_k}$	3.12	Another equation *
$\overline{u_i u_j u_k}$	3.12	Modelled in 4.2.4 *
$\overline{\rho \frac{\partial u_i}{\partial x_j}}$	3.12	Modelled in 4.2.3 *

(In addition, we must prescribe the values of the fluid properties ν and ρ , assumed constant for our purpose, which appear in equations (3.2), (3.3) and (3.12).)

It is at this point that we have particular need of Hypotheses A and B of Appendix A. We must call a halt to the process at some point, and we need to use intuition to decide when that is to be. Chou, for example [1945], who first performed the derivation in Section 3.2, felt that an appropriate point would be at the level of the triple-correlations, on the ground that the quadruple correlations could be neglected.

However, there is no evidence that the quadruple correlations are negligible in general, so that this particular argument for proceeding further does not really hold. As we saw, Chou's closure would involve ten further equations: this would stretch the capabilities of most computers to the point where such a procedure would be academic in interest rather than economically feasible.

The alternative to the production of further equations for the transport of the triple correlations is to model them in terms of the lower-order correlations and mean-flow quantities. By analogy with the energy-balance for kinetic energy of turbulence, we shall see the triple correlations arise in connection with the diffusion of the normal stresses, and it would thus be reasonable to expect a gradient-type model of the triple-correlations to perform as well as von Kármán's gradient model of the diffusion of turbulent kinetic energy (von Kármán [1937]). Such models have been entirely adequate in the context of one- and two-equation models of turbulence.

If, as we shall seek to show, the triple correlations can be modelled with fair precision in terms of simpler quantities, Hypothesis B assures us that any residual error will not be troublesome. This is especially likely to be so, as the error will arise in the context of a quantity that we know to make a very small contribution to the energy balance – the diffusion. This will be all the more relevant in the near-wall region, of particular interest to us, where the production and dissipation of turbulent energy will dominate the energy balance.

As there would thus seem to be no reason to assume that we should necessarily obtain greater detail or improved accuracy merely by manipulating our limited store of information to generate ever

more complicated equations, we feel justified in calling a halt at this point. We summarize the reasons for choosing a Reynolds-stress closure:

- ★ The Reynolds stresses arise naturally as the representation of the turbulence in equations (3.3)', while quantities such as the triple correlations do not.
- ★ A Reynolds-stress closure is the simplest that enables us to escape from the Boussinesq eddy-viscosity approach.
- ★ If we proceed to a higher order of closure, quantities will arise which do not admit of a simple intuitive interpretation. Apart from the danger of a consequent loss of contact with practical reality, this may lead to serious problems of modelling.
- ★ The Reynolds stresses are well documented experimentally, while the triple correlations are not. In practice, this would mean that even if we could predict accurately the values of certain quantities, we should not be able to adduce practical evidence that we had done so.
- ★ Even the best modern computers are fully stretched by the demands that a closure at the Reynolds-stress level makes on them: more elaborate models would raise problems of time and expense.
- ★ There can be no reason for *not* trying the Reynolds-stress level of closure before expending further effort in developing the techniques required by a more sophisticated level of closure.

Already in the two-dimensional case, we need four equations for the Reynolds stresses, in addition to the mean momentum equation and the continuity equation, and a further equation for the quantity $(\overline{\partial u_i / \partial x_k})(\overline{\partial u_j / \partial x_k})$, as we shall discuss in Section 4.2.2 below. In a three-dimensional case, we shall need two additional Reynolds-stress equations as well as the equations for the extra mean velocities.

Our next task is to close the Reynolds-stress equations (3.12): i.e. to find differential or algebraic equations for the quantities starred in Table 3-1. This will be performed in Chapter 4.

4

THE REYNOLDS-STRESS MODEL

4.1 The Equations

Each term in equation (3.12) is customarily given a designation as follows:

$$\begin{aligned}
 \left\{ \frac{\partial}{\partial t} + \bar{U}_k \frac{\partial}{\partial x_k} \right\} \overline{u_i u_j} &= \text{CONVECTION} \\
 &= \\
 - \left\{ \overline{u_j u_k} \frac{\partial \bar{U}_i}{\partial x_k} + \overline{u_i u_k} \frac{\partial \bar{U}_j}{\partial x_k} \right\} &\text{ PRODUCTION} \\
 &- \\
 - 2\nu \overline{\frac{\partial u_i}{\partial x_k} \frac{\partial u_j}{\partial x_k}} &\text{ DISSIPATION} \quad (4.1) \\
 &+ \\
 + \frac{p}{\rho} \overline{\left\{ \frac{\partial u_i}{\partial x_j} + \frac{\partial u_j}{\partial x_i} \right\}} &\text{ REDISTRIBUTION} \\
 &+ \\
 - \frac{\partial}{\partial x_k} \left\{ \overline{u_i u_j u_k} - \nu \frac{\partial}{\partial x_k} \overline{u_i u_j} \right\} &\text{ DIFFUSION} \\
 - \frac{1}{\rho} \overline{\left\{ \frac{\partial}{\partial x_j} (p u_i) + \frac{\partial}{\partial x_i} (p u_j) \right\}} &
 \end{aligned}$$

We have split up the terms involving the pressure, but shall occasionally have to refer to them collectively as the *pressure terms*.

In Section 4.2 we shall tackle the problem of closure in the order indicated, dealing with the individual terms as grouped in equation (4.1).

4.1.1, The trace of equation (4.1)

It is convenient first to consider the trace of equation (4.1), which we derive by setting i equal to j

$$\begin{aligned} \left\{ \frac{\partial}{\partial t} + \bar{U}_k \frac{\partial}{\partial x_k} \right\} \overline{u_i u_i} &= -2 \overline{u_i u_k} \frac{\partial \bar{U}_i}{\partial x_k} \\ &\quad - 2\nu \overline{\left\{ \frac{\partial u_i}{\partial x_k} \right\}^2} \\ &\quad + 2 \overline{p \frac{\partial u_i}{\partial x_i}} \\ &\quad - \frac{\partial}{\partial x_k} \left\{ \overline{u_i^2 u_k} - \nu \frac{\partial}{\partial x_k} \overline{u_i^2} \right\} - 2 \frac{\partial}{\partial x_i} \overline{p u_i} \end{aligned}$$

Dividing by 2, we get, if we write k for $\overline{u_i u_i} / 2$,

$$\begin{aligned} \left\{ \frac{\partial}{\partial t} + \bar{U}_m \frac{\partial}{\partial x_m} \right\} k &= -\overline{u_i u_m} \frac{\partial \bar{U}_i}{\partial x_i} - \nu \overline{\left\{ \frac{\partial u_i}{\partial x_m} \right\}^2} \\ &\quad - \frac{\partial}{\partial x_m} \left\{ \overline{\frac{1}{2} u_m u_i^2} - \nu \frac{\partial}{\partial x_m} k \right\} \\ &\quad - \frac{\partial}{\partial x_i} \overline{p u_i} \end{aligned} \tag{4.2}$$

which is the *equation for the turbulent kinetic energy k* .

It is easier to see from equation (4.2) what the true roles of the various terms in equation (4.1) must be. In particular, the *redistribution* term justifies its designation by disappearing altogether from equation (4.2). The three remaining terms on the right-hand side of (4.2) have distinct effects, which become even more obvious when we consider degenerate cases, such as the two-dimensional boundary-layer, where the equation takes the form:

$$\begin{aligned} \frac{Dk}{Dt} = & -\overline{u_1 u_2} \frac{\partial \overline{U}_1}{\partial x_2} - \nu \overline{\frac{\partial u_i}{\partial x_j} \frac{\partial u_i}{\partial x_j}} \\ & - \frac{\partial}{\partial x_2} \left\{ \overline{u_i^2 u_2} - \nu \frac{\partial k}{\partial x_2} \right\} - \frac{\partial}{\partial x_2} \overline{\rho u_2} \end{aligned} \quad (4.3)$$

Now the term $-\overline{u_1 u_2} \partial \overline{U}_1 / \partial x_2$ is positive near a wall, as $-\overline{u_1 u_2}$ will tend to the value U_τ^2 , which (in the nature of friction) will tend to oppose the velocity. Experimentally, even for flows in which $\overline{u_1 u_2}$ must change its sign — such as boundary-layers between two walls — the quantities $-\overline{u_1 u_2}$ and $\partial \overline{U}_1 / \partial x_2$ are observed to be of the same sign for almost all the flow. The presence of the term $-\overline{u_1 u_2} \partial \overline{U}_1 / \partial x_2$ in equation (4.3) will normally tend to enhance the amount of turbulent kinetic energy present: hence the designation *production term*.

Clearly the term $-\nu \overline{\partial u_i / \partial x_j \partial u_i / \partial x_j}$ is negative semi-definite. It can thus be seen to destroy k , and its significance is therefore that of a *dissipative* term depending on the viscosity for its effect. We shall henceforth write

$$\begin{aligned} \epsilon = & -\nu \overline{\frac{\partial u_i}{\partial x_j} \frac{\partial u_i}{\partial x_j}} \\ \text{or } & -\nu \overline{\left\{ \frac{\partial u_i}{\partial x_j} \right\}^2} \end{aligned}$$

4.2. The terms of equations (3.12)

4.2.1 *The production term*

The first term on the right-hand side of equations (4.1) requires no “modelling” as such, as it is composed of precisely the type of quantity that we seek: the mean velocities \bar{U}_i (in this case their gradients) and the $\overline{u_i u_j}$: i.e. the quantities to be generated by our solution procedure.

The fact that the term $\overline{u_i u_j}$ appears in equation (3.3) and $\partial \bar{U}_i / \partial x_j$ in equation (4.1) merely shows that the equations are strongly coupled. In fact, it is already becoming evident that the coupling of the equations is almost complete: almost every one of the dependent variables appears inextricably in each of the equations – and not merely in the equation of which it is nominally the subject.

It is easily seen from equations (3.12) that the production of turbulence energy occurs only in relation to u_α^2 in a boundary-layer, where \hat{u}_α is the direction of mean motion.

4.2.2 *The dissipation term*

In equations (3.12) we saw that one term in particular,

$$\epsilon_{ij} \equiv \nu \frac{\partial u_i}{\partial x_k} \frac{\partial u_j}{\partial x_k}; \quad \epsilon_{ii} = \epsilon$$

would require ingenuity in modelling. ϵ , the second term in equation (4.3), represents the dissipation of the kinetic energy of turbulence. If we were to adopt a one-equation approach, or to use a scheme involving an equation for the transport of a length-scale ℓ_e , we should need to relate ϵ and ℓ as follows:

$$\epsilon \propto k^{3/2} / \ell_e \quad (4.4a)$$

(cf. Prandtl (1945)).

However, as we saw in § 1, we shall find it more useful to treat (4.4a) as a means of constructing a length-scale ℓ_e appropriate to the turbulent motion:

$$\ell_e \propto k^{3/2} / \epsilon \quad (4.4b)$$

The alternative to a purely algebraic model of ϵ is for us to try to construct, first, an exact equation for ϵ , and then a simplified version of that equation involving only the quantities appearing in Table 3.1 (i.e. those appropriate to our chosen level of closure). In constructing this equation, we follow the derivation given by Harlow & Nakayama [1967].

Equation (3.1) may be written as

$$\begin{aligned} \frac{\partial}{\partial t} (\bar{U}_i + u_i) + (\bar{U}_k + u_k) \frac{\partial}{\partial x_k} (\bar{U}_i + u_i) \\ = -\frac{1}{\rho} \frac{\partial}{\partial x_i} (\bar{P} + p) + \nu \frac{\partial^2}{\partial x_j^2} (\bar{U}_i + u_i) \end{aligned}$$

Subtracting equation (3.3)' we get

$$\begin{aligned} \frac{\partial u_i}{\partial t} + \bar{U}_k \frac{\partial u_i}{\partial x_k} + u_k \frac{\partial \bar{U}_i}{\partial x_k} + u_k \frac{\partial u_i}{\partial x_k} \\ = -\frac{1}{\rho} \frac{\partial p}{\partial x_i} + \nu \frac{\partial^2 u_i}{\partial x_k^2} - \frac{\partial}{\partial x_k} \overline{u_i u_k} \end{aligned} \quad (4.5)$$

Next we differentiate equation (4.5) with respect to x_q , and multiply throughout by $\partial u_i / \partial x_q$: i.e. we apply the operator $\partial u_i / \partial x_q \partial / \partial x_q$ to equation (4.5).

$$\begin{aligned} \frac{\partial u_i}{\partial x_q} \frac{\partial}{\partial x_q} \left\{ \frac{\partial u_i}{\partial t} \right\} + \frac{\partial u_i}{\partial x_q} \frac{\partial \bar{U}_k}{\partial x_q} \frac{\partial u_i}{\partial x_k} + \frac{\partial u_i}{\partial x_q} \bar{U}_k \frac{\partial^2 u_i}{\partial x_q \partial x_k} \\ + \frac{\partial u_i}{\partial x_q} \frac{\partial u_k}{\partial x_q} \frac{\partial \bar{U}_i}{\partial x_k} + \frac{\partial u_i}{\partial x_q} u_k \frac{\partial^2 \bar{U}_i}{\partial x_q \partial x_k} \\ + \frac{\partial u_i}{\partial x_q} \frac{\partial u_k}{\partial x_q} \frac{\partial u_i}{\partial x_k} + \frac{\partial u_i}{\partial x_q} u_k \frac{\partial^2 u_i}{\partial x_k \partial x_q} \\ = -\frac{1}{\rho} \frac{\partial u_i}{\partial x_q} \frac{\partial^2 p}{\partial x_i \partial x_q} + \nu \frac{\partial u_i}{\partial x_q} \frac{\partial^3 u_i}{\partial x_k \partial x_k \partial x_q} + \frac{\partial u_i}{\partial x_q} \frac{\partial^2 \overline{u_i u_k}}{\partial x_k \partial x_q} \end{aligned} \quad (4.6)$$

Assuming that u_i satisfies the criterion for

$$\frac{\partial^2 u_i}{\partial x_m \partial x_q} = \frac{\partial^2 u_i}{\partial x_q \partial x_m} \quad (4.7)$$

and observing that

$$\begin{aligned} \text{(a)} \quad & \frac{\partial \bar{U}_k}{\partial x_q} \frac{\partial u_i}{\partial x_k} \frac{\partial u_i}{\partial x_q} \equiv \frac{\partial \bar{U}_i}{\partial x_k} \cdot \frac{\partial u_q \partial u_q}{\partial u_i \partial u_k} \\ \text{(b)} \quad & \frac{\partial}{\partial x_k} \left\{ u_k \cdot \frac{1}{2} \left(\frac{\partial u_i}{\partial x_q} \right)^2 \right\} \equiv \frac{\partial u_k}{\partial x_k} \cdot \frac{1}{2} \left(\frac{\partial u_i}{\partial x_q} \right)^2 + u_k \frac{\partial u_i}{\partial x_q} \frac{\partial^2 u_i}{\partial x_k \partial x_q} \\ & = u_k \frac{\partial u_i}{\partial x_q} \frac{\partial^2 u_i}{\partial x_k \partial x_q} \\ \text{(c)} \quad & \frac{\partial}{\partial x_k} \left\{ \frac{\partial u_i}{\partial x_q} \frac{\partial^2 u_i}{\partial x_q \partial x_k} \right\} \equiv \left(\frac{\partial^2 u_i}{\partial x_k \partial x_q} \right)^2 + \frac{\partial u_i}{\partial x_q} \frac{\partial^3 u_i}{\partial x_k \partial x_k \partial x_q} \\ & \Rightarrow \frac{\partial u_i}{\partial x_q} \cdot \frac{\partial^3 u_i}{\partial x_q \partial x_k \partial x_q} = \frac{\partial}{\partial x_k} \left\{ \frac{\partial u_i}{\partial x_q} \frac{\partial^2 u_i}{\partial x_q \partial x_k} \right\} - \left(\frac{\partial^2 u_i}{\partial u_k \partial x_q} \right)^2 \\ & = \frac{\partial}{\partial x_k} \left\{ \frac{\partial}{\partial x_k} \left[\frac{1}{2} \left(\frac{\partial u_i}{\partial x_q} \right)^2 \right] \right\} - \left(\frac{\partial^2 u_i}{\partial x_k \partial x_q} \right)^2 \\ \text{(d)} \quad & \frac{\partial}{\partial x_i} \left\{ u_i \frac{\partial p}{\partial x_q} \frac{\partial u_i}{\partial x_q} \right\} \equiv \frac{\partial u_i}{\partial x_i} \frac{\partial p}{\partial x_q} \frac{\partial u_i}{\partial x_q} + u_i \frac{\partial^2 p}{\partial x_q \partial x_i} \frac{\partial u_i}{\partial x_q} \\ & + u_i \frac{\partial p}{\partial x_q} \frac{\partial^2 u_i}{\partial x_i \partial x_q} = u_i \frac{\partial^2 p}{\partial x_q \partial x_i} \frac{\partial u_i}{\partial x_q} \end{aligned}$$

by (3.2), its corollary,

$$\frac{\partial}{\partial x_i} \left\{ \frac{\partial^n u_i}{\partial x_{\alpha_1} \dots \partial x_{\alpha_k}} \right\} = 0$$

subject as usual to (4.7).

We can now write equation (4.6) in the form

$$\begin{aligned}
& \frac{\partial}{\partial t} \left\{ \frac{1}{2} \left(\frac{\partial u_i}{\partial x_q} \right)^2 \right\} + U_k \frac{\partial}{\partial x_k} \left\{ \frac{1}{2} \left(\frac{\partial u_i}{\partial x_q} \right)^2 \right\} & \text{A} \\
= & - \frac{\partial U_i}{\partial x_k} \left\{ \frac{\partial u_i}{\partial x_q} \frac{\partial u_k}{\partial x_q} + \frac{\partial u_q}{\partial x_i} \frac{\partial u_q}{\partial x_k} \right\} & \text{B} \\
& - \frac{\partial u_i}{\partial x_q} \frac{\partial u_k}{\partial x_q} \frac{\partial u_i}{\partial x_k} & \text{C} \\
& - \frac{\partial}{\partial x_k} \left\{ u_k \frac{1}{2} \left(\frac{\partial u_i}{\partial x_q} \right)^2 \right\} & \text{D} \\
& - \frac{\partial u_i}{\partial x_q} u_k \frac{\partial^2 U_i}{\partial x_q \partial x_k} & \text{E} \quad (4.8) \\
& - \frac{1}{\rho} \frac{\partial}{\partial x_i} \left\{ \frac{\partial p}{\partial x_q} \cdot \frac{\partial u_i}{\partial x_q} \right\} & \text{F} \\
& - \nu \left(\frac{\partial^2 u_i}{\partial x_k \partial x_q} \right)^2 & \text{G} \\
& + \nu \frac{\partial^2}{\partial x_k^2} \left\{ \frac{1}{2} \left(\frac{\partial u_i}{\partial x_q} \right)^2 \right\} & \text{H} \\
& + \frac{\partial u_i}{\partial x_q} \frac{\partial^2 \overline{u_i u_k}}{\partial x_k \partial x_q} & \text{I}
\end{aligned}$$

where we have dropped the overbars on U_i , as we shall have no further occasion to refer to the unaveraged U_i 's.

As we have defined

$$\epsilon_{ii} \equiv \epsilon \equiv \nu \left(\frac{\partial u_i}{\partial x_q} \right)^2$$

we must now multiply equation (4.8) throughout by 2ν and time-average the whole equation. If we further define the unaveraged equivalent of ϵ as

$$\epsilon' \equiv \nu \left(\frac{\partial u_i}{\partial x_q} \right)^2$$

we obtain an *exact equation for ϵ* , due to Harlow and Nakayama [1967]:

$$\begin{aligned}
 & \frac{\partial \epsilon}{\partial t} + U_k \frac{\partial \epsilon}{\partial x_k} && \text{A} \\
 & = -2\nu \frac{\partial U_i}{\partial x_k} \left\{ \overline{\frac{\partial u_i}{\partial x_q} \frac{\partial u_k}{\partial x_q} + \frac{\partial u_q}{\partial x_i} \frac{\partial u_q}{\partial x_k}} \right\} && \text{B} \\
 & \quad - 2\nu \overline{\frac{\partial u_i}{\partial x_q} \frac{\partial u_k}{\partial x_q} \frac{\partial u_i}{\partial x_k}} && \text{C} \\
 & \quad - \frac{\partial}{\partial x_k} \overline{u_k \epsilon'} && \text{D} \\
 & \quad - 2\nu \overline{\frac{\partial u_i}{\partial x_q} u_k \frac{\partial^2 U_i}{\partial x_q \partial x_k}} && \text{E} \quad (4.9) \\
 & \quad - \frac{2\nu}{\rho} \frac{\partial}{\partial x_i} \left\{ \overline{\frac{\partial \rho}{\partial x_q} \frac{\partial u_i}{\partial x_q}} \right\} && \text{F} \\
 & \quad - 2\nu \overline{\left\{ \frac{\partial^2 u_i}{\partial x_k \partial x_q} \right\}^2} && \text{G} \\
 & \quad + \frac{1}{2} \nu \overline{\frac{\partial^2 \epsilon}{\partial x_k^2}} && \text{H} \\
 & \quad + \overline{\frac{\partial u_i}{\partial x_q} \left\{ \dots \right\}} && \text{I}
 \end{aligned}$$

Defining R as $u'\ell/\nu$, where ℓ is the ('integral') length scale of turbulence and noting that, if λ is the microscale, $\lambda/\ell = O(R^{-1/2})$,

Term A is of order u'^4/ℓ^2

Term C is of order $u'^4/\ell^2 \times R^{1/2}$

Term D is of order u'^4/ℓ^2

Term E is of order $u'^4/\ell^2 \times R^{-1/2}$ and can thus be neglected in any fully-turbulent zone.

Term F can be resolved (by analogy with our analysis, below, of the pressure-strain term in, §4.2.3) into two terms, which as Hanjalić and Launder [1972] argue, both contain higher-order derivatives of the mean and fluctuating velocities than appear in the pressure-strain term. It is thus consistent with our chosen level of closure to neglect *Term F*.

Term G is again of order u'^4/ℓ^2

Term H is of order $(u'^4/\ell^2) \times R^{-1/2}$ and is thus negligible for high Reynolds numbers.

Term I disappears by continuity (3.2).

Term B

Earlier workers (Rodi [1972], Hanjalić & Launder [1972]) relied on *term B* for the source of generation of dissipation. Lumley and Khajeh-Nouri [1974] argue that this term, by virtue of the relative isotropy of the small scales at large R , can be written roughly as

$$\nu \cdot \frac{\partial U_i}{\partial x_k} \cdot \frac{\partial u_i}{\partial x_\ell} \frac{\partial u_k}{\partial x_\ell} \sim \frac{\epsilon u'}{\ell} \cdot \frac{\delta_{ik}}{3} \quad (4.10)$$

neglecting off-diagonal, i.e. anisotropic terms. The difference between the two sides of (4.10) represents the degree of anisotropy and is proportional to the time-scale ratio between the small and large scales. If we further define

$$a_{ij} \equiv \frac{\overline{u_i u_j}}{k} - \frac{2}{3} \delta_{ij} \quad (4.11)$$

we see that the difference is

$$\frac{u'^2}{\ell^4} \frac{\lambda}{\ell} a_{ij} \sim R^{-1/2} a_{ij} \cdot \frac{u'^2}{\ell^4}$$

and can thus be neglected. This means, therefore, that *term B* should be neglected for high R .

Lumley and Khajeh-Nouri argue that the source of dissipation must therefore lie in term **C**. (Term **D** is a diffusive term, and Term **G** is negative semi-definite, so that – if only by elimination – Term **C** is the sole term capable of positive generation)

Regardless of the individual sources responsible, the imbalance between generation and destruction can thus be modelled as a term of the form

$$\epsilon \frac{\partial U_i}{\partial x_j} \left\{ \frac{\overline{u_i u_j}}{k} - \frac{2}{3} \delta_{ij} \right\} \left\{ (a R^{-1/2} + b) + O(R^{-1}) \right\}$$

$R^{-1/2}$ is a non-dimensional quantity here representing the imbalance between generation and destruction of dissipation: a suitable measure is the ratio ϵ/P between dissipation and production ($-\overline{u_i u_j} \partial U_i / \partial x_j$) of turbulence energy.

This leads to the model

$$\frac{\epsilon}{k} \left\{ -c_{\epsilon 1} \overline{u_i u_j} \frac{\partial U_i}{\partial x_j} - c_{\epsilon 2} \epsilon \right\} \quad (4.12)$$

recognising that the term in δ_{ij} disappears by continuity, and neglecting higher order terms in $R^{-1/2}$.

Thus far, all workers are in agreement to the extent that the models to which their arguments lead all reduce to (4.12) for high R . However, Lumley and Khajeh-Nouri proceed to advocate the replacement of P in (4.12) by $\Pi \equiv \frac{1}{4} a_{ij} a_{ji}$ (with a suitably-dimensioned coefficient). Π , they argue, does not vanish in regions of flows where P does vanish, ensuring the continued generation of dissipation even in the absence of generation of turbulence energy. Attempts to incorporate this, and other aspects of Lumley and Khajeh-Nouri's proposal by the present author led to negative conclusions and it was deduced that for the (simple one-dimensional) flows considered, a single set of constants did not suffice. There would thus appear to be no advantage in incorporating the model in a two-dimensional situation. However, we must concede that more favourable conclusions were drawn by Launder [1975] from investigations performed by A.P. Morse. As we shall see, the results obtained from the model

(4.12) are sufficiently close to experimental data where these are available to justify confidence in its predictive powers.

The remaining term \mathbf{D} represents the diffusion of dissipation by turbulent fluctuations. By a similar argument to that which leads from the exact triple-correlation equations to a gradient-type (von Kármán) model of diffusion, Hanjalić and Launder [1972] showed that, to the same level of approximation as used to justify the derivation of the expressions for the generation and destruction of dissipation, the diffusive term \mathbf{D} could be modelled as

$$\overline{\epsilon u_k} = -c_{\epsilon 3} \frac{k}{\epsilon} \overline{u_k u_q} \frac{\partial \epsilon}{\partial x_q}$$

in a thin shear flow.

The modelled equation for dissipation thus reads

$$\begin{aligned} \frac{D\epsilon}{Dt} = & -c_{\epsilon 1} \epsilon \frac{\overline{u_i u_k}}{k} \frac{\partial U_i}{\partial x_k} - c_{\epsilon 2} \frac{\epsilon^2}{k} \\ & + c_{\epsilon 3} \frac{\partial}{\partial x_k} \left\{ \frac{k}{\epsilon} \overline{u_k u_q} \frac{\partial \epsilon}{\partial x_q} \right\} \end{aligned} \quad (4.13)$$

Determination of the values of $c_{\epsilon 1}$, $c_{\epsilon 2}$, and $c_{\epsilon 3}$.

Like Hanjalić and Launder we consider the decay of turbulence behind a grid (Batchelor & Townsend [1948]). Noting that the decay is governed by a law of the form

$$k \propto x^{-1-\delta}$$

where δ is small and positive, we have

$$k = Ax^{-1-\delta}$$

$$\frac{\partial k}{\partial x} = A(-1-\delta)x^{-2-\delta}$$

Then (4.3) gives

$$U_0 A (-1-\delta) x^{-2-\delta} = -\epsilon$$

$$\Rightarrow \epsilon = U_0 A (1+\delta) x^{-2-\delta}$$

(4.13) then gives

$$(-2-\delta) U_0^2 A (1+\delta) x^{-3-\delta} = -c_{\epsilon 2} \frac{U_0^2 A^2 (1+\delta)^2 x^{-4-2\delta}}{A x^{-1-\delta}}$$

$$\Rightarrow c_{\epsilon 2} = \frac{2+\delta}{1+\delta}$$

$$c_{\epsilon 2} = \left. \begin{array}{l} 1.91 \text{ if } \delta = 0.1 \\ 2.0 \text{ if } \delta = 0.0 \end{array} \right\}$$

Hanjalić and Launder took the value $\delta = 0$. If we examine the data of Batchelor and Townsend, we soon recognize that each of the graphs they present for U/k vs. x curves upwards, away from the straight line as x increases, suggesting a value of δ greater than zero. We have therefore taken $c_{\epsilon 2} = 1.91$ rather than Hanjalić & Launder's value of 2.0. This was suggested by the work of Rodi [1972].

To determine $c_{\epsilon 1}$ and $c_{\epsilon 3}$, we consider the log-law region of a fully-developed boundary-layer near a wall, where production and dissipation of turbulent kinetic energy are known to be in balance (see Hanjalić & Launder [1972]). Here

$$U_1 = \frac{u_\tau}{\kappa} \ln \frac{x_2 U_\tau}{\nu} + \text{const.}$$

$$\frac{\partial U_1}{\partial x_2} = \frac{U_\tau}{\kappa x_2} \quad ; \quad \text{also} \quad -\overline{u_1 u_2} = U_\tau^2$$

$$\epsilon = -\overline{u_1 u_2} \frac{\partial U_1}{\partial x_2} = \frac{U_\tau^3}{\kappa x_2}$$

The appropriate values of k and $\overline{u_2^2}$ indicated by various experiments (e.g. Hanjalić and Launder [1972])

$$k \simeq 4.2 U_\tau^2; \quad \overline{u_2^2} \simeq U_\tau^2$$

We have

$$\begin{aligned} \frac{D\epsilon}{Dt} = & -c_{\epsilon 1} \epsilon \frac{\overline{u_i u_k}}{k} \frac{\partial U_i}{\partial x_k} - c_{\epsilon 2} \frac{\epsilon^2}{k} \\ & + c_{\epsilon 3} \frac{\partial}{\partial x_k} \left\{ \frac{k}{\epsilon} \overline{u_k u_q} \frac{\partial \epsilon}{\partial x_q} \right\} \end{aligned} \quad (4.13)$$

whence

$$\begin{aligned} 0 = & c_{\epsilon 1} \frac{U_\tau^3}{\kappa x_2} \frac{U_\tau}{\kappa x_2} \frac{U_\tau^2}{4.2 U_\tau^2} - c_{\epsilon 2} \frac{U_\tau^6}{\kappa^2 \cdot 4.2 U_\tau^2 x_2^2} \\ & + c_{\epsilon 3} \frac{\partial}{\partial x_2} \frac{4.2 \overline{u_2^2}}{U_\tau^3} \cdot \kappa x_2 \cdot U_\tau^2 \cdot \frac{-U_\tau^3}{\kappa x_2^2} \end{aligned}$$

which simplifies to

$$c_{\epsilon 1} = c_{\epsilon 2} - (4.2)^2 \kappa^2 c_{\epsilon 3}$$

which, with $\kappa = 0.41$, gives

$$c_{\epsilon 1} = c_{\epsilon 2} - 3.0 c_{\epsilon 3} \quad (4.14)$$

It is perhaps comforting to note that, despite all the differences in detail between our argument and that of Hanjalić and Launder (e.g. they take $\overline{u_2^2} = 1.6 U_\tau^2$ while we take $\overline{u_2^2} = U_\tau^2$), they derive a relationship

$$c_{\epsilon 1} = c_{\epsilon 2} - 3.5 c_{\epsilon 3}$$

which does not differ radically from our equation (4.14).

Our choice of $\overline{u_2^2} = U_\tau^2$ and $k = 4.2 U_\tau^2$ is, in fact, based on Hanjalić and Launder's own published measurements [1972a].

The discrepancies between their choices and ours for the ratios must be attributed to their use of the values associated with homogeneous shear flows such as that of Champagne, Harris & Corrsin [1970], which we suggest may not be so appropriate as those derived from Hanjalić & Launder's own channel-flow measurements. Relationship (4.14) leads to the result

$$c_{\epsilon 1} = 1.91 - 3.0 c_{\epsilon 3} \quad (4.15)$$

if we insert our calculated value for $c_{\epsilon 2}$.

Measurement of the dissipation

One fundamental problem attendant upon our treatment of the dissipation term in equation (4.1) is the absence of reliable direct experimental data. Such energy-balance measurements as there are, e.g. those of Hanjalić & Launder [1972], contain results for the dissipation only as a by-product of the remaining measurements. If we consider, for a moment, the measurement of the energy balance for a fully-developed boundary-layer flow, the kinetic energy of turbulence being governed by the equation (4.3), we have:

$$\begin{aligned} 0 &= P - \epsilon + D \\ \epsilon &= P + D \end{aligned} \quad (4.16)$$

Clearly, if D is measured as being small, ϵ (the dissipation) will inevitably be seen to be roughly equal to P . But if P is derived from the product of two measured quantities $\partial U_1 / \partial x_2$ and $\overline{u_1 u_2}$, in the case of a two-dimensional boundary-layer, and D is taken as equal to the measured values of the triple-correlation gradient, each measured quantity f being subject to the error δf :

$$\begin{aligned} \epsilon + \delta\epsilon &= (-\overline{u_1 u_2} + \delta(-\overline{u_1 u_2})) \left\{ \frac{\partial U_1}{\partial x_2} + \delta \left(\frac{\partial U_1}{\partial x_2} \right) \right\} \\ &+ (D + \delta D) \end{aligned}$$

Thus

$$\delta\epsilon \approx \delta(-\overline{u_1 u_2}) \cdot \frac{\partial U_1}{\partial x_2} + (-\overline{u_1 u_2}) \cdot \delta \left(\frac{\partial U_1}{\partial x_2} \right) + \delta D \quad (4.17)$$

Unfortunately, therefore, $\delta\epsilon$ is not merely the sum of the errors in $\overline{u_1 u_2}$, $\partial U_1 / \partial x_2$ and D , but is the *weighted* sum shown in equation (4.17). Worse still: the errors are likely to be largest when the coefficients are largest (e.g. near a wall).

We can therefore not rely on energy-balance measurements for accurate information on the dissipation.

Evidence of isotropy

If these were the only available checks on the values of ϵ , we should be in doubt as to the validity of the model. However, it is a well established experimental fact (cf. Hinze [1975]) that the production and dissipation of turbulent energy occur at opposite ends of the frequency scale. Energy is produced in large eddies (at low wave numbers) and dissipated in small eddies (at high wave numbers) (see, e.g., Tennekes & Lumley [1972], §8.3). The further fact that these ranges are clearly separated in the flows we consider by a well-defined 'inertial subrange' enables us to confirm, by examining spectral decompositions of the turbulent fluctuations (e.g. those in Hanjalić and Launder [1972a]), that the small-scale turbulence is *isotropic*, as first suggested by Kolmogorov [1941].

In view of this evidence, we are able to allocate the dissipation of turbulence energy equally among the normal stresses $\overline{u_\alpha^2}$:

$$\epsilon_{\alpha\alpha} = \frac{1}{3} \epsilon_{ii}$$

It is reassuring to note that these observations are in accord with the common-sense view that the small-scale activities occur over such short times and distances that they are bound to be insensitive to gross quantities such as mean velocities and mean strain with large characteristic time- and length-scales.

Again, in accordance with experimental evidence, we allocate no dissipative activity to the off-diagonal (shear) Reynolds stresses.

A different model:

$$\epsilon_{ij} = \epsilon \frac{\overline{u_i u_j}}{2k}$$

was proposed by Daly and Harlow [1970] but is not supported by the data of Hanjalić & Launder [1972].

4.2.3 The pressure-strain term

The next term to engage our attention is the “redistribution” term of equation (4.1):

$$\Pi_{ij} \equiv \frac{1}{\rho} \overline{p \left(\frac{\partial u_i}{\partial x_j} + \frac{\partial u_j}{\partial x_i} \right)} \quad (4.18)$$

This term, as we have remarked (in Section 4.1.1), is redistributive of turbulent kinetic energy as between the $\overline{u_\alpha u_\alpha}$ (the Reynolds normal stresses). If, for a moment, we think of the Reynolds normal-stress equations as a separate closed system of equations (which of course they are not) this term acts merely to allocate k to $\overline{u_1^2}$, $\overline{u_2^2}$ and $\overline{u_3^2}$ after allowing for the effects of production and dissipation, and of diffusion; it thus neither creates k nor destroys it. Now, relaxing our view, and admitting that the subsystem of normal-stress equations is not in fact closed, we see, for example, that the term (4.18) also appears in the turbulent shear-stress equations (as, of course, do also the normal stresses themselves) and that it is thus capable of influencing the mean-velocity profiles and the rate of production of turbulent kinetic energy. We shall, nevertheless, have occasion to think of the term (4.18) in its redistributive role, neglecting its interactive influence.

Our main concern in “modelling” the term (4.18) will be to provide a representation which will serve to allocate k in the correct ratios (i.e. in accordance with the empirical data) to the normal stresses. The consequence of our approach will be to allow the effect on the turbulent shear stresses to emerge naturally from the model. If our assumptions are correct, the requisite ratios of the normal stresses will provide sufficient information to determine any unknown coefficients in the model. *If* our assumptions are correct, we shall then find the effect on the $\overline{u_i u_j}$ ($i \neq j$) correctly predicted.

It is perhaps worth pointing to the crucial differences implied by our choice of a full Reynolds-stress model, compared, for example, with Hanjalić and Launder [1972] who solved equations for k , ϵ and $\overline{u_1 u_2}$ in the two-dimensional boundary-layer, replacing the normal stresses by fractions of k wherever they arose. This implies an essential difference in the importance to be attached to the term

(4.18). For us it is a redistributive term for the normal stresses with consequent effects on the shear stress, while for Hanjalić and Launder the term was significant only in respect of its non-redistributive role. The consequences of the effects on the shear stresses are far from trivial and will appear as effects on the predicted mean-velocity profile; they are responsible for the decay of $\overline{u_1 u_2}$. In a sense, therefore, we are more rigidly constrained by the present model than Hanjalić and Launder were by theirs: we approach indirectly the crucial problem of producing an equation for $\overline{u_1 u_2}$ in a two-dimensional boundary-layer – a problem which Hanjalić and Launder were able to tackle head-on.

Eliminating the pressure

Equation (4.5) states that

$$\begin{aligned} \frac{\partial u_i}{\partial t} + U_k \frac{\partial u_i}{\partial x_k} + u_k \frac{\partial U_i}{\partial x_k} + u_k \frac{\partial u_i}{\partial x_k} \\ = -\frac{1}{\rho} \frac{\partial p}{\partial x_i} + \nu \frac{\partial^2 u_i}{\partial x_k^2} - \frac{\partial}{\partial x_k} \overline{u_i u_k} \end{aligned} \quad (4.5)$$

Following Chou [1945] we take the divergence ($\partial/\partial x_i$) of equation (4.5) and recall that continuity dictates (3.2) that $\partial u_i/\partial x_i = 0$:

$$-\frac{1}{\rho} \frac{\partial^2 p}{\partial x_i^2} = \frac{\partial u_i}{\partial x_k} \frac{\partial U_k}{\partial x_i} + \frac{\partial u_k}{\partial x_i} \frac{\partial U_i}{\partial x_k} + \frac{\partial u_k}{\partial x_i} \frac{\partial u_i}{\partial x_k} - \frac{\partial^2}{\partial x_k \partial x_i} \overline{u_i u_k}$$

Therefore, as

$$\begin{aligned} \frac{\partial}{\partial x_k} \left\{ \frac{\partial}{\partial x_i} (u_i u_k) \right\} &= \frac{\partial}{\partial x_k} \left\{ u_i \frac{\partial u_k}{\partial x_i} \right\} = \frac{\partial u_i}{\partial x_k} \cdot \frac{\partial u_k}{\partial x_i} \\ \frac{1}{\rho} \nabla^2 p &= -2 \frac{\partial u_i}{\partial x_k} \frac{\partial U_k}{\partial x_i} - \frac{\partial^2 u_i u_k}{\partial x_k \partial x_i} + \frac{\partial^2 \overline{(u_i u_k)}}{\partial x_i \partial x_k} \end{aligned} \quad (4.19)$$

Now, taking $(\partial/\partial x_k)$ of (4.19) we see that

$$\begin{aligned} \frac{1}{\rho} \nabla^2 \left(\frac{\partial \rho}{\partial x_k} \right) &= -2 \frac{\partial}{\partial x_k} \left\{ \frac{\partial U_m}{\partial x_n} \frac{\partial u_n}{\partial x_m} \right\} \\ &\quad + \frac{\partial^3 \overline{u_m u_n}}{\partial x_m \partial x_n \partial x_k} - \frac{\partial^3 u_m u_n}{\partial x_m \partial x_n \partial x_k} \end{aligned} \quad (4.20)$$

Green's Theorem states that

$$u = -\frac{1}{4\pi} \int_V \frac{\nabla^2 u}{r} dV + \frac{1}{4\pi} \int_{\Sigma} \frac{1}{r} \frac{\partial u}{\partial n} d\Sigma - \frac{1}{4\pi} \int_{\Sigma} u \frac{\partial}{\partial n} \left(\frac{1}{r} \right) d\Sigma$$

whence

$$\begin{aligned} \frac{1}{\rho} \frac{\partial \rho}{\partial x_k} &= \frac{1}{2\pi} \int_V \frac{1}{r'} \frac{\partial}{\partial x_k} \left(\frac{\partial U_m'}{\partial x_n} \frac{\partial u_n'}{\partial x_m} \right) dV' \\ &\quad + \frac{1}{4\pi} \int_V \frac{1}{r'} \left\{ \frac{\partial^3 \overline{u_m' u_n'}}{\partial x_m \partial x_n \partial x_k} - \frac{\partial^3 u_m' u_n'}{\partial x_m \partial x_n \partial x_k} \right\} dV' \quad (4.21) \\ &\quad + \frac{1}{4\pi\rho} \int_{\Sigma} \frac{1}{r'} \frac{\partial}{\partial n'} \left(\frac{\partial \rho'}{\partial x_k} \right) d\Sigma \\ &\quad - \frac{1}{4\pi\rho} \int_{\Sigma} \frac{\partial \rho'}{\partial x_k} \frac{\partial}{\partial n'} \left(\frac{1}{r} \right) d\Sigma \end{aligned}$$

ρ is a function of x_0, y_0 , and z_0 (fixed); all the terms of the right-hand-side of equation (4.21) are evaluated with respect to x', y' and z' (moving over the volume or surface as appropriate).

If we now multiply (4.21) throughout by u_i , evaluated at (x_0, y_0, z_0) , and put bars over appropriate terms, we see that

$$\begin{aligned} \frac{1}{\rho} \overline{u_i \frac{\partial p}{\partial x_k}} &= \frac{1}{2\pi} \int_v \frac{\partial}{\partial x_k'} \left\{ \frac{\partial U_m'}{\partial x_n'} \cdot \frac{\partial \overline{u_n' u_i}}{\partial x_m'} \right\} \frac{1}{r'} dV' \\ &+ \frac{1}{4\pi} \int_v \frac{\partial^3 \overline{u_m' u_n' u_i}}{\partial x_m' \partial x_n' \partial x_k'} \cdot \frac{1}{r'} dV' \\ &+ \frac{1}{4\pi\rho} \int_\Sigma \left\{ \frac{1}{r'} \frac{\partial}{\partial n'} \left(\frac{\partial p'}{\partial x_k} u_i \right) - \frac{\partial(\overline{p' u_i})}{\partial x_k} \frac{\partial}{\partial n'} \left(\frac{1}{r} \right) \right\} d\Sigma' \end{aligned} \quad (4.22)$$

Chou suggests that the surface-integral term in equation (4.22) may be neglected if $\overline{u_i \partial p' / \partial x_k'}$ is small, which it is, provided the point $P(x_0, y_0, z_0)$ is not too close to the boundary.

This argument then leads to the following expression for the correlation $\frac{1}{\rho} \overline{u_i \frac{\partial p}{\partial x_j}}$

$$\begin{aligned} \phi_{ij} &= -\frac{1}{\rho} \frac{\partial}{\partial x_j} \overline{(p u_i)} + \frac{\overline{p \partial u_i}}{\rho \partial x_j} = -\frac{1}{\rho} \frac{\partial p}{\partial x_j} \overline{u_i} \\ &= S_{ij} + \frac{1}{4\pi} \int_v \underbrace{\left\{ \left(\frac{\partial^2 (u_c u_m)}{\partial x_c \partial x_m} \right)' \right\}}_{\phi_{ij,1}} \frac{\partial U_i}{\partial x_j} \\ &\quad + 2 \underbrace{\left\{ \left(\frac{\partial U_c}{\partial x_m} \right)' \left(\frac{\partial u_m}{\partial x_c} \right)' \left(\frac{\partial u_i}{\partial x_j} \right) \right\}}_{\phi_{ij,2}} \frac{dV}{|x-y|} \end{aligned} \quad (4.23)$$

with the primed values taken at y , unprimed ones at x .

Equation (4.23) thus shows that the pressure-strain correlation can be divided into two parts: the first involving purely fluctuating quantities, and the second involving the mean rate of strain. In fact, Chou's argument covers, as we have seen, not merely the "redistributive" part of the pressure term, but also that part of the original pressure term in equation (4.1) which we have tended to separate out as more akin to the diffusion. However, it should always be borne in mind that over the largest part of any near-wall turbulent flow, the production and dissipation of turbulent kinetic energy are in balance, and the diffusion is altogether relatively small; it is thus virtually immaterial whether or not we include the separated-out part of the pressure term when we model the pressure-strain term.

A model of $\phi_{ij,1}$

We follow Rotta's suggestion (1951) that

$$(\phi_{ij,1} + \phi_{ji,1}) = -c_{\phi 1} \frac{\epsilon}{k} (\overline{u_i u_j} - \frac{2}{3} \delta_{ij} k) \quad (4.24)$$

Rotta argued that in the absence of external influences the most probable distribution of the turbulent fluctuations was the isotropic one. Hence, the effect of the term Π_{ij} (4.18) was to cause a return to isotropy. (4.24) was the obvious initial choice for a model of $\phi_{ij,1}$, setting it as proportional to the degree of anisotropy. As we have seen, for a boundary-layer, in the absence of diffusion, the pressure-strain terms are the *only* ones capable of generation in the u_α^2 equations where \hat{i}_α is any direction normal to that of the mean motion. This enables us to use experimental data for a boundary-layer flow to assess the effect of the pressure-strain terms.

In particular, Rotta was able to derive a formula for the coefficient $c_{\phi 1}$. We apply Rotta's analysis to the data of Champagne, Harris and Corrsin [1970]. This process leads to precisely the same conclusion as that drawn by Rotta — a value of $c_{\phi 1}$ roughly equal to 1.4 (Rotta gave the reciprocal as 0.7). (We present a more detailed derivation in the context of the determination of $c_{\phi 2}$, below.)

Intervening writers have found different values for $c_{\phi 1}$: in every case, this can be related to the level of anisotropy of the flows con-

sidered. Expression (4.24) shows that the greater the anisotropy the larger will be the required value of $c_{\phi 1}$. Rotta himself revised his estimate [1962] to 2.8, a value which has been used by Hanjalić and Launder [1972], and close to the value of 2.5 used by Wolfshtein and his co-workers [1969].

Thus far we have tried to maintain a high level of generality in the argument. At this point, however, we adjourn the discussion of $\phi_{ij,1}$ pending a detailed discussion of the effects of the proximity of a wall (§5 below). Everything we have said up to now has been of particular relevance to flows remote from walls.

The term $\phi_{ij,2}$

From (4.23)

$$\phi_{ij,2} \equiv \frac{1}{2\pi} \int_V \left(\frac{\partial U_q}{\partial x_m} \right)' \left(\frac{\partial u_m}{\partial x_q} \right)' \left(\frac{\partial u_i}{\partial x_j} \right) \frac{dV}{|x-y|} \quad (4.25)$$

For convenience, we define $\xi \equiv x - y$.

If

$$\begin{aligned} R_{mi} &\equiv \overline{u_i(r_0) u_m(r_0 + r)} \\ &= \overline{u_i u_m'}, \text{ say.} \\ \frac{\partial}{\partial x_j} \overline{(u_i u_m')} &= \overline{\frac{\partial u_i}{\partial x_j} u_m'} = \frac{\partial}{\partial x_j} R_{mi} = \frac{-\partial}{\partial \xi_j} R_{mi} \end{aligned} \quad (4.26)$$

as the u_m' are independent of the x_j .

Then

$$\begin{aligned} \frac{\partial}{\partial x_q'} \left(\overline{\frac{\partial u_i}{\partial x_j} u_m'} \right) &= - \frac{\partial}{\partial x_q'} \left(\frac{\partial R_{mi}}{\partial \xi_j} \right) \\ &= \frac{-\partial^2 R_{mi}}{\partial \xi_q \partial \xi_j} = \frac{\partial u_m}{\partial x_q} \frac{\partial u_i'}{\partial x_j'} \end{aligned}$$

whence

$$\frac{\partial u_m}{\partial x_q} \frac{\partial u_i}{\partial x_j} = - \frac{\partial^2 R_{mi}}{\partial \xi_q \partial \xi_j}$$

(these results were obtained by von Kármán and Howarth [1938]).

If we now define:

$$\begin{aligned} \phi_{ij,2} \equiv & \frac{\partial U_q}{\partial x_m} \bigg|_{r=0} a_{qj}^{mi} + \frac{\partial^2 U_q}{\partial x_m \partial x_n} \bigg|_{r=0} {}_n b_{qj}^{mi} \\ & + \frac{\partial^3 U_q}{\partial x_m \partial x_n \partial x_p} \bigg|_{r=0} {}_{np} c_{qj}^{mi} + \dots \end{aligned} \quad (4.27)$$

we see also that, by Taylor's theorem,

$$\begin{aligned} \phi_{ij,2} & \equiv \frac{1}{2\pi} \int_v \frac{\partial U_q(r_0+r)}{\partial x_m} \frac{\partial u_m(r_0+r)}{\partial x_q} \frac{\partial u_i(r_0)}{\partial x_j} \frac{dV}{r} \\ & = \frac{\partial U_q}{\partial x_m} \frac{1}{2\pi} \int_v \frac{\partial u_m(r_0+r)}{\partial x_q} \frac{\partial u_i(r_0)}{\partial x_j} \frac{dV}{r} \\ & + \frac{\partial^2 U_q}{\partial x_m \partial x_n} \frac{1}{2\pi} \int_v \xi_m \frac{\partial u_m(r_0+r)}{\partial x_q} \frac{\partial u_i(r_0)}{\partial x_j} \frac{dV}{r} \\ & + \frac{\partial^3 U_q}{\partial x_m \partial x_n \partial x_p} \cdot \frac{1}{2\pi} \int_v \xi_m \xi_n \cdot \frac{1}{2!} \frac{\partial u_m(r_0+r)}{\partial x_q} \frac{\partial u_i(r_0)}{\partial x_j} \frac{dV}{r} + \dots \end{aligned} \quad (4.28)$$

which shows, by comparing co-efficients, that

$$a_{ij}^{mi} = -\frac{1}{2\pi} \int_v \frac{\partial^2 R_{mi}}{\partial \xi_r \partial \xi_j} \frac{dV}{r} \quad (4.29)$$

$${}_n b_{ij}^{mi} = -\frac{1}{2\pi} \int_v \xi_n \frac{\partial^2 R_{mi}}{\partial \xi_r \partial \xi_j} \frac{dV}{r} \quad (4.30)$$

$${}_{np} c_{ij}^{mi} = -\frac{1}{4\pi} \int_v \xi_n \xi_p \frac{\partial^2 R_{mi}}{\partial \xi_r \partial \xi_j} \frac{dV}{r} \quad (4.31)$$

Rotta showed that by considerations of continuity and symmetry (1951, Appendix), the following conditions must be satisfied:

$$a_{ij}^{mi} = a_{ij}^{in} = a_{jr}^{im} \quad (4.32)$$

$$a_{ri}^{mi} = 0 \quad (4.33)$$

In addition, we have the following consequence of Green's Theorem:

$$a_{jj}^{mi} = -\frac{1}{2\pi} \int_v \nabla^2 R_{mi}(r) \frac{dV}{r} = 2R_{mi}(0) = 2\overline{u_i u_m} \quad (4.34)$$

Rotta [1951] assumed values for the a_{ij}^{mi} derived from isotropic turbulence data. The observation that some of the a_{ij}^{mi} were linear combinations of the Reynolds stresses led Hanjalić and Launder [1972] to deduce a model based on the assumption that the a_{ij}^{mi} could *all* be modelled as linear combinations of the Reynolds stresses. Launder [1971] proposed a more rigorous version of the earlier model, the basis of which is as follows.

The most general such tensor capable of satisfying is

$$\begin{aligned}
 a_{ij}^{ml} = & \alpha_1 \delta_{ij} \overline{u_m u_l} + \alpha_2 \delta_{il} \overline{u_m u_j} + \alpha_3 \delta_{im} \overline{u_l u_j} \\
 & + \alpha_4 \delta_{jl} \overline{u_m u_i} + \alpha_5 \delta_{jm} \overline{u_l u_i} + \alpha_6 \delta_{im} \overline{u_l u_j} \\
 & + \alpha_7 \delta_{ij} \delta_{ml} \overline{u_k u_k} + \alpha_8 \delta_{il} \delta_{mj} \overline{u_k u_k} + \alpha_9 \delta_{im} \delta_{jl} \overline{u_k u_k}
 \end{aligned} \tag{4.35}$$

In Appendix B we solve the system of equations (4.32)–(4.34) for the coefficients α_n in terms of α_6 . This gives the model in precisely the form in which Launder originally proposed it:

$$\begin{aligned}
 a_{ij}^{ml} = & \alpha \delta_{ij} \overline{u_m u_l} + \beta (\delta_{ml} \overline{u_i u_j} + \delta_{mj} \overline{u_l u_i} + \delta_{il} \overline{u_m u_j} + \delta_{ij} \overline{u_m u_l}) \\
 & + c_{\phi 2} \delta_{ml} \overline{u_i u_j} + [\eta \delta_{ml} \delta_{ij} + \nu (\delta_{ml} \delta_{ij} + \delta_{mj} \delta_{il})] k
 \end{aligned} \tag{4.36}$$

where

$$\begin{aligned}
 \alpha_1 & \equiv \alpha = (4c_{\phi 2} + 10)/11 \\
 \alpha_2 = \alpha_3 = \alpha_4 = \alpha_5 & \equiv \beta = (-2 - 3c_{\phi 2})/11 \\
 2\alpha_7 & \equiv \eta = (-50c_{\phi 2} - 4)/55 \\
 2\alpha_8 = 2\alpha_9 & \equiv \nu = (20c_{\phi 2} + 6)/55 \\
 \alpha_6 & \equiv c_{\phi 2}
 \end{aligned} \tag{4.37}$$

If we define

$$\begin{aligned}
 P_{ij} & \equiv - \{ \delta_{ij} \overline{u_m u_l} + \delta_{il} \overline{u_m u_j} \} \frac{\partial U_l}{\partial x_m} \\
 & = - \{ \overline{u_m u_l} \frac{\partial U_j}{\partial x_m} + \overline{u_m u_j} \frac{\partial U_l}{\partial x_m} \} \\
 D_{ij} & \equiv - \{ \overline{u_l u_m} \frac{\partial U_m}{\partial x_j} + \overline{u_j u_m} \frac{\partial U_m}{\partial x_l} \} \\
 P & \equiv - \overline{u_m u_l} \frac{\partial U_l}{\partial x_m} = \text{rate of production of} \\
 & \quad \text{turbulent kinetic energy}
 \end{aligned} \tag{4.38}$$

By comparing coefficients, it is easily seen that

$$\begin{aligned}
 \Pi_{ij,2} &\equiv \frac{\partial U_k}{\partial x_m} \{a_{kj}^{mi} + a_{ki}^{mj}\} \\
 &= -\frac{(c_{\phi 2} + 8)}{11} \{P_{ij} - \frac{2}{3} \delta_{ij} P\} \\
 &\quad - \frac{(8c_{\phi 2} - 2)}{11} \{D_{ij} - \frac{2}{3} \delta_{ij} P\} \\
 &\quad - \frac{(30c_{\phi 2} - 2)}{11} k \left\{ \frac{\partial U_i}{\partial x_j} + \frac{\partial U_j}{\partial x_i} \right\}
 \end{aligned} \tag{4.39}$$

This is in fact the form of the model proposed by Naot, Shavit and Wolfshtein [1972]: their proposal and that of Launder [1971] are thus wholly equivalent. (This was shown by Launder [1973].) Their " ϕ " and Launder's " $c_{\phi 2}$ " are related simply by:

$$105 c_{\phi 2} + 4 - 88 \phi = 0$$

Naot, Shavit & Wolfshtein included only the P_{ij} term in an earlier proposal. This model, as we shall show in Chapter 6, is quite powerful in its own right.

The determination of $c_{\phi 2}$

The form (4.39) is much easier to manipulate than the rather clumsier expression (4.36), though, of course, (4.39) is merely an algebraic rewriting of (4.36).

It remains for us to determine the value of the sole parameter $c_{\phi 2}$ in (4.39). To do so, we return to equation (4.1) and consider the ratios of $\overline{u_1^2} : \overline{u_2^2} : \overline{u_3^2}$ generated by a nearly-homogeneous shear flow, such as that reported by Champagne, Harris and Corrsin [1970].

Before proceeding, we draw up a table of values of the various components of the modelled term (4.39) for a two-dimensional boundary-layer. Table 4.1 illustrates another, aesthetically pleasing, aspect

of the model when written in the form (4.39), viz. that each of the components of the "redistribution" term is itself redistributive, i.e. has zero trace.

Using Table 4.1, we see that if production and dissipation are in balance, i.e. $-\overline{u_1 u_2} \partial U_1 / \partial x_2 = \epsilon$,

(i) for $\overline{u_1^2}$:

$$\frac{\overline{u_1^2}}{k} - \frac{2}{3} = \frac{8 + 12 c_{\phi 2}}{33 c_{\phi 1}} \quad (4.40)$$

(ii) for $\overline{u_2^2}$:

$$\frac{\overline{u_2^2}}{k} - \frac{2}{3} = \frac{2 - 30 c_{\phi 2}}{33 c_{\phi 1}} \quad (4.41)$$

whence

$$\frac{\overline{u_3^2}}{k} - \frac{2}{3} = \frac{-10 + 18 c_{\phi 2}}{33 c_{\phi 1}} \quad (4.42)$$

Now the data of Champagne, Harris and Corrsin [1970] suggest that the values of the normal stresses are such that

$$\frac{\overline{u_1^2}}{k} - \frac{2}{3} = 0.28$$

$$\frac{\overline{u_2^2}}{k} - \frac{2}{3} = -0.21$$

$$\frac{\overline{u_3^2}}{k} - \frac{2}{3} = -0.07$$

With these values, the equations (4.40) – (4.42) form a pair of simultaneous equations in the two unknowns $c_{\phi 1}$ and $c_{\phi 2}$. There are, of course, only two independent equations as we must always have $\overline{u_i^2} = 2k$.

The solution of the pair of equations

$$8 + 12 c_{\phi 2} = 33 \times 0.28 c_{\phi 1}$$

$$2 - 30 c_{\phi 2} = 33 \times (-0.21) c_{\phi 1}$$

is easily seen to be

$$\left. \begin{array}{l} c_{\phi 2} = 0.38 \\ c_{\phi 1} = 1.36 \end{array} \right\} \quad (4.43a)$$

The pair of values that we have chosen to use:

$$c_{\phi 2} = 0.4; c_{\phi 1} = 1.5$$

is clearly not in any significant disagreement with the values (4.43). No single set of data can be regarded as absolutely conclusive in the determination of constants intended to serve over a very wide range of flows (ideally, of course, all flows), and our aim is not to predict perfectly one simple flow, but to predict well a whole set of complicated flows. Moreover it is readily seen that the pair of equations (4.40) – (4.41) is highly sensitive to small changes in the values of the normal stresses: i.e. to experimental error.

Thus, if we had chosen to interpret the Champagne, Harris & Corrsin data as yielding

$$\frac{\overline{u_1^2}}{k} - \frac{2}{3} = 0.30$$

$$\frac{\overline{u_2^2}}{k} - \frac{2}{3} = -0.18$$

$$\frac{\overline{u_3^2}}{k} - \frac{2}{3} = -0.12$$

– a perfectly tenable interpretation – we should have concluded that

$$\left. \begin{array}{l} c_{\phi 1} = 1.17 \\ c_{\phi 2} = 0.30 \end{array} \right\} \quad (4.43b)$$

Component Term	$\overline{u_1^2}$ $i=j=1$	$\overline{u_2^2}$ $i=j=2$	$\overline{u_3^2}$ $i=j=3$	$\overline{u_1 u_2}$ $i=1; j=2$
$\{P_{ij} - \frac{2}{3} \delta_{ij} P\}$	$-\frac{4}{3} \overline{u_1 u_2} \frac{\partial U_1}{\partial x_2}$	$\frac{2}{3} \overline{u_1 u_2} \frac{\partial U_1}{\partial x_2}$	$\frac{2}{3} \overline{u_1 u_2} \frac{\partial U_1}{\partial x_2}$	$-\overline{u_2^2} \frac{\partial U_1}{\partial x_2}$
$\{D_{ij} - \frac{2}{3} \delta_{ij} P\}$	$\frac{2}{3} \overline{u_1 u_2} \frac{\partial U_1}{\partial x_2}$	$-\frac{4}{3} \overline{u_1 u_2} \frac{\partial U_1}{\partial x_2}$	$\frac{2}{3} \overline{u_1 u_2} \frac{\partial U_1}{\partial x_2}$	$\overline{u_1^2} \frac{\partial U_1}{\partial x_2}$
$k \left(\frac{\partial U_i}{\partial x_j} + \frac{\partial U_j}{\partial x_i} \right)$	0	0	0	$k \frac{\partial U_1}{\partial x_2}$

Table 4-1. The components of the modelled term $\phi_{ij,2}$ for a 2-D boundary-layer.

4.2.4 The diffusion terms

The remaining terms of equation (4.1) are diffusive in effect. We write

$$\begin{aligned} -\tau_{ij} &\equiv \frac{\partial}{\partial x_k} \{ \overline{u_i u_j u_k} - \nu \frac{\partial}{\partial x_k} \overline{u_i u_j} \} + \frac{\partial}{\partial x_j} \overline{p u_i} + \frac{\partial}{\partial x_i} \overline{p u_j} \\ &= \frac{\partial}{\partial x_k} \{ \overline{u_i u_j u_k} - \nu \frac{\partial}{\partial x_k} \overline{u_i u_j} \} + \frac{\partial}{\partial x_k} (\delta_{jk} u_i + \delta_{ik} u_j) p \quad (4.44) \end{aligned}$$

Following common practice since von Kármán [1937] we assume a gradient-type model of diffusion (see §1 above). We isolate the second and third terms as respectively

- (i) the laminar diffusion of Reynolds stresses, which is negligible by comparison with the first term:

$$O(\text{first term}) = \frac{u^3}{\ell}$$

$$O(\text{second term}) = \frac{u^2}{\ell^2} \cdot \frac{u\ell}{R} = \frac{u^3}{\ell} \cdot \frac{1}{R}$$

i.e. it diminishes with R^{-1} as $R \rightarrow \infty$;

- (ii) the pressure-diffusion term: this was incorporated in equation (4.23) above.

Essentially, our aim must be to provide an acceptable simulation of the term $\overline{u_i u_j u_k}$. To be "acceptable", the model must be (i) a tensor of the right order. (ii) invariant with respect to cyclic permutations of the suffices, (iii) composed of Reynolds stresses and mean-flow quantities.

For the moment, let us relax the second of these conditions – and consider the suggestion of Daly and Harlow [1970], *viz.*

$$(A) \quad \tau_{ij} = -c_s \frac{\partial}{\partial x_k} \left\{ \frac{k}{\epsilon} \overline{u_k u_l} \frac{\partial}{\partial x_l} \overline{u_i u_j} \right\} \quad (4.45)$$

We shall neglect the operator $-c_s \partial/\partial x_k k/\epsilon$. The factor k/ϵ is introduced for dimensional reasons – it is the appropriate time-scale for the diffusive activity (see Tennekes & Lumley [1972]).

It will be noted immediately that there is a distinction in (4.45) between the suffices i and j on the one hand, and k on the other. As we intend initially to examine a two-dimensional boundary-layer, this distinction will be in order, provided that k represents the single direction in which we suppose derivatives to exist.

This model, which we shall designate “Model A”, has in fact been thoroughly tested by various workers (e.g. Rodi [1972]) and found satisfactory. For a two-dimensional boundary-layer, it gives the following matrix of diffusion (each location corresponding to the Reynolds stress in question):

$$\begin{bmatrix} \overline{u_2^2} \frac{\partial}{\partial x_2} \overline{u_1^2} & \overline{u_2^2} \frac{\partial}{\partial x_2} \overline{u_1 u_2} & 0 \\ \overline{u_2^2} \frac{\partial}{\partial x_2} \overline{u_1 u_2} & \overline{u_2^2} \frac{\partial}{\partial x_2} \overline{u_2^2} & 0 \\ 0 & 0 & \overline{u_2^2} \frac{\partial}{\partial x_2} \overline{u_3^2} \end{bmatrix}$$

Next, we consider the simplest model satisfying the criterion of invariance, having regard to the fact that Model A gives a good representation of the term. The obvious way to make such a biased model invariant is to take three similarly-biased models, and add them together. In this way we arrive at the model, which we shall call B_1 (the reason for the suffix will emerge later), first announced by Hanjalić and Launder [1972]:

$$(B_1) \quad \overline{u_k u_l} \frac{\partial}{\partial x_l} \overline{u_i u_j} + \overline{u_i u_l} \frac{\partial}{\partial x_l} \overline{u_j u_k} + \overline{u_j u_l} \frac{\partial}{\partial x_l} \overline{u_k u_i} \quad (4.46)$$

Model B_1 has 2-D matrix

$$\begin{bmatrix} \overline{u_2^2} \frac{\partial}{\partial x_2} \overline{u_1^2} + 2 \overline{u_1 u_2} \frac{\partial}{\partial x_2} \overline{u_1 u_2} & 2 \overline{u_2} \frac{\partial}{\partial x_2} \overline{u_1 u_2} + \overline{u_1 u_2} \frac{\partial}{\partial x_2} \overline{u_2^2} & 0 \\ 2 \overline{u_2} \frac{\partial}{\partial x_2} \overline{u_1 u_2} + \overline{u_1 u_2} \frac{\partial}{\partial x_2} \overline{u_2^2} & 3 \overline{u_2} \frac{\partial}{\partial x_2} \overline{u_2^2} & 0 \\ 0 & 0 & \overline{u_2^2} \frac{\partial}{\partial x_2} \overline{u_3^2} \end{bmatrix}$$

However, B_1 is by no means the only invariant model of the type we seek. By simply inverting the order of operations (multiplication and differentiation), we immediately arrive at the model which we shall call B_2 :

$$(B_2) \quad \overline{u_i u_j} \frac{\partial}{\partial x_j} \overline{u_k u_l} + \overline{u_j u_k} \frac{\partial}{\partial x_j} \overline{u_l u_i} + \overline{u_k u_i} \frac{\partial}{\partial x_i} \overline{u_j u_l} \quad (4.47)$$

which has the matrix

$$\begin{bmatrix} \overline{u_1^2} \frac{\partial}{\partial x_2} \overline{u_2^2} + 2 \overline{u_1 u_2} \frac{\partial}{\partial x_2} \overline{u_1 u_2} & 2 \overline{u_1 u_2} \frac{\partial}{\partial x_2} \overline{u_2^2} + \overline{u_2^2} \frac{\partial}{\partial x_2} \overline{u_1 u_2} & 0 \\ \overline{u_1^2} \frac{\partial}{\partial x_2} \overline{u_1 u_2} + 2 \overline{u_1 u_2} \frac{\partial}{\partial x_2} \overline{u_2^2} & 3 \overline{u_2} \frac{\partial}{\partial x_2} \overline{u_2^2} & 0 \\ 0 & 0 & \overline{u_2^2} \frac{\partial}{\partial x_2} \overline{u_3^2} \end{bmatrix}$$

Unfortunately, B_2 , through *a priori* of the same status as B_1 , leads to the intuitively unacceptable result that there is no diffusion of the normal stresses parallel to a wall in a boundary-layer along the wall. It would be aesthetically more pleasing, of course, if B_1 and B_2 led to the same results.

The next possibility is given by a further rearrangement of the relative roles of the dummy and active suffices in the model:

$$(C_1) \quad \overline{u_i u_j} \left\{ \frac{\partial}{\partial x_j} \overline{u_k u_i} + \frac{\partial}{\partial x_k} \overline{u_i u_j} + \frac{\partial}{\partial x_i} \overline{u_j u_k} \right\} \quad (4.48)$$

with matrix

$$\begin{bmatrix} k \frac{\partial \overline{u_1^2}}{\partial x_2} & 2k \frac{\partial \overline{u_1 u_2}}{\partial x_2} & 0 \\ 2k \frac{\partial \overline{u_1 u_2}}{\partial x_2} & 3k \frac{\partial \overline{u_2^2}}{\partial x_2} & 0 \\ 0 & 0 & k \frac{\partial \overline{u_3^2}}{\partial x_2} \end{bmatrix}$$

and obverse

$$(C_2) \quad \left\{ \overline{u_k u_i} \frac{\partial}{\partial x_j} + \overline{u_i u_j} \frac{\partial}{\partial x_k} + \overline{u_j u_k} \frac{\partial}{\partial x_i} \right\} \overline{u_i u_j} \quad (4.49)$$

with matrix

$$\begin{bmatrix} \overline{u_1^2} \frac{\partial k}{\partial x_2} & 2\overline{u_1 u_2} \frac{\partial k}{\partial x_2} & 0 \\ 2\overline{u_1 u_2} \frac{\partial k}{\partial x_2} & 3\overline{u_2^2} \frac{\partial k}{\partial x_2} & 0 \\ 0 & 0 & \overline{u_3^2} \frac{\partial k}{\partial x_2} \end{bmatrix}$$

Unfortunately, the second of these models, C_2 , is quite unrealistic, as it suggests that there is no diffusion of the normal stresses as such, but merely of the turbulent kinetic energy k . On the other hand, with C_1 we have reached a model due to Donaldson [1968]. It is, moreover, in fact, the model used by Hanjalić and Launder in generating their predictions. Although Hanjalić and Launder announced Model B_1 , they simulated the normal stresses by replacing $\overline{u_2^2}$ by $0.5 k$, and also rejected as negligibly small those terms (in locations (1.1), (2.1) and (1.2) of the diffusion matrix for Model B_1) which distinguish the resulting model from Model C_1 . We thus see that Model C_1 , subject to certain plausible simplifying assumptions, can be regarded as a degenerate form of Model B.

The final possibility is:

$$(D) \quad \overline{u_i u_j} \frac{\partial}{\partial x_i} \overline{u_k u_l} + \overline{u_j u_l} \frac{\partial}{\partial x_j} \overline{u_i u_k} + \overline{u_k u_l} \frac{\partial}{\partial x_l} \overline{u_i u_j} \quad (4.50)$$

with matrix

$$\begin{array}{ccc}
 \overline{u_1^2} \frac{\partial}{\partial x_2} \overline{u_1^2} + \overline{u_1 u_2} \frac{\partial}{\partial x_2} \overline{u_1 u_2} & \overline{u_1 u_2} \frac{\partial}{\partial x_2} (\overline{u_1^2} + \overline{u_2^2}) + (\overline{u_1^2} + \overline{u_2^2}) \frac{\partial}{\partial x_2} \overline{u_1 u_2} & 0 \\
 \overline{u_1 u_2} \frac{\partial}{\partial x_2} (\overline{u_1^2} + \overline{u_2^2}) + (\overline{u_1^2} + \overline{u_2^2}) \frac{\partial}{\partial x_2} \overline{u_1 u_2} & 3 \overline{u_2^2} \frac{\partial}{\partial x_2} \overline{u_2^2} + 3 \overline{u_1 u_2} \frac{\partial}{\partial x_2} \overline{u_1 u_2} & 0 \\
 0 & 0 & \overline{u_3^2} \frac{\partial}{\partial x_2} \overline{u_3^2}
 \end{array}$$

where, it will be noted, we have not made use of a suffix.. This is because, as is immediately obvious, Model D is "self-obverse". By permuting the suffices in an exactly analogous way to that used to get from B_1 to B_2 , or from C_1 to C_2 , we get from D to itself. Model D has an additional heuristic attraction, which is, however, not of itself sufficiently compelling a reason for us to abandon Models A, B_1 and C_1 . Indeed, as we shall see, Model A, for all its appearance of non-invariance, gives the best results. This is because the result of making the model invariant is inevitably to increase the effective (2,2) component of the appropriate matrix for the two-dimensional case by a factor 3. However, the measured values of $\overline{u_1 u_2 u_3}$ shown by, e.g. Hanjalić and Launder [1972], simply do not support this: the diffusion of u_2^2 is not three times as fast as that of u_1^2 . Though Model D does tend to compensate for the overlarge coefficient of the (2,2) component of the diffusion matrix by taking the value of $\overline{u_2^2}$ rather than $\overline{u_1^2}$ for the coefficient, we do not find in practice a great improvement over the results of Model B, and none whatsoever over those of Model A.

The principal objection to Model A is its apparent non-invariance. However, it is clear that not only are all the Models B_1 , B_2 , C_1 , C_2 and D possible invariant models of the diffusion, but so is any linear combination of these models.

The question of invariance

We consider the most general linear combination of the invariant models:

$$G = \alpha B_1 + \beta B_2 + \gamma C_1 + \delta C_2 + \eta D \quad (4.51)$$

We shall show that it is possible to choose values of α, \dots, η that make the invariant model to **G** (4.51) capable of simulating the numerical values of the *non*-invariant Model **A**.

If we take, e.g. $k = \overline{u_1^2} = 3\overline{u_2^2}$, $\overline{u_3^2} = 2\overline{u_2^2}$, $\overline{u_1 u_2} = \overline{u_2^2}$ we obtain the four equations:

$$\begin{aligned} 11(\alpha + \beta) + 27(\gamma + \delta) + 28\eta &= 9 \\ 9(\alpha + \beta + 27(\gamma + \delta) + 10\eta) &= 3 \\ (\alpha + \beta) + 3(\gamma + \delta) + 2\eta &= 1 \\ 3(\alpha + \beta) + 6(\gamma + \delta) + 8\eta &= 1 \end{aligned} \tag{4.53}$$

As these 4 equations have only 3 independent unknowns this is a consequence of the simplification (4.52) we solve the last three exactly:

$$\begin{aligned} (\alpha + \beta) &= -4 \\ (\gamma + \delta) &= 7/6 \\ \eta &= 3/4 \end{aligned}$$

Substituting into the first of equations (4.53) we get:

$$-44 + 27 \cdot 7/6 + 28 \cdot 3/4 = 8\frac{1}{2} \simeq 9$$

Thus to a very high degree of approximation we find that the first equation is satisfied.

We have thus shown that where (4.52) holds, the matrices and hence the models satisfy, e.g., the relation

$$\mathbf{A} \simeq -4 \mathbf{B}_1 + \frac{7}{6} \mathbf{C}_1 + \frac{3}{4} \mathbf{D} \tag{4.54}$$

We are thus justified in treating Model **A** as an apparently non-invariant combination (4.54) of invariant models. The apparent non-invariance can be attributed to the replacement of terms like $(3\overline{u_2^2} + \overline{u_3^2})$ by the corresponding fractions of k .

However, we must recall that our search is for a feasible model of turbulence: one which (in Lumley & Khajeh-Nouri's [1974] words) is 'not beyond the willingness or ability of reasonable men to pay for'. We recall that the diffusion is only a small component of the energy balance (typically 5% of the largest term in a boundary layer except for regions where the mean velocity gradient is small), and that measurements of triple correlations are relatively scarce, with consequent doubts as to the accuracy to which the *gradients* of the triple correlations are known. We feel justified in concluding that Models A – D are all of equal status.

One *caveat*, however, is that Model A cannot be generalized without care (and regard for the data) to diffusion in three dimensions. This is discussed in § 7 below.

The determination of the constant c_s

To determine the value of c_s , we first turn to Table 4-2 for guidance. We see that the value of c_s that this suggests is in the region of 0.1. Hanjalić and Launder, using Model C_1 , gave a value of 0.08: this was, however, on the basis of taking the ratio $\overline{u_2^2} : k = 0.5$, which we consider rather high. Our choice, for Model B_1 (as opposed to its degenerate form C_1) is $c_s = 0.11$. This is the result of many thousands of computer calculations, and can be regarded as thoroughly optimized in the context of two-dimensional boundary-layers.

We shall clearly need a different value of c_s for use with Model A. To see roughly what this value must be, let us consider the net effective diffusion of k :

Model A:

$$c_{sA} \overline{u_i'} \frac{\partial}{\partial x_i} (\overline{u_1'} + \overline{u_i'} + \overline{u'}) \quad (4.55)$$

Model B:

$$c_{sB} \left[\text{terms in (4.55)} + \overline{u'} \frac{\partial}{\partial x} \overline{u_1' u'} - \overline{u_i'} \frac{\partial}{\partial x_i} \overline{u'} \right] \quad (4.56)$$

x_2/D	0.2	0.4	0.6	0.8
A Values of triple correlation	-0.09	-0.21	-0.22	-0.06
B Gradient-modelled terms	-0.32	-0.9	-1.2	-0.3
$A/B = c_s$	0.4	0.23	0.18	0.20

Table 4-2. Values of the diffusion coefficient deduced from data of Hanjalić & Launder [1972].

for these net rates of diffusion to be equal, as they must be, we see that if $\overline{u_1 u_2} \simeq \overline{u_2^2} \simeq 0.4 k$

$$c_{sA} \simeq 1.8 c_{sB} \quad (4.57)$$

From Table 4-2 we see that the value of c_s must be about 0.2. We find, indeed that the best results are obtained from Model A with $c_{sA} = 1.8 \times 0.11 \simeq 0.2$.

4.2.5 Summary

The Reynolds stress model is in principle now closed. The missing details in Table 3-1 are now available:

- The term $\overline{\partial u_i / \partial x_k \cdot \partial u_j / \partial x_k}$ is now the subject of equation (4.13).
- The term $\overline{u_i u_j u_k}$ is modelled in §4.2.4.
- The term $p \overline{\partial u_i / \partial x_j}$ is modelled in §4.2.3.

However, in §5 we shall show that although the model is closed, it is not yet quite complete.

5

THE SITUATION NEAR RIGID BOUNDARIES

5.1 The Data

If we collate the available data on Reynolds stresses in flows near walls, we obtain Table 5-1. If we then collate similar information on flows uninfluenced by walls, we obtain Table 5-2.

Comparing the consensus of Table 5-1 with the results from Table 5-2 we see that $\overline{u_1^2}$ is greater near walls and $\overline{u_2^2}$ smaller, than would be the case in regions remote from walls.

5.2 Explanation of the phenomenon

We now examine the various terms in (4.1) to determine which of them is capable of causing a transfer of turbulence energy from $\overline{u_2^2}$ to $\overline{u_1^2}$ leaving $\overline{u_3^2}$ more or less unchanged.

5.2.1 *The Production Term P*

This arises only in the equation for $\overline{u_1^2}$ and is treated exactly. Any alteration, even indirect, in the rate of production of turbulent kinetic energy would in any case be felt equally by both the other components, and thus cannot be the source of a transfer from the one to the other.

	$\frac{\overline{u_1^2}}{k} - \frac{2}{3}$	$\frac{\overline{u_2^2}}{k} - \frac{2}{3}$	$\frac{\overline{u_3^2}}{k} - \frac{2}{3}$	$\frac{\overline{u_1 u_2}}{k}$
Laufer [1954]	+0.55	- 0.38	- 0.17	0.17
Klebanoff [1954]	+0.57	- 0.46	- 0.11	0.23
Comte-Bellot [1964]	+0.61	- 0.45	- 0.16	0.22
Hanjalić & Launder [1972]	+0.56	- 0.45	- 0.11	0.24
<i>Consensus</i>	+0.57	-0.45	-0.12	0.22

TABLE 5.1 Reynolds-stress distribution near walls

	$\frac{\overline{u_1^2}}{k} - \frac{2}{3}$	$\frac{\overline{u_2^2}}{k} - \frac{2}{3}$	$\frac{\overline{u_3^2}}{k} - \frac{2}{3}$	$\frac{\overline{u_1 u_2}}{k}$
Champagne, Harris & Corrsin [1970]	+0.29	- 0.18	- 0.11	0.30

TABLE 5.2 Reynolds-stress distribution in homogeneous-shear flow

5.2.2 The Dissipation term ϵ

This term is certainly capable of causing a redistribution from any $\overline{u_\alpha^2}$ to any other. In §4 we gave our reasons for supposing that the effect of ϵ was isotropic. Those grounds, based both on physical arguments and on reference to the general data, remain firm. We recall that

- (i) the small-scale motions in which the dissipation occurs are likely to be insensitive to large-scale quantities – such as distances from walls – and
- (ii) the measurements of k -spectra by, e.g. Hanjalic & Launder [1972], show not only a general isotropy at the high-frequency end of the spectrum but also (and more significantly for our present purpose) the *same* high degree of isotropy at all positions in the flow – i.e. regardless of the proximity of a wall.

Moreover

- (iii) any departure from local isotropy must tend to enhance the value of ϵ_{11} and reduce that of ϵ_{22} – the opposite of the required effect.

We therefore see no reason to depart from the isotropic model of dissipation.

5.2.3 The Diffusion

It is again necessary to recall just how small the contribution from the diffusion is to the overall energy balance. In the region near a wall, moreover, the diffusion is very small (see, e.g. Figure 6.13) – and we are looking for a term capable of producing a transfer of energy to $\overline{u_1^2}$ from $\overline{u_2^2}$ of about 30% of $\overline{u_2^2}$. It is thus quite impossible for such an effect to be caused by the diffusion. Any such effect associated with $\overline{u_2^2}$ would also be extremely difficult to divorce from the $\overline{u_3^2}$ term.

5.2.4 The Pressure-Strain Terms

Thus, having eliminated all the other terms in equation (3.12), we are left attributing the near-wall transfer of energy from $\overline{u_2^2}$ to $\overline{u_1^2}$ to the remaining (pressure-strain) term,

$$\Pi_{ij} = \phi_{ij,1} + \phi_{ij,2}.$$

Therefore workers since Harlow & Hirt [1969], and particularly since the detailed proposals of Daly & Harlow [1970], have recognized the need for a near-wall component to be incorporated into the pressure-strain term.

The earlier proposals

The suggestion of Harlow & Hirt was for a transport equation for the wall-effect tensor $P_{\alpha\beta}$. This was superseded by the proposal of Daly & Harlow, which was to replace the tensor by an explicit integral formulation of the coefficients P_{ij} in the wall-effect expression:

$$\Phi_{\text{wall}ij} \propto P_{il} \overline{u_l u_j} + P_{jl} \overline{u_l u_i} - \frac{2}{3} P_{lm} \overline{u_l u_m} \delta_{ij}$$

Shir [1972] replaced the Daly-Harlow tensor decay function P_{ij} by the scalar decay function ψ , where

$$\psi = \frac{1}{\pi \kappa^2} \int_{\Sigma} \frac{\mathcal{L}^2}{|r - r'|^4} d\Sigma$$

and

$$P_{ij} = n_i n_j \psi$$

\hat{n}_a being the unit vector normal to the wall. No explanation was offered for the particular form chosen for ψ . The results generated were satisfactory, but were presented only for the axisymmetric pipe, and for the symmetric channel.

Many workers have generated equally successful sets of predictions without the use of a wall-effect modification. Such a practice will certainly be capable of leading to success if (as in the case of the work of Hanjalic & Launder) the method used involves the solution of only one Reynolds stress. The coefficients for the shear-stress equation can — or even, as we have seen, *must* — be chosen in the light of the experimental data. The solutions generated are thus very likely to match the data used. However, the consequent lack of generality of such a procedure is bound to reveal itself

in an inability to predict certain flows. In the work of Hanjalic & Launder, this arose in the case of the plane wall jet, for which the predictions of shear stress were too high.

It is perfectly possible to generate a successful Reynolds-stress model without introducing a separate near-wall term, but rather taking the presence of a wall into account when choosing the values of the constants c_{ϕ_1} and c_{ϕ_2} . This is the approach adopted by, e.g., Naot, Shavit & Wolfshtein. It is possible to adapt a model to cope with near-wall conditions, or with flows remote from walls. To enable a model to deal with both situations involves compromises which will detract from its accuracy.

Our aim in the present chapter is to generate a model which is not merely satisfactory in the context of two-dimensional flow, but which is also capable of straightforward generalisation to three dimensions.

The present proposals

Let us assume that the additional energy transfer can be written in the form of an *additional* pressure-strain term $\phi_{ij, w}$. Clearly $\phi_{ij, w}$ will have to satisfy the following criteria:

- (i) it must diminish with increasing distance from a wall
- (ii) it must conform to the analysis of §4.2.3.

The second criterion suggests that we should, in fact, set

$$\phi_{ij, w} = \phi_{ij, 1, w} + \phi_{ij, 2, w} + \phi_{ij, 3, w}$$

where $\phi_{ij, 1, w}$ behaves like $\phi_{ij, 1}$, $\phi_{ij, 2, w}$ like $\phi_{ij, 2}$, and $\phi_{ij, 3, w}$ contains any terms in $\phi_{ij, w}$ which are not of the same form as $\phi_{ij, 1}$ or $\phi_{ij, 2}$. It will be simplest for us to consider the terms in reverse order.

(i) *The term* $\phi_{ij,3,w}$

$\phi_{ij,3,w}$ can arise only from such terms as we have chosen to neglect from $\phi_{ij,1}$ and $\phi_{ij,2}$. Returning to the analysis of §4.2.3 (equations (4.26)–(4.27)), we see that this implies that

$$\phi_{ij,3,w} = p b_{mj}^{qj} \frac{\partial^2 U_m}{\partial x_q \partial x_p} + p q c_{mi}^{qj} \frac{\partial^3 U_m}{\partial x_q \partial x_p \partial x_q} + \dots$$

as these are the only terms we neglected.

The term in $\partial^2 U / \partial x_m \partial x_p$ vanishes identically for homogeneous turbulence and will therefore be small in general; the term in $\partial^3 U / \partial x_m \partial x_p \partial x_q$ will generally be present. In a wall boundary layer, the rapid spatial changes of velocity imply very large values of $\partial^3 U / \partial x_m \partial x_n \partial x_p$.

We recall that in the (near-wall) region in question the ‘log-law’ holds

$$\begin{aligned} U &= \frac{U_\tau}{k} \ln \frac{y U_\tau}{\nu} + C \\ \frac{\partial U}{\partial y} &\propto \frac{1}{y} \\ \frac{\partial^2 U}{\partial y^2} &\propto \frac{1}{y^2} \\ \frac{\partial^3 U}{\partial y^3} &\propto \frac{1}{y^3} \end{aligned} \tag{5.1}$$

In other words, the second and third derivatives of mean velocity fall off at least as fast as y^{-2} . The principal contribution would have to come from the third derivative, i.e. a quantity falling off as y^{-3} . This leads to a model of the following type:

$$\phi_{ij,3,w} = p q c_{mj}^{qj} \frac{\partial^3 U_m}{\partial x_q \partial x_p \partial x_q} \cdot \varrho^2 \tag{5.2}$$

* We have adopted the boundary-layer convention of writing the sole mean velocity as U , i.e. without a subscript, and the normal distance from a wall as y .

where the term ℓ^2 is introduced to preserve the dimensions of (5.2) as u^3/ℓ , presuming the ${}_{pq}c_{mj}^{ii}$ to be linear functions of the $u_i u_j$.

However, the effect that we are trying to model falls off at most as y^{-1} . This can be seen from the work of Hanjalic & Launder (e.g. Figure 6.9), or from that of Klebanoff (Figure 6.24), from which it is clear that the wall-effect is noticeable at normal distances which would be incompatible with a decay faster than $\sim y^{-1}$.

An appropriate length-scale to use for ℓ would be

$$L_\epsilon = \frac{k^{3/2}}{\epsilon}$$

which is known to be proportional, in a two-dimensional boundary layer, to the normal distance from the wall. This gives us a choice of normalising factors, of which the most obvious ones are L_ϵ/y and $\partial L_\epsilon/\partial y$. The choice of L_ϵ/y is dictated by the following considerations.

If there are two walls, as in a channel flow, with respective subscripts A and B, the use of $\partial L_\epsilon/\partial y$ leads to:

$$\begin{aligned} \phi_{ij,3,3A} &= c_{\ell j}^{mi} \frac{U_{\tau A}}{\kappa y_A} \left(\frac{\partial L_\epsilon}{\partial y} \right)^2 & * \\ \phi_{ij,3,3B} &= c_{\ell j}^{mi} \frac{U_{\tau B}}{\kappa y_B} \left(\frac{\partial L_\epsilon}{\partial y} \right)^2 \end{aligned} \quad (5.3)$$

If we now examine an *asymmetric* channel flow -- that of Hanjalic & Launder [1972] -- we see that for the two length-scales to match at the meeting-point of the two boundary layers, about 70% of the channel width from the rough side, the values of $\partial L_\epsilon/\partial y$ on the smooth-wall side must rise to very high levels. Figure 6.18 shows how this arises. $\partial L_\epsilon/\partial y$ is therefore not a satisfactory normalizing factor.

We thus have, in a two-dimensional boundary layer

$$\phi_{ij,3,w} = c_{\ell j}^{mi} \frac{U_\tau}{\kappa y} \left(\frac{L_\epsilon}{y} \right)^2 \quad (5.4)$$

* We have dropped the ${}_{22}$ prefix from the c 's, as an extension of the boundary-layer convention, for ease of reading. They remain, of course, sixth-order tensors.

The model leads to a simple additive term (5.4) in which the c_{mj}^{xi} are subject to the same constraints as the b_{mj}^{xi} used in $\phi_{ij,2,w}$ (derived below) and are hence equal to them.

(ii) *The term $\phi_{ij,2,w}$*

This term is assumed to be composed in exactly the same way as $\phi_{ij,2}$ itself. It must therefore satisfy the same invariance criteria; hence, if we let

$$\phi_{ij,2,w} = b_{\rho j}^{mi} \frac{\partial U_{\rho}}{\partial x_m}$$

we have:

$$b_{\rho j}^{mi} = b_{\rho j}^{im} = b_{j\rho}^{im} \quad (5.5)^*$$

$$b_{\rho i}^{mi} = 0 \quad (5.6)$$

as before, if we assume again that the $b_{\rho j}^{mi}$ are linear combinations of the $\overline{u_i u_j}$, we see that

$$b_{\rho j}^{mi} = \alpha' \delta_{\rho j} \overline{u_m u_i} + \dots \quad (5.7)$$

(cf. (4.31): (5.7) is the same equation with primes on the coefficients, with b replacing a).

We have three equations (5.5) and (5.6) in five unknowns α', \dots, ν' (5.6) gives:

$$\begin{aligned} b_{\rho i}^{mi} &= \alpha' \overline{u_m u_{\rho}} + \beta' (2\delta_{m\rho} k + 5 \overline{u_m u_{\rho}}) \\ &+ \nu' (4\delta_{m\rho} k) + \eta' \delta_{m\rho} k + c_{\phi 2} \overline{u_{\rho} u_m} = 0 \end{aligned}$$

so

$$\alpha' + 5\beta' + c_{\phi 2}' = 0 \quad (5.8a)$$

$$2\beta' + 4\nu' + \eta' = 0 \quad (5.8b)$$

* These $b_{\rho j}^{mi}$ are not, of course, the $b_{\rho j}^{mi}$ of equation (4.27). The notation $a_{\rho j}^{mi}$ would be too cumbersome.

In particular

$$\begin{aligned}c_{11}^{21} &= \alpha' \overline{u_1 u_2} + 2\beta' \overline{u_1 u_2} \\c_{12}^{22} &= 4\beta' \overline{u_1 u_2} + 2c_{\phi 2}' \overline{u_1 u_2} \\c_{13}^{23} &= 2\beta' \overline{u_1 u_2}\end{aligned}$$

If, as seems clear from Tables 5-1 and 5-2, there is almost no extra redistribution to or from $\overline{u_3^2}$ as a result of the proximity of a wall,

$$\begin{aligned}b_{13}^{23} &= 2\beta' \overline{u_1 u_2} = 0 \\b_{12}^{22} &= 2c_{\phi 2}' \overline{u_1 u_2} \\b_{11}^{21} &= \alpha' \overline{u_1 u_2}\end{aligned}$$

Applying (5.8a), $b_{12}^{22} + b_{12}^{21} = 0$, whence

$$\left. \begin{aligned}b_{12}^{22} &= -\alpha' \overline{u_1 u_2} \\b_{12}^{21} &= \alpha' \overline{u_1 u_2}\end{aligned} \right\} \quad (5.9)$$

Eqn (5.9) is a simple model of the additional redistribution of the normal stresses. It further implies that, by (5.8b)

$$4\nu' + \eta' = 0$$

We now deduce the redistributive effect on the shear stress:

$$\begin{aligned}b_{12}^{21} + b_{11}^{22} &= \alpha' \overline{u_2^2} + \beta' (\overline{u_1^2} + \overline{u_2^2}) + (\eta' + \nu')k + c_2' \overline{u_1^2} \\&= \alpha' (\overline{u_2^2} - \overline{u_1^2}) + (\eta' + \nu')k \\&= \alpha' (\overline{u_2^2} - \overline{u_1^2}) + \xi' k\end{aligned} \quad (5.10)$$

($\xi' \equiv \eta' + \nu'$)

The values of α' and ξ'

α' can be determined by the measured level of additional redistribution indicated by the data in Table 5-1. Clearly, in order that the value of the redistribution should fall off as the wall recedes, α' must not be simply an additional constant, but must be suitably damped. We

find that

$$\alpha'_{\max} = 0.06 \quad (5.11)$$

and that the non-dimensional factor

$$\frac{L}{x_2} \quad (5.12)$$

appears to provide the correct form of the decay for a single wall. If there are two walls, we assume the effects to be additive, so that the factor (5.12) should be revised to read

$$\left(\frac{L}{x_2} + \frac{L}{D-x_2} \right) \quad (\text{where } D \text{ is the channel width}) \quad (5.13)$$

Consideration of the shape of (5.13) shows that it does not allow much decay in a channel but permits an effect to be felt in each boundary layer from the *remote* wall. We shall see (§6) that this accounts for certain hitherto unexplained effects.

The value of ξ'

From equation (5.10) we see that the net extra generation of $\overline{u_1 u_2}$ in a two-dimensional boundary layer by pressure-strain interaction near a wall is

$$\begin{aligned} \alpha' (\overline{u_1^2} - \overline{u_2^2}) + \xi' k &= +.06 (\overline{u_1^2} - \overline{u_2^2}) + \xi' k \\ &\simeq (\xi' + .06) k \end{aligned}$$

which, from Tables 5-1 and 5-2 is equal to roughly $0.09 k$, so that

$$\xi' \simeq .03$$

This is a maximum value, so that we are justified in neglecting the term altogether. Indeed, if we deduce a value from the Hanjalic & Launder [1972] data,

$$\xi' \simeq -0.01$$

The models derived for $\phi_{ij, 2, w}$ and $\phi_{ij, 3, w}$ differ only in the following respects:

(i) in a 2-D boundary layer,

$$\phi_{ij, 2, w} = b_{1j}^{2i} \frac{\partial U}{\partial x_2} \cdot \left(\frac{L_\epsilon}{x_2} \right)$$

$$\phi_{ij, 3, w} = c_{1j}^{2i} \frac{\partial U}{\partial x_2} \left(\frac{L_\epsilon}{x_2} \right)^2$$

L_ϵ/x_2 is nearly constant in regions where $\partial U/\partial x_2$ is large, so that the decision as to whether to include both terms is not crucial.

(ii) Any term $\phi_{ij, 2, w}$ can arise only from the distortion of the turbulence caused by the pressure of a wall. Since the terms $\phi_{ij, 1}$ and $\phi_{ij, 2}$ were associated with eddies of similar large size, the need for a term $\phi_{ij, 2}$ implies that a non-zero $\phi_{ij, 1}$ will be found; this argument does not follow from the assumption of a *separate* wall term $\phi_{ij, 3}$.

The term $\phi_{ij, 1, w}$

The available data suggest that the effect of a wall is felt in regions where the mean strain rate is small: this is further evidence that the term $\phi_{ij, 1}$ must also be regarded as subject to the addition of a wall-correction term

$$\phi_{ij, 1, w} = c_{\phi 1} \frac{\epsilon}{k} \left(\overline{u_i u_j} - \frac{2}{3} \delta_{ij} k \right) f \left(\frac{\rho}{x_2} \right) \quad (5.14)$$

The whole term (neglecting $\phi_{ij, 3, w}$) reads as follows:

$$\Pi_{ij, w} = \left\{ c_{\phi 1} \frac{\epsilon}{k} \left(\overline{u_i u_j} - \frac{2}{3} \delta_{ij} k \right) + \frac{\partial U_\rho}{\partial x_m} (b_{2i}^{mi} + b_{2i}^{mj}) \right\} f \left(\frac{\rho}{x_2} \right) \quad (5.15)$$

where, so far, we have assumed that $f(\ell/x_2)$ was simply proportional to ℓ/x_2 . We assume, moreover, that the same decay law applies to $\phi_{ij,1,w}$ as to $\phi_{ij,2,w}$. These assumptions are largely borne out by computations (see §6).

The value of c_{ϕ_1}'

If we take the equations (3.12) and neglect the transport terms, as we may, e.g., in the equilibrium layer of a fully-developed 2D flow, we are left with

$$0 = (c_{\phi_1} - c_{\phi_1}') \left(\overline{u_1^2} - \frac{2}{3}k \right) \frac{\epsilon}{k} - \left(\frac{8 + 12c_{\phi_2}}{33} + 2c_{\phi_2}' \right) \epsilon$$

$$0 = (c_{\phi_1} - c_{\phi_1}') \left(\overline{u_2^2} - \frac{2}{3}k \right) \frac{\epsilon}{k} - \left(\frac{2 - 30c_{\phi_2}}{33} - 2c_{\phi_2}' \right) \epsilon$$

$$0 = (c_{\phi_1} - c_{\phi_1}') \left(\overline{u_3^2} - \frac{2}{3}k \right) \frac{\epsilon}{k} - \left(\frac{-10 + 18c_{\phi_2}}{33} \right) \epsilon$$

Setting $c_{\phi_1} = 1.5$, $c_{\phi_2} = 0.4$ (cf. §4.2.3 above) and $c_{\phi_2}' = 0.06$, we see that

$$\overline{u_1^2} - \frac{2}{3}k = \frac{0.51}{1.5 - c_{\phi_1}'}$$

$$\overline{u_2^2} - \frac{2}{3}k = \frac{-0.18}{1.5 - c_{\phi_1}'}$$

$$\overline{u_3^2} - \frac{2}{3}k = \frac{-0.09}{1.5 - c_{\phi_1}'}$$

giving the values in Table 5-1 if

$$1.5 - c_{\phi_1}' = 1.0$$

i.e.

$$c_{\phi_1}' = 0.5$$

An alternative approach

Irwin [1974] assumed approximate local homogeneity and isotropy to deduce expressions for the pressure-strain term in the Reynolds-stress equations. This is an approach of potential generality, but Irwin was obliged to acknowledge that the wall effect was subject to a decay that did not follow directly from the analysis. Just as in the present work, Irwin used the empirical data to determine a decay factor, and also came to the conclusion that the most suitable form was a decay $\sim L_e/x_2$.

By rewriting (4.21) in the form

$$\begin{aligned} \overline{\frac{p}{\rho} \frac{\partial u_i}{\partial x_j}} = & \frac{1}{4\pi} \int_{\text{Vol.}} \left\{ \overline{\left(\frac{\partial^2 (u_q u_m)}{\partial x_q \partial x_m} \right)'} \left(\frac{\partial u_i}{\partial x_j} \right)} + \right. \\ & \left. + 2 \left(\frac{\partial U_1}{\partial x_2} \right)' \left(\frac{\partial u_2}{\partial x_1} \right)' \frac{\partial u_i}{\partial x_j} \right\} \\ & \times \left\{ \frac{1}{|y-x|} + \frac{1}{|y^*-x|} \right\} d(\text{Vol.}) \end{aligned}$$

Irwin is able to deduce the effect of a wall on the stress distribution.

Irwin's work:

- confirms the need for a 'near-wall' correction to the pressure-strain term;
- confirms that a decay $\sim L_e/y$ is consistent with the required behaviour of such a term;
- suggests that the 'near-wall' modification should affect not merely merely the 'second' part (Launder, Wolfshtein) of the pressure-strain model but should in fact (contrary to Irwin's own view) be extended to embrace the 'first' (Rotta) part of the term.

6

PREDICTION OF TWO-DIMENSIONAL FLOWS

6.1 Introduction

The models derived in Chapters 4 and 5 have been applied to a number of two-dimensional flows. The most exacting test is that provided by the asymmetric plane channel studied by Hanjalic & Launder [1972]. Other flows to which the models have been applied, and for which the resulting predictions are presented here are:

- (i) the symmetric plane channel*
- (ii) the flow on a flat plate*
- (iii) the plane wall-jet in stagnant surroundings.*

The models are categorized in Table 6.1. For brevity, the labels attached to the models in the Table will be used to describe them: thus Model 2 denotes the closure effected by using the Wolfshtein et al. model of the pressure-strain terms, together with the Daly-Harlow model of diffusion. In every case, the near-wall correction derived in Chapter 5 has been applied in addition to the pressure-strain model, as it would not be possible otherwise to evaluate the performance of the various models objectively.

The flows will be examined in the order in which they are listed above.

Pressure-Strain

<i>1.</i>	<i>2.</i>
Launder's model, as given by Eq. 4.39	The model of Wolfshtein et al.; also given by Eq. 4.39 but omitting the term D_{ij}
Near-wall correction terms derived in Chapter 5	

Diffusion

<i>A</i>	<i>B</i>
The invariant model due to Hanjalic & Launder [1972]	The model due to Daly & Harlow

TABLE 6-1 The models used to effect closure

6.2 The Asymmetric Plane Channel Flow of Hanjalić & Launder

The asymmetric plane channel flow of Hanjalić & Launder [1972] was produced by attaching square ribs to one wall, at a pitch-height ratio of 10:1, the height being 1/17 of the distance between the walls. The effect of this roughening is to cause a shear-stress ratio of 5:1 as between the rough and smooth walls, and a consequent displacement of both the position of zero shear-stress and the position of maximum velocity. As noted in Section 3.2 above, any eddy-viscosity type of model of turbulence must necessarily imply that the positions of maximum velocity and of zero shear-stress must coincide. However, the measurements of Hanjalić and Launder show quite clearly that the two points do not coincide.

The boundary conditions applied to the various equations are listed in Table 6.2. The constants used are shown in Table 6.3. Figures 6.1–6.4 show the mean-velocity profiles given by Models 1A, 1B, 2A and 2B. Figures 6.5–6.8 show the shear-stress distributions; Figures 6.9–6.12 give the normal-stress profiles, and Figures 6.13–6.16 the predicted energy-balances. Figures 6.17–6.19 show the length-scale profile and the behaviour of the positions of zero shear stress and maximum velocity against increasing Reynolds' number.

The first conclusion to be drawn from the profiles is that they provide little support for the invariant Hanjalić-Launder model (A) of diffusion. Certainly in no case does this model perform better than the Daly-Harlow model (B). Specifically, it is clear that model A implies too high a level of diffusion of $\overline{u_2^2}$; any attempt to reduce the diffusion coefficient to compensate for this results in too low an overall diffusion of turbulent kinetic energy.

The pressure-strain models are also clearly distinguished by the fact that the predictions of mean-velocity profiles using model 2 are not so satisfactory as those of model 1. The excessive 'fullness' of the profiles generated by model 2 means also that the ratio of maximum mean velocity to bulk mean velocity is too low (actually by about 3%). The ratio predicted by model 1 is correct to within 1%.

<i>Equation</i>	<i>Wall</i>	<i>Free Stream</i>
U	$U/U_\tau = (1/\kappa)\ln(x_2 U_\tau/\nu) + 5.4$ SMOOTH $U/U_\tau = (1/\kappa)\ln(x_2/e) + 3.5$ ROUGH where e is the height of the roughness elements	U_G
$\overline{u_1 u_2}$	$-U_\tau^2$	0
$\overline{u_1^2}$	$5.1 U_\tau^2$	0
$\overline{u_2^2}$	U_τ^2	0
$\overline{u_3^2}$	$2.3 U_\tau^2$	0
ϵ	$U_\tau^3 / \kappa x_2$	0

TABLE 6-2 The boundary conditions applied

6.3 The Symmetric Channel [Comte-Bellot, 1965]

The predictions of models 1 and 2 for the fully-developed symmetric channel are broadly in line with those for the asymmetric channel. It will be noted from Figure 6.21 that the distribution of Reynolds stresses in this flow would appear from the data to be somewhat different from that which obtains in either the asymmetric channel flow already examined or, as we shall see, in the near-wall region of the flat-plate boundary layer. As there is no known mechanism for the establishment of such a distinction, we are forced to conclude that the discrepancies among the near-wall distributions of Reynolds normal stresses must be attributable to errors of measurement. The predictions, naturally, do not take account of the idiosyncracies of individual sets of data: this is the most probable explanation of the apparently poor predictions shown in Figure 6.21.

The predictions of mean velocity are consistent with those generated for the asymmetric channel, and offer the same measure of accord with the data. The normalized shear-stress profile is of course of no interest to us here, as the zero-point is constrained by the boundary-conditions to lie at the centre of the channel. All the predictions shown were obtained by using Model B of the diffusion; we have already seen that in a flow which could be expected to display any benefits of a precise model of diffusion none were to be discerned.

6.4 The Boundary-layer on a Flat Plate

The third two-dimensional flow to be considered is the high-Reynolds'-number flow along a flat plate. This flow was first considered in detail by Klebanoff [1954], and it is with Klebanoff's data that we present comparisons of our predictions. This set of data lies close to the mean of Table 5.1, and it is therefore one which we should hope to predict with accuracy. Figures 6.22–6.26 bear this out. Indeed, it is possible to draw from these predictions the conclusion that the particular model of the near-wall redistribution is satisfactory, and further that the linear decay assumed (in the single-wall case)

provides the correct rate of falling-off as we leave the wall. One especially pleasing aspect of the predictions is that we faithfully reproduce the point of inflection in the $\overline{u_1^2}$ curve. The predictions of dissipation length-scale also reinforce the overall impression, displaying as they do the correct falling-off at the free-stream edge of the flow.

6.5 The Plane Wall Jet

The final two-dimensional flow examined is the plane wall-jet in stagnant surroundings for which measurements were obtained by Mathieu and Tailland in 1967. Although the sole difference between this flow and the flat-plate boundary-layer lies in the zero-free-stream velocity, this difference leads to considerable computational complications related to the existence of two regions of high velocity-gradients and to the need to solve the mean-momentum equation accurately also in the outer region of low velocity and low velocity-gradients.

The predictions of mean velocity and of turbulent shear-stress are satisfactory (Figures 6.27–6.28).

6.6 Conclusions

Viewed overall, the predictions in Figures 6.1–6.28 of two-dimensional flows provide confirmation of the satisfactoriness of the model of turbulence developed in Chapters 4 & 5 above. In each case, the correct falling-off of the additional redistribution induced by the presence of a wall confirms the suitability of the model developed in Chapter 5.

We see that Model 1 of the pressure-strain terms in the Reynolds stress equations consistently produces better results than the truncated version which we have called Model 2. The diffusion models A and B are not quite so clearly distinguished, but on the evidence of the predictions obtained we can deduce that there is no evidence that the more complicated, albeit *obviously* invariant, Model A is superior in any case. Therefore we apply Occam's razor and choose the simpler Model B for further work.

Symbol	Equation of first mention	Value	Significance	How determined
c_{ϕ_1}	4.24	1.5	coefficient of 'Rotta' term in pressure-strain correlation	normal stress levels in nearly-homogeneous shear flow
c_{ϕ_2}	4.32	0.4	parameter governing 'second' part of pressure-strain term	normal stress levels in nearly-homogeneous shear flow
$c_{\phi'_1}$	5.14	0.5	near-wall correction term to 'Rotta' pressure-strain term	normal stress levels near walls
α'	5.7	0.06	near-wall correction term to 'second' part of pressure-strain term	normal stress levels near walls
ξ'	5.10	0.00	redistribution of shear stress by 'second' part of pressure-strain term	normal stress levels near walls
c_{ϵ_1}	4.13	1.44	generation of dissipation	normal stress levels near walls
c_{ϵ_2}	4.13	1.91	viscous destruction of dissipation	decay of turbulence behind a grid
c_{ϵ_3}	4.13	0.15	coefficient of diffusive transport of dissipation	computer optimisation
c_s	4.45	Model A: 0.11 Model B: 0.20	coefficient of diffusion of Reynolds stresses	computer optimisation

TABLE 6-3 The value and significance of the constants, and the basis for their choice

The shear-stress profiles give further support to model 1 against model 2; the predictions of model 1B are indistinguishable from the data of Hanjalić & Launder, while those of model 2 are not satisfactory, showing an excessive displacement of the position of zero shear stress with respect to that of maximum velocity.

The validity of the form of the near-wall correction is borne out by the normal stress levels, particularly in the region $0.2 < x_2 < 0.6$, measured from the rough wall. The choice of decay factor

$$f(x_2) \equiv \mathcal{L} (x_2^{-1} + (D - x_2)^{-1})$$

is justified by the fact that we are able to predict correctly the slight inflexion in the u_1^2 curve at about 0.4 of the distance across the channel. This inflexion is also present in the data for the symmetric channel, and occurs most pronouncedly in the flat-plate boundary-layer (*vide infra*).

The values of the constants chosen, and given in Table 6.3, were confirmed by systematic and detailed exploration of the effect of allowing them to vary within the bounds indicated by the experimental data.

Conclusions

1. There appears to be no reason to prefer model A to model B for the diffusion.
2. The evidence for the models 1 and 2 of the pressure-strain terms appears to favour model 1.
3. The form of the near-wall correction chosen appears to be vindicated.

7

THREE-DIMENSIONAL BOUNDARY-LAYER FLOWS

7.1 Introduction

In the real world, most flows are not only turbulent but also three-dimensional. So far we have considered exclusively those flows for which one of the dimensions is degenerate as a consequence of the effective absence 'at infinity' of some of the containing boundaries.

Many flows of practical interest are fully three-dimensional, but may yet be regarded as boundary layers, for they have a single predominant direction of flow. This is the case for, e.g., all uniform pipes, whatever their cross-sectional shape,* provided only that the curvature of the pipe is negligible. Under certain assumptions we shall be able to deduce a three-dimensional boundary-layer form of the governing equations. We shall solve these equations for the case of flows in rectangular ducts.

Secondary Flows

Turbulent flows in three dimensions exhibit one feature of particular interest to us which is absent from flows in two dimensions and from laminar flows. This feature is the phenomenon of non-negligible *secondary* mean flows locally normal to the principal direction of mean flow. These flows are typically two orders of magnitude smaller than the principal mean velocity. Their effect is to promote the transport of high-momentum (principal component) fluid into the extremities of a duct; e.g. into the corners of a square or triangular duct. Similar effects are observed in the (elliptic) flow of, e.g. a river round a bend.

* Strictly, of course, a perfectly circular duct is degenerate by one degree

The most striking manifestation of the effect of secondary flows is the fact that in the case of an open-channel flow (such as that in a river or canal) the maximum velocity occurs not at the surface but some way below it. The facts that such flows are not amenable to laminar-flow analysis, that secondary flows occur in open channels, and that these secondary flows are responsible for the displacement of the position of maximum velocity, were all observed by Thomson * in 1878.

In view of the claims of priority made by Nikuradse, in 1926, and implicitly on Nikuradse's behalf by Schlichting [1975]† it is worth quoting some passages from Thomson's 1878 paper *On the flow of water in uniform regime*, and reprinting as our Figure 7.1a one of the diagrams of secondary flows measured by Thomson, and shown in his 1879 paper *On the flow of water round river bends*. In 1878 Thomson wrote:

The experimentally derived and perplexing suggestionis that inconsistently with the imagination of the water's motion conceived under the laminar theory, the forward velocity of the water in rivers is, in actual fact, sometimes or usually not greatest at the surface with gradual abatement from the surface to the bottom.....

[Drawing on the work of Boileau (1854) Thomson dismisses the then current theory that the effect was due to drag at the air-water interface, and observes that, for fully developed flow]

.....even if the channel face is extremely smooth, so as to present no sensible asperities, still there is good reason to assert that transverse flows will come to be instituted in consequence of the rapid flow of the main body of the current.....

Presumably unaware of the painstaking work of Thomson or of that of Stanton [1911], or of van der Hegge Zijnen [1924], Nikuradse wrote in 1926 that

Ueber die Geschwindigkeitsverteilung in turbulenten Stroemungen sind bisher, soweit bekannt, keine Untersuchungen angestellt.....

Nikuradse's measurements were, however, the best and most detailed ones made of turbulent flow up to 1926. Figure 7.1b shows the contours he produced for flow in a rectangular-sectioned duct, showing clearly the 'bulging' of the contours towards the corners

* The remarkable James Thomson, elder brother of William, later Lord Kelvin, who introduced the terms *laminar flow*, *torque*, *poundal* and (of perhaps lesser value in the light of modern usage) *interface*.

† cf. Tatchell [1975] who asserts that Nikuradse was the first to *observe* secondary flows. In fact, Nikuradse (unlike Thomson) made neither direct observation nor measurement of secondary flows. Figure 7.1a settles the question of priority; unfortunately, Thomson relied on the measurements of others for *fully-developed* secondary flow observations and was thus unable to present similarly quantitative analysis in that context.

of the duct. The results obtained by Nikuradse for open-channel flow will be used in Section 7.5.3 below, and are illustrated in Figure 7.21. Nikuradse's measurements of axial mean velocities show very clearly the 'bulging' of the contours towards the corners. They represent, historically, the first detailed quantitative evidence of the phenomenon so clearly described by Thomson.

Since about 1960 it has been possible, thanks to the refinement of experimental technique, to obtain detailed measurements of turbulent flows in non-circular ducts. The fully-developed secondary flows were first measured by Hoagland [1960], and measurements of turbulence quantities were reported by Leutheusser [1963], Brundrett & Baines [1964], Gessner [1964] and Launder & Ying [1972]. Recently [1975], Melling has presented extensive measurements of turbulence quantities in a developing square-duct flow, using laser-Doppler techniques. The data obtained by Melling are in broad qualitative agreement with those of earlier workers. Melling's work revealed some aspects of the phenomena in question that had not been recognized by earlier workers: for example, by measuring turbulence quantities throughout a quadrant (rather than restricting measurements to an octant), Melling noted that it was not necessarily possible to assume the symmetry that would seem *prima facie* to be required by the boundary conditions. The cause of the asymmetry must necessarily lie in an asymmetry of the boundaries too small to be detected. However, the fact that an apparently negligible asymmetry in the boundaries can cause non-negligible asymmetries in the flow must cast a certain amount of doubt on earlier results. For our present purpose, we shall assume that, as is most likely, the asymmetries will have disappeared by the time the flow is fully-developed. We therefore rely on Melling's data for developing flow, and on earlier results for the fully-developed,[†] flow.

[†] *faute de mieux* — Melling measured only up to 40 hydraulic diameters downstream of the inlet.

7.2 Equations of motion in three dimensions

Equations (3.3)' apply, as before:

$$\begin{aligned} \frac{\partial U_i}{\partial t} + \bar{U}_j \frac{\partial}{\partial x_j} \bar{U}_i &= -\frac{1}{\rho} \frac{\partial \bar{P}}{\partial x_i} + \nu \nabla^2 \bar{U}_i - \frac{\partial}{\partial x_j} \overline{u_i u_j} \\ &= -\frac{1}{\rho} \frac{\partial}{\partial x_j} \left\{ \bar{P} \delta_{ij} - \mu \frac{\partial \bar{U}_i}{\partial x_j} + \rho \overline{u_i u_j} \right\} \end{aligned} \quad (7.1)$$

Mass continuity, again, gives

$$\frac{\partial U_i}{\partial x_i} = 0$$

A three-dimensional boundary-layer form of equations (7.1) can be deduced under the following assumptions:

(i) terms in $\partial U_2/\partial x_1$ and $\partial U_3/\partial x_1$ are neglected, as in a boundary-layer flow $\partial U_2/\partial x_1 \ll \partial U_1/\partial x_3$, etc.

(ii) axial stress gradients are neglected.

(iii) the axial and lateral pressure fields are 'decoupled' by setting $\partial \bar{P}/\partial x_1 \equiv \partial \bar{P}/\partial x_1$, where \bar{P} is the space-averaged mean pressure, in the equation for which $i = 1$; this (cf. Tatchell [1975]) prevents the introduction of an elliptic-type term into the pressure equation.

The lateral pressure gradients will be negligible compared with the axial gradients in most boundary-layer flows. Pressures are derived from overall mass-continuity considerations: the details are presented by Tatchell [1975].

In this way we obtain the following equations:

$$\frac{DU_1}{Dt} = -\frac{1}{\rho} \frac{\partial \bar{P}}{\partial x_1} + \nu \nabla^2 U_1 - \frac{\partial}{\partial x_2} \overline{u_1 u_2} - \frac{\partial}{\partial x_3} \overline{u_1 u_3} \quad (7.2)$$

$$\frac{DU_2}{Dt} = -\frac{1}{\rho} \frac{\partial \bar{P}}{\partial x_2} + \nu \nabla^2 U_2 - \frac{\partial}{\partial x_2} \overline{u_2^2} - \frac{\partial}{\partial x_3} \overline{u_2 u_3} \quad (7.3)$$

$$\frac{DU_3}{Dt} = -\frac{1}{\rho} \frac{\partial \bar{P}}{\partial x_3} + \nu \nabla^2 U_3 - \frac{\partial}{\partial x_2} \overline{u_2 u_3} - \frac{\partial}{\partial x_3} \overline{u_3^2} \quad (7.4)$$

7.3 Reynolds-stress closure

Once again, we see that closure of the mean-momentum equations for turbulent flow is a question of providing a satisfactory model of the Reynolds stresses appearing in equation (7.1). The same considerations as to the best approach apply as before, but with renewed force. For example it is no longer possible to prescribe a satisfactory single length scale. As recently in 1975 it was possible for Tatchell to state that a barrier to the use of turbulence models involving differential equations for the Reynolds stresses was "uncertainty regarding the appropriate form of the modelled stress-transport equations". The extensive tests to which the models described in the present work have been subjected in two dimensions [cf. §6 above] together with the fact that they allow of easy generalization to three dimensions, suggests that this reservation need no longer apply. Other considerations such as economy of computer time may, of course, still deter future users from the use of a solution procedure involving three momentum equations, one continuity equation and six equations for the Reynolds stresses, together with an equation for the dissipation.

Launder and Ying [1973] neglected the effects of convection and diffusion in the region near the duct walls, where the generation of secondary flows is most powerful (see Brundrett & Baines [1964]). They then used a model of the pressure-strain redistribution derived from the work of Rotta [1951] and of Hanjalić & Launder [1972] to obtain algebraic expressions for the stresses $\overline{u_2^2}$, $\overline{u_3^2}$ and $\overline{u_2 u_3}$ which appear in the U_2 and U_3 equations (7.2–7.3). Gessner & Emery [1976] have shown that the Hanjalić–Launder pressure-strain model, under these assumptions, reduces to an *isotropic* eddy-viscosity model for the shear stresses $\overline{u_1 u_2}$ and $\overline{u_1 u_3}$. They show that

$$\overline{u_1^2} = c_1 k \quad (7.5-a)$$

$$\overline{u_2^2} = -c_2 c_4 \frac{k^3}{\epsilon^2} \left\{ \frac{\partial U_1}{\partial x_2} \right\}^2 + c_3 k \quad (7.5-b)$$

$$\overline{u_3^2} = -c_2 c_4 \frac{k^3}{\epsilon^2} \left\{ \frac{\partial U_1}{\partial x_3} \right\}^2 + c_3 k \quad (7.5-c)$$

$$\overline{u_1 u_2} = -c_4 \frac{k^2}{\epsilon} \frac{\partial U_1}{\partial x_2} \quad (7.5-d)$$

$$\overline{u_1 u_3} = -c_4 \frac{k^2}{\epsilon} \frac{\partial U_1}{\partial x_3} \quad (7.5-e)$$

$$\overline{u_2 u_3} = -c_2 c_4 \frac{k^3}{\epsilon^2} \frac{\partial U_1}{\partial x_2} \frac{\partial U_1}{\partial x_3} \quad (7.5-f)$$

where

$$c_1 = \frac{22(c_{\phi 1} - 1) - 6(4c_{\phi 2} - 5)}{33(c_{\phi 1} - 2c_{\phi 2})}$$

$$c_2 = \frac{4(3c_{\phi 2} - 1)}{11(c_{\phi 1} - 2c_{\phi 2})} \quad (7.6a)$$

$$c_3 = \frac{22(c_{\phi 1} - 1) - 12(3c_{\phi 2} - 1)}{33(c_{\phi 1} - 2c_{\phi 2})}$$

$$c_4 = \frac{44c_{\phi 1} - 22c_{\phi 1}c_{\phi 2} - 128c_{\phi 2} - 36c_{\phi 2}^2 + 10}{165(c_{\phi 1} - 2c_{\phi 2})^2}$$

Equations 7.5 d–e contain the result referred to above: the *same* proportionally constant c_4 for $\overline{u_1 u_2}$ and $\overline{u_1 u_3}$ gives

$$\mu_{\tau_{12}} \equiv \mu_{\tau_{13}} = c_4 \frac{k^2}{\epsilon}$$

The constants $c_{\phi 1}$ and $c_{\phi 2}$ for the Hanjalić–Launder model are 2.5 and 0.4 respectively. The Hanjalić–Launder model differs from that presented in Chapter 4 otherwise only in respect of one term; it does *not*, however, properly satisfy conditions (4.32)–(4.34).

If the same process of analysis is applied to the fully-consistent model proposed in Chapter 4 of the present work, it can easily be shown that the corresponding result is

$$\begin{aligned}
 c_1 &= \frac{22 c_{\phi 1} + 12 c_{\phi 2} + 8}{33 c_{\phi 1}} \\
 c_2 &= \frac{16 c_{\phi 2} - 4}{11 c_{\phi 1}} \\
 c_3 &= \frac{10 + 22 c_{\phi 1} + 18 c_{\phi 2}}{33 c_{\phi 1}} \\
 c_4 &= \frac{-44 c_{\phi 1} + 30 c_{\phi 2}^2 + 60 c_{\phi 2} - 10}{165 \times c_{\phi 1}^2}
 \end{aligned} \tag{7.6b}$$

With the appropriate choice of constants for each model, we obtain the values of c_1, \dots, c_4 given in Table 7.1 below.

For consistency, $\Sigma \overline{u_i^2} = 2k$, and this can easily be seen to imply that

$$c_1 - c_2 + 2c_3 = 2$$

which condition is satisfied by the values in both columns of Table 7.1.

The value of μ_r implied by the present model is somewhat higher than might be expected. The constant 0.09 is generally accepted (e.g. Launder & Ying [1973], Tatchell [1975]) as desirable. However, the present pressure-strain model is not intended for use as it stands in situations like those to which Gessner & Emery – or for that matter Launder & Ying – applied it. In near-wall situations including those involving corners, the near-wall modification of Chapter 5 must be used in addition to the pressure-strain model of Chapter 4. This has the effect of reducing the value of μ_r in line with the value of 0.09 for the constant of proportionality.

Unfortunately, the analysis which led Gessner and Emery to derive the results in equations 7.6a, and us to those of equations 7.6b, cannot be performed for the full model (including near-wall terms), as the general form of the associated decay function (5.13) will preclude this.

	HL $c_{\phi 1} = 2.5, c_{\phi 2} = 0.4$	Present model $c_{\phi 1} = 1.5, c_{\phi 2} = 0.4$
c_1	0.95	0.925
c_2	0.04	0.145
c_3	0.545	0.610
c_4	.09	.127

TABLE 7.1 The values of the constants c_1, \dots, c_4

7.4 The Reynolds-stress Equations

Equations (4.1) still apply:

$$\begin{aligned}
 \left\{ \frac{\partial}{\partial t} + \bar{U}_k \frac{\partial}{\partial x_k} \right\} \overline{u_i u_j} = & - \left\{ \overline{u_j u_k} \frac{\partial \bar{U}_i}{\partial x_k} + \overline{u_i u_k} \frac{\partial \bar{U}_j}{\partial x_k} \right\} && \text{PRODUCTION} \\
 & - 2\nu \overline{\frac{\partial u_i}{\partial x_k} \frac{\partial u_j}{\partial x_k}} && \text{DISSIPATION} \\
 & + \overline{\frac{p}{\rho} \left\{ \frac{\partial u_i}{\partial x_j} + \frac{\partial u_j}{\partial x_i} \right\}} && \text{REDISTRIBUTION,} \\
 & - \frac{\partial}{\partial x_k} \left\{ \overline{u_i u_j u_k} - \nu \frac{\partial}{\partial x_k} \overline{u_i u_j} \right\} && \text{+} \\
 & - \frac{1}{\rho} \overline{\left\{ \frac{\partial}{\partial x_j} (p u_i) + \frac{\partial}{\partial x_i} (p u_j) \right\}} && \text{DIFFUSION}
 \end{aligned}$$

The convection and production terms are, as before, treated exactly. The dissipation is again assumed to be isotropic and not to affect the off-diagonal terms of the stress tensor. The remaining terms (redistribution and diffusion) will be modelled in the light of the findings of Chapters 4–6.

Diffusion

The simpler diffusion model of Daly & Harlow was seen in Chapter 6 to give better results than the invariant model of Hanjalić & Launder. We therefore, choose the Daly–Harlow model for all 3-D computations. The Hanjalić–Launder model, it should be noted, implies six non-zero elements in each component of the 3-D diffusion tensor. The diffusion is, in any case, not an important contributor to the energy balance.

Pressure-Strain

The pressure-strain terms are modelled according to the prescription of Chapter 4.

Near-wall correction

The near-wall correction terms are specified by the general form presented in Chapter 5. However, a certain ambiguity is necessarily associated with the scalar function f , defined in formula (5.13) for the two-dimensional two-wall case.

For the present purpose we restrict the generalization of the near-wall modification to the case of rectangular ducts, illustrated in Figure 7.2. Equation (5.13) may be written as

$$f = \frac{k^{3/2}}{\epsilon} \frac{D_2}{x_2 \tilde{x}_2}$$

As in the two-dimensional case, we treat the effects of the various walls as additive. However, a simple generalization would lead to implausibilities, especially in the corners, where the fact that the walls are not parallel and remote from each other but perpendicular and adjacent will be crucial.

The relative intensity of the turbulent fluctuations parallel to a wall and at right angles to the plane of dominant strain, as we saw in Chapter 6, are unaffected to within experimental error by the presence of the wall. We shall assume that the turbulent fluctuations *normal* to a wall are affected exactly as in two dimensions, and that the decay of the effect is governed by the normal distance from the wall alone. Common sense dictates that the effect which is insensitive to the presence of a wall parallel to the fluctuations is unlikely to be a function of the distance from that wall. For the purpose of the near-wall correction term alone, we are thus entitled to treat the three-dimensional duct as effectively equivalent to the superposition of two orthogonal two-dimensional ducts.

This leads to the following effective near-wall corrections corresponding to the second part of the pressure-strain term in the normal-stress equations:

$$\phi_{11,2,w} \propto \frac{D_2}{x_2 \tilde{x}_2} \overline{u_1 u_2} \frac{\partial U_1}{\partial x_2} + \frac{D_3}{x_3 \tilde{x}_3} \overline{u_1 u_3} \frac{\partial U_1}{\partial x_3}$$

$$\phi_{22,2,w} \propto \frac{-D_2}{x_2 \tilde{x}_2} \overline{u_1 u_2} \frac{\partial U_1}{\partial x_2}$$

$$\phi_{33,2,w} \propto \frac{-D_3}{x_3 \tilde{x}_3} \overline{u_1 u_3} \frac{\partial U_1}{\partial x_3}$$

The shear-stress equations are subject to the additional corrections :

$$\phi_{12,2,w} = f_2 \{c'_2 (\overline{u_2^2} - \overline{u_1^2}) + \zeta' k\} \frac{\partial U_1}{\partial x_2} + f_3 \{c'_2 \overline{u_2 u_3}\} \frac{\partial U_1}{\partial x_3}$$

$$\phi_{13,2,w} = f_4 \{c'_2 \overline{u_2 u_3}\} \frac{\partial U_1}{\partial x_2} + f_5 \{c'_2 (\overline{u_3^2} - \overline{u_1^2}) + \zeta' k\} \frac{\partial U_1}{\partial x_3}$$

where f_2, \dots, f_5 are decay factors, to be determined.

The two-dimensional limits must in any case be equal to the forms already determined for two dimensions.

This criterion is evidently satisfied by

$$f_4 f_2 = \frac{D_2}{x_2 \tilde{x}_2}; f_5 f_3 = \frac{D_3}{x_3 \tilde{x}_3}$$

This is the simplest solution, and it is consistent with the result found for the normal stresses: viz. that the decay factor $D_\alpha / x_\alpha \tilde{x}_\alpha$ was associated throughout with the operator $\partial / \partial x_\alpha$.

Physically, this solution is little different in practice from the solution

$$f_2 = f_3 = f_4 = f_5 = \frac{D_2}{x_2 \tilde{x}_2} + \frac{D_3}{x_3 \tilde{x}_3}$$

as the values of $\partial U_1 / \partial x_3$ will tend to be important mainly where the term $D_2 / x_2 \tilde{x}_2 \ll D_3 / x_3 \tilde{x}_3$ (and similarly for $\partial U_1 / \partial x_2$).

The final term is

$$\phi_{23,2,w} = -c'_2 \left\{ \overline{u_1 u_3} \frac{\partial U_1}{\partial x_2} + \overline{u_1 u_2} \frac{\partial U_1}{\partial x_3} \right\} \cdot f_6$$

By symmetry,

$$f_6 = \frac{D_2}{x_2 \tilde{x}_2} + \frac{D_3}{x_3 \tilde{x}_3}$$

The 'first' part of the near-wall correction must be treated differently. It will readily be seen that it would not be possible for this term to be purely redistributive if we were to associate different rates of decay with the $\phi_{22,3,w}$ and $\phi_{33,3,w}$ components. The 'first' term, free of mean strain effects, must therefore behave in all components under the influence of both walls: the decay factor will thus be $\propto \{D_2 / x_2 \tilde{x}_2 + D_3 / x_3 \tilde{x}_3\}$. This will not affect the argument used to deduce the form of the mean-strain part of the near-wall correction, as $u_3^2 \simeq 2/3 k$ near a wall to which the u_3 fluctuations are parallel (and likewise for u_2^2/k), except possibly near a corner. The whole component $\phi_{33,w}$ is thus still roughly zero near a wall parallel to the u_3 fluctuations.

7.5 Applications in three dimensions

The model developed in earlier chapters, and extended to three dimensions in the foregoing sections of the present chapter, has been applied to developing duct flow. In this section, we examine the results generated and review the model in the light of its ability to cope with this generalised problem.

7.5.1 Preliminaries

Before proceeding to the application of the model to three-dimensional flows, the program (see Appendix C) into which the model was incorporated was adapted to produce two-dimensional predictions in order to verify that it was as accurate as the two-dimensional procedure used to generate the results described in Chapter 6 above. This was done in two distinct ways: first, the duct was given a large aspect ratio (5:1 was sufficient for this purpose) in order to make the flow at the mid-plane parallel to the shorter sides effectively two-dimensional; the second method was to modify the boundary conditions at one wall to replace the wall by a plane of symmetry. While the first approach was more interesting from the physical point of view, in that it predicted the actual flow in the type of duct used for two-dimensional measurements (e.g. Hanjalić & Launder, who used such a duct), the second was more economical as it permitted the reduction of the number of grid nodes in the direction of the normal to the wall to three. With this approach, it was possible to predict the symmetric channel flow to within 0.8% of the results given in Chapter 6. The more exacting test of the asymmetric boundary layers in Chapter 6 would have necessitated solving over the whole duct, and would have been less relevant to the prediction of flows in ducts with two centre planes of symmetry. The first approach was used to confirm the two-dimensionality of the flow in ducts of 5:1 aspect ratio. This test is illustrated in Figure 6.20, where the results are superimposed on those of a 2D procedure

7.5.2 Square duct flows

Figures 7.3–7.20 show the results obtained for the developing square duct flow, with comparisons with the data of Melling [1975]. Over the first 40 diameters, measured by Melling, Figure 7.3 shows that the model gives excellent agreement with the data for the variation of mean velocity along the axis of the duct. Figures 7.4–7.8 show the level of agreement obtained with the mean velocity contours at 5.6, 13.2, 20.7, 29.0 and 36.8 diameters downstream of the grid respectively (we shall refer to these as stations A–E for brevity in what follows). Figures 7.9–7.13 show the contours of $u_1^{1/2}$ at stations A–E respectively, where u_1 denotes the axial direction. Already in these contours we can detect a tendency for the high-intensity lines to be somewhat too close to the centre plane away from the corners, and to point too noticeably towards the corners. This ‘bulging’ of the contours is common to all the prediction procedures so far developed. The most striking example is the 0.06 contour on Figure 7.13: the discrepancy is none too great, and would be insignificant if it were not mimicked in all the predictions. Contours of $u_1 u_2$, and

$\overline{u_3^2}^{1/2}$ at station E are shown in Figures 7.14 and 7.15. Here we see very good agreement: it is the accuracy of, in particular, the turbulent shear-stress modelling that must govern the accuracy of the mean velocity profiles in the developing region. As we have seen, the centre-line velocity (Figure 7.3) is indeed well predicted. Figure 7.16 shows the predictions of turbulent kinetic-energy profiles: these must be expected, in line with the results in two dimensions, to parallel those of u_1 in Figure 7.13, which is confirmed by comparison. Figure 7.17 presents the contours of the quantity $(\overline{u_2^2} - \overline{u_3^2})$. Figure 7.17 illustrates well the difficulty described in Section 7.1 above: the contours should, in principle, be perfectly anti-symmetrical, with a zero line fixed along the diagonal, given perfectly symmetrical initial and boundary conditions. (Indeed, for sufficiently-developed flow, the initial conditions must tend to irrelevance.) The predictions must therefore be quite different from the data in this instance. Close examination of the data shown on the other contour plots in the present sequence reveals that all suffer to a varying degree of severity from the same defect. Figure 7.18, drawn from Melling [1975] shows the lack of agreement among the various workers who have measured the axial velocity and the axial component of turbulence intensity; not all the discrepancies can be accounted for by the differences in Reynolds numbers involved, as the variation is not monotonic with Reynolds number.

Figure 7.19 shows the profiles of secondary flows at station A; Figures 7.20 and 7.21 shows those at stations C and E. No data exist for comparison with Figures 7.19 or 7.20. As these represent results in developing flow, there will be a net momentum flux away from the wall, as the boundary layer develops, and this is confirmed by the predictions. Figures 7.23 and 7.24 show the axial mean-velocity profiles at stations B and E. The profiles lie below the 'universal' logarithmic profile, which is shown superposed on Figure 7.24.

Comparison with earlier work For the purpose of comparison, Figure 7.3 shows also the predictions made by Tatchell of the variation of mean velocity along the axis of the duct. From this graph, and also from the contours in Figures 7.8 and 7.16, it is quite clear that the agreement achieved by the present model is considerably better than that obtained by Tatchell. The maximum departure of the predictions of maximum axial velocity shown by the present model is roughly 2%, while that used by Tatchell gave disagreements (with respect to the data of Melling) of order 10%. The model used by Tatchell was that developed by Launder & Ying, with additional assumptions described in Section 7.2 above to enable predictions to be made of developing flow.

Fully-developed flow As noted earlier, we rely on the work of Launder & Ying [1972] for the data on fully-developed flow: their data are the most extensive and Figure 7.18 suggests that their results represent something close to a consensus.

Figure 7.25 shows the predictions of fully-developed axial mean velocity contours using the present model, compared with the data and predictions of Launder & Ying, and with the predictions of Naot [1972]. Figure 7.26 shows the predictions of secondary velocity profiles, against the data and predictions of Launder & Ying. Figure 7.27 gives the present predictions of kinetic energy contours, and Figure 7.28 those of shear stress around the perimeter of a smooth duct, using the data of Brundrett & Baines and of Leutheusser, as shown. In all cases, there is good agreement with the data, albeit showing vestigial traces of all the deficiencies of the predictions of developing flow (mainly in respect of the excessive bulging of the contours towards the corners of the duct – see 7.5.4 below). Figure 7.27 reveals considerable improvement in the predictions of turbulent kinetic energy, as compared with those of Launder & Ying. This is the first point at which the full Reynolds stress model can be said to have improved significantly the results for fully-developed flows. Figure 7.25 can be regarded as vindicating the use of the present form of the pressure-strain model rather than that of Naot et al., once the use of a stress model is accepted as justified. The predictions of turbulent kinetic energy and of axial mean velocity confirm the observation of Brundrett & Baines [1964] that the secondary flows cause greater distortion of the former than of the latter. Like Launder & Ying we conclude that the discrepancies observed between prediction and experiment are 'quite typical' of those 'to be found between different sets of experimental data for the more extensively examined flow geometries (e.g. the plane channel).' The predictions of the variation in wall shear stress reflect very closely the measurements of Leutheusser, as shown in Figure 7.28. Figure 7.29 shows the variation in friction factor with increasing Reynolds number. The predictions show some improvement on those of Launder & Ying, especially at lower Reynolds numbers. The improvement must be attributed to that in the velocity contours, which in turn owe their increased accuracy to the near-wall model used.

Verification of numerical accuracy The fact that several workers have already obtained solutions of the equations for fully-developed flow, this provides us with the opportunity to test the present procedure for numerical accuracy. The program was adapted to 'simulate' the work of Naot, Shavit & Wolfshtein [1972] by modifying the various components (pressure-strain model, choice of constants) and eliminating the near-wall correction, to correspond to the model used by Naot et al. The detailed comparisons are shown in Figure 7.30, and are entirely satisfactory.

It was found that an 11×11 grid gave excellent results, provided that the grid was compressed near the walls and allowed to spread near the planes of symmetry. With a 15×15 grid it was not necessary to take these precautions. To obtain stable solutions in the initial region (up to 30 hydraulic diameters) of a developing flow, it was found necessary to take very small 'forward steps'

(not greater than .03 of the hydraulic diameter), though these could be allowed to grow exponentially to 0.75 of the hydraulic diameter after 20 diameters had been covered. For all these recommendations, the criterion of accuracy has been a local variation of not more than 0.75% in the mean velocities and 1% in the turbulence quantities. To obtain fully-developed flow, it is not necessary to proceed so slowly as for developing flow: an initial forward step of 0.25 hydraulic diameters is permissible if a maximum inaccuracy of 5% *en route* (though not ultimately present) is overlooked. The results for fully-developed flow shown in Figures 7.25–7.30 were obtained with settings suitable for developing flow. By observing all these numerical constraints it was possible to ensure that all the symmetries imposed by the physical nature of the problem were reflected in the predictions to within one part in 10^5 . Grid-independence was verified by increasing the fineness (*i*) to 22×22 and then (*ii*) to 11×33 , and noting that in neither case was any discrepancy produced, to within .1% locally in any predicted quantity.

7.5.3 Free-surface flows

An interesting extension of the techniques used for duct flows is the application of the model to the flow in an open channel. Data for such a flow were presented by Nikuradse [1926]. The free surface presents considerable difficulties, particularly in respect of the correct specification of boundary conditions.

The free surface was treated as a symmetry plane, with the following exception: *the liquid–air interface was presumed to act on the Reynolds stresses as a wall.* * Accordingly the wall-effect (Chapter 5) with its associated decay (7.4 above) were imposed on the flow from the symmetry plane, with the results shown in Figure 7.31. These results confirm that the boundary conditions imposed lead to essentially correct prediction of the velocity distribution, and in particular to the correct prediction of the descent of the velocity maximum from the surface. As the only change in the boundary conditions as between the (quadrant of the) square duct and the (half of the) open channel is the introduction into the latter of the near-wall correction term at the surface, we may deduce that one way of generating correct predictions of the flow in an open channel is to treat it as we have done.

* The effect in this sense of causing a redistribution of the stresses as given by the model of Chapter 5 with the decay function expressed in terms of the distance from the surface.

While this is not presented as a solution to the problem of the prediction of such flows, it does suggest a line along which such a solution might well be pursued: the free surface does generate an additional redistribution of the Reynolds normal stresses, it seems, which only direct measurement can confirm.

7.5.4 *Summary of results*

Figures 7.3–7.20 show that the model can predict the developing flow in a square duct with a good degree of accuracy. In common with earlier attempts by Naot [1972] and Tatchell [1975] (the latter having predicted developing flow; the former having used a model of the same order as the present one to predict fully-developed flow), the axial mean velocity contours show an excessive ‘bulging’ towards the corners. The present predictions are comfortably within the envelope of the data for fully-developed flow shown in Figure 7.18. For developing flow, the contours of turbulent kinetic energy and of axial mean velocity are quite satisfactory: the other quantities can not be regarded as experimentally ‘known’ to within the accuracy required for a definitive judgement.

The excessive ‘bulging’ of the axial mean velocity contours towards the corners can (in order of decreasing likelihood) be attributed to :

- (a) the neglect of the effect of lateral pressure variations on the axial mean velocity (for developing flow only);
- (b) an inadequacy in the log law wall functions used near the corners; the law may clearly not hold in the region of intersection of the two wall boundary layers;
- (c) possible inadequacies for three dimensions of a Reynolds-stress model of turbulence that was derived on the basis of measurements and correlations for two-dimensional phenomena.

However, it must be pointed out that the predictions of the present model appear to lie consistently closer to the data than those produced by earlier models.

8

GENERAL CONCLUSIONS

8.1 Summary of achievements

The model described in Chapters 3–5 has been subjected to exhaustive testing in two-dimensional near-wall situations, and applied to three-dimensional flows – in all cases with satisfactory results.

8.1.1 Objective and achievement

We have stated our objective as the production of ‘a properly heuristic model of turbulence’ (cf. Appendix A). In so far as our model was heuristically derived, in Chapters 3–5, and was shown in Chapters 6–7 to be capable of the correct prediction of most features of the turbulent flows considered, our objective has been achieved.

8.1.2 The prediction of two-dimensional flows

Excellent agreement with experiment was achieved in the single-wall flows treated.

Especially pleasing successes were

- + the accurate predictions of the wall jet in stagnant surroundings;
- + the correct prediction of the point of inflexion in the u_1^2 curve in all two-dimensional flows;
- + the good agreement achieved with the data of Hanjalic & Launder for the asymmetric channel flow.

The near-wall correction devised clearly produces excellent results in one-wall flows and is generally successful in channel flows.

The diffusion models considered can not be regarded as a really satisfactory representation of the physical world. The model which best reflects the data is not clearly invariant, though we have shown that its non-invariance may perhaps be due to the over-simplified way in which we have chosen to write it. We have, in the absence of entirely reliable measurements of the diffusion, no way of pursuing this matter further at this point of time. As it stands, the model recommended (that of Daly & Harlow) does not provide an unequivocal generalisation to three dimensions. However, this failing should not be overstressed, relating as it does to a very small fraction of the overall turbulent kinetic energy balance.

8.1.3 The prediction of three-dimensional flows

The model derived for two dimensions was extended to three dimensions in Chapter 7. This enabled us to produce predictions for the square duct which were

- (a) in good general overall agreement with the best available data;
- (b) much more accurate over the entrance region than those generated by lower-order models (cf. Tatchell [1975], who correctly guessed that this would happen);
- (c) deficient in respect of the overprediction of the secondary flows, leading to an excessive 'bulging' into the corners of a duct; this excess is less than that indicated by earlier predictions, an improvement that can be attributed to the use of the near-wall correction.

The predictions of flow in open channels are of interest, and are in line with those of flow in ducts.

The deficiencies in the predictions may be due to shortcomings in the Reynolds-stress modelling, but (since they are common to all models so far applied) are much more likely to be due to neglect of significant terms in the mean-momentum equations.

8.1.4 General assessment

The predictions obtained justify the use of the model. However, we must concede that the model requires, in its three-dimensional form, slightly over 150% more computer time than, say, a $k-\epsilon$ model. Whether this additional investment is justified in terms of the increased accuracy and extra information available from the present approach is a question that must be answered in the light of the requirements of each particular user of a turbulence model. We have shown

- that the use of a Reynolds-stress model permits the incorporation of a modification which represents the effect of a wall on both the stress distribution and, hence, on the mean flow pattern;
- that it is possible to incorporate such a model into standard parabolic partial-differential equation solution algorithms without causing instability or requiring excessive computer time and storage;
- that the values of the additional constants required by the model can be deduced from physical considerations, and that the results generated with the use of these constants are both stable and optimal with respect to small variations in the values of the constants.

8.2 The future

There is clearly room for further improvement. As topics which are suggested by the present work we submit:

- the refinement of the modelling of the dissipation of turbulent kinetic energy: the isotropic model is probably satisfactory in the present context, but there may be better ways of modelling the production, destruction and diffusion of dissipation than those of Chapter 4;
- a 'causal' explanation of the origins of the near-wall redistribution of the Reynolds stresses, leading to a consequent improvement on the present phenomenological approach;

- a thorough investigation of the phenomenon of diffusion of turbulent stresses, leading — it is hoped — to a model which reflects the undoubted invariance of the physical world, and is also able to predict the phenomena of turbulence better than an apparently non-invariant one;
- the implementation of the present model in the context of a more exact treatment of the mean-momentum equations in three dimensions;
- the constant refinement of the methods of turbulence modelling in the light of the the data generated by ever-improving techniques of measurement.

APPENDIX A

MODELLING IN HYDRODYNAMICS

We assume that the problem of solving the equations of motion for a Newtonian viscous incompressible fluid satisfies the following “plausible intuitive hypotheses” first enunciated in this form by Birkhoff [1960].

- A. Intuition suffices for determining which physical variables require consideration.*
- B. Small causes produce small effects, and infinitesimal causes produce infinitesimal effects.*
- C. Symmetric causes produce effects with the same symmetry.*
- D. The flow topology can be guessed by intuition.*
- E. The processes of analysis can be used freely: the functions of rational hydrodynamics can be freely integrated, differentiated, and expanded in series (Taylor, Fourier) or integrals (Laplace, Fourier).*
- F. Mathematical problems suggested by intuitive physical ideas are “well set” (i.e. have one and only one solution depending continuously on the boundary conditions (Hadamard [1923])).*

Hypothesis (A)

Thus, strictly speaking in combination with (B), allow us to disregard e.g. relativistic effects, electrostatic forces, impurities, compressibility of “incompressible” fluids, quantum-mechanical considerations, etc. The failure to invoke and operate correctly Hypothesis (A) can be regarded as the source of many so-called

paradoxes of classical hydrodynamics. Thus, if we assume incompressibility, we are inexorably led to the conclusion that in a two-dimensional theory a bubble requires infinite energy to expand. Correct, albeit implicit rather than explicit, use of the hypothesis, on the other hand, led Prandtl to derive his theory of the boundary-layer [1904]. This hypothesis amounts to a decision on the contents of what Bradshaw, for example, [1967] calls "the list of important variables".

Hypothesis (B)

This hypothesis lies at the heart of our search for a solution of the problem of turbulence. In deliberately neglecting certain terms that properly appear in the Navier-Stokes equations we not only assume that they are small, but also that their inclusion would lead to a negligible change in the results obtained. Similarly, we shall replace unmanageable terms by tractable ones in the belief that the difference between the true term and its modelled form is not merely negligible but of infinitesimal effect on the solutions obtained.

That this hypothesis is neither so obvious nor so innocent as it may seem can be seen from the fact that it does not hold for, e.g.

- (a) Any quantum-mechanical phenomenon
- (b) any macroscopic transition of a truly "sudden" nature: such as the problem of the determination of the exact height from which a given egg can be dropped without breaking,

or, as we saw earlier (page above),

- (c) the transition of a given flow from a laminar regime to a turbulent one. The hypothesis thus implies a stability of the solutions obtained by its use. This fact leads to a further complication: viz, that the effect of non-zero viscosity is not a symmetrical, and thus ordinary, type of perturbation. Clearly, the result of letting $\nu \rightarrow 0+$ may be quite different from whatever would result from letting $\nu \rightarrow 0-$ (i.e. through negative values).

The point is probably best made in terms of an example.

Example. Consider the equation

$$\ddot{x} = kx$$

If $k < 0$ this has the solution:

$$x = A \sin(k^{1/2}t) + B \cos(k^{1/2}t)$$

which satisfies the condition

$$|x| < \sqrt{A^2 + B^2} \text{ for all } t.$$

If $k > 0$, the general solution is

$$x = A e^{k^{1/2}t} + B e^{-k^{1/2}t}$$

which tends to infinity as $t \rightarrow \infty$ or $t \rightarrow -\infty$ however small the value of k .

The value $k = 0$ thus represents a dividing-point between two essentially different types of solution.

In the case of the Navier-Stokes equations, $\nu < 0$ makes the equations hyperbolic, not elliptic. This suggests that a fruitful approach might be *via* 'catastrophe theory' (see e.g. Thom []) which deals with bifurcations of this kind. However, the theory is currently restricted to the derivation of an intuitive understanding of 'pure' differential equations. Ours being a physical problem, we are handicapped not by a lack of physical, intuitive understanding: what we lack is an adequate mathematical justification for its solution.

Hypothesis (B) is also the basis of the justification of a finite-difference approach. We invoke it implicitly every time we seek 'grid-independence', by saying, in effect, that if we can produce the results that we seek (i.e. to within a specified tolerance) with a given grid fineness, and no problems of inaccuracy arise if we refine the grid slightly further, we may deduce that we should not change the results however much further we refined the grid.

Hypotheses (C), (D) & (E)

These hypotheses allow us, above all, to apply common sense to save time, and (particularly in the case of (E)) to avoid unpleasantly tricky and repetitive continuity considerations.

Hypothesis (F)

On page above, we give certain reasons for believing that this hypothesis, in effect, held. Further evidence is provided by the facts that:

- (a) the results of all predictive work so far based on the Navier-Stokes equations have not conflicted with the experimental data;
- (b) the equations have close links with the physics of the problem: thus, we can measure individually most of the terms in the equations – convective, generative, diffusive, etc. effects – and thus have a good intuitive understanding of the internal structure of the equations;
- (c) experimental results, being self-consistent to within the accuracy of the techniques used, have led to satisfactory simple algebraic correlations (e.g. laws of boundary-layer growth, and ‘universal’ velocity profiles) – just as one would expect from a ‘well-set’ problem.

In the last analysis, however, no set of rules can be as effective in ensuring good practice as the simple expedient of constant reference to the empirical data. In all that follows, we shall draw on the available experimental information to assist in establishing the models we examine or propose. We shall conclude by comparing the results obtained from those models with a wide range of well-established data. In this way, we should be able to produce what we seek – a properly heuristic model of turbulence.

APPENDIX B

THE SOLUTION OF EQUATIONS (4.32)–(4.34) as linear functions of the Reynolds stresses

From condition (4.32) we see that

$$\begin{aligned} 0 = & \alpha_1 \overline{u_m u_l} + \alpha_2 \overline{u_m u_l} + \alpha_3 \delta_{lm} \overline{u_i u_i} \\ & + 3\alpha_4 \overline{u_m u_l} + \alpha_5 \overline{u_m u_l} + \alpha_6 \overline{u_m u_l} \\ & + (\alpha_7 + \alpha_8 + \alpha_9) \delta_{ml} \overline{u_k u_k} \end{aligned}$$

From equation (4.34) we see that

$$\begin{aligned} 2 \overline{u_m u_l} = & (3\alpha_1 + \alpha_2 + \alpha_3) \overline{u_m u_l} \\ & + \alpha_4 \delta_{lm} \overline{u_i u_i} - (\alpha_5 + \alpha_6) \overline{u_m u_l} \\ & + (3\alpha_7 + \alpha_8 + \alpha_9) \delta_{ml} \overline{u_k u_k} \end{aligned}$$

Next, we note that the conditions (4.32)–(4.33) have no effect on terms other than the groupings

$$\alpha_2 \quad \alpha_3 \quad \alpha_4 \quad \alpha_5$$

and

$$\alpha_6 \quad \alpha_7$$

which they cause to be permuted among themselves. Consequently, as (4.32) is an identity, the four permutations (the fourth is a corollary of the other three) merely serve to show that

$$\alpha_2 = \alpha_3 = \alpha_4 = \alpha_5$$

and that

$$\alpha_6 = \alpha_7$$

Therefore we may write

$$\begin{aligned}
 a_{\ell j}^{mi} &= \alpha_1 \delta_{\ell j} \overline{u_m u_i} + \alpha_2 (\delta_{\ell i} \overline{u_m u_j} + \delta_{\ell m} \overline{u_i u_j} + \delta_{jm} \overline{u_i u_\ell} \\
 &\quad + \delta_{ij} \overline{u_m u_\ell}) \\
 &\quad + \alpha_6 \delta_{im} \overline{u_\ell u_j} + \alpha_7 \delta_{\ell j} \delta_{mi} \overline{u_k u_k} \\
 &\quad + \alpha_8 (\delta_{\ell i} \delta_{mj} \overline{u_k u_k} + \delta_{\ell m} \delta_{ij} \overline{u_k u_k})
 \end{aligned}$$

and applying (4.33) we see that if $i=j$

$$\begin{aligned}
 0 &= \alpha_1 \overline{u_m u_\ell} + \alpha_2 (5 \overline{u_m u_\ell} + \delta_{\ell m} \overline{u_i u_i}) + \alpha_6 \overline{u_\ell u_m} \\
 &\quad + \alpha_7 \delta_{m\ell} \overline{u_k u_k} + \alpha_8 (\delta_{m\ell} \overline{u_k u_k} + 3 \delta_{m\ell} \overline{u_k u_k})
 \end{aligned}$$

If further $\ell=m$, this gives

$$0 = \alpha_1 + 8\alpha_2 + \alpha_6 + 3\alpha_7 + 12\alpha_8$$

while if $\ell \neq m$, we have

$$0 = \alpha_1 + 5\alpha_2 + \alpha_6$$

Equation (4.34) gives, for $\ell=j$,

$$\begin{aligned}
 2 u_m u_i &= 3\alpha_1 \overline{u_m u_i} + 4\alpha_2 \overline{u_m u_i} + \alpha_6 \delta_{im} \overline{u_\ell u_j} + 3\alpha_7 \delta_{mi} \overline{u_k u_k} \\
 &\quad + 2\alpha_8 \delta_{mi} \overline{u_k u_k}
 \end{aligned}$$

If $i=m$, we see that

$$2 = 3\alpha_1 + 4\alpha_2 + 3\alpha_6 + 9\alpha_7 + 6\alpha_8$$

while if $i \neq m$, we have

$$2 = 3\alpha_1 + 4\alpha_2$$

Thus, in all, we have the four equations:

$$\begin{aligned}
 \alpha_1 + 5\alpha_2 + \alpha_6 &= 0 \\
 3\alpha_2 + 3\alpha_7 + 12\alpha_8 &= 0 \\
 3\alpha_1 + 4\alpha_2 &= 2 \\
 3\alpha_6 + 3\alpha_7 + 6\alpha_8 &= 0
 \end{aligned}$$

which have the solutions

$$\begin{aligned}\alpha_2 &= (-2-3\alpha_6)/11 \\ \alpha_1 &= (4\alpha_6 + 10)/11 \\ \alpha_7 &= (-25\alpha_6 - 2)/11 \\ \alpha_8 &= (10\alpha_6 + 3)/55\end{aligned}$$

If we write $k = \overline{u_i u_i} / 2$ in the terms associated with α_7 and α_8 , these coefficients will have to appear doubled. If we now write

$$\begin{aligned}\alpha &= \alpha_1 \\ \beta &= \alpha_2 = \alpha_3 = \alpha_4 = \alpha_5 \\ c_{\phi 2} &= \alpha_6 \\ \eta &= 2\alpha_7 \\ \nu &= 2\alpha_8 = 2\alpha_9\end{aligned}$$

we derive the model in precisely the form in which Launder [1971] originally presented it:

$$\begin{aligned}a_{\phi j}^{mi} &= \alpha \delta_{\phi j} \overline{u_m u_i} + \beta (\delta_{m\phi} \overline{u_i u_j} + \delta_{mj} \overline{u_i u_\phi} + \delta_{i\phi} \overline{u_m u_j} + \delta_{ij} \overline{u_m u_\phi}) \\ &\quad + c_{\phi 2} \delta_{mi} \overline{u_\phi u_j} + [\eta \delta_{mi} \delta_{\phi j} + \nu (\delta_{m\phi} \delta_{ij} + \delta_{mj} \delta_{i\phi})] k\end{aligned}$$

where

$$\begin{aligned}a &= (4c_{\phi 2} + 10)/11 \\ \beta &= (-2-3c_{\phi 2})/11 \\ \eta &= (-50c_{\phi 2}-4)/55 \\ \nu &= (20c_{\phi 2} + 6)/55\end{aligned}$$

Recalling that the relevant term in the stress equations is in fact

$$\Pi_{ij} \equiv \overline{p \left(\frac{\partial u_i}{\partial x_j} + \frac{\partial u_j}{\partial x_i} \right)} / \rho$$

we next write:

$$\begin{aligned}
\frac{\partial U_q}{\partial x_m} \{a_{2j}^{mi} + a_{2i}^{mj}\} &= \alpha (\delta_{2j} \overline{u_m u_i} + \delta_{2i} \overline{u_j u_m}) \frac{\partial U_q}{\partial x_m} \\
&+ \beta (2\delta_{m2} \overline{u_i u_j} + \delta_{mj} \overline{u_i u_2} + \delta_{mi} \overline{u_j u_2} \\
&+ \delta_{i2} \overline{u_m u_j} + \delta_{j2} \overline{u_m u_i} + 2\delta_{ij} \overline{u_m u_2}) \frac{\partial U_q}{\partial x_m} \\
&+ c_{\phi 2} (\delta_{mi} \overline{u_2 u_j} + \delta_{mj} \overline{u_2 u_i}) \frac{\partial U_q}{\partial x_m} \\
&+ \nu (\delta_{mi} \delta_{2j} + \delta_{2i} \delta_{mj}) k \frac{\partial U_q}{\partial x_m} \\
&+ \eta (\delta_{mi} \delta_{2j} + \delta_{mj} \delta_{i2} + 2\delta_{m2} \delta_{ij}) k \frac{\partial U_q}{\partial x_m} \\
&= (\alpha + \beta) \{ \delta_{2j} \overline{u_m u_i} + \delta_{2i} \overline{u_m u_j} \} \frac{\partial U_q}{\partial x_m} \\
&+ (\beta + c_{\phi 2}) \{ \delta_{mj} \overline{u_i u_2} + \delta_{mi} \overline{u_j u_2} \} \frac{\partial U_q}{\partial x_m} \\
&+ (\eta + \nu) \{ \delta_{mi} \delta_{2j} + \delta_{2i} \delta_{mj} \} \frac{\partial U_q}{\partial x_m} \\
&+ 2\beta \{ \delta_{m2} \overline{u_i u_j} + \delta_{ij} \overline{u_m u_2} \} \frac{\partial U_q}{\partial x_m} \\
&+ 2\eta \delta_{m2} \delta_{ij} k \frac{\partial U_q}{\partial x_m} \\
&= -(\alpha + \beta) P_{ij} - (\beta + c_{\phi 2}) D_{ij} \\
&+ (\eta + \nu) \left\{ \frac{\partial U_j}{\partial x_i} + \frac{\partial U_i}{\partial x_j} \right\} k \\
&- 2\beta P \delta_{ij}
\end{aligned} \tag{B.1}$$

where

$$\begin{aligned}
 P_{ij} &\equiv - \{ \delta_{ij} \overline{u_m u_i} + \delta_{ij} \overline{u_m u_j} \} \frac{\partial U_q}{\partial x_m} \\
 &= - \{ \overline{u_m u_i} \frac{\partial U_j}{\partial x_m} + \overline{u_m u_j} \frac{\partial U_i}{\partial x_m} \} \\
 D_{ij} &\equiv \{ \overline{u_i u_m} \frac{\partial U_m}{\partial x_j} + \overline{u_j u_m} \frac{\partial U_m}{\partial x_i} \} \\
 P &\equiv - \overline{u_m u_q} \frac{\partial U_q}{\partial x_m} = \text{rate of production of} \\
 &\quad \text{turbulent kinetic energy}
 \end{aligned}$$

By comparing coefficients, it is easily seen that (B.1) reduces to:

$$\begin{aligned}
 \Pi_{ij,2} &\equiv \frac{\partial U_q}{\partial x_m} \{ a_{ij}^{mq} + a_{ij}^{mq} \} \\
 &= - \frac{(c_{\phi 2} + 8)}{11} \{ P_{ij} - \frac{2}{3} \delta_{ij} P \} \\
 &\quad - \frac{(8c_{\phi 2} - 2)}{11} \{ D_{ij} - \frac{2}{3} \delta_{ij} P \} \\
 &\quad - \frac{(30c_{\phi 2} - 2)}{11} k \left\{ \frac{\partial U_i}{\partial x_j} + \frac{\partial U_j}{\partial x_i} \right\}
 \end{aligned}$$

APPENDIX C

THE 2-D COMPUTER PROGRAM

Appendix D contains a full listing of the program used for computing two-dimensional boundary-layers. The finite-difference procedure is that of Patankar & Spalding [1967, 1969].

The main differences in structure between the original GENMIX code and the one in Appendix D are all attributable to the fact that the computations were obtained using the 'interactive' systems of the University of London and of Imperial College, London. The input of data is normally assumed to be from a teletype or VDU, through 'default' settings are left available for the use of the program by 'batch' processing. The advantages of interactive use as against batch processing were comparable to those of owning and driving ones own vehicle rather than relying on public services. Thus the program, when run interactively, has controls corresponding to an 'accelerator' (forward - step - size) and a 'brake' ('pause' or 'stop'). One 'steers' the program by choosing models and constants in the light of information received. Against this must be set the sole disadvantage of limited (interactive) core: 25000₁₀ words on the Imperial College CDC 6400/CYBER 7314 system.

To facilitate compilation within this limited region of core, the original STRIDE subroutine was divided in such a way as to ensure that no one subroutine was much larger than the others. The subroutine HELP is nothing more than Patankar & Spalding's STRIDE (3), with appropriate variables common to HELP and the rest of STRIDE.

Structure of Program:

The basic structure of the program is (except as already indicated) as documented by Patankar & Spalding. The particular modification introduced are as follows:

MAIN

- (i) Common blocks include turbulence-model constants and sufficiently large arrays to accommodate the dependent variable, and their 'sources';
- (ii) Chapter 1 includes default settings of constants for different models for batch running; the 'rib-height' (RIBHI) for a rough wall;
- (iii) Chapter 2 allows for strongly non-uniform grid-spacing (required by strongly asymmetric flows);
- (iv) Chapter 5 sets initial values of all appropriate variables. The profiles chosen for dependent variables were found to have less than 1% influence at $x/D > 2$.
- (v) Chapter 7 includes provision for an automatically-expanding forward step; this is not needed for interactive operation.
- (vi) In Chapter 10, a number of Patankar – Spalding variables are redefined and used as locations for values of quantities of interest. (e.g. FUFLUX contains the value of the "E"-wall shear stress). The quantity U_{\max} is calculated for the purpose of deriving R_M . The position of zero shear-stress is also obtained, as are the values of \bar{U} for the regions of flow on either side of U_{\max} .
In Chapter 10(d) the intermediate output (but not input) is relegated to the new SUBROUTINE WRITE.
Finally, provision is made for the boundary conditions on each equation.

WRITE

This subroutine

- (i) gives output of dependent variables
- (ii) provides values of normalized quantities
- (iii) allows for selective output in interactive mode (default values are also provided in order to restrict line-width)
- (iv) is structured to allow for 'debugging' information to be generated.

AUX:

Calculates $\partial U/\partial y$ by interpolation, to give a value suitable for inclusion in the source terms.

The sources are calculated for the various equations. In the case of the near-wall corrections, it was found necessary to include these by stages. The "DO 14" loop effectively incorporates the correction terms by an ad hoc under-relaxation over the first 200 steps.

The PREF's (coefficients of the diffusion term) are selected according to the model invoked.

STRIDE:

This subroutine has been modified to allow:

- (i) use of the calculated shear stress as source for momentum
- (ii) the incorporation of fixed boundary values ϕ_{i_w} by setting, e.g.,

$$C(1, 2) = 2 * \phi_{i_w}$$

The shear-stress modification will be found on page 175 (foot) where the SULA term represents the integrated momentum source due to the turbulent shear stress

HELP:

Contains STRIDE (3) of the Patankan–Spalding code. Also incorporates automatic correction for instabilities revealed by negative normal stresses, and warnings if this scheme is invoked. [This facility is not intended for normal operation and results so generated are not, of course, used for any but ‘debugging’ purposes].

WF

This subroutine incorporates the wall-boundary conditions of Table 6–1.

The rough-wall boundary condition is explicit. It cannot work satisfactorily if YREF is allowed to be less than RIBHT (the ‘rib-height’ of roughness elements); this dictates a minimum spacing of the first node from the rough wall, effected by use of a strongly non-linear grid.

Running

Generally, the calculations were made using 30–40 nodes. This is not a minimum figure it is sufficiently large to generate grid-invariant predictions. (variation $< 0.5\%$ everywhere). Neither precise optimization of grids nor paring of the redundancies in the program was performed as there were no restrictions on the free use of Imperial College computing facilities for research. Current users of the program are not so fortunate.

Running times were about 28/CDC 6400 seconds to fully-developed flow using FUN–compiled binary codes. Other compilers would perform much better. Recent tests indicate that compilation and running under MNF would effect savings of about 60% in compilation time and about 40% in running time. Optimization of the code could certainly be expected to produce still further substantial improvement.

3-D Procedure

For reasons of claimed copyright, it is not possible to publish a listing of the procedure used for 3D computations. This makes it pointless to describe the modifications performed. Suffice it to say that the methods used were exactly in line with the 2D procedure described here.

Other workers have incorporated the present model in publicly available 3D parabolic programs, and forthcoming publications from Imperial College will doubtless provide full details.

APPENDIX D
LISTING OF THE 2-D COMPUTER PROGRAM

Introduction

The listing given in the following pages of this Appendix is that of the program used to solve two-dimensional boundary-layer flow (it is here 'set up' for solving the asymmetric channel flow of Hanjalić & Launder). No attempt has been made to 'clean up' the appearance of the program. Redundancies abound – most of them the debris of early versions – but it was felt that the advantages of publishing the actual program used outweighed the marginal benefits of subsequent polishing.


```

PROGRAM BUNGLA(INPUT,OUTPUT,TAPES=INPUT,TAPES=OUTPUT)
CHAPTER 0 ***** PRELIMINARY *****
CHAPTER 0 ***** DIMENSIONS AND COMMON BLOCKS *****
COMMON/GENERAL/AJE(6),AJI(6),OSALFA,OPDX(83),DX,EMU(83),F(6,83),
1  FS(6,83),H,IFIN,INDE(6),INDI(6),ISTEP,ITEST,IUTRAP,KEX,KIN,KRAD,
2  N,NEQ,NPH,NP1,NP2,IP3,O4(83),PEI,PMJREF,PREF(6,83),PSIE,PSII,
3  R(83),RHO(83),RME,RMI,RU(83),SU(6,83),SU(9,83),TAUE,TAUI,U(83),
4  XU,XU,Y(83),YE,YI,FO(2,83),EMUL(83)
COMMON/GM4/ AK,ALMG,EWALL,IPRINT,FR,PRESS,
1  UBAR,U=AC,
2  KRUF
COMMON/GM4A/RIBHI
COMMON/K/ALPHA,BETA,PNU,CFI2,ETA,GAMMA,C1,C2,CMU,CE,CE1,CE2,CE3
COMMON/L/CFI1,CS,ALFANN,CASEP,CASED,THETA,Z1,Z2,Z3,K3,K4,K5,FRA
COMMON/WRIT/M,M11,M12,UMAX,I4,I5,I6,ITEL
COMMON/FEED/M5,M6
CHAPTER 1 ***** PARAMETERS AND CONTROL INDICES *****
PRINT 1750
C-----CAUTION SET UP FOR AUTOMATIC BATCH RUNNING FOR 4 MODEL
C-----COMBINATIONS
DO 12 I=1,3,2
C-----CASEJ REFERS TO CHOICE OF DIFFUSION MODEL --- 1 FOR INVARIANT
C----- 2 FOR DALY HARLOW, 3 FOR DONALDSON 4 FOR THESIS MODEL 'D'
C-----CASEP REFERS TO THE PRESSURE STRAIN MODEL CHOSEN-----
C-----A FOR NAOT ET AL MODEL---3 FOR HANJALIC-LAUNDER
C-----C FOR THESIS CHAPTER 4 MODEL
DO 12 I=1,4
IF(I100.EQ.1)CASED=141
IF(I100.EQ.1)CASEP=14A
IF(I100.EQ.2)CASED=141
IF(I100.EQ.2)CASEP=14C
IF(I100.EQ.3)CASED=142
IF(I100.EQ.3)CASEP=14A
IF(I100.EQ.4)CASED=142
IF(I100.EQ.4)CASEP=14C
1750 FORMAT(' CHANNEL FLOW, ASYMMETRIC OR SYMMETRIC*/ *')
C-----SELECT ITEL=1 FOR BATCH, ITEL FOR TELEX RUNNING
ITEL=3
CONSTANTS SET HERE FOR DEFAULT [BATCH] RUNNING
C-----WITH DEFINITIONS OF MAIN FORTRAN NAMES USED
C-----REM IS REYNOLDS NUMBER BASED ON HYDRAULIC DIAMETER AND MAX VEL
C-----AND IS USED TO INITIALISE THE VISCOSITY
C-----CE1, CE2, CE3 ARE CONSTANTS FOR EPSILON (DISSIPATION) EQN
C-----Z3 IS CFI1-PRIME

```

```

C-----KRUF IS SWITCH FOR SMOOTH CHANNEL (=0)
C-----ONE ROUGH WALL (=1 OR =2, ACCORDING TO
C-----WHICH WALL IS ROUGH)
C-----TWO ROUGH WALLS (=3)
C-----N IS NO OF NODES
C-----OMDIST CONTROLS SPREAD OF THE NODES (OMEGA DISTRIBUTION)
C-----=0 FOR LINEAR .....GT.1 FOR SPREAD
C-----FRA IS INITIAL FORWARD STEP---BUT SEE CHAPTER 7
C-----ALFANW IS ALPHA-PRIME (NEAR WALL CORRECTION COEFFICIENT)
C-----OTHER VARIABLES EITHER SELF-EXPLANATORY OR STANDARD 'GENMIX'
C-----NOTATION.

```

```

      REM=57000.

```

```

      CE1=1.45

```

```

      CE2=1.92

```

```

      CE3=.14

```

```

      Z3=.33

```

```

      KKRU=2

```

```

      K3=K5=0

```

```

      K4=1

```

```

      N=4

```

```

      OMDIST=.4

```

```

      FRA=.3

```

```

      ALFANW=-.05

```

```

      NSTA=1

```

```

      LASTEP=600

```

```

      I4=2

```

```

      I5=N+2

```

```

      I6=1

```

```

CONSTANTS FOR ROUGHNESS, M-L AND REYNOLDS NUMBER

```

```

      RIBHI=.00568

```

```

      L=1

```

```

      M5=0

```

```

      ALMG=C.13

```

```

      IF (L.GT.7) ALMG=.13

```

```

      IF (L.GE.3) RIBHI=.011

```

```

      PRINT 14+E

```

```

1440 FORMAT(* RE(M)= -----,*)

```

```

      IF (ITER.EQ.1) READ(5,1540) REM

```

```

1540 FORMAT(F7.0)

```

```

      PMUREF=.018/REM

```

```

9 CONTINUE
CONSTANTS FOR MODEL B (ROTTA-HANJALIC-LAUNDER) OF PRESSURE STRAIN
1431 FORMAT(* CE1= -.----*)
1531 FORMAT(F5.3)
CE2=2.75
CE3=.157
CE1=1.57
CFI1=2.8
C2=.35
C1=2.
CFI2=0.45
ALPHA=(12.-3.*CFI2)/11.
BETA=(-2.+6.*CFI2)/11.
PNU=-CFI2
Z2=1.
Z1=2.
GAMMA=(12.*CFI2-4.)/55.
ETA=(6.-3.*CFI2)/55.
CASE SETTING - 'G' '1B' FOR NON-INV'T DIFFUSION + R-H-L PRESS-STRAIN
PRINT 1471
1471 FORMAT(* CASE:*)
IF(ITEML.EQ.1)READ(5,1551)CASED,CASEP
IF(CASEP.EQ.1HB)GO TO 1301
1551 FORMAT(2A1)
CONSTANTS FOR MODEL A (ROTTA-WOLFSHTEIN-REYNOLDS) OF PRESSURE-STRAIN
Z2=1.
CFI1=1.5
Z1=0.
CFI2=0.5+FLOAT(I101)/2.
CE1=1.43
CE2=1.9
CE3=.157
THETA=0.
CONSTANTS FOR MODEL C (ROTTA-LAUNDER) OF THE PRESSURE-STRAIN CORRELATION
IF(CASEP.EQ.1HA)GO TO 1301
CE3=.157
CE2=1.92
CE1=1.47
PRINT 1431
IF(ITEML.EQ.1)READ(5,1531)CE1
PRINT 1431
1451 FORMAT(* CE2= -.----*)

```

```

IF (ITEL.EQ.1) READ(5,1531) CE2
CFI1=1.5
THETA=.4
1590 FORMAT(* THETA=,----*)
1591 FORMAT(F4.3)
PRINT 1591
IF (ITEL.EQ.1) READ(5,1591) THETA
PRINT 1591
IF (ITEL.EQ.1) READ(5,1512) CFI1
BETA=-(2.+3.*THETA)/11.
ETA=(2).*THETA+6.)/55.
GAMMA=-(50*THETA+4.)/55
PNU=1.
CFI2=0.
ALPHA=(4.*THETA +11.)/11.
Z1=2.
1801 CONTINUE
1412 FORMAT(* CFI1=,---*)
1512 FORMAT(F4.2)
CONSTANTS FOR TWO DIFFERENT DIFFUSION MODELS: '2' IS INVARIANT, '1' IS NOT
IF (CASE0.EQ.1H1) CS=.195
IF (CASE0.EQ.1H2) CS=.11
IF (CASE0.EQ.1H3) CS=.16
IF (CASE0.EQ.1H4) CS=.13
IF (CASE0.EQ.1H1) CE3=.157
IF (CASE0.EQ.1H2) CE3=.145
1414 FORMAT(* CE=,----*)
PRINT 1414
IF (ITEL.EQ.1) READ(5,1514) Z3
1514 FORMAT(F4.3)
PRINT 1514
1593 FORMAT(* KRJF=,---*)
IF (ITEL.EQ.1) READ(5,1594) KRJF
C-----CMU USED IN KINETIC-ENERGY EQN ONLY (NORMALLY SUPPRESSED)
PRINT 7001
7001 FORMAT(* USUAL TAU: 0; HANJALIG TAU:1 :*)
IF (ITEL.EQ.1) READ(5,1594) K3
PRINT 7002
7002 FORMAT(* ADDNL TERM IN TAU: 0; SUPPRESS: 1:*)
IF (ITEL.EQ.1) READ(5,1594) K4
PRINT 7003
7003 FORMAT(* TO SUPPRESS ADDNL NORMAL STRESS TERM: 1 OTHERWISE 0*)
IF (ITEL.EQ.1) READ(5,1594) K5

```

```

1485 PRINT 1485
      FORMAT(*,CC=.----4)
      IF (ITEL.EQ.1) READ(5,1585) CS
1585 FORMAT(F4.3)
1594 FORMAT(I1)
      CE=.41
      CMU=.125/CE/(CFI1-.9)
      IF (KRUF.==1.3) RIBHI=.
      IPRINT=0
      ITEST=0
      IUTRAP=1

```

C -----
CHAPTER22222222222222222222222222222222 GRID AND GEOMETRY 22222222222222222222

```

      FRA=.3
      PRINT 1410
1410 FORMAT(*,N=--*)
      IF (ITEL.EQ.1) READ(5,1510) N
1510 FORMAT(I2)
      NP1=N+1
      NP2=N+2
      NP3=N+3
      OM(1)=1.
      OM(IP3)=1.

      ROUT=.1
      IRIBHI=RIBHI*FLOAT(N)/ROUT
      M6=IRIBHI
      IF (KRUF.==1.0) M1=0
      IF (KRUF.==2.0) M2=0
      IF (KRUF.==3.1) M1=1
      IF (KRUF.==3.1) M2=1
      IF (KRUF.==4.2) M1=1
      IF (KRUF.==4.2) M2=1
      IF (KRUF.==4.3) M1=1
      IF (KRUF.==4.3) M2=2
      L1=N/2
      PRINT 1409
1409 FORMAT(*,OMDIST=.----*)
      IF (ITEL.EQ.1) READ(5,1509) OMDIST
1509 FORMAT(F4.3)
      DO 11 I=3,101
      OM(I)=FLOAT(I-2+M1*IRIBHI)/FLOAT(N+M2*IRIBHI)
      OMDIS=1.-OMDIST*OM(I)
      IF (OMDIST.NE.0.) OM(I)=OM(I)**OMDIS
11 CONTINUE

```



```

TA=RI9HI
TB=LASTEP
TC=AK
REY=12.35/29./PMUREF
EQRAT=FLCAT(KRUF)
AMACH=ALMG
107 FORMAT(1H,1P3E 11.3,4I6)
108 FORMAT(1H,1P3E 11.3,4I6)
IF(OMDIST.EQ.0.)WRITE(6,1011) (OM(I),I=1,NP3)
1011 FORMAT(6H,OM'S,11F5.3 / (1H,+,11F6.3 ))
101 FORMAT(1H,9G8.2 )
PRESS1=PRESS
106 CONTINUE
CHAPTER 108 ----- TESTS FOR PRINTOUT
IPRINT=0
IF(ISTEP.EQ.0) GO TO 102
IF(ITEST.EQ.1) GO TO 102
IF(IFIN.EQ.1) GO TO 102
IF(FLOAT(ISTEP/NSTA).EQ.FLOAT(ISTEP)/FLOAT(NSTA)) GO TO 102
IF(ISTEP.EQ.LASTEP) GO TO 102
IF(ISTEP.GE.IEND.AND.ISTEP.LT.IEND+3) GO TO 102
IF(ISTEP.GE.IAX.AND.ISTEP.LT.IAX+3) GO TO 102
IF(ISTEP.EQ.IOUT) GO TO 102
IF(ISTEP.GE.IOUT.AND.ISTEP.LT.IOUT+1.) GO TO 102
IPRINT=0
GO TO 105
CHAPTER 109 ----- STATION VARIABLES
102 IPRINT=1
103 IPRINT=IPRINT+1
PRDRP=(PRESS1-PRESS)
TAUEJ=TAUE/DYNHED
FUFLUX=0.
FIFLUX=0.
FIBAR=0.
FUFLUX=TAUI
FIFLUX=TAUE
REXD=(Y(NP3)-ROUT)/ROUT
AJED=TAUI/(TAUE+TAUI)
1012 FORMAT(3X,24XU,9X,5HPRDRP,6X,5HTAUEJ,6X,5HYEXD,7X,4HUBAR,7X,
1 6HTAUI,5X,6HTAUE,5X,4HTAUI,7X,5HISTEP,1X,4HIEND,2X,3HIAX,5X,
24HIOUT/1H,1P3E 11.3,4I6)
DO 1020 I=3,NP1

```

```

M=I
UMAX=U(I)
IF(U(I+1).LT.UMAX) GO TO 1024
1020 CONTINUE
1024 DO 1022 I=3, NP1
MIS=I
AKMIN=F(1, I)
IF(F(1, I+1).GT.AKMIN) GO TO 1023
1022 CONTINUE
1023 CONTINUE
1021 REM=0.5*UMAX*ROUT/PMUREF
AJED=Y(M)
OM=CM(M-1)+(AJED-Y(M-1))*(OM(M+1)-OM(M-1))/(Y(M+1)-Y(M-1))
STORE=OM(1)
OM(M)=OM(1)
UBARI=OM(1)/AJED
UBARE=(1.-OM(M))/(ROUT-AJED)
FI=2.*TAUI/UBARI**2*RHOEF
FE=2.*TAUI/UBARE**2*RHOEF
REI=4.*UBARI*AJED
REE=4.*(ROUT-AJED)*UBARE
REE=REE/PMUREF
REI=REI/PMUREF
YZEROI=FI/FE
YZEROE=1.-YZEROI
UBA=0.
DO 121 I=1, NP2
121 UBA=UBA+(J(I)+U(I+1))*(Y(I+1)-Y(I))
UBA=0.5*UBA
REYC=UBA+2.*ROUT/PMUREF
IF(ISTEP.NE.0) GO TO 1077
IF(CASED.EQ.1H1) PRINT 1070
1070 FORMAT(* DIFFUSION MODEL USED: DALY-HARLOW (I.E. NON*
1*-INVARIANT)*)
IF(CASED.EQ.1H2) PRINT 1071
1071 FORMAT(* DIFFUSION MODEL USED: HANJALIC'-LAUNDER (TM/TN/A/8)*)
IF(CASED.EQ.1H3) PRINT 1072
1072 FORMAT(* DIFFUSION MODEL USED: DONALDSON - I.E. SIMPLIFIED*
1* HANJALIC'-LAUNDER*)
IF(CASED.EQ.1H4) PRINT 1073
1073 FORMAT(* NEW MODEL USED FOR DIFFUSION*)

```

```

IF(CASEP.EQ.1HA) PRINT 1074
1074 FORMAT(* PRESSURE-STRAIN MODEL USED: ROTTA-WOLFSHSTEIN-REYNOLDS*)
IF(CASEP.EQ.1HB) PRINT 1075
1075 FORMAT(* PRESSURE-STRAIN MODEL USED: LAUNDER (EARLY VERSION)*)
IF(CASEP.EQ.1HC) PRINT 1076
1076 FORMAT(* PRESSURE-STRAIN MODEL USED: LAUNDER (LATER VERSION)*)
1077 CONTINUE
PRINT 1014,XU,YZEROI,UMAX,REM
1014 FORMAT(*F6.2* METRES DOWNSTREAM, FI/FE=*F6.2*, UMAX=*F6.2* REM=*
1 F8.3)
1015 FORMAT(* ZERO SHEARSTRESS AT *F6.3*, UMAX AT *F6.3*, KMIN AT *
1 F6.3)
1013 FORMAT(3X,2HFI,9X,2HFE,9X,3HREM,3X,3HREI,6X,3HREE, 8X,6HFI/FE ,
15X,4HUMAX,7X,3HUBA,3X,5HUBARI,6X,5HUBAPE,6X,4HREYC/1H ,11F6.3 )
CHAPTER 100 ----- PROFILE VARIABLES
OM(M)=STORE
C ----- TEST 6
IF(ITEST.EQ.0) GO TO 1006
TEST=1006
WRITE (6,100) TEST
1006 CONTINUE
IF(IPRINT.LT.2) GO TO 105
C----- CALL THE WRITE SUBROUTINE WHICH PROVIDES OUTPUT OF STATION
C----- VARIABLES
CALL WRITE
IF(ISTEP.EQ.1.0) GO TO 105
PRINT 14)2
C----- IN THE INTERACTIVE MODE, NOW CHOOSE NEW FORWARD STEP SIZE
C----- IN THE LIGHT OF OUTPUT RECEIVED
C----- AND THEN SELECT THE NEXT STATION FOR WHICH OUTPUT IS
C----- DESIRED
IF(ITEMP.EQ.1) READ(5,15)2) FRA
PRINT 14)2
IF(ITEMP.EQ.1) READ(5,15)4) NSTA
1240 CONTINUE
105 CONTINUE
113 IF (IFIN.EQ.1) GO TO 110
IF (ISTEP.LT.LASTEP.AND).XU.LT.XULAST) GO TO 112
GO TO 110
112 F(1,NP3)=TAUE+4.3
F(1,1)=TAJI+7.3
F(2,1)= 1.19*F(1,1)
F(2,NP3)=1.19*F(1,NP3)
F(3,1)=.030*F(1,1)

```

```

F(3,NP3)=.250*F(1,NP3)
F(4,1)=.550*F(1,1)
F(4,NP3)=.550*F(1,NP3)
F(5,1)=-TAUI
F(5,NP3)=-TAUE
F(6,NP3)=TAUE**1.5/AK/YE
F(6,1)=TAUI**1.5/AK/YI
CALL STRIDE(3)
GO TO 60
110 CONTINUE
120 CONTINUE
STOP
END
*DECK, WRITE
SUBROUTINE WRITE
DIMENSION A(4,83)
COMMON/GE PRAL/AJE(6),AJI(6),CSALFA,DPOX(83),JX,EMU(83),F(6,83),
1 FS(6,83),I,IFIN,INDI(6),INDI(6),ISTEP,ITEST,IUTRAP,KEX,KIN,KRAD,
2 N,NEG,NPH,NP1,NP2,NP3,OM(83),PEI,PIURF,UREF(6,83),PSIE,PSII,
3 R(83),RHO(83),RME,RHI,RU(83),S(6,83),SU(9,83),TAUE,TAUI,U(83),
4 XD,XU,Y(83),YE,YI,FD(2,83),EMUL(83)
COMMON/GM,A/RIGHT
COMMON/K/ALPHA,BETA,PNU,CFI2,ETA,GAMMA,C1,C2,CMU,CE,CE1,CE2,CE3
COMMON/L/CFI1,CS,ALFANW,CASE3,CASE5,THETA,Z1,Z2,Z3,K3,K4,K5,FRA
COMMON/WPIT/M,M10,M11,M12,UMAX,I4,I5,I6,ITEL
COMMON/ABC/DU(83)
L=1
IF(L.EQ.1)GO TO 10
  UTAUI=SQRT(TAUI)
  UTAUE=SQRT(TAUE)
  PRINT 1005,UTACI,UTAUE
1096 FORMAT(1H** UTAUI=+G10.4*   JTAUE=+G10.4)
  IF(ISTEP.GT.0)PRINT 1005
  1005 FORMAT(1H** THE VARIABLES ARE TABULATED AS FOLLOWS; Y,U,UV,K,DISS,
1 U1,U2,U3,L*)
  JUMP=(NP1-3)/9+1
  IF(ISTEP.GT.0)GO TO 2001
  PRINT 3010
  PRINT 3011
3011 FORMAT(1H** *CONSTANTS AND ANY ERROR MESSAGES*)
  WRITE(6,101)ALPHA,BETA,GAMMA,ETA,THETA,PNU,CFI1,CFI2,ALFANW,
1 CE1,CE2,CE3,CS
  RETURN

```

```

2001 WRITE(6,3010)
3010 FORMAT(72(14+))
PRINT 2003
2000 FORMAT(* PRINTOUT CONTROLS: FIRST NODE, LAST NODE, SKIP*)
      IF(IT.L.EC.1) READ(5,3000) I4, I5, I6
      IF(I4.L.2) RETURN
3000 FORMAT(I2,1X,I2,1X,I2)
1995 FORMAT(6H Y'S ,11F6.3 / ( 6X,11F6.3 ))
      DO 1920 I=I4, I5, I6
1920 W(1, I)=Y(I)/Y(NP3)
      WRITE(6,101) (W(1, I), I=I4, I5, I6)
      DO 1921 I=I4, I5, I6
1921 W(1, I)=U(I)/UMAX
      WRITE(6,101) (W(1, I), I=I4, I5, I6)
1994 FORMAT(6H U'S ,11F6.2 / ( 6X,11F6.2 ))
      DO 1925 I=I4, I5, I6
1925 W(1, I)=F(5, I)/TAUI
      WRITE(6,101) (W(1, I), I=I4, I5, I6)
      DO 2030 I=I4, I5, I6
2030 W(1, I)=SU(5, I)
      WRITE(6,101) (W(1, I), I=I4, I5, I6)
      DO 2031 I=I4, I5, I6
2031 W(1, I)=SU(7, I)
      WRITE(6,101) (W(1, I), I=I4, I5, I6)
      DO 1910 I=I4, I5, I6
1910 W(1, I)=F(1, I)/TAUI
      WRITE(6,101) (W(1, I), I=I4, I5, I6)
      DO 1911 I=I4, I5, I6
1911 W(1, I)=F(3, I)*Y(NP3)/TAUI**1.5
      WRITE(6,101) (W(1, I), I=I4, I5, I6)
      DO 1912 I=I4, I5, I6
1912 W(1, I)=SQRT(F(2, I)/TAUI)
PRINT 1007
1007 FORMAT(14*)
      WRITE(6,101) (W(1, I), I=I4, I5, I6)
      DO 1913 I=I4, I5, I6
1913 W(1, I)=SQRT(F(3, I)/TAUI)
      WRITE(6,101) (W(1, I), I=I4, I5, I6)
      DO 1914 I=I4, I5, I6
1914 W(1, I)=SQRT(F(4, I)/TAUI)
      WRITE(6,101) (W(1, I), I=I4, I5, I6)
      WRITE(6,101) (FD(2, I), I=I4, I5, I6)

```

```

2150 DO 2150 I = I4, I5, I5
2151 W(1, I) = F(1, I) / (Y(NP3) - Y(I))
      WRITE(6, 101) (W(1, I), I = I4, I5, I6)
      DOBYUT3 = 0.5 * TAUI * SU(3, I)
1051 WRITE(6, 105) (W(1, I), I = I4, I5, I6)
      DO 1101 I = I4, I5, I6
1101 W(1, I) = CS * F(1, I) / (Y(NP3) - Y(I))
      WRITE(6, 101) (W(1, I), I = I4, I5, I6)
      IF (CASE).EQ.1H1) J3=1
      IF (CASE).EQ.1H2) J4=1
      IF (CASE).EQ.1H3) J5=1
      IF (CASE).EQ.1H4) J6=1
      IF (CASE).EQ.1H5) J7=1
      IF (CASE).EQ.1H6) J8=1
      IF (CASE).EQ.1H7) J9=1
      IF (CASE).EQ.1H8) J10=1
      IF (CASE).EQ.1H9) J11=1
      IF (CASE).EQ.1H10) J12=1
1931 W(1, I) = CS * F(1, I) / (Y(NP3) - Y(I)) + J2 * (FS(3, I) * F(J1, I) + J5 * SU(3, I))
      WRITE(6, 101) (W(1, I), I = I4, I5, I6)
      DO 1932 I = I4, I5, I6
      IF (CASE).EQ.1H1) J3=1
      IF (CASE).EQ.1H2) J4=1
      IF (CASE).EQ.1H3) J5=1
      IF (CASE).EQ.1H4) J6=1
      IF (CASE).EQ.1H5) J7=1
      IF (CASE).EQ.1H6) J8=1
      IF (CASE).EQ.1H7) J9=1
      IF (CASE).EQ.1H8) J10=1
      IF (CASE).EQ.1H9) J11=1
      IF (CASE).EQ.1H10) J12=1
1932 W(1, I) = CS * F(1, I) / (Y(NP3) - Y(I)) + F(6, I) + J5 * SU(6, I) + F(J1, I) +
      WRITE(6, 101) (W(1, I), I = I4, I5, I6)
      DO 1933 I = I4, I5, I6
      J3=1
      IF (CASE).EQ.1H1) J3=1
      J4=1
      IF (CASE).EQ.1H2) J4=1
      W(1, I) = CS * F(1, I) / (Y(NP3) - Y(I)) + (J4 * F(5, I) * FS(3, I) + J3 * F(3, I) * FS(5, I)) / TAUI
1 *+ 1.5

```

```

      IF (CASED.EQ.1H4) W(1,I)=CS*F(1,I)/F(6,I)*((F(2,I)+F(3,I))*FS(5,I)
1+F(5,I)+(FS(3,I)+(F(2,I+1)-F(2,I-1))/(Y(I+1)-Y(I-1))))/TAUI**1.5
1933 CONTINUE
      WRITE(6,101) (W(1,I),I=I4,I5,I6)
      DO 2131 I=2,NP2
      IF(ISTEP.LS.600) RETURN
      W(1,I)=(DU(I+1)-DU(I-1))/(Y(I+1)-Y(I-1))
2131 CONTINUE
      WRITE(6,905) (W(1,I),I=I4,I5,I6)
      DO 2132 I=I4,I5,I6
      W(1,I)=W(1,I)*FD(2,I)/UMAX
2132 CONTINUE
      WRITE(6,905) (W(1,I),I=I4,I5,I6)
      DO 2133 I=I4,I5,I6
2133 W(1,I)=W(1,I)*UMAX/FD(2,I)
      DO 2134 I=I4,I5,I6
2134 SU(7,I)=(W(1,I+1)-W(1,I-1))/(Y(I+1)-Y(I-1))
      DO 2201 I=I4,I5,I6
2201 W(1,I)=SU(7,I)
      WRITE(6,905) (W(1,I),I=I4,I5,I6)
      DO 2135 I=I4,I5,I6
      W(1,I)=W(1,I)*FD(2,I)**2/UMAX
2135 CONTINUE
      WRITE(6,905) (W(1,I),I=I4,I5,I6)
      DO 2136 I=I4,I5,I6
2136 W(1,I)=W(1,I)*UMAX
      WRITE(6,905) (W(1,I),I=I4,I5,I6)
      WRITE(6,905) (SU(9,I),I=I4,I5,I6)
905 FORMAT(/(9F3.2))
31 CONTINUE
      IF(L.EQ.1) RETURN
10 CONTINUE
101 FORMAT(1H*,9F3.3 )
      RETURN
      END
*DECK,AUX
SUBROUTINE AUX
C***** FOR BOUNDARY LAYERS
DIMENSION YEDGE(6)
COMMON/GENERAL/ AJE(6),AJI(6),CSALFA,DPDX(83),DX,EMU(83),F(6,83),
1 FS(6,83),H,IFIN,INDE(6),INJI(6),ISTEP,ITEST,IUTRAP,KEX,KIN,KRAD,
2 N,NEQ,NPH,NP1,NP2,NP3,OM(83),PEI,PMJREF,PREF(6,83),PSIE,PSII,
3 R(83),R40(83),RME,RMI,RU(83),SD(6,83),SU(9,83),TAUE,TAUI,U(83),

```



```

C ----- LAMINAR CONTRIBUTION
EMU(I)=EMU(I)+EMUT
20 CONTINUE
DO 21 I=2, NP1
21 EM U(I)=.5*(EM U(I)+ EMU(I+1))
C ----- TEST 10
IF(ITEST.EQ.0) GO TO 1010
TEST=1010
WRITE(6,101) TEST
WRITE(6,101) (EMU(I),I=1, NP3)
WRITE(6,101) (S D(1,I),I=1, NP3)
1010 CONTINUE
C ----- MODIFICATION OF EMU ARRAY -----
DO 24 I=2, NP1
EM UL(I)=PUREF/(Y(I+1)-Y(I))
24 EM U(I)=EMU(I)/(Y(I+1)-Y(I))
IF(KRAD.EQ.0) GO TO 25
DO 26 I=2, NP1
26 EM U(I)=EM U(I)*.5*(R(I)+R(I+1))
25 CONTINUE
DO 14 I=1, NP3
FD(2,I)=ALMG*Y(NP3)/AK
C----- THE CALCULATED LENGTH-SCALE IS INTRODUCED GRADUALLY
IF(FD(2,I).GT.Y(I)) FD(2,I)=Y(I)
IF (FD(2,I).GT.(Y(NP3)-Y(I))) FD(2,I)=Y(NP3)-Y(I)
IF(ISTEP.GT.100) FD(2,I)=(ISTEP-100)/100*F(1,I)**1.5/F(6,I)*
1 Y(3)/F(1,3)**1.5*F(6,3)+FD(2,I)*(200-ISTEP)/100
IF(ISTEP.GE.200) FD(2,I)=F(1,I)**1.5/F(6,I)*Y(3)*F(6,3)/F(1,3)
1 **1.5
FD(2,1)=FD(2,2)=FD(2, NP2)=FD(2, NP3)=1.E-15
14 CONTINUE
DO 291 I=1, NP3
FD(1,I)=F(6,I)
IF(F(3,I).LE.0.) PRINT 1420, F(3,I), ISTEP, I
1420 FORMAT(* U2 NEGATIVE =+G11.4* STEP +I3* NODE +I2)
C----- FS4 IS SHEAR STRESS
C----- FD2 IS LENGTH SCALE
C----- FS3 IS GRADIENT OF U2**2
C----- FS1 IS GRADIENT OF LENGTH SCALE
C----- FS5 IS GRADIENT OF SHEAR STRESS
291 FS(4,I)=F(5,I)

```

```

DO 232 I=2, NP2
  FS(1,I)=(F(2,I+1)-F(2,I-1))/(Y(I+1)-Y(I-1))
  FS(3,I)=(F(3,I+1)-F(3,I-1))/(Y(I+1)-Y(I-1))
  IF(ISTEP.LE.20) FS(1,I)=.05*ISTEP*FS(1,I)
292 FS(5,I)=(F(5,I+1)-F(5,I-1))/(Y(I+1)-Y(I-1))
DO 27 I=1, NP3
C 3 3 3 3 3 3 3 3 3 3 3 3 3 SOURCES
C SOURCE TERM FOR TURBULENT KINETIC ENERGY *****
IF(I.EQ.1.OR.I.EQ.2.OR.I.EQ.NP2.OR.I.EQ.NP3) GO TO 13J1
C-----PROVISION HAS BEEN MADE FOR THE USE OF A T K E EQN
IF(NEG.GT.4) F(1,I)=.5*(F(2,I)+F(3,I)+F(4,I))
IF(NEG.LE.4) F(4,I)=2.*F(1,I)-F(2,I)-F(3,I)
F(1,2)=F(1,1)
F(1,NP2)=F(1,NP3)
IF(F(1,I).LE.0.) F(1,I)=1.E-15
IF(F(1,I-1).LE.0.) F(1,I-1)=1.E-15
IF(F(1,I+1).LE.0.) F(1,I+1)=1.E-15
C-----SU1 IS SOURCE FOR T K E EQN IF NEEDED
C-----SA IS ADDITIONAL SOURCE TERM IMPLIED BY H-L DIFFUSION
C-----MODEL FOR U1**2
C-----S3 IS SAME FOR THE SHEAR STRESS EQ1
SU(1,I)=(CMU*F(1,I)**2+DU(I)**2+FD(2,I)-FD(1,I))*1.5*(Y(I+1)
1-Y(I-1))
FS(5,NP3)=FS(5,NP2)=FS(5,NP1)
FS(5,1)=FS(5,2)=FS(5,3)
SA(I)=.5*(S+(F(1,I+1)/FD(1,I+1)+2.*FS(4,I+1)+FS(5,I+1)
1 F(1,I-1)/FD(1,I-1)+2.*FS(4,I-1)+FS(5,I-1))
IF(K5.EQ.1) SA(I)=0.
SB(I)=.5*(S*(F(1,I+1)/FD(1,I+1)+F(5,I+1)*FS(3,I+1)-
1 F(1,I-1)/FD(1,I-1)+F(5,I-1)*FS(3,I-1))
IF(K4.EQ.1) SB(I)=0.
IF(CASED.NE.1H2.AND.CASED.NE.1H4) SA(I)=SB(I)=0.
IF(CASED.NE.1H4) GO TO 41
SA(I)=.5+SA(I)
41 CONTINUE
C-----SHSRLX IS RELAXED VALUE OF SHEAR-STRESS NW CORRECTION
C-----IMPLIED BY THIS IS CHAPTER 5
SHSRLX=(-.5*ALFANW*(F(3,I)-F(2,I))+0.*F(1,I))
1 +SQRT(TAU1)/AK/(Y(I))
2 +(-.5*ALFANW*(F(3,I)-F(2,I))+0.*F(1,I))
1+(-SQRT(TAU1))/AK/(Y(NP3)-Y(I))

```

```

IF(ISTEP.LE.20)SHSRLX=.
IF(ISTEP.LE.100)SHSRLX=ISTEP/100*SHSRLX
C-----RNSCOR IS EFFECTIVE RELAXED NW CORRECTION IN 2ND PART OF PS
RNSCCR=ALFANW*ABS(F(5,I))*SQRT(TAUJ)/AK/Y(I)
1 +ALFANW*ABS(F(5,I))*SQRT(TAUJ)/AK/
1 (Y(NP3)-Y(I))
SU(9,I)=RNSCOR
IF(ISTEP.LE.100)RNSCOR=RNSCOR*ISTEP/100
N4=4
IF(KRUF.EQ.0) N4=8
IF(I.LE.(NP3/N4))A1=2.
IF(I.GT.(NP3/N4))A1=0.
IF(I.GT.(NP3-NP3/N4).AND.KRUF.EQ.0)A1=2.
IF(I.GT.(N-2))A1=2.
C-----DECAY IS THE DECAY FACTOR APPLIED TO THE WHOLE NW CORRECTION
DECAY=F(2,I)/Y(I)+FD(2,I)/(Y(NP3)-Y(I))
C-----CF01 IS THE EFFECTIVE VALUE OF THE COEFFICIENT OF THE FIRST
C----- (ROTTA) TERM OF THE PS MODEL USED
CF01=CFI1+Z3*DECAY
C-----SU2-4 ARE THE SOURCE TERMS FOR NORMAL STRESSES 1-3 RESPECTIVELY
SU(2,I)=(Z2*CFI2*.75.*F(5,I)*DU(I) +A1*(FD(1,I)+FS(4,I)*DU(I))
1 -2.*FS(4,I)*DU(I)-2.*F(1,I)/3.-CF01*FD(1,I)/F(1,I)*
1 (F(2,I)-2.*F(1,I)/3.)+Z1*FS(4,I)*(ALPHA+2.*BETA+(CFI2+2.*PNU)
2 *F(2,I)/F(1,I)+ALFRLX*DECAY)*DU(I)+.5*(Y(I+1)-Y(I-1))+SA(I)
SU(3,I)=-Z2*CFI2*.75.*F(5,I)*DU(I)
1 -.667*FD(1,I)-CF01*F(1,I)/F(1,I)+(F(3,I)
1)-.667*F(1,I))+Z1*FS(4,I)*(THETA+2.*BETA+(CFI2+2.*PNU)*F(3,I)/
2 F(1,I)-ALFRLX*DECAY)*DU(I)
SU(3,I)=SU(3,I)+.5*(Y(I+1)-Y(I-1))
IF(CASE).EQ.1H4) SU(3,I)=SU(3,I)+3.*SA(I)
SU(4,I)=(-Z2*CFI2*.75.*F(5,I)*DU(I)+.5*CFI2*RNSCOR
1 -2.*F(1,I)/3.-CF01*FD(1,I)/F(1,I)*(F(4,I)-.667*F(1,I))
1 +Z1*FS(4,I)*(BETA+PNU)*F(4,I)/F(1,I)*DU(I)+.5*(Y(I+1)-Y(I-1)
2))
C-----SUR IS SOURCE TERM FOR THE SHEAR STRESS
C-----HMOD IS CORRESPONDING TERM TO MODIFY THIS TO GIVE EARLIER
C----- (HANJALIC-LAUNDER) MODEL OF PRESSURE-STRAIN TERM
SU(5,I)=(Z2*CFI2*F(3,I)*DU(I) -F(3,I)*DU(I)+.5*Z1*(
1 (BETA+ALPHA) *F(3,I)+BETA*F(2,I)+(ETA+JAMMA)*F(1,I)
1 + THETA*F(2,I)+ALFPLX*(F(3,I)-F(2,I))*DECAY
2 -2.*CFI2*(F(5,I)+.2/F(1,I))*DU(I)-CF01*FD(1,I)*F(5,I)/F(1,I)
SU(5,I)=(SU(5,I)+SHSRLX)*0.5*(Y(I+1)-Y(I-1))+S5(I)
HMOD=-2.3*(.67*F(1,I)*DU(I)+F(5,I)*F(6,I)/F(1,I))
HMOD=HMOD*.5*(Y(I+1)-Y(I-1))

```

```

IF(K3.EQ.1)SU(5,I)=4M00
DISS=13.*NP3
IF(F(6,I).GE.(DISS).OR.F(6,I).LE.0.)F(6,I)=(DISS)
SU(6,I)=F(6,I)/F(1,I)*(CE1*(-F(5,I))*DU(I)-CE2*F(6,I))
SU(6,I)=SU(6,I)*(Y(I+1)-Y(I-1))*5
SU(8,I)=SA(I)
SU(7,I)=SB(I)
GO TO 1300
1300 SU(1,I)=SU(2,I)=SU(3,I)=SU(4,I)=0.
SU(2,2)=4.*FD(1,2)+YI/3.
SU(2,NP2)=4.*FD(1,NP2)+YE/3.
SU(3,2)=3J(4,2)=-.5*SU(2,2)
SU(3,NP2)=3J(4,NP2)=-.5*SU(2,NP2)
SU(5,2)=3J(5,NP2)=1.
SU(5,1)=3J(5,NP3)=0.
SU(6,1)=3J(6,NP3)=1.
SU(6,2)=SU(5,NP2)=0.
IF(I.LT.P.LE.1)GO TO 29
IF(PREF(5,2).EQ.0..OR.YI.EQ.1..OR.AK.EQ.0.)GO TO 29
IF(PREF(5,NP2).EQ.1..OR.YE.EQ.0.)GO TO 29
SU(5,2)=1.0*(U(2)/PREF(5,2)+(OPDX(2)+PMUREF*SQRT(TAUI)/AK/YI/YI)*
1 (Y(3)-Y(2))
SU(5,NP2)=EM U(NP1)/PREF(5,NP2)*(OPDX(NP2)+PMUREF*SQRT(TAUE)
1 /AK/YI/YE)*(Y(NP2)-Y(NP1))
IF(PREF(6,2).EQ.0..OR.PREF(6,NP2).EQ.0.)GO TO 29
SU(6,2)=1.0*(U(2)/PREF(6,2)*((F(5,2)+F(5,1))**2+.25/TAUI)**1.5/AK/
1 YI/YI+(Y(3)-Y(2))
SU(6,NP2)=EM U(NP1)/PREF(6,NP2)*((F(5,NP1)+F(5,NP2))**2+.25/TAUE)
1 **1.5/AK/YE/YE*(Y(NP2)-Y(NP1))
29 CONTINUE
IF(I.EQ.NP3)GO TO 27
1301 CONTINUE
SU(7,I)=FS(4,I)*DU(I)
IF(TAUI.EQ.0.)TAUI=+.1-15
DUYUT3=Y(NP3)/TAUI**1.5
SD(1,I)=SD(2,I)=SD(3,I)=SD(4,I)=SD(5,I)=SD(6,I)=0.
IF(ISTEP.EQ.3)GO TO 28
C-----SET THE DIFFUSION COEFFICIENTS FOR THE VARIOUS EQUATIONS
PREF(1,I)=PREF(1,1)
PREF(2,I)=1.
PREF(3,I)=1./3.
PREF(4,I)=1.

```

```

PREF(5,I) = .5
PREF(6,I) = CS/CE3
IF(CASED, EQ, 1H1) PREF(3,I) = PREF(5,I) = 1.
IF(CASED, NE, 1H4) GO TO 40
PREF(1,I) = 1.
PREF(2,I) = F(3,I)/F(2,I)
PREF(4,I) = F(3,I)/F(4,I)
PREF(5,I) = F(3,I)/(F(2,I)+F(3,I))
40 CONTINUE
23 CONTINUE
27 CONTINUE
1001 FORMAT(1H ,1X,6G11.4 )
1011 CONTINUE
RETURN
END
*DECK, STRIDE
SUBROUTINE STRIDE(ISW)
COMMON/S/A(6,83),AU(33),B(6,33),BU(33),C(6,83),CU(33),FDIFE(6),
1 FDIFI(6),GE(6),GI(6),ITPF(6),D04,
2 BOMP,PG04P,PG04,PX,THLP,RMIJ2,G04,TTP
COMMON/G/NRAL/AJE(6),AJI(6),CSALFA,DPDX(83),DX,FMU(83),F(6,83),
1 FS(6,83),H,IFIN,INDE(6),INJI(6),ITEP,ITEST,IUTRAP,KEA,KIN,KRAC,
2 N,NEQ,NPH,NP1,NP2,NP3,OM(83),PEI,PMUREF,PREF(6,83),PSIE,PSII,
3 R(83),RHO(83),RME,RMI,RU(83),SD(6,83),SU(9,83),TAUL,TAUI,U(83),
4 XD,XU,Y(83),YE,YI,FD(2,83),EMUL(83)
COMMON/GM4/AK,ALMG,EWALL,IPRINT,FR,PRESS,
1 UEAR,UFAO,KRUF
COMMON/K/ALPHA,BETA,PNU,CFI2,ETA,GAYMA,C1,C2,OMU,CE,CE1,CE2,CE3
COMMON/L/CFI1,CS,ALFANN,CASEP,CASID,THETA,Z1,Z2,Z3,K3,K4,K5,FRA
COMMON/F/D/M5,M6
GO TO (1000,2000,3000), ISW

```

```

C ***** STRIDE 1 *****
1000 IF(ISTEP.GT.0) GO TO 1100
OM(1)=0.
OM(2)=0.
OM(NP2)=1.
OM(NP3)=1.
ONI = .5*CM(3)
OME = .5*(1.-OM(NP1))
BPE=1.
BPI=1.
Y(1)=0.

```

```

      IF(KRAD.EQ.1) GO TO 1100
      DO 1101 I=1, NP3
1001  R(I)=1.
      R25=1.
      RN15=1.
      IF(ITEST.EQ.0) GO TO 9018
      WRITE(6,9010) (R(I),I=1, NP3), R25, RN15
9010  FORMAT(1H, 11F6.3)
9018  CONTINUE
C ----- CALCULATION OF RHO*U 'S -----
1100  DO 1101 I=1, NP3
      IF(RHO(I).GT.0.) GO TO 1101
      WRITE(6,1108) RHO(I), I, RHO(1)
1108  FORMAT(25H NEGATIVE OR ZERO RHO(I)=, 1PE11.3, 6H AT I=, I3, 6X,
      121HSET TO ABS OF RHO(1)=, E11.3)
      RHO(I)=ABS(RHO(1))
1101  RU(I)=RHO(I)*U(I)
      RU3=RU(3)
      RUN1=RU(NP1)
      DO 1102 I=2, NP1
      RU(I)=.5*(RU(I)+RU(I-1))
1102  CONTINUE
      IF(ITEST.EQ.0) GO TO 9019
      WRITE(6,9010) (RU(I),I=1, NP3), RUN1, RU3, PEI
9019  CONTINUE
C ----- CALCULATION OF Y 'S AND R 'S -----
C ----- Y 'S FOR PLANE GEOMETRY -----
      YI=PEI*OMI/(3PI*RU(2))
      Y(3)=YI+PEI*OM(3)/(RU(2)+RU3)
      Y(2)=2.*YI-Y(3)
      DO 1103 I=4, NP1
1103  Y(I)=Y(I-1)+PEI*(OM(I)-OM(I-1))/RU(I-1)
      YN15=Y(NP1)+PEI*(1.-OM(NP1))/(RU(NP1)+RUN1)
      YE=PEI*OMI/(3PEI+RU(NP1))
      Y(NP3)=YN15+YE
      Y(NP2)=2.*YN15-Y(NP1)
      IF(KRAD.EQ.1) RETURN
C ----- Y 'S AND R 'S FOR AXISYMMETRICAL GEOMETRY -----
      IF(CSALFA.EQ.0.) GO TO 1110
C ----- CSALFA NE ZERO -----
      COSD2=.5*CSALFA
      IF(R(1).NE.0.) GO TO 1105

```

C----- R(1)=0.

```
DO 1106 I=2, NP3
Y(I)=SQRT(ABS(Y(I)/COSD2))
1106 R(I)=Y(I)*CSALFA
YI=SQRT(ABS(YI/COSD2))
YN15=SQRT(ABS(YN15/COSD2))
GO TO 1107
```

C----- R(1) NE 0.

```
1105 R1D2=.5*R(1)
R1D2SQ=R1D2*R1D2
DO 1104 I=2, NP3
Y(I)=Y(I)/(R1D2+SQRT(ABS(R1D2SQ+COSD2*Y(I))))
1104 R(I)=R(1)+Y(I)*CSALFA
YI=YI/(R1D2+SQRT(ABS(R1D2SQ+COSD2*YI)))
YN15=YN15/(R1D2+SQRT(ABS(R1D2SQ+COSD2*YN15)))
1107 R25=R(1)+YI*CSALFA
RN15=R(1)+YN15*CSALFA
YE=Y(NP3)-YN15
RETURN
```

C----- CSALFA EQ ZERO

```
1110 DO 1111 I=2, NP3
Y(I)=Y(I)/R(1)
1111 R(I)=R(1)
YI=YI/R(1)
YN15=YN15/R(1)
R25=R(1)
RN15=R(1)
YE=Y(NP3)-YN15
RETURN
```

C***** S T R I D E 2 *****

C----- PRELIMINARIES FOR COEFFICIENTS

```
2000 PX=PEI/DX
G=R4I-RME
PD3=.125*PX
PD4=.25*PX
PG=DX+G
PGD3=.125*PG
PGD4=PGD0+PGD3
RMI02=.5*RMI
GD4=.25+G
BOMP=OM(3)-OM(2)
PGOMP=PGD4+BOMP
P4OMP=PD4+BOMP
```



```

C ----- GRID POINT 2
C ----- TAUI, BPI, T1
IF(KIN.NE.1) GO TO 2001
CALL WF(J,1,2,3,BPI,T1,TAUI)
GO TO 2002
2001 T1=0.
IF(KRAD.EQ.1) BPI=.33333+.66667*RU(1)/RU(2)
IF(KRAD.EQ.1) BPI=(R(1)*(5.*RU(1)+RU(2))+3.*R25+
1 (RU(1)+RU(2)))/6./(R(1)+R25)/RJ(2)
C ----- BOUNDARY COEFFICIENTS FOR VELOCITY
2002 HLP=R MID2-GD4*(OM(2)+CM(3))
AHL=ABS(HLP)
THLP=HLP+HL
TP=EM UL(2)
IF(U(2).NE.U(3))TP=TP-(F(5,2)+F(5,3))/2./(U(3)-U(2))
TTP=TP+AHL+ABS(TP-AHL)
AD=TTP-THLP-T1-PGOMP
BD=2.*(T1+RMI)
CD=P4OMP*(3.*U(2)+U(3))-DPDX(2)*(R(1)+R25)*YI
TTP=EM UL(2)+AHL+ABS(EM UL(2)-AHL)
DU=AD+BD+PX*BOMP
AU(2)=AD/JJ
BU(2)=BD/JJ
CU(2)=CD/JJ
TP=EMU(2)
C ----- BOUNDARY COEFFICIENTS FOR F'S
IF(NEQ.EQ.1) GO TO 2304
DO 2300 J=2,NPH
TPF2=TP/P2=F(J,2)
TTPF(J)=TTPF2+AHL+ABS(TPF2-AHL)
IF(KIN.NE.1) GO TO 2301
CALL WF(J,1,2,3,FDIFI(J),T1F,GI(J))
IF(I DI(J).EQ.2) GO TO 2303
AJI(J)=GI(J)*(F(J,1)-.5*(F(J,2)+F(J,3))-FDIFI(J))
GO TO 2302
2301 T1F=0.
FDIFI(J)=0.
C ----- COEFFICIENTS
2302 ADF=TTPF(J)-THLP-T1F-PGOMP+.5*SD(J,2)
BDF=2.*(T1F+RMI)
DF=ADF+BDF+PX*BOMP-2.*SD(J,2)
T=-T1F*FDIFI(J)
GO TO 2305

```

```

2303 ADF=TTPF(J)-THLP-PGOMP+.5*SD(J,2)
      BDF=J.
      DF=ADF+PX*3OMP-2.*SD(J,2)+RMI*2.
      T=RMI*F(J,1)+AJI(J)*R(1)
2305 TT=3.*F(J,2)+F(J,3)
      CDF=P4OMP*TT+2.*(T+SU(J,2))
      IF(J.EQ.5) A(J,2)=ADF/DF
      A(J,2)=0.
      B(J,2)=-1.
      IF(J.EQ.5) C(J,2)=ADF/DF
      IF(J.EQ.5) D(J,2)=BDF/DF
2308 IF(J.EQ.5) C(J,2)=CDF/DF
      C(1,2)=3.5*TAUI
      C(2,2)=1.19*C(1,2)
      C(3,2)=.255*C(1,2)
      C(4,2)=0.55*C(1,2)
      IF(ISTEP,3E,1) C(6,2)=TAUI**1.5/AK/YI*2.
      IF(ISTEP,7,0) C(8,2)=0.
C ----- GRID POINT NP2
C ----- TAUE, 3PE, TNP3
2304 IF(KEX.NE.1) GO TO 2003
      CALL WF(J, NP3, NP2, NP1, 3PE, TNP3, TAUE)
      GO TO 2311
2003 TNP3=0.
      IF(KRAD.EQ.0) 3PE=.33333+.56567*RU(NP3)/RU(NP1)
      IF(KRAD.NE.1) 3PE=(R(1P3)*(E.*RU(NP3)+RU(NP1))+3.*RN15*
1      (RU(NP3)+RU(NP1)))/6./(R(NP3)+RN15)/RU(NP1)
C ----- BOUNDARY COEFFICIENTS FOR VELOCITY
2311 BOMM=OM(NP2)-OM(NP1)
      HLM=RMID2-GO4*(CM(NP1)+OM(NP2))
      AHLM=ABS(HLM)
      THLM=HLM+ILM
      TM=EM UL(NP1)
      IF(U(NP2).LE.U(NP1)) TM=TM-(F(5,NP1)+F(5,NP2))/2./(U(NP2)-U(NP1))
      TTM=TM+AHLM+ABS(TM-AHLM)
      PGOMM=PGO4*3OMM
      P4OMM=P4O4*3OMM
      AD=2.*(TNP3-RME)
      BD=TTM+THLM-TNP3-PGO14
      CD=P4OMM*(3.*U(NP2)+J(NP1))-JPDJ(NP2)+(RN15+R(NP3))*YE
      DU=AD+BD+PX*BOMM
      AU(NP2)=AJ/DU

```

```

BU(NP2)=3J/5U
CU(NP2)=CJ/5U
IF(NEQ.EG.1) RETURN

```

C ----- BOUNDARY COEFFICIENTS FOR F'S

```

      TM=EMU(NP1)
DO 2320 J=2,NPH
  TMF=TM/PRIF(J,NP1)
  TTMF=TMF+AHLM+ABS(TMf-AHLM)
  IF(KEX.NE.1) GO TO 2311
  CALL WF(J,NP3,NP2,NP1,FDIFE(J),TNP3F,GE(J))
  IF(INDE(J).EQ.2) GO TO 2313
  AJE(J)=GE(J)*(.5*(F(J,NP2)+F(J,NP1))+FDIFE(J)-F(J,NP3))
  GO TO 2312
2311 TNP3F=.
  FDIFE(J)=.

```

C ----- COEFFICIENTS

```

2312 ADF=2.*(TNP3F-RME)
      BDF=TTMF+HLM-TNP3F-PGOMM+.5*SD(J,NP2)
      DF=ADF+6JF+PX*3OMM-2.*SD(J,NP2)
      T=-TNP3F+FDIFE(J)
      GO TO 2315
2313 ADF=J.
      BDF=TTMF+HLM-PGOMM+.5*SD(J,NP2)
      DF=BDF+PX*3OMM-2.*SD(J,NP2)-RME*2.
      T=-RME*F(J,NP3)-AJE(J)*R(NP3)
2315 TT=3.*F(J,NP2)+F(J,NP1)
      CDF=P4OMM*TT+2.*(T+SU(J,NP2))
      A(J,NP2)=.
      B(J,NP2)=3JF/DF
      B(J,NP2)=J.
      IF(J.EQ.5) A(J,NP2)=ADF/DF
      IF(J.EQ.5) B(J,NP2)=3JF/DF
2320 IF(J.EQ.5) C(J,NP2)=CDF/DF
      C(1,NP2)=3.5*TAUE
      C(2,NP2)=1.19*C(1,NP2)
      C(3,NP2)=.251*C(1,NP2)
      C(4,NP2)=.55*C(1,NP2)
      IF(ISTEP.1) C(6,NP2)=TAUE**+1.5/AK/YE*2.
      IF(ISTEP.1) C(6,NP2)=.
RETURN

```

C***** STRIDE 3 *****

3000 CALL HELP

C-----THE HELP SUBROUTINE CONTAINS THE STRIDE (3) OF GENMIX

C-----AS OTHERWISE THE STRIDE SUBROUTINE IS DISPROPORTIONATELY

C-----LONG AND CAUSES INEFFICIENT USE OF THE COMPUTER

RETURN

END

*DECK, HELP

SUBROUTINE HELP

COMMON/S/A(6,83),AU(83),B(6,33),BU(83),C(6,83),CU(83),FDIFI(6),

1 FDIFI(6),GI(6),GI(6),ITPF(6),PG4,

2 BOMP,PGOIP,PGO4,PX,THLP,RMID2,GD4,TTP

COMMON/GENERAL/AJE(6),AJI(6),CSALFA,JPOX(43),OX,EMU(53),F(6,83),

1 FS(6,83),I,IFIN,INDE(6),INDI(6),ISTEP,ITEST,IUTRAP,KTX,KIN,KRAD,

2 N,NEQ,NPH,NP1,NP2,NP3,OM(83),PEI,PHUREF,PREF(6,83),PSIE,PSII,

3 R(83),RHO(83),RME,RMI,RU(33),S(6,33),SU(3,53),TAUE,TAUI,U(83),

4 XD,XU,Y(83),YE,YI,FD(2,83),EMUL(83)

COMMON/K/ALPHA,BETA,PNU,CFI2,ETA,GAMMA,C1,C2,CMU,CE,CE1,CE2,CE3

COMMON/L/CFI1,CS,ALFA IN,CASE3,CASED,THETA,Z1,Z2,Z3,K3,K4,K5,FRA

COMMON/F()/M5,M6

DO 3005 I=3,NP1

BOMM=BOMP

BOMP=OM(I+1)-OM(I)

BO1=BOMM+BOMP

BO173=BO1*3.

PGO11=PGOMP

PGOMP=PGO4*BOMP

PJOM=PX+3OM

THLM=THLP

HLP=RMID2-GD4+(OM(I+1)+OM(I))

THLP=HLP+HLP

AHLP=ABS(HLP)

TTM=ITP

TP=EMUL(I)

TTP=IP+AHLP+ABS(TP-AHLP)

AD=TTP-THLP-PGOMP

BD=TTM+THLP-PGOMM

SUUA=F(5,I-1)-F(5,I+1)

CU=PGO4*(3OMT3*U(I)+3OMP*U(I+1)+3OMM*U(I-1))-

1 DPCX(I)*R(I)+(Y(I+1)-Y(I-1))+SUUA

DU=AD+BD+PBOM

AU(I)=AD/DU

BU(I)=BD/DU

CU(I)=CD/CU

C----- START OF J LOOP

```

          IF (NEQ.EQ.1) GO TO 3005
          DO 3004 J=2,NPH
3002  TTMF=TTPF(J)
3003  TPF=EM U(I)/PRIF(J,I)
          TTPEF(J)=TPF+AHLP+A3S(TPF-AHLP)
          AD=TTPEF(J)-THLP-PGOMP
          BD=TTMF+THLM-PGOMM
          CD=PD4*(DO IT3+F(J,I)+BOMP*F(J,I+1)+BOMM*F(J,I-1))
          DD=CD+2.*SU(J,I)
          DF=AD+3D+3OM-2.*SD(J,I)
          A(J,I)=AD/DF
          B(J,I)=3D/DF
          C(J,I)=CD/DF

```

```

3004  CONTINUE
3005  IF(ITEST.EQ.0) GO TO 3013
          WRITE(6,9001) (AU(I),I=2,NP2)
          WRITE(6,9002) (BU(I),I=2,NP2)
          WRITE(6,9003) (CU(I),I=2,NP2)
9001  FORMAT(7H AU(I) ,11F6.3 )
9002  FORMAT(7H BU(I) ,11F6.3 )
9003  FORMAT(7H CU(I) ,11F6.3 )
          IF (NEQ.EQ.1) GO TO 9013
          DO 9004 J=2,NPH
          WRITE(6,9004) (A(J,I),I=2,NP2)
          WRITE(6,9005) (B(J,I),I=2,NP2)
          WRITE(6,9006) (C(J,I),I=2,NP2)
9004  FORMAT(8H A(J,I) ,11F6.3 )
9005  FORMAT(8H B(J,I) ,11F6.3 )
9006  FORMAT(8H C(J,I) ,11F6.3 )
9013  CONTINUE

```

C-----
 IF(KIN.EQ.2.AND.RU(1).NE.0.) U(1)=U(1)-DPDX(1)*DX/RU(1) ;
 IF(KEX.EQ.2.AND.RU(NP3).NE.0.) U(NP3)=U(NP3)-DPDX(NP3)*DX/RU(NP3)
 C----- SOLVE FOR DOWNSTREAM U 'S -----

```

3047  BU(2)=BU(2)+U(1)+CU(2)
          DO 3048 I=3,NP2
          T=1.-BU(I)*AU(I-1)
          IF(T.EQ.0) PRINT 1024,T,ISTEP,I,AU(I-1),BU(I)
1024  FORMAT(* NOTE T FOUND EQUAL TO *F6.7*AT STEP *
          1I3* NODE *I2/* AU(I-1)=*F6.3* , BU(I)=*F6.3)
          IF(T.EQ.0) T=1.E-15
          AU(I)=AU(I)/T

```

```

3048 BU(I)=(BU(I)+BU(I-1)+CU(I))/T
DO 3050 IDASH=2,NP2
I=N+4-IDASH
U(I)=AU(I)*U(I+1)+BU(I)
C TEST FOR NEGATIVE VELOCITY
C IUTRAP=0 TO ACTION, =1 SET U'S TO ZERO, =2 PRINT AND STOP
IF(IUTRAP.EQ.0) GO TO 3050
IF(I.EQ.2.OR.I.EQ.NP2.OR.U(I).GE.0.) GO TO 3050
IF(IUTRAP.EQ.1) GO TO 3051
IFIN=1
ITEST=1
WRITE(6,3120)
3120 FORMAT(10X,33HAT LEAST ONE VELOCITY IS NEGATIVE)
RETURN
3051 U(I)=1.E-15
3050 CONTINUE
IF(KIN.EQ.3) U(1)=.5*(U(2)+U(3))
IF(KEX.EQ.3) U(NP3)=.5*(U(NP1)+U(NP2))
72 IF(N.Q.EQ.1) GO TO 3160
DO 3320 J=2,NPH
C----- SOLVE FOR DOWNSTREAM F 'S -----
B(J,2)=B(J,2)+F(J,1)+C(J,2)
DO 3148 I=3,NP2
T=1.-B(J,I)+A(J,I-1)
IF(T.EQ.0.) PRINT 1023,J,I,ISTEP
1023 FORMAT(* SERIOUS WARNING - T FOUND ZERO AT LOCATION W1*
1* AND REPLACED BY 1.E-15,EQ 4 *I1*, NODE *I2*, STEP *I3)
C***** LOCATION W111111111111111111111111111111*****
IF(T.EQ.0.) T=1.E-15
A(J,I)=A(J,I)/T
3148 B(J,I)=(B(J,I)+B(J,I-1)+C(J,I))/T
DO 3150 IDASH=2,NP2
I=N+4-IDASH
3150 F(J,I)=A(J,I)*F(J,I+1)+B(J,I)
GO TO(3210,3220,3230)KIN
3210 IF(INDI(J).EQ.2) F(J,1)=FDIFI(J)+.5*(F(J,2)+F(J,3))+AJI(J)/GI(J)
GO TO 3220
3230 F(J,1)=.5*(F(J,2)+F(J,3))
3220 GO TO(3310,3320,3330)KEX
3310 IF(INDE(J).EQ.2) F(J,NP3)=FDIFE(J)+.5*(F(J,NP2)+F(J,NP1))
1 - AJE(J)/GE(J)
GO TO 3320
3330 F(J,NP3)=.5*(F(J,NP1)+F(J,NP2))

```

```

3320 CONTINUE
1020 FORMAT(+U1: +F3.1* AT +I3*(+I2+)* )
1021 FORMAT(+U2: +F3.1* AT +I3*(+I2+)* )
1022 FORMAT(+U3: +F3.1* AT +I3*(+I2+)* )
3060 XU=XD
      PSII=PSII-RMI*DX
      PSIE=PSIE-RME*DX
      PEI=PSII-PSII
C-----THE LOOP WHICH NOW FOLLOWS IS FOR AUTOMATIC DEBUGGING
C-----PURPOSES...THE RESULTS GENERATED SHOULD NOT BE REGARDED
C-----AS SATISFACTORY UNTIL THEY HAVE BEEN REPRODUCED WITHOUT ITS
C-----USE...ANY RESETTING SHOULD BE PERFORMED AT THE OUTSET OF THE
C-----NEXT RUN.
      DO 3061 I=1, NP3
      IF(ISTEP.LE.20) GO TO 1025
      IF(F(2,I).LE.0.) PRINT 1021, F(2,I), ISTEP, I
      IF(F(3,I).LE.0.) PRINT 1022, F(3,I), ISTEP, I
      IF(F(4,I).LE.0.) PRINT 1022, F(4,I), ISTEP, I
1025 CONTINUE
      IF(F(1,I).GE.0.) GO TO 3062
      WRITE(6,9015) ISTEP, I, F(1,I)
      F(1,I)=1.
9015 FORMAT(+WARNING--AT STEP*I4+, NODE*I4+, A VALUE OF*
1 1X, PE11.3, 2X, +WAS FOUND FOR K AND REPLACED BY UNITY*)
      MS=MS+1
      IF(MS.NE.20) GO TO 3064
      FRA=.2*FRA
      PRINT 9017, FRA
9017 FORMAT(+AS THE PREVIOUS ADJUSTMENT DID NOT WORK, FRA HAS NOW*
1 * BEEN RESET TO +,G11.4)
3064 CONTINUE
      IF(MS.NE.5) GO TO 3062
3062 CONTINUE
3061 CONTINUE
      ISTEP=ISTEP+1
      RETURN
      END

```

```

SUBROUTINE WF(J,I1,I2,I3,OUT1,OUT2,OUT3)
COMMON/GENERAL/AJE(6),AJI(6),CSALFA,JPDX(83),DX,EMU(33),F(6,33),
1 FS(6,83),H,IFIN,INDE(6),INJI(6),ISTEP,ITEST,IUTRAP,KEX,KIN,KRAD,
N N,NEQ,NPH,NP1,NP2,NP3,OM(33),PEI,PMURF,PREF(6,83),PSIE,OSII,
F R(83),RHO(83),RME,RMI,RU(83),SD(6,83),SU(9,83),TAUE,TAUI,U(83),
N XD,XU,Y(33),YE,YI,FJ(2,83),EMUL(33)
COMMON/G41/AK,ALMG,EWALL,IPRINT,FR,PRESS,
N USAR,U=AC,
KRUF
COMMON/GM4A/RIBHI
COMMON/K/ALPHA,BETA,PNU,OFI2,ETA,GAMMA,C1,C2,CMU,CE,CE1,CE2,CE3
COMMON/L/DFI1,CS,ALFANH,CASED,CASED,THETA,Z1,Z2,Z3,K3,K4,K5,FRA
COMMON/ABO/DOU(33)
C EFFECTS OF PRESSURE GRADIENT, MASS TRANSFER AND
C RADIUS VARIATION ARE NEGLECTED
C FOR VELOCITY, OUT1=3P, OUT2=T, OUT3=TAU
C FOR F'S, OUT1=FIDIF, OUT2=T, OUT3=S

DATA SHALE/.04/
I25=I3-1/I1
JDASH=J+1
GO TO (100,200,250,299,299,299,299,299), JDASH
----- VELOCITY
100 UREF=.5*(U(I2)+U(I3))
RHOREF=.5*(RHO(I1)+.25*(RHO(I2)+RHO(I3)))
RREF=.5*(R(I2)+R(I3))
VREF=EMU(I1)
YREF=YI+(YE-YI)*OM(I1)
RE=UXREF+RHOREF*YREF/VREF
RRURREF=RRREF+RU(I25)
----- LOG LAW

*****
MODIFICATION FOR EITHER OR BOTH WALLS TO BE ROUGH *****
*****
IF NO WALL ROUGH PUT KRUF = 0
IF EWALL IS ROUGH PUT KRUF=1
IF IWALL IS ROUGH PUT KRUF=2
IF BOTH WALLS ARE ROUGH PUT KRUF=3
*****
KRUF AND RIBHI SHOULD BE SET IN CHAPTER ONE OF MAIN AS THEY ARE IN CCM
*****

```



```

C      CAPP=AK
      CRUF=3.5
C      IF((KRUF.NE.1.OR.I2.NE.NP2).AND.(KRUF.NE.2.OR.I2.NE.2).AND.
1      (KRUF.NE.3.OR.I2.NE.NP2).AND.(KRUF.NE.3.OR.I2.NE.2)) GO TO 9990
      SHALF=ALOG(YREF/RISHI)/CAPP + CRUF
      SHALF=1./SHALF
      GO TO 102
9990  CONTINUE
C      *****
      IF(RE.LT.120.) GO TO 110
      ER=RE*EWALL
      NIT=J
101   SHALF1=SHALF
      SHALF=AK/ALOG(ER*SHALF)
      IF(ABS(SHALF -SHALF1).LT..0001.OR.NIT.GT.20) GO TO 112
      NIT=NIT+1
      GO TO 101
102   S=SHALF**2
      OUT1=AK/(AK+SHALF)
      GO TO 103
C      ----- LAMINAR FLOW
110   S=1./RE
      OUT1=.5
      EM U(I25)=VREF*REFF/ABS(Y(I3)-Y(I2))
103   OUT2=S*RXJREF
      OUT3=OUT2*JREF/R(I1)
      RETURN
C      -----
200   OUT1=1.000000
      OUT2=1.000000
      OUT3=1.000000
      RETURN
      END

```

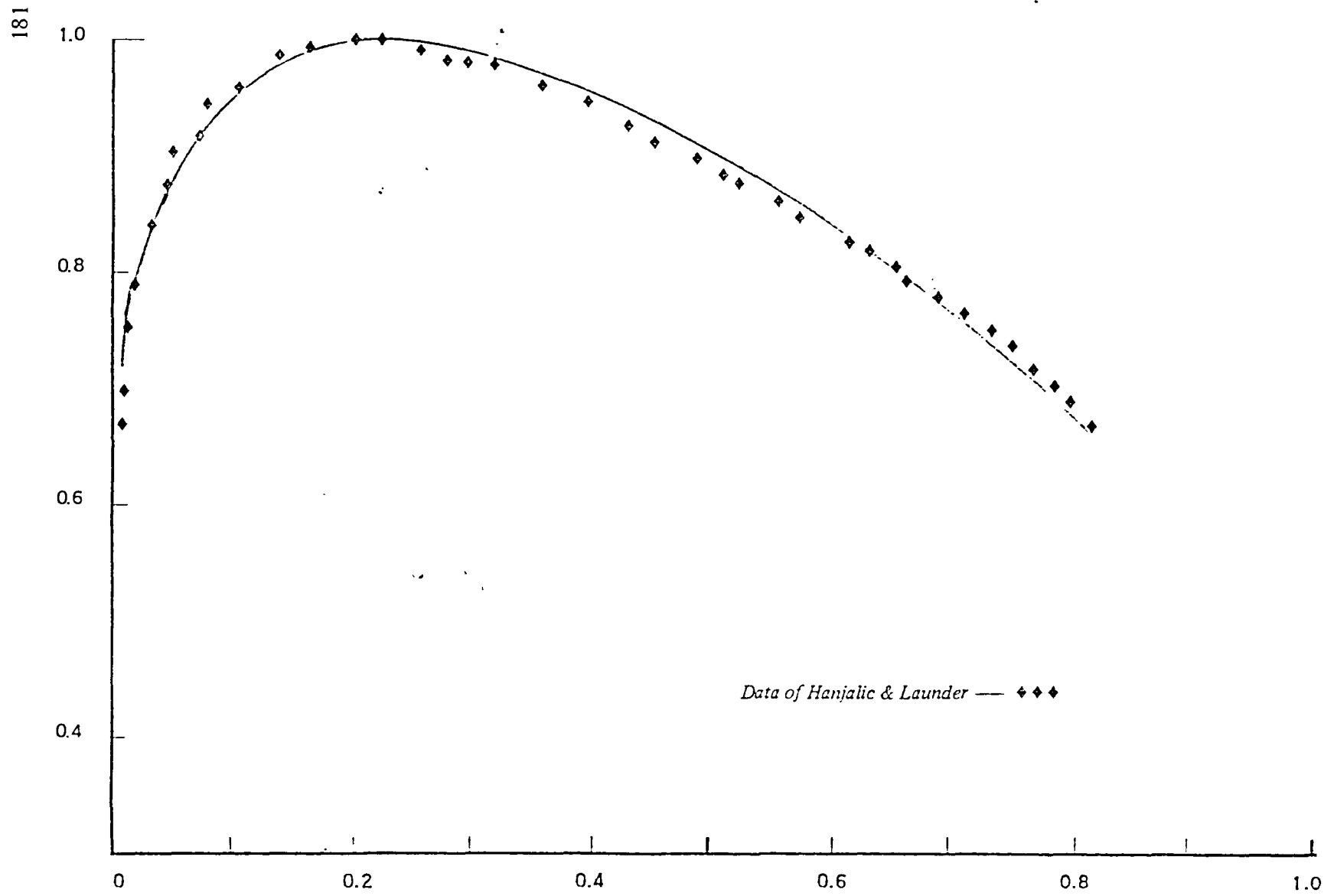


Figure 6.1 Asymmetric plane channel: mean velocity profile Model 1A

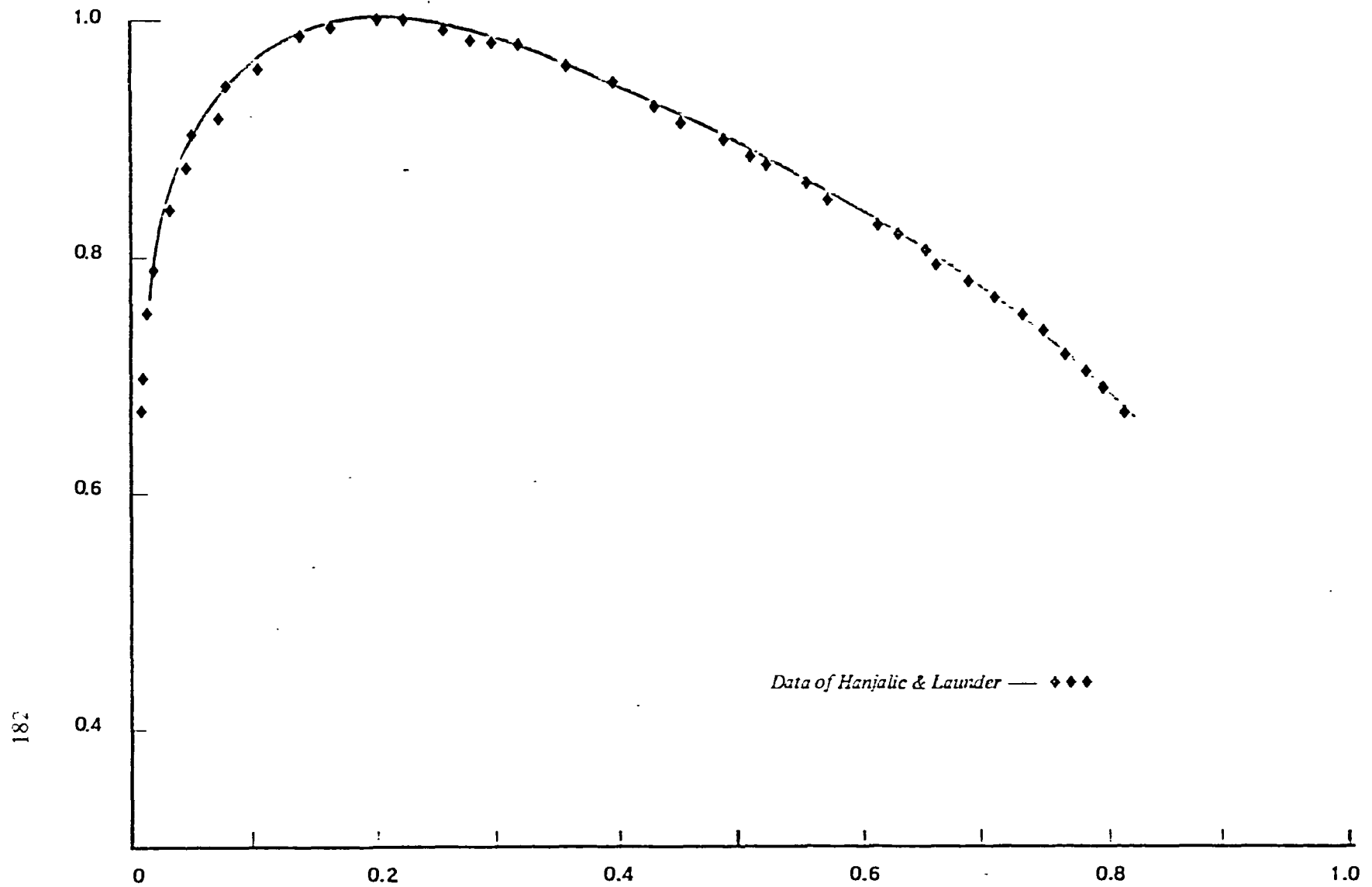


Figure 6.2 Asymmetric plane channel: mean velocity profile Model 1B

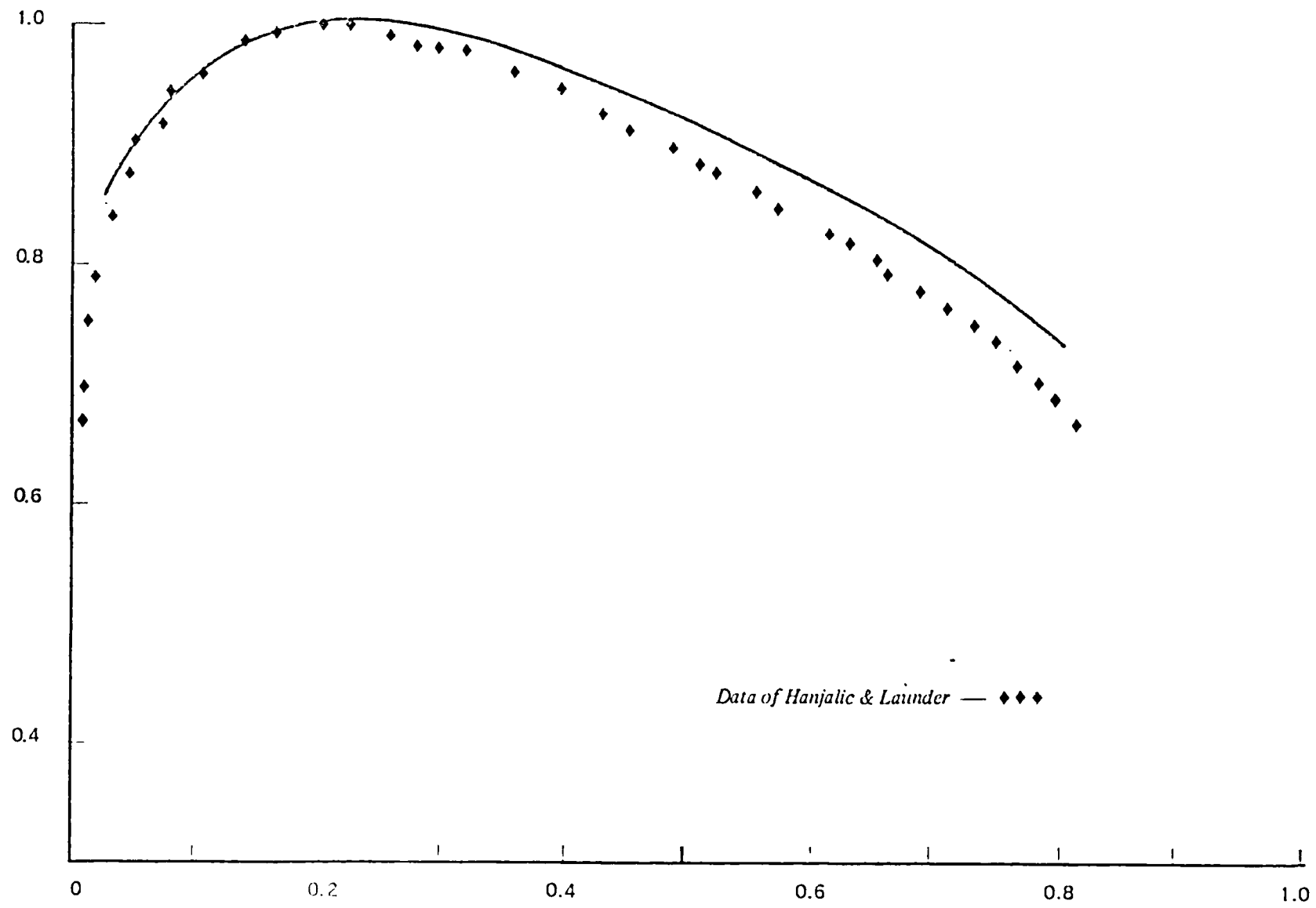


Figure 6.3 Asymmetric plane channel: mean velocity profile Model 2A

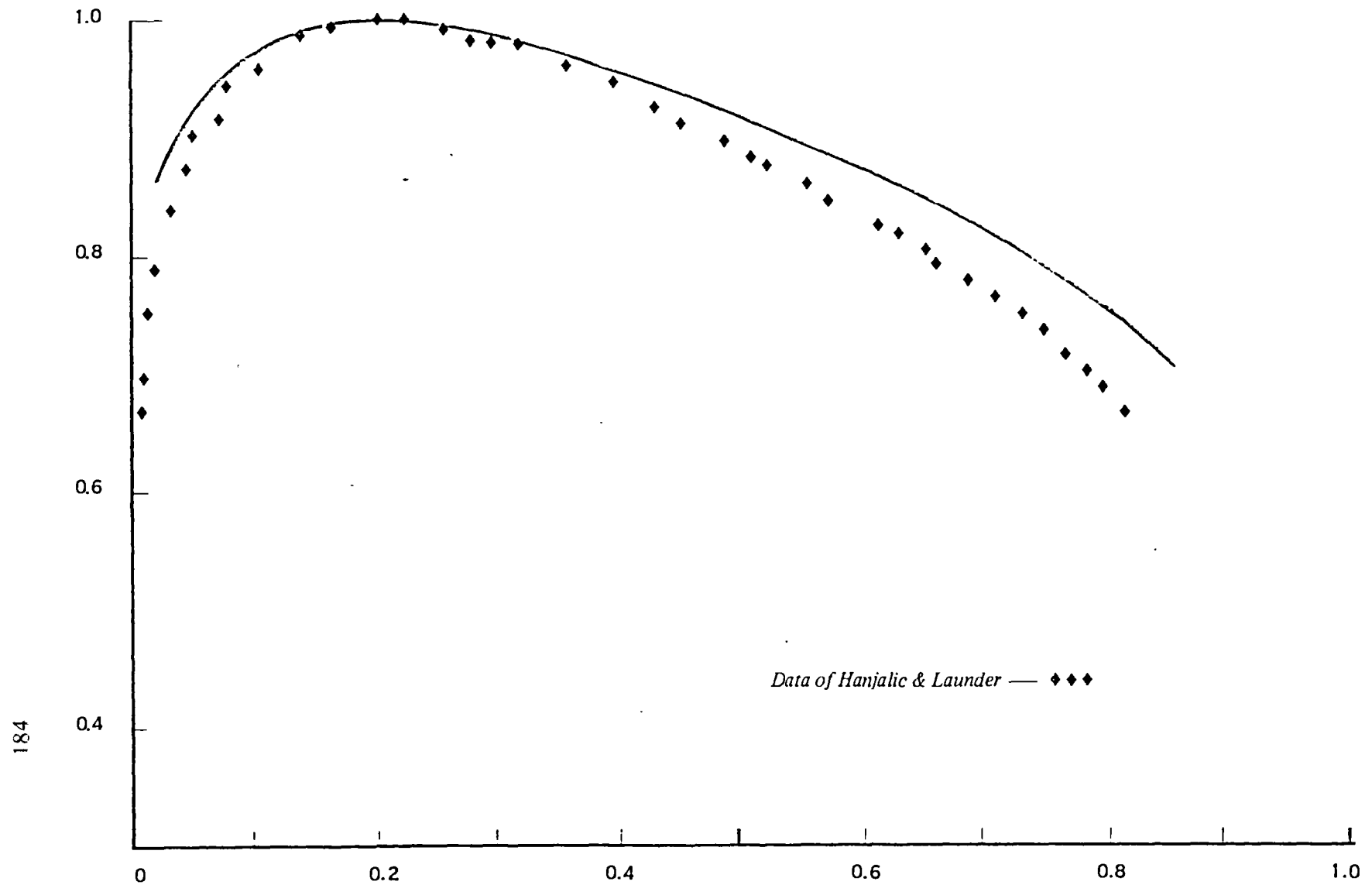


Figure 6.4 Asymmetric plane channel: mean velocity profile Model 2B

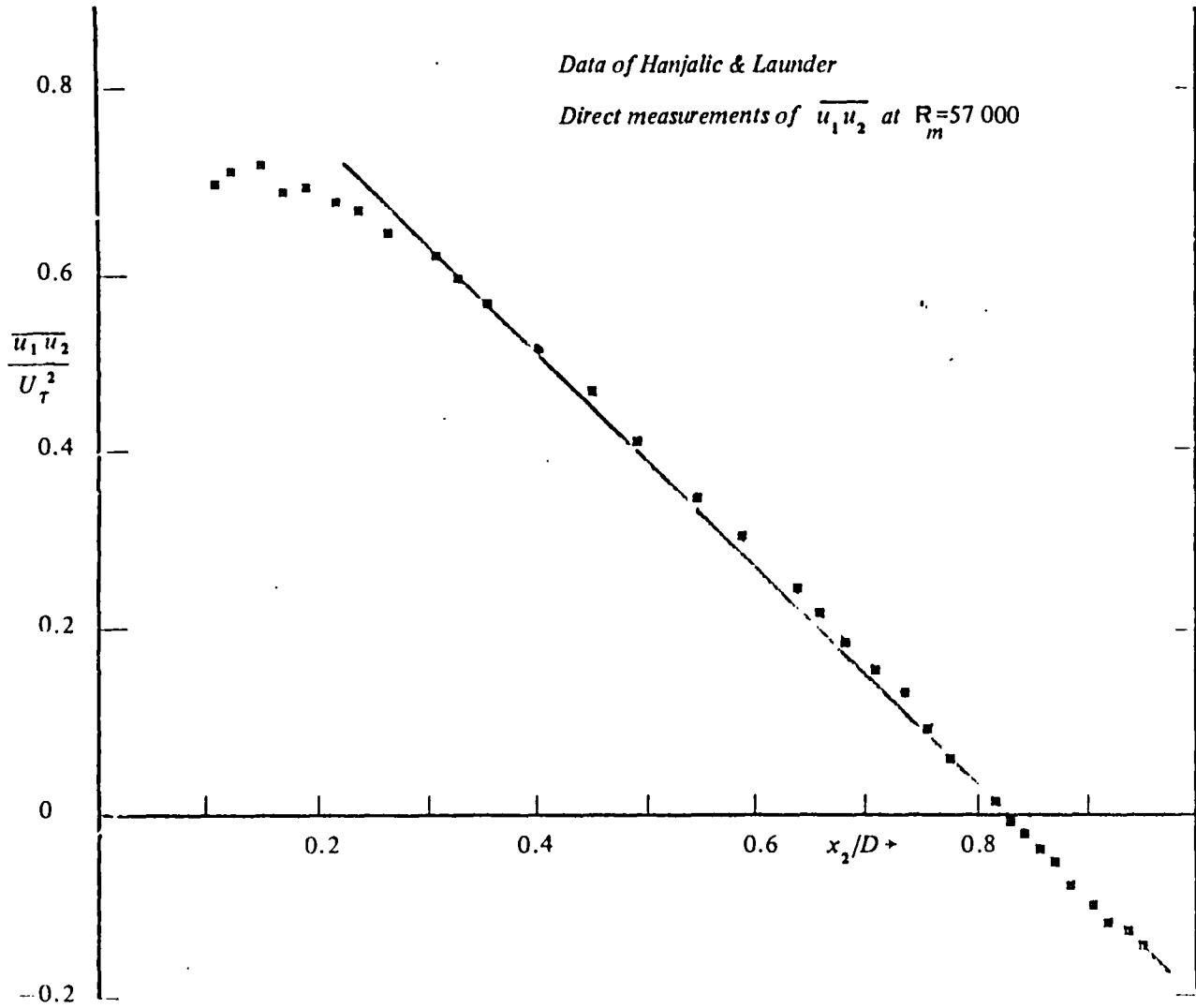
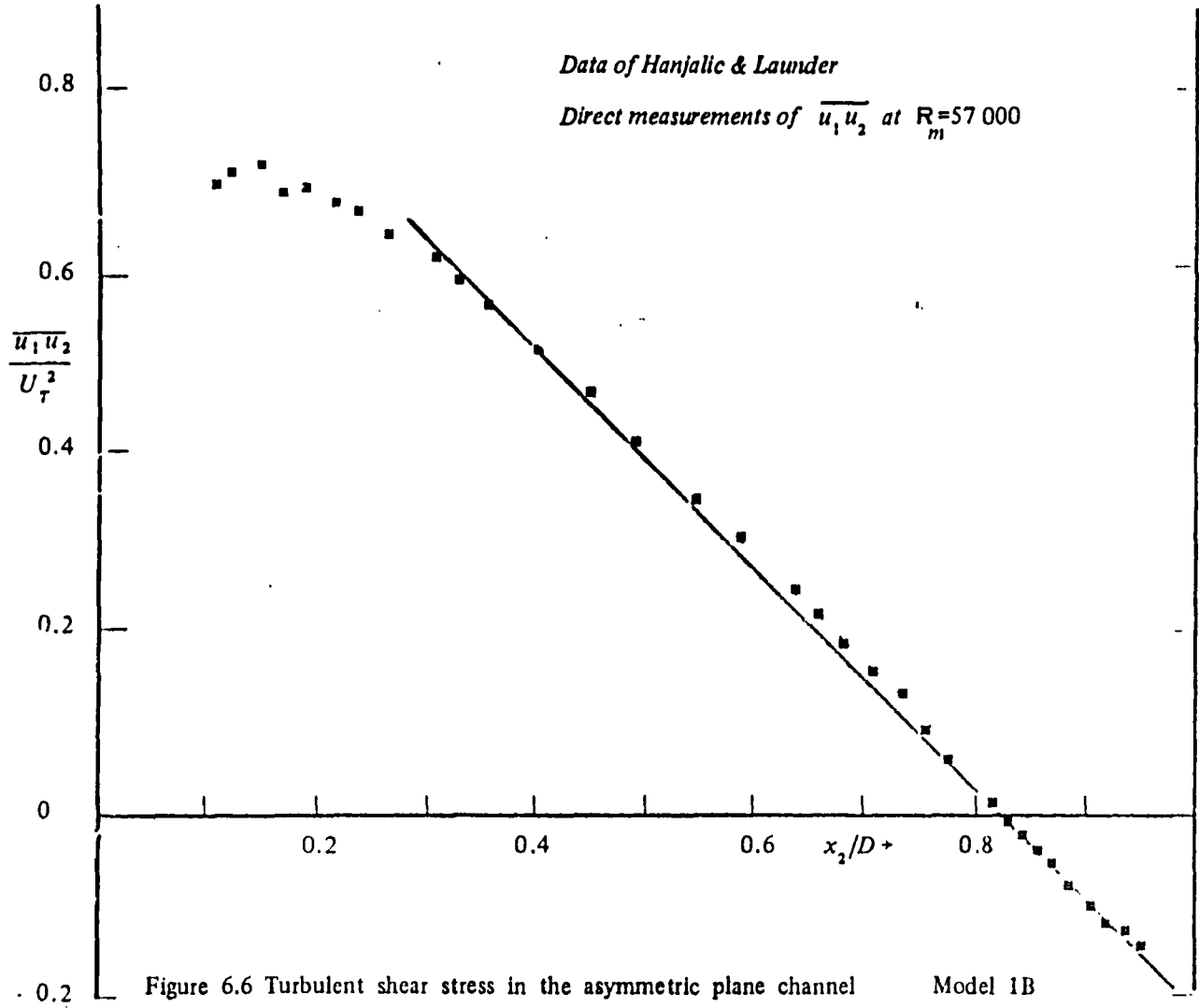


Figure 6.5 Turbulent shear stress in the asymmetric plane channel

Model 1A



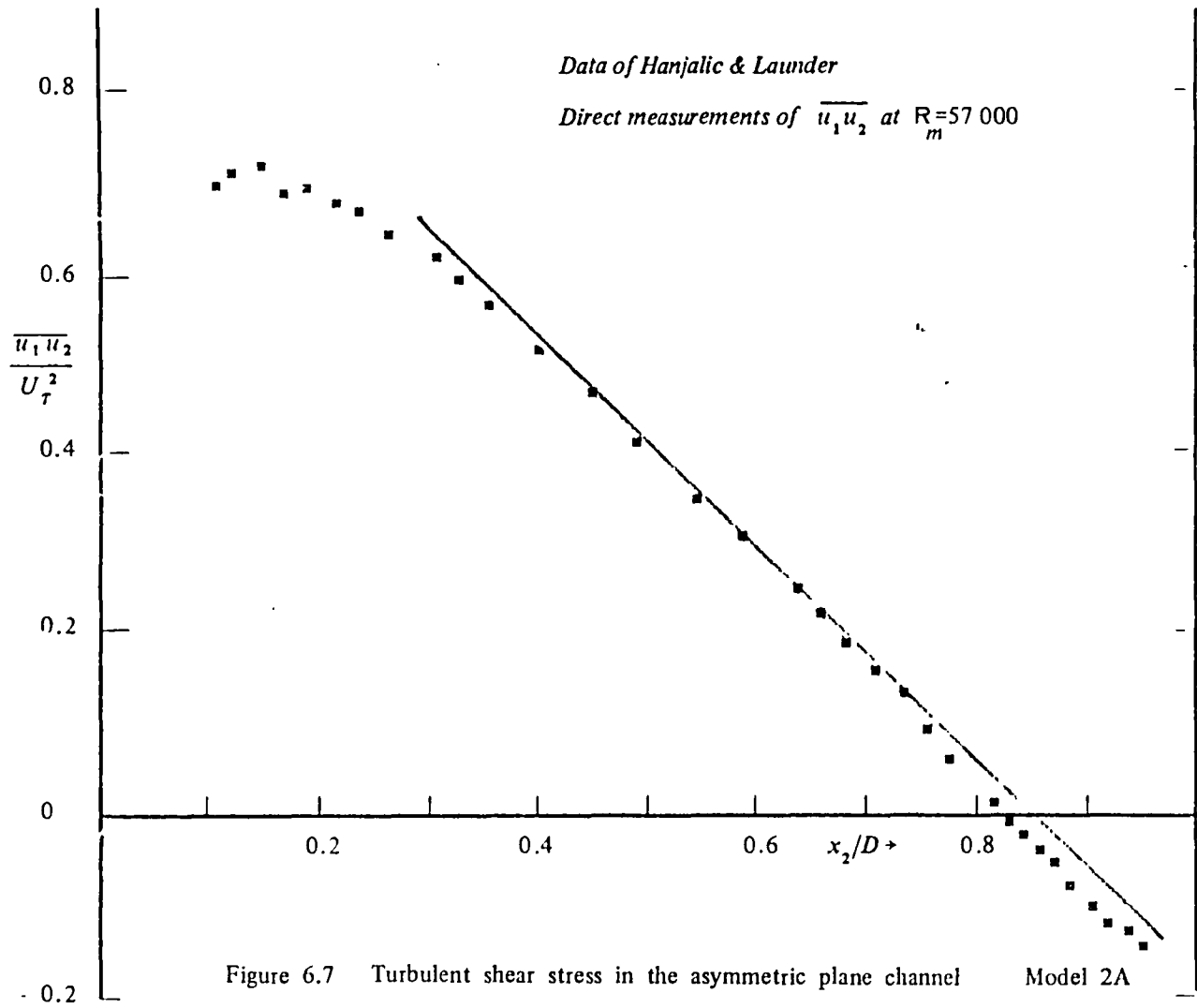


Figure 6.7 Turbulent shear stress in the asymmetric plane channel

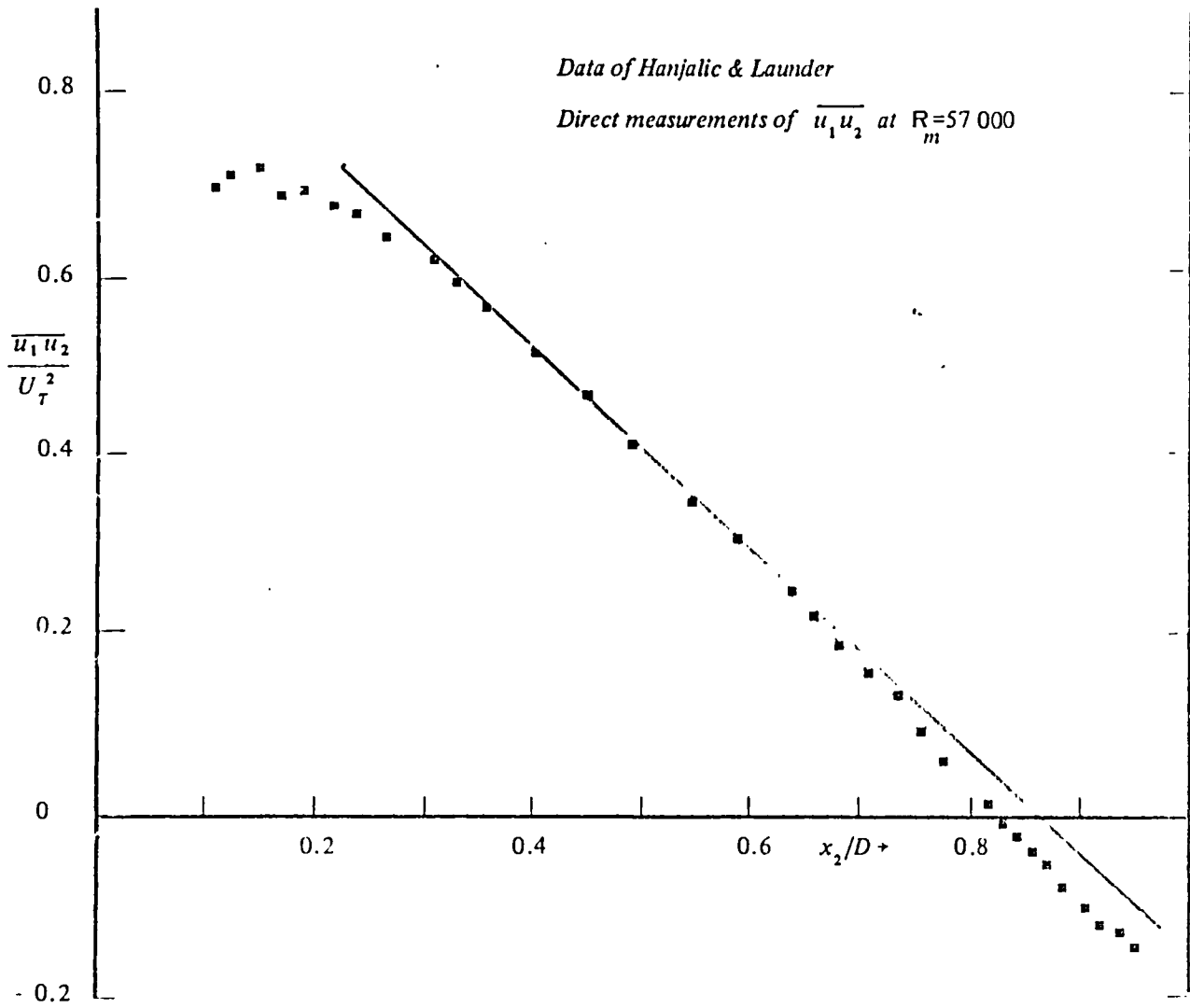


Figure 6.8 Turbulent shear stress in the asymmetric plane channel Model 2B

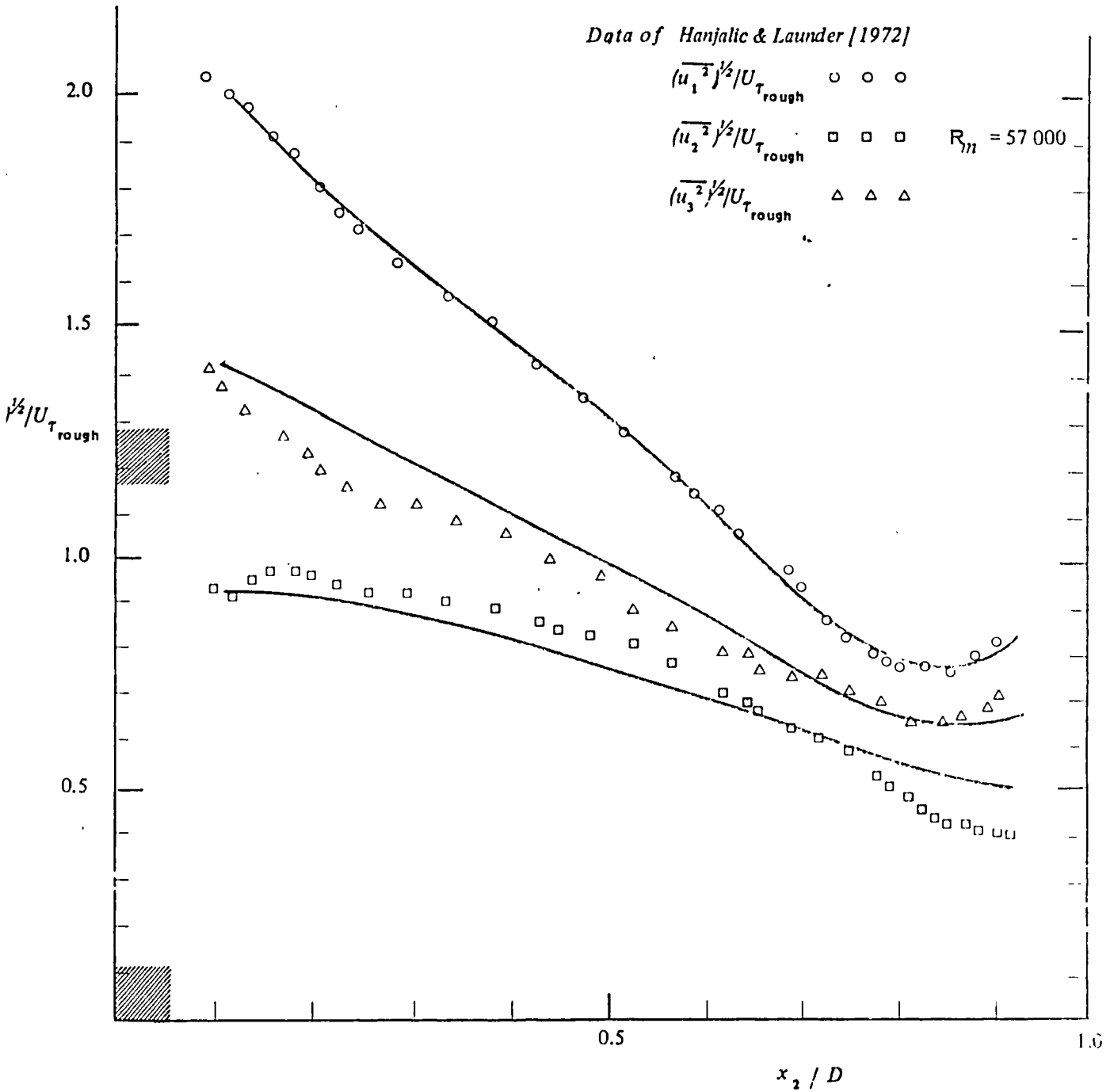


Figure 6.9
 Asymmetric Channel: Turbulence Intensities.
 Model 1A

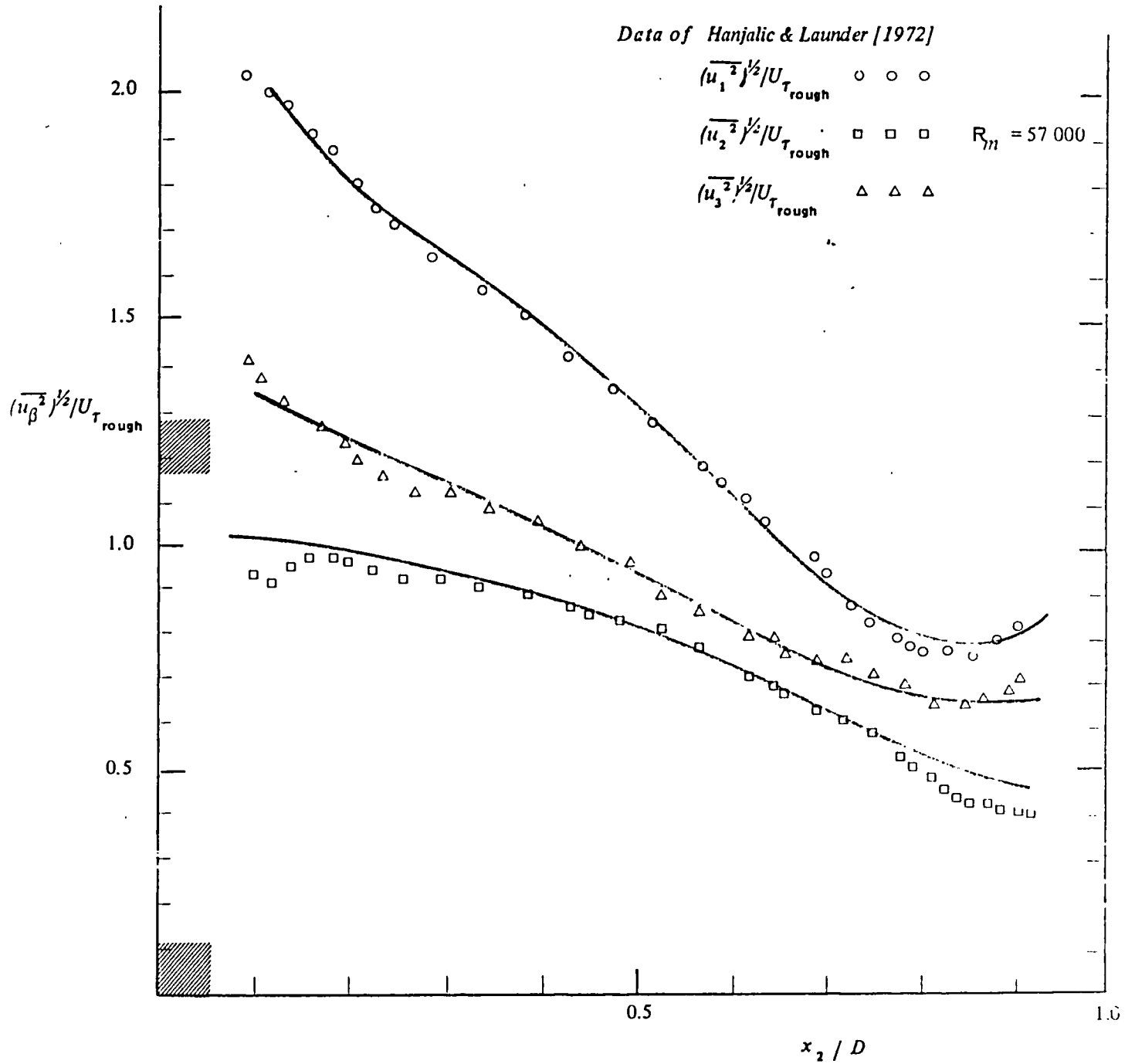


Figure 6.10
 Asymmetric Channel: Turbulence Intensities.
 Model 1B

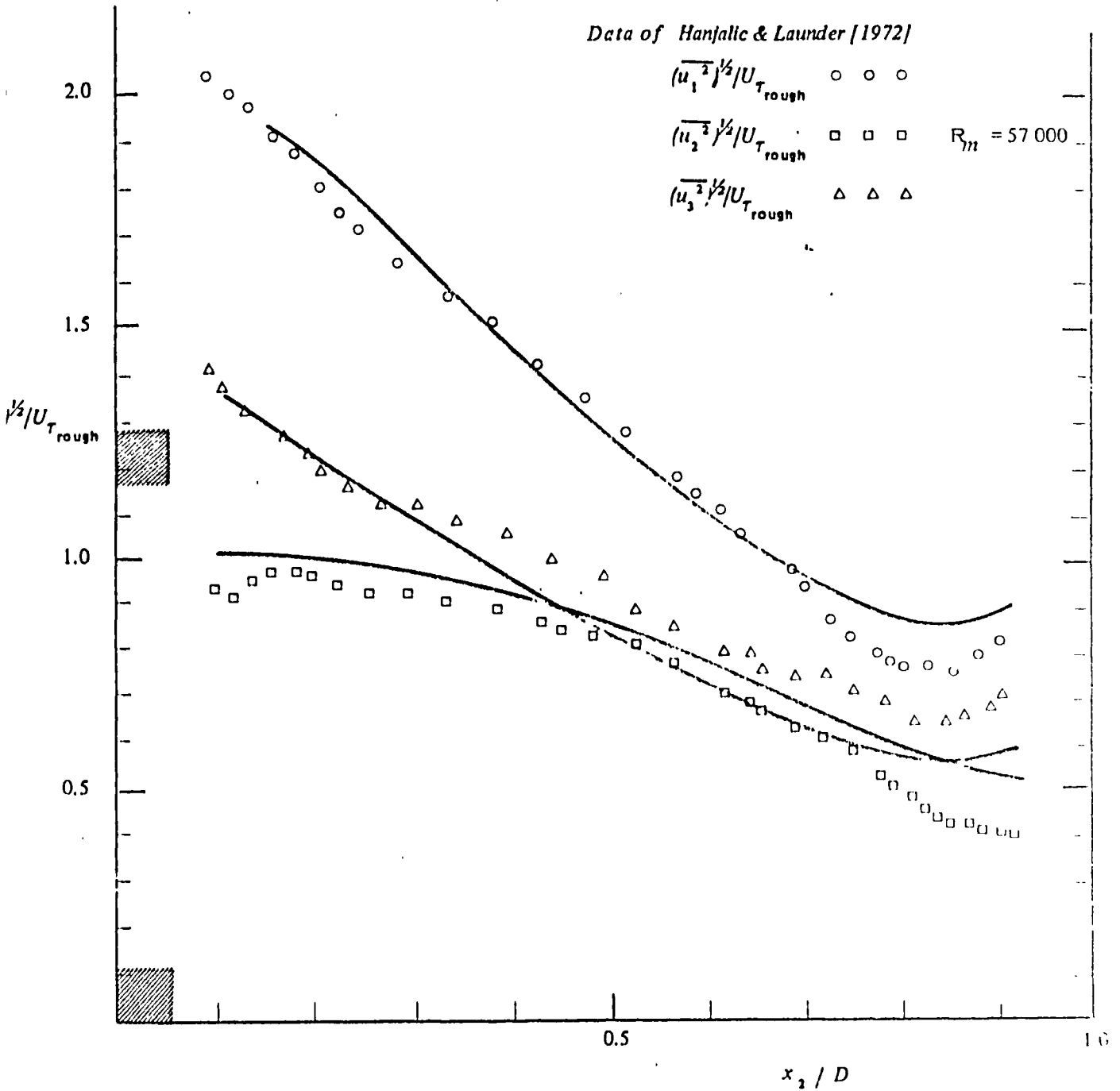


Figure 6.11
 Asymmetric Channel: Turbulence Intensities.
 Model 2A

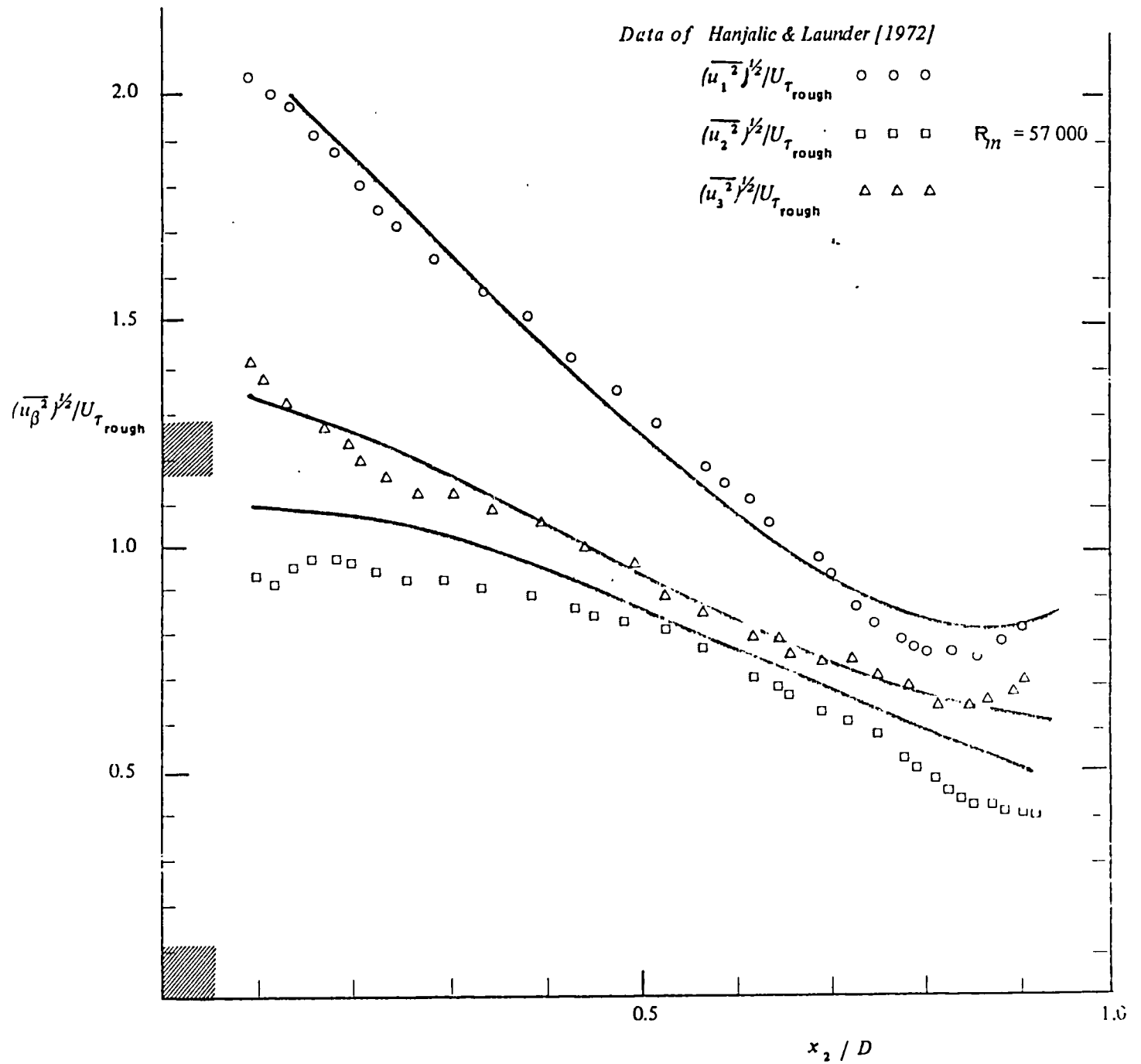


Figure 6.12
Asymmetric Channel: Turbulence Intensities.
 Model 2B

turbulence energy gain ($\times D/U_{\tau_{rough}}^3$)

Production : \circ
Dissipation : \square Data of Hanjalic & Launder
Diffusion : \triangle

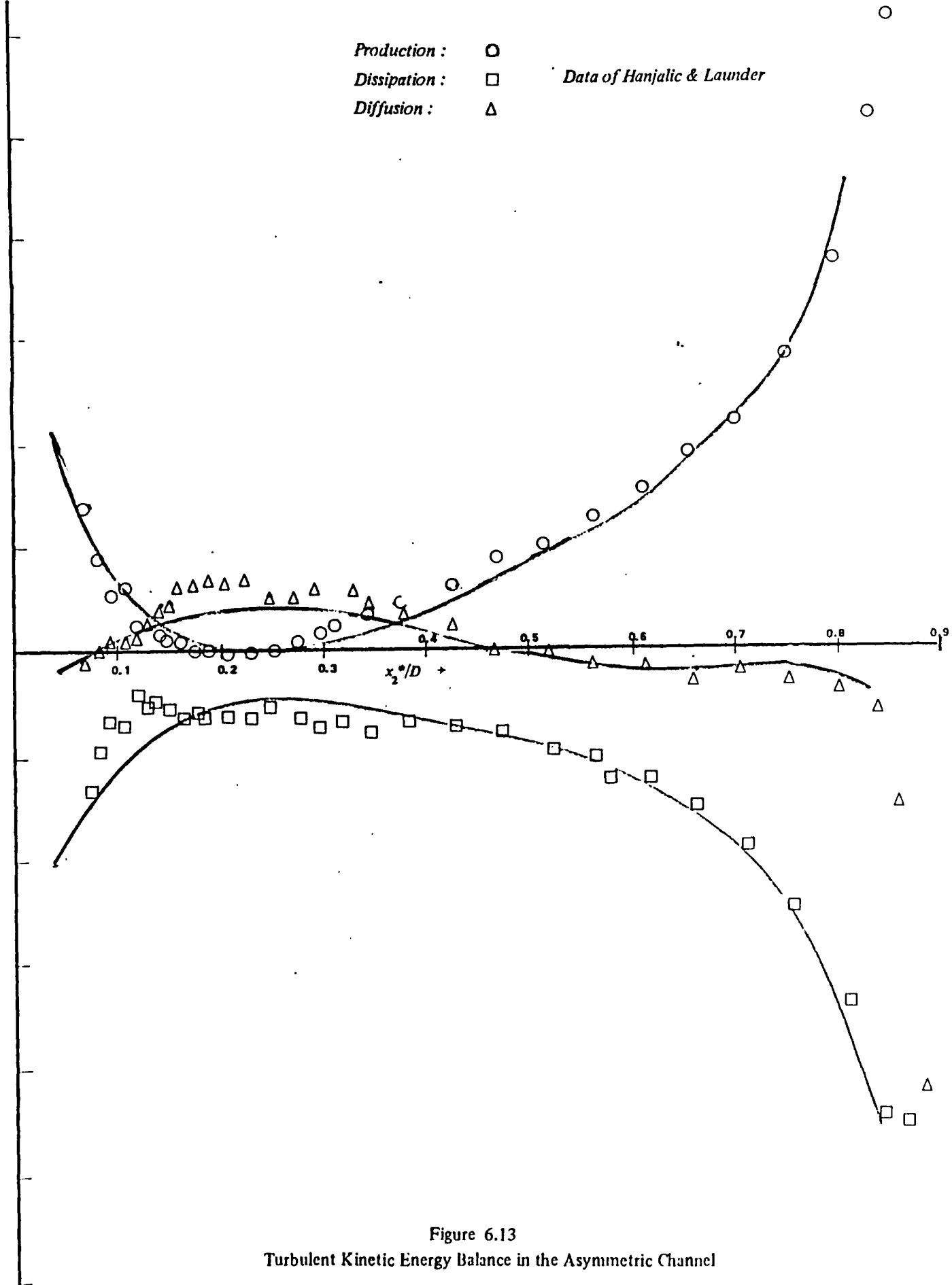


Figure 6.13
Turbulent Kinetic Energy Balance in the Asymmetric Channel

Model 1A

turbulence energy loss

Turbulence energy gain ($\times D/U_{Trough}^3$)

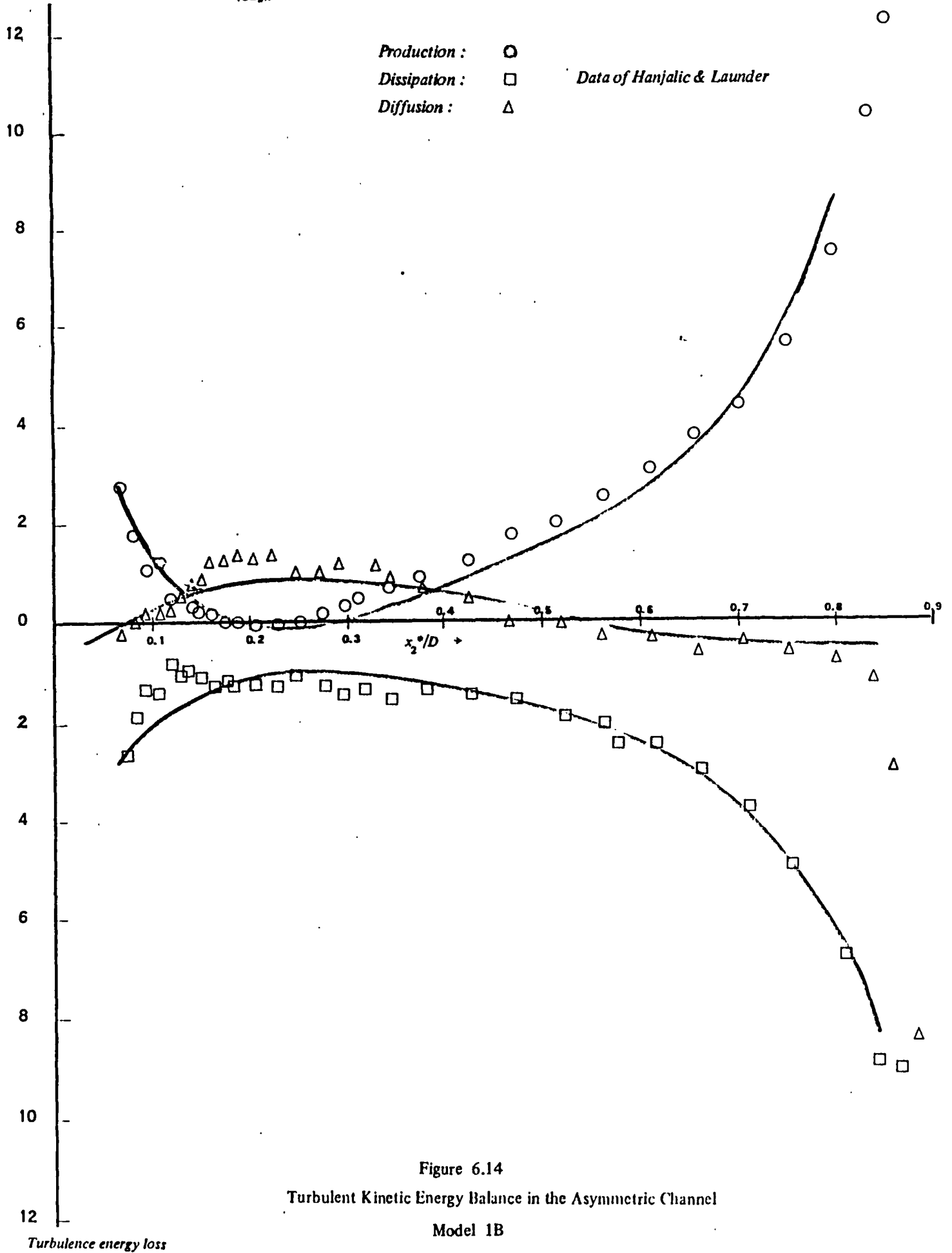
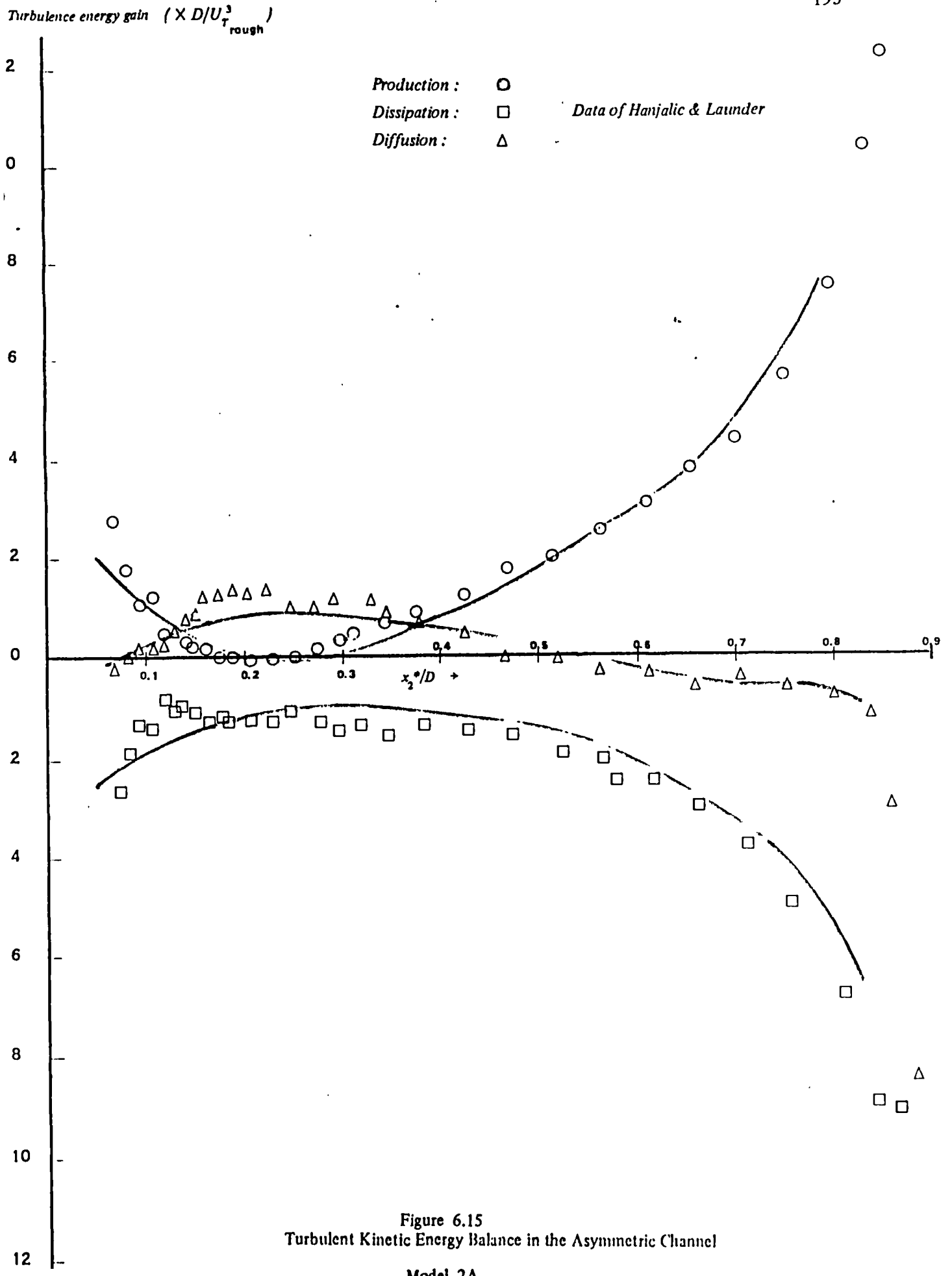


Figure 6.14
 Turbulent Kinetic Energy Balance in the Asymmetric Channel
 Model 1B



Turbulence energy gain $(\times D/U_{\tau_{rough}}^3)$

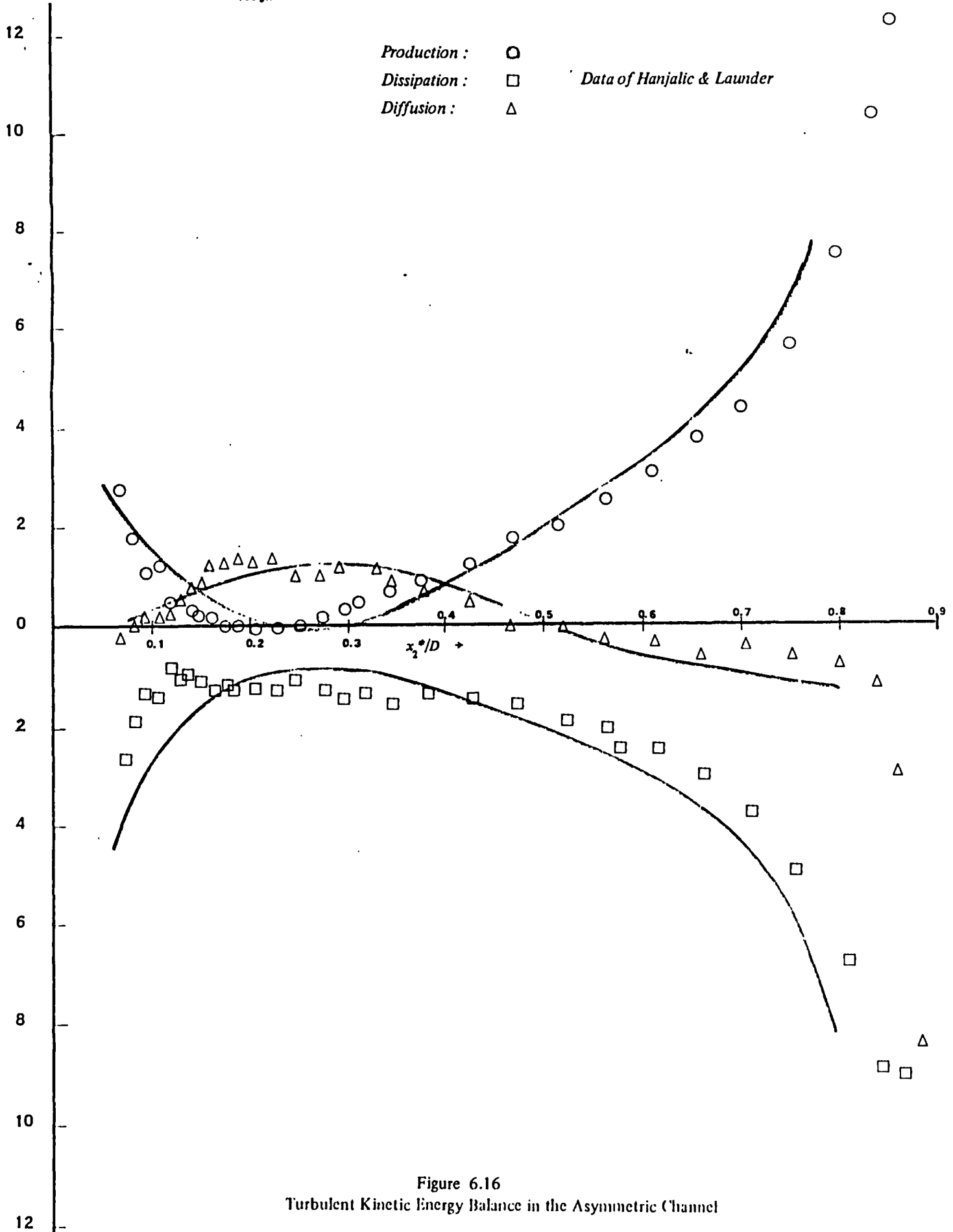


Figure 6.16
 Turbulent Kinetic Energy Balance in the Asymmetric Channel

Model 2B

Turbulence energy loss

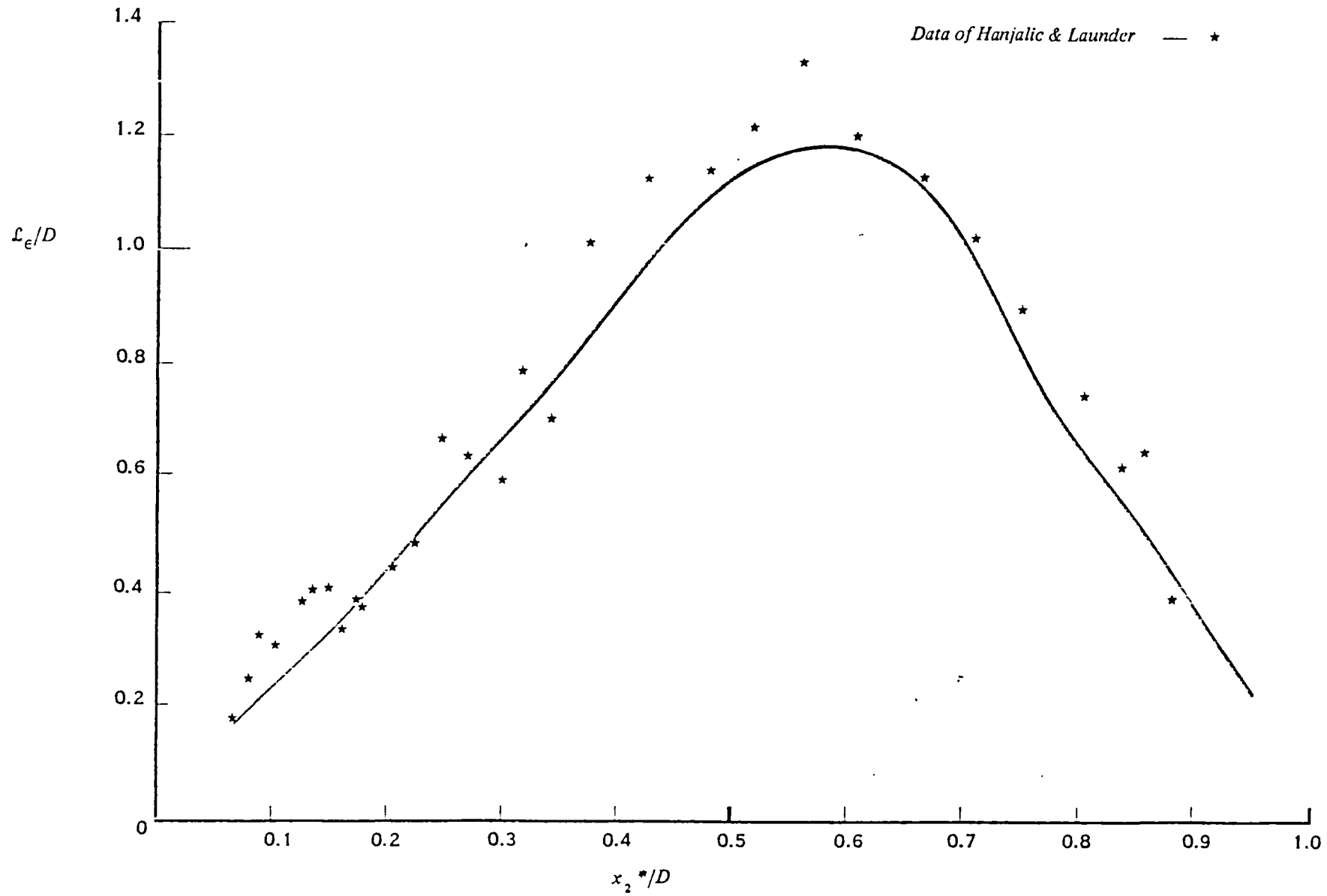


Figure 6.17 Profile of Dissipation Length-scale (plotted against distance from the smooth wall)

Model 1

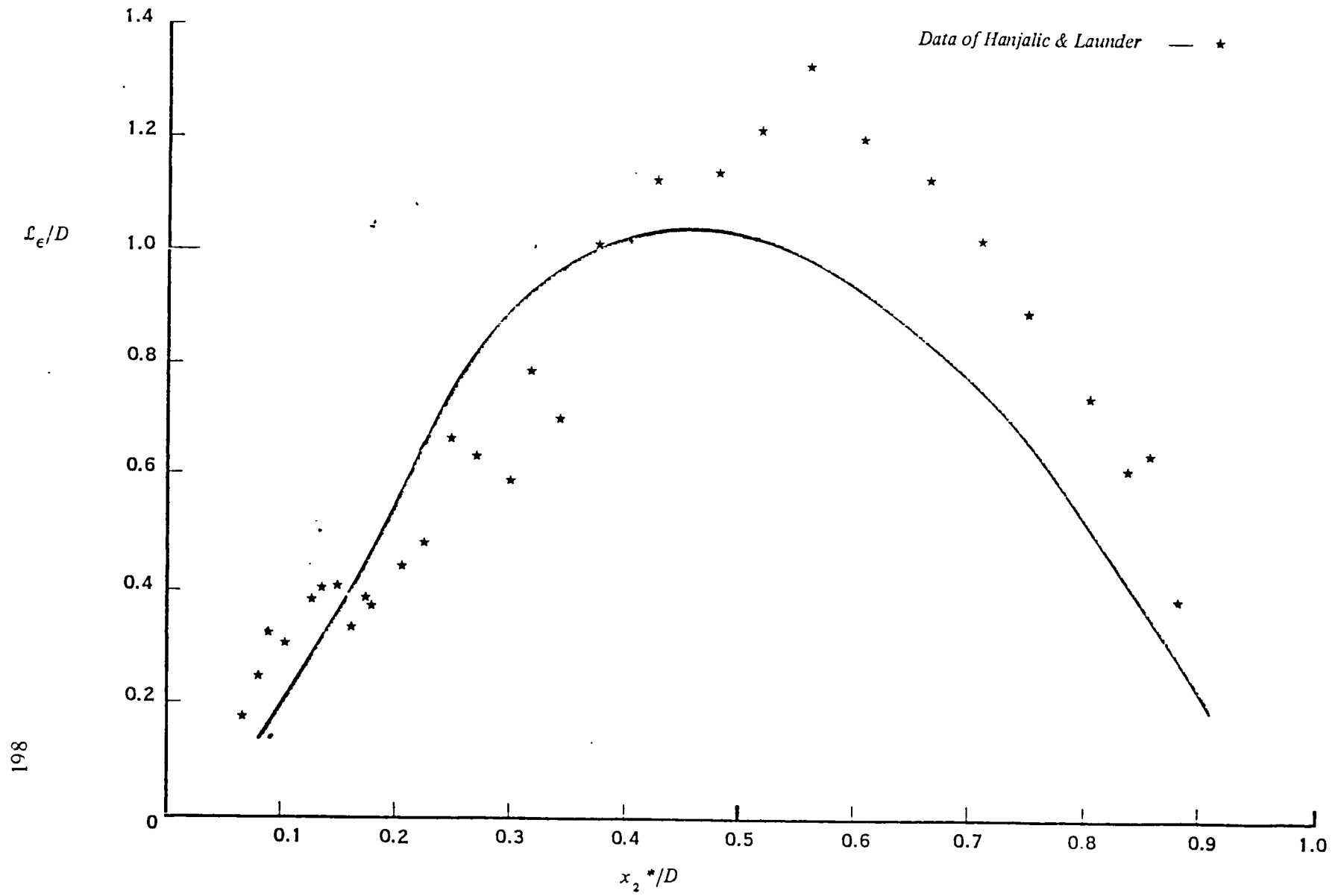


Figure 6.18 Profile of Dissipation Length-scale (plotted against distance from the smooth wall) Model 2

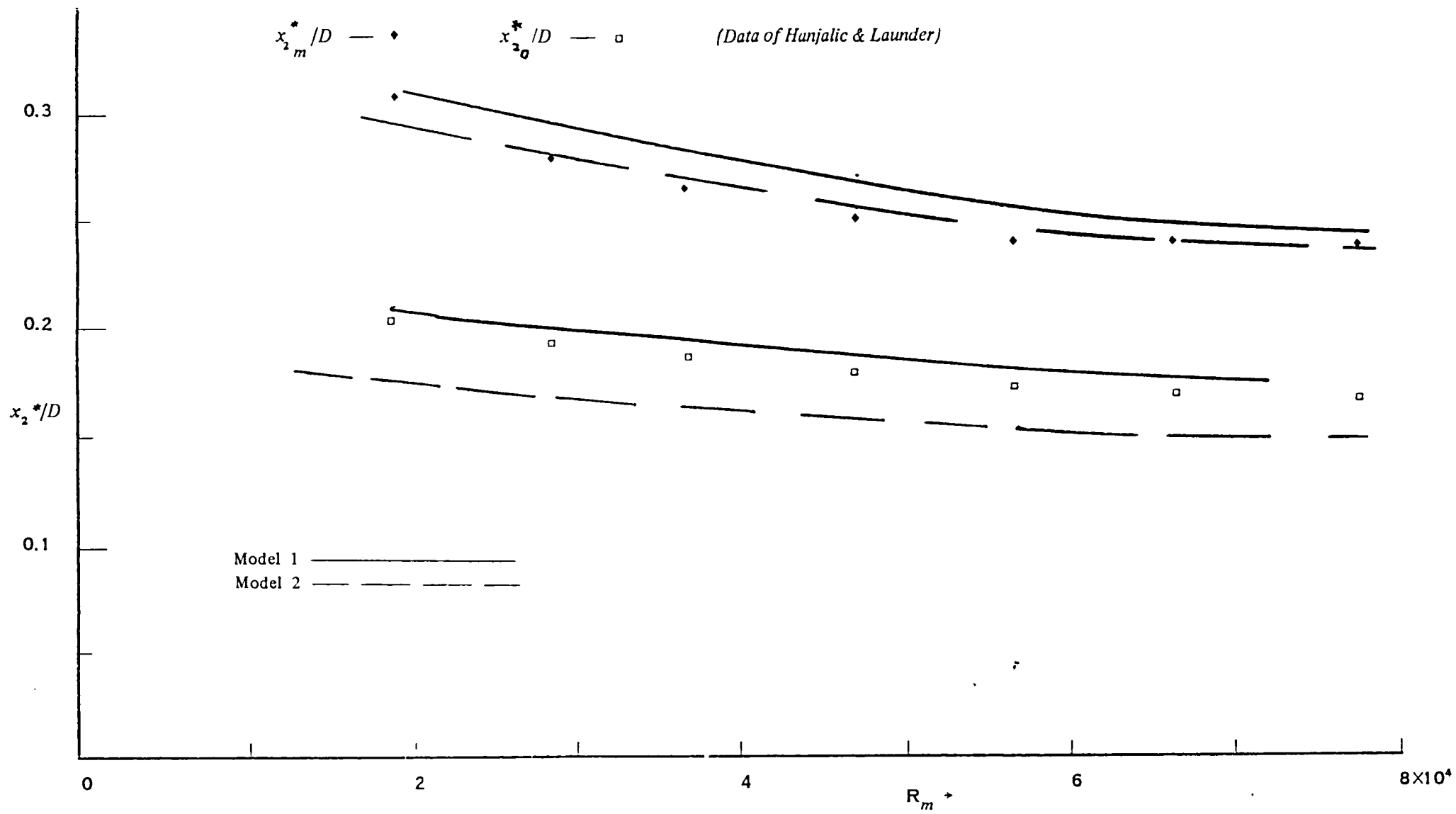


Figure 6.19

Variation of position of maximum mean velocity and of position of zero shear stress (relative to smooth wall) with R_{m1}

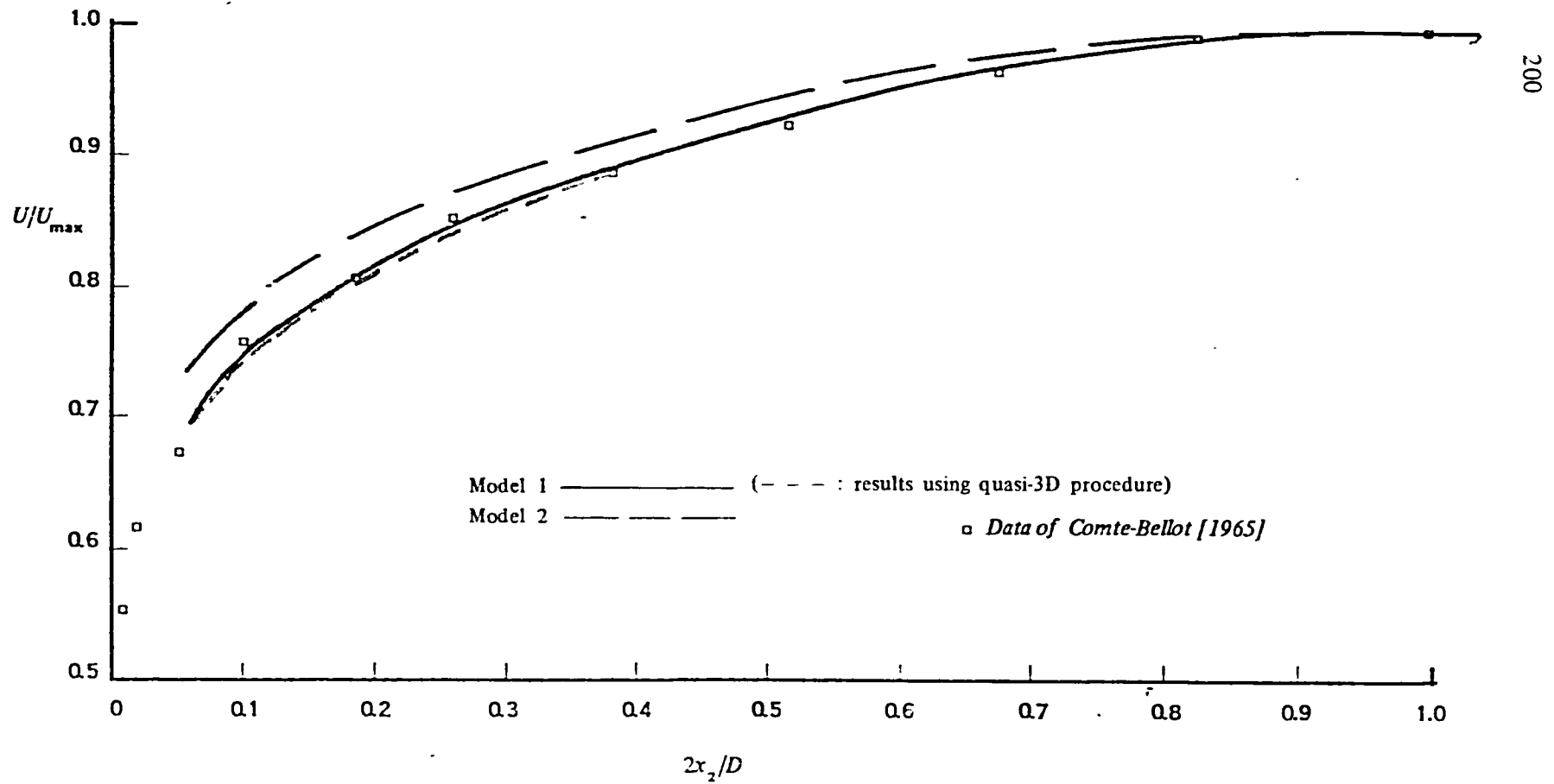


Figure 6.20 Mean velocity distribution in the fully-developed symmetric channel

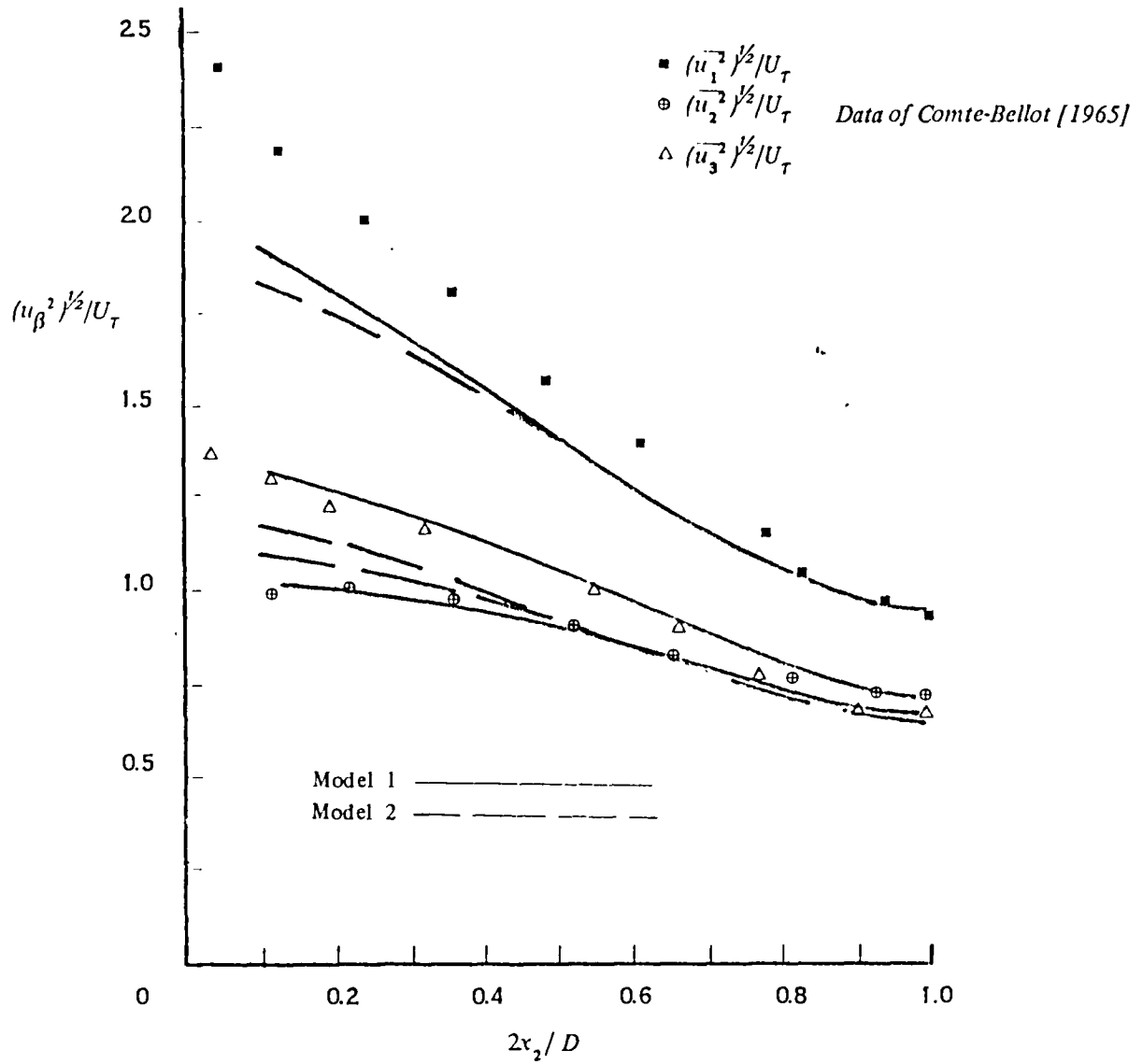


Figure 6.21 Distribution of turbulence intensities in the symmetric channel

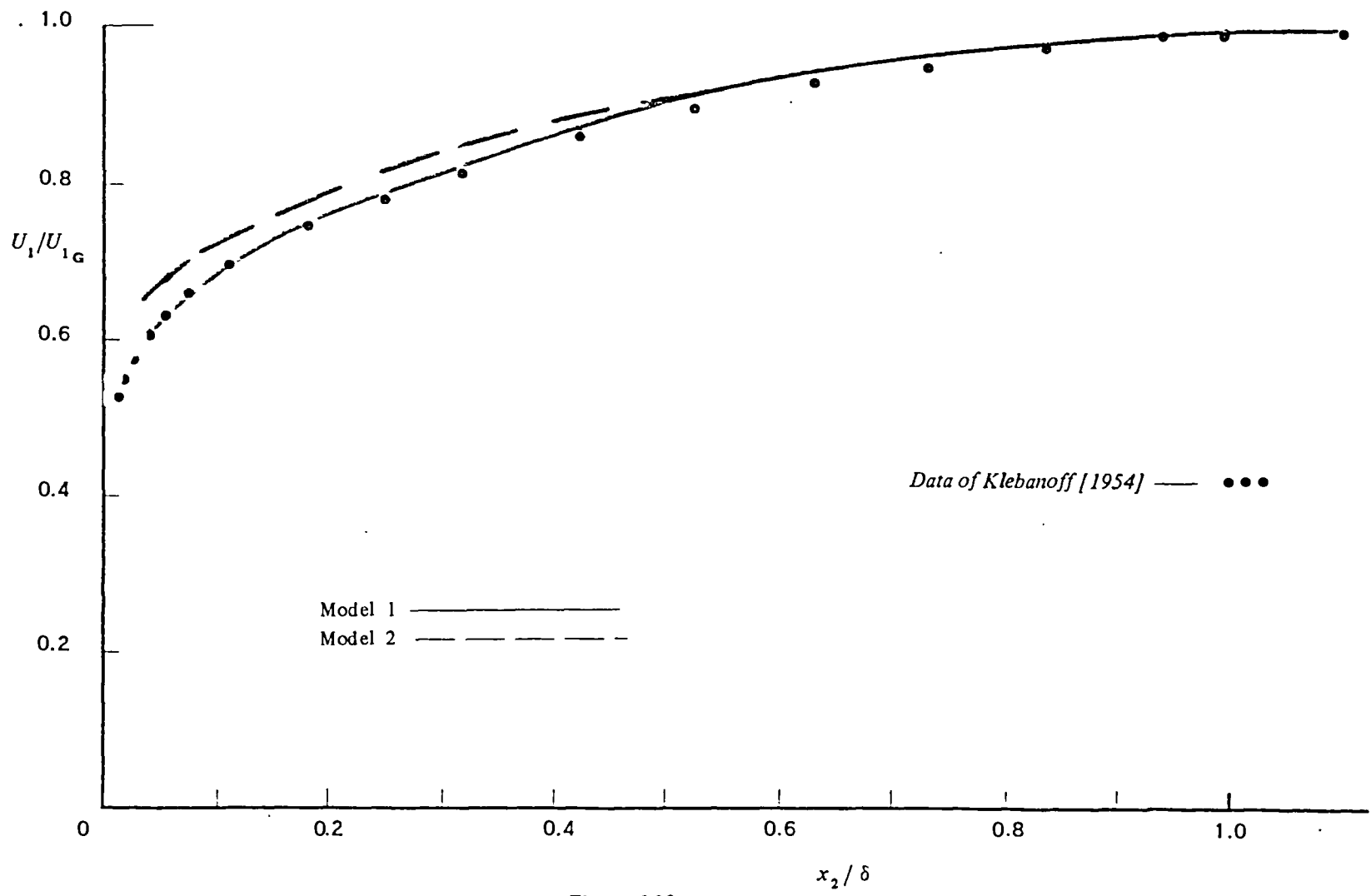


Figure 6.22
Mean-velocity distribution in the flat-plate boundary-layer

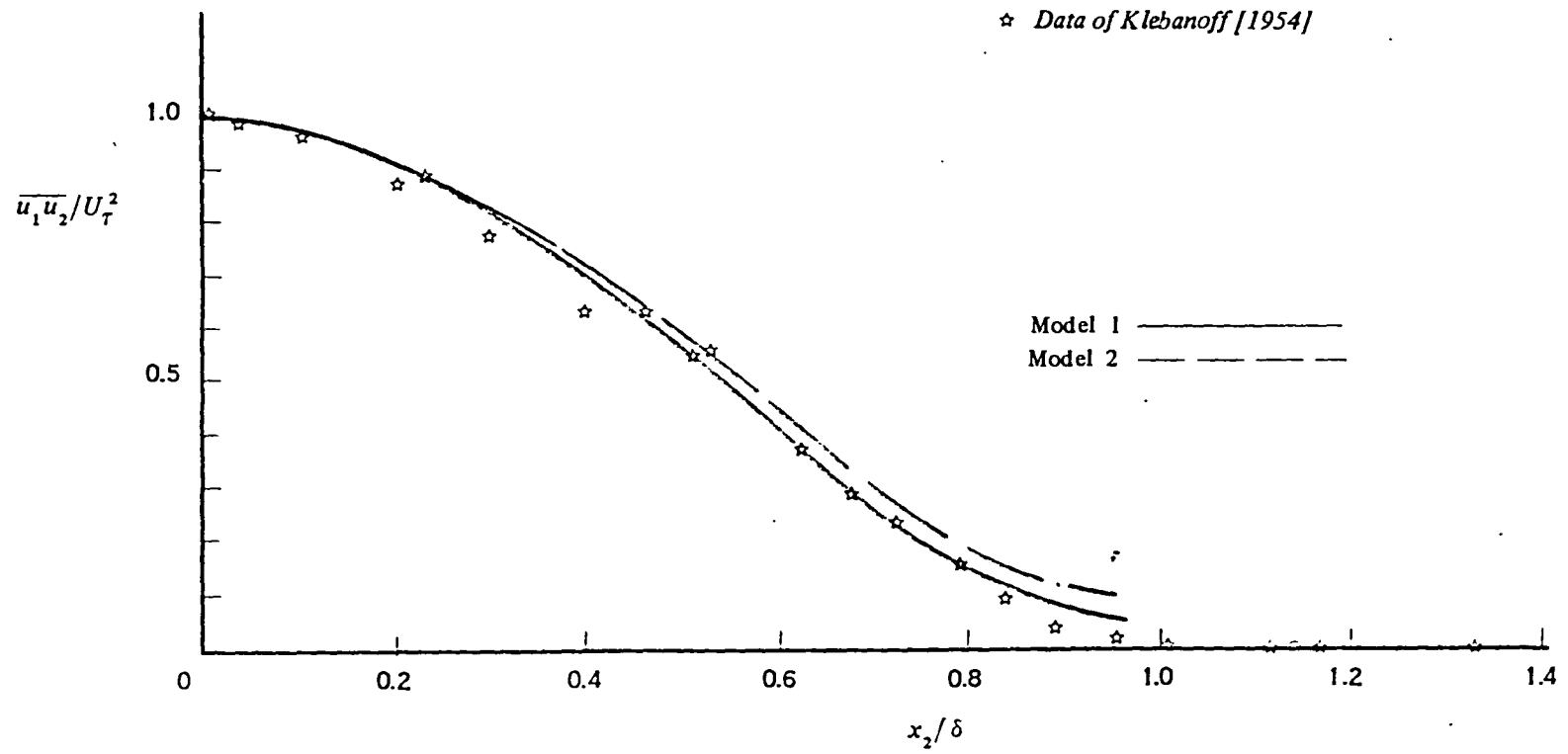


Figure 6.23

Distribution of turbulent shear stress in the flat plate boundary-layer

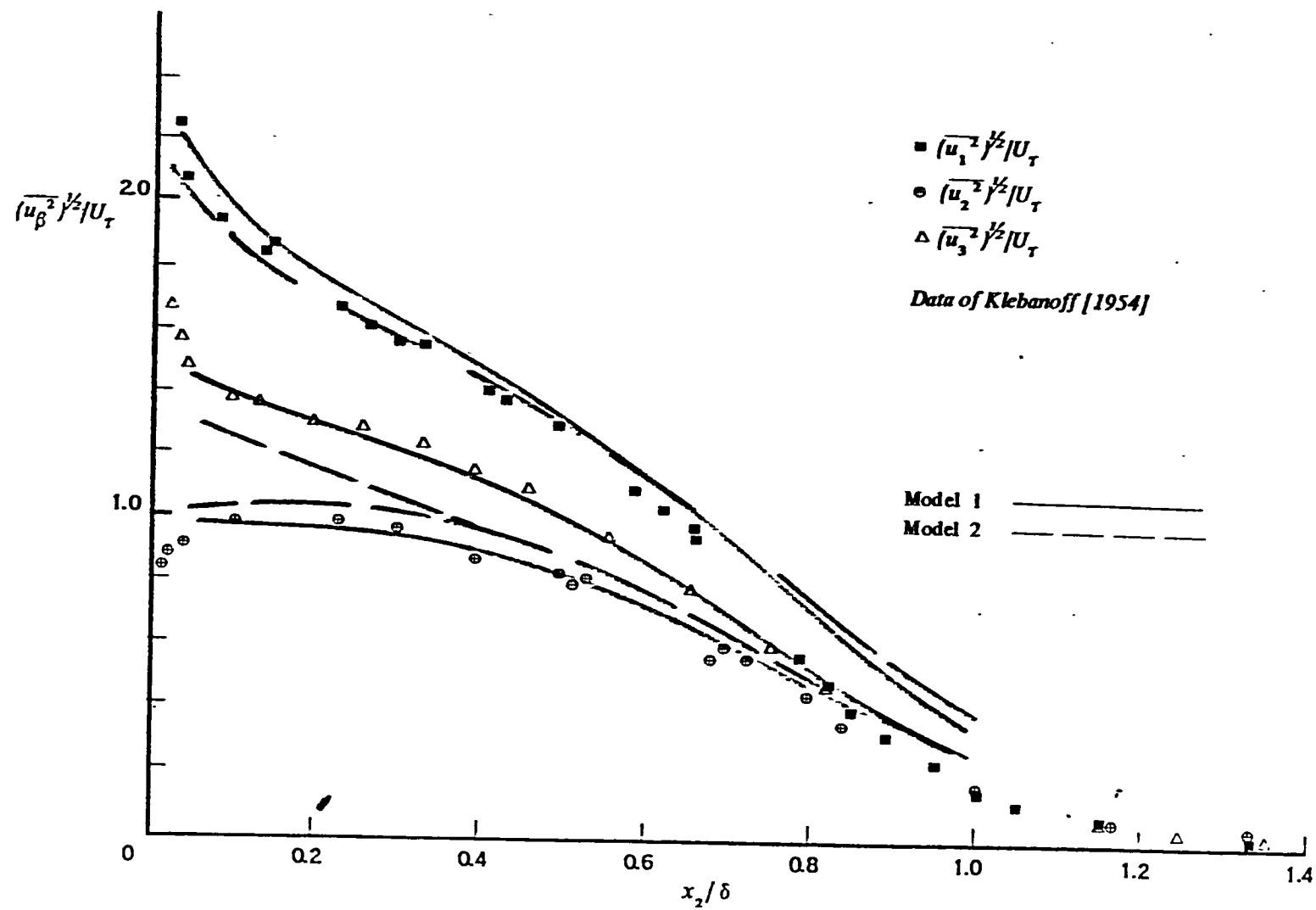


Figure 6.24
The distribution of turbulence intensities in the flat-plate boundary-layer

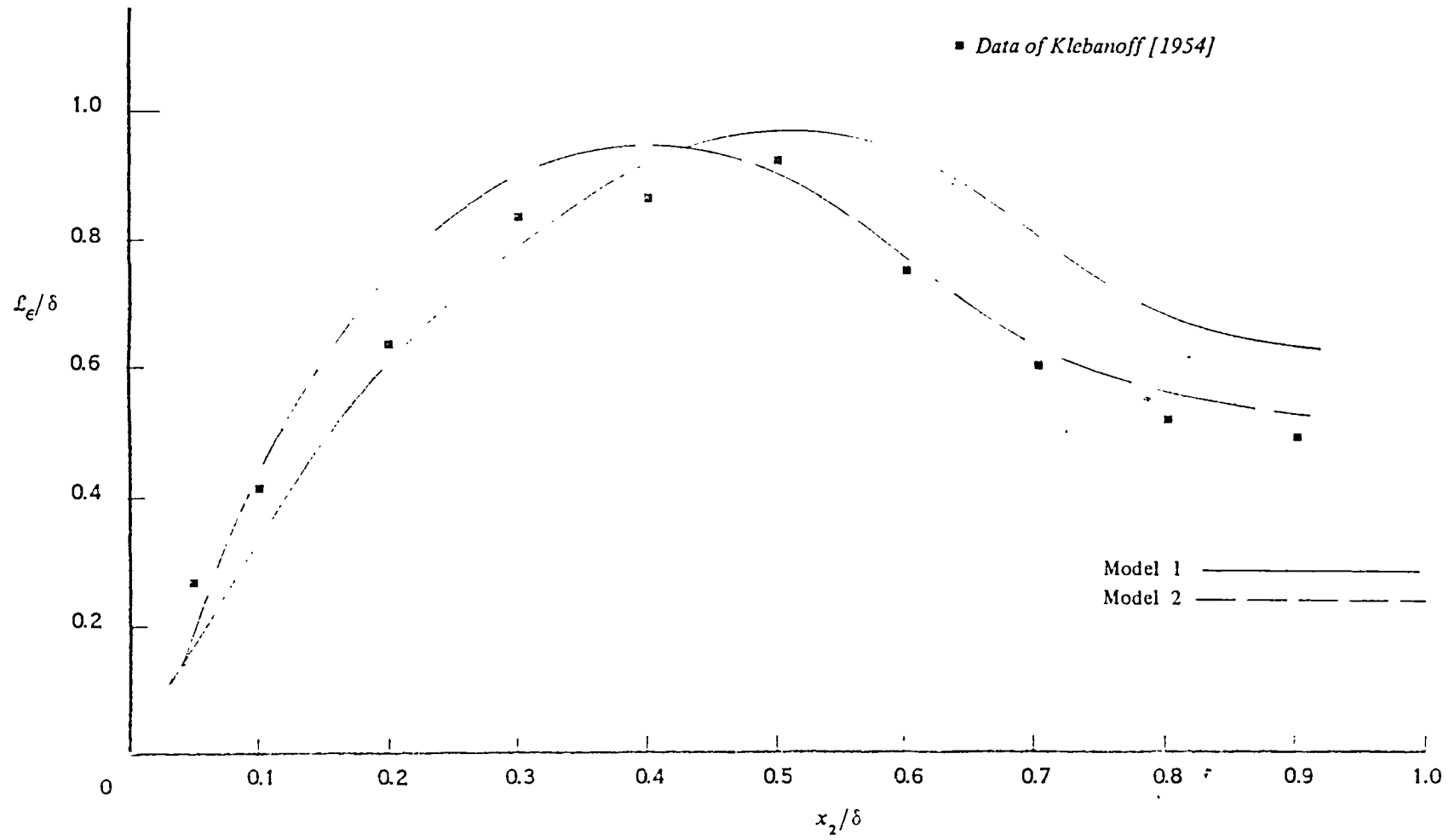
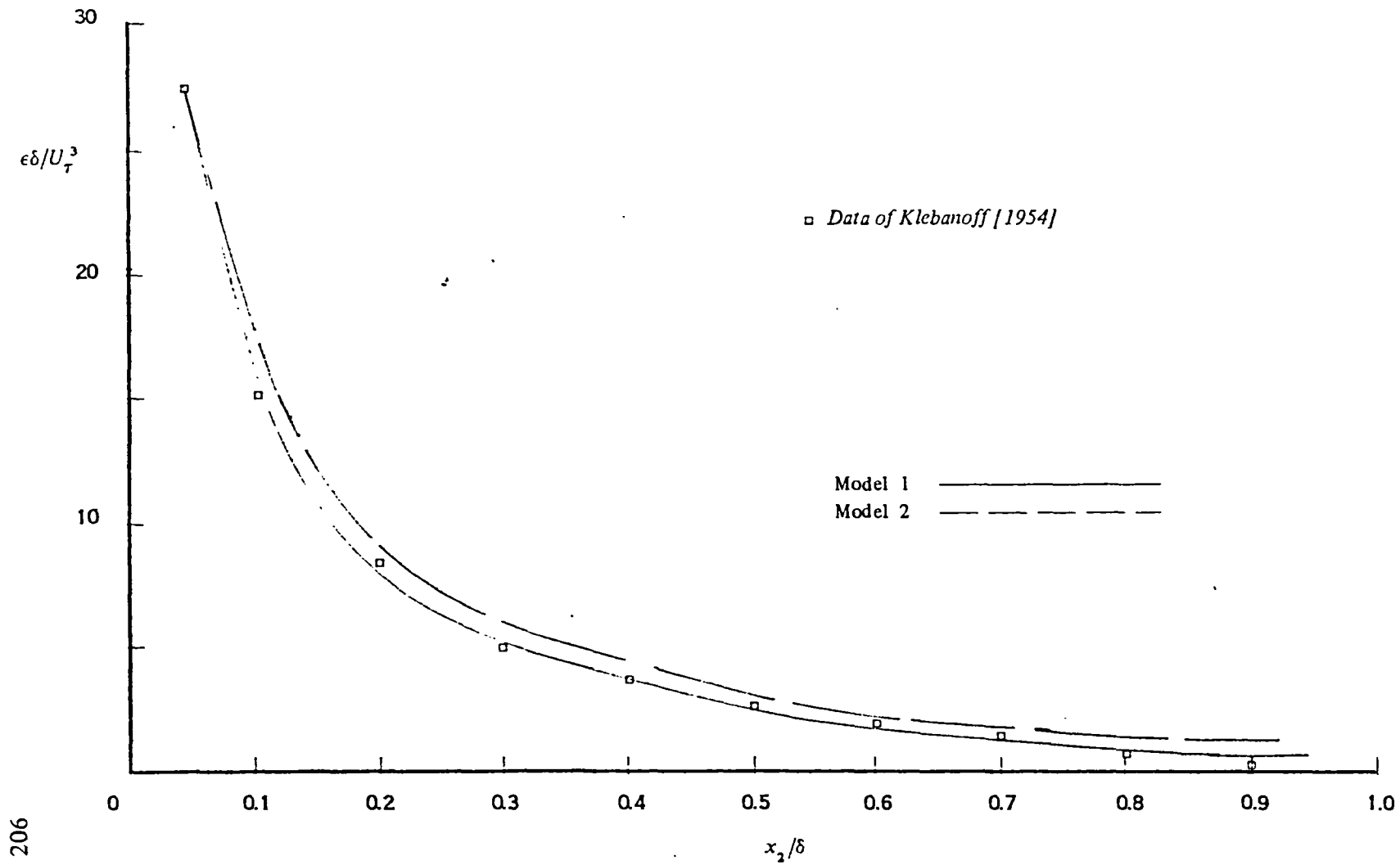


Figure 6.25 Distribution of dissipation length-scale in the flat-plate boundary-layer



206

Figure 6.26 Distribution of turbulence dissipation across a flat-plate boundary-layer

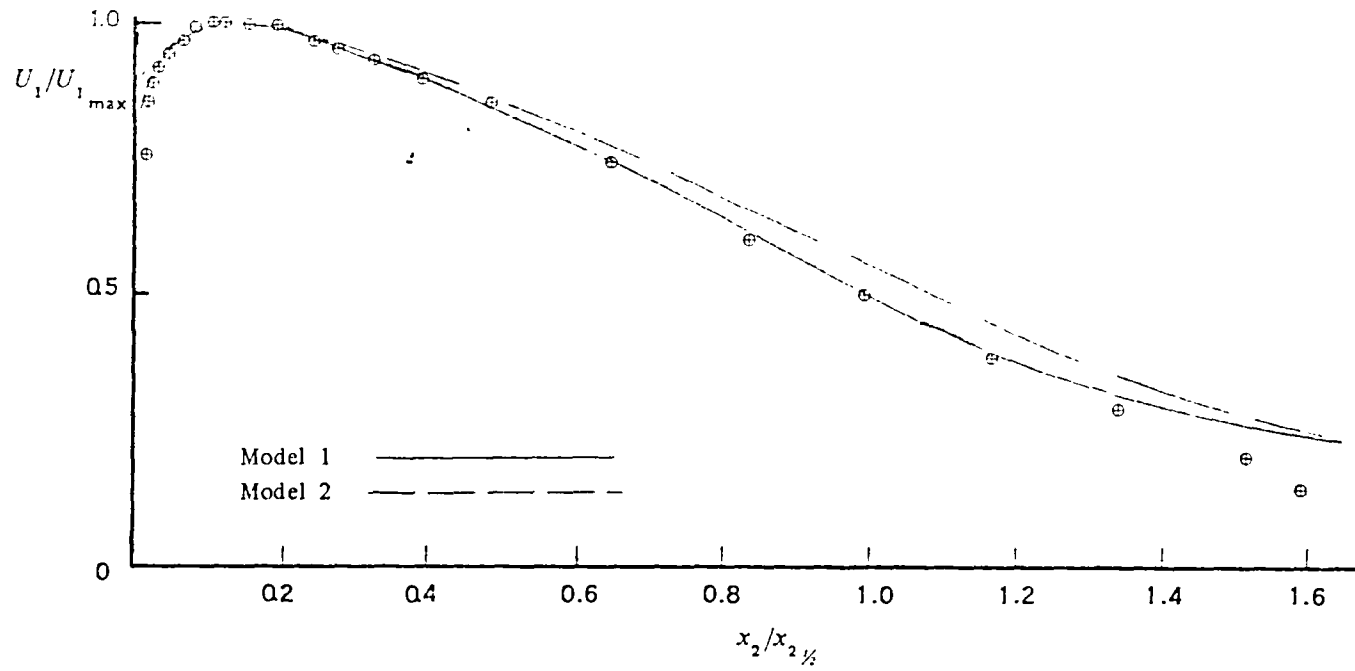


Figure 6.27 Mean velocity profile in a plane wall jet (Data of Tailland & Mathieu [1967])

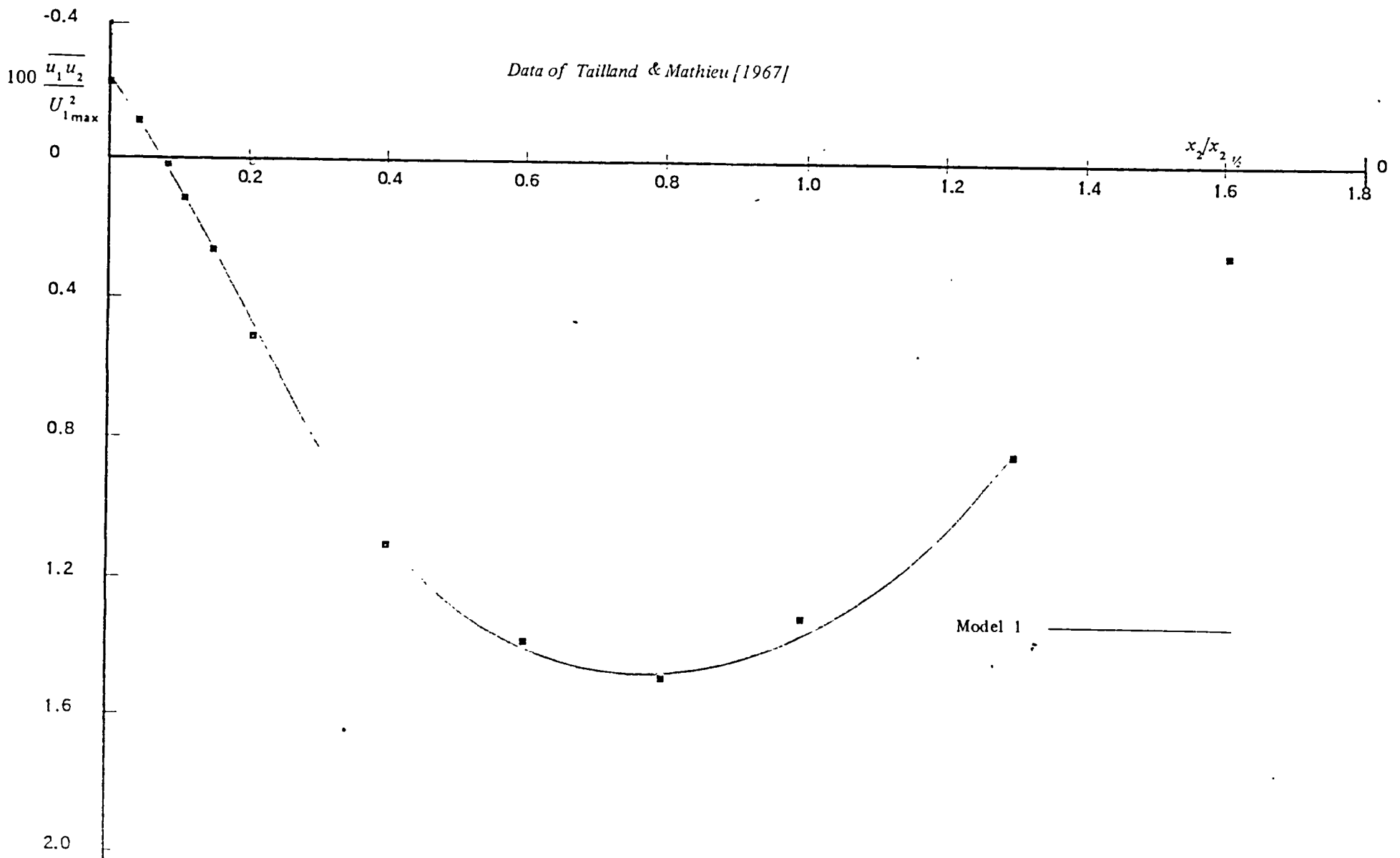


Figure 6.28 Shear-stress profiles in the plane wall jet

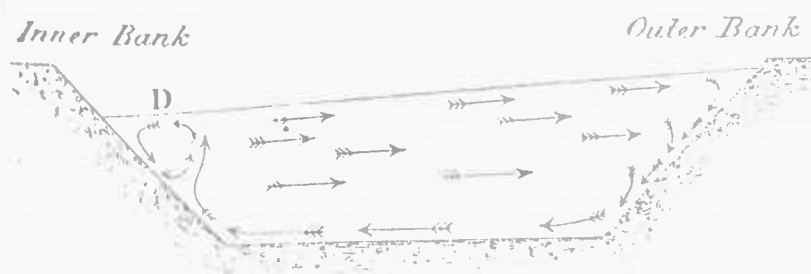


Figure 7.1a Measurements of secondary flows
in rivers by Thomson [1879]

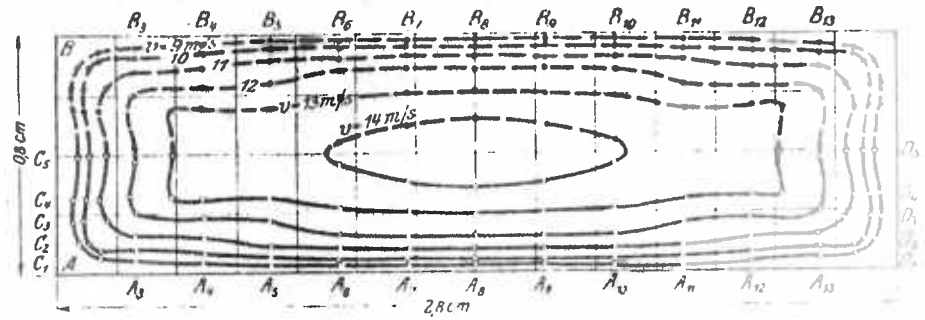


Figure 7.1b Measurements of axial velocity by Nikuradse [1926]

The domain of solution is shown shaded

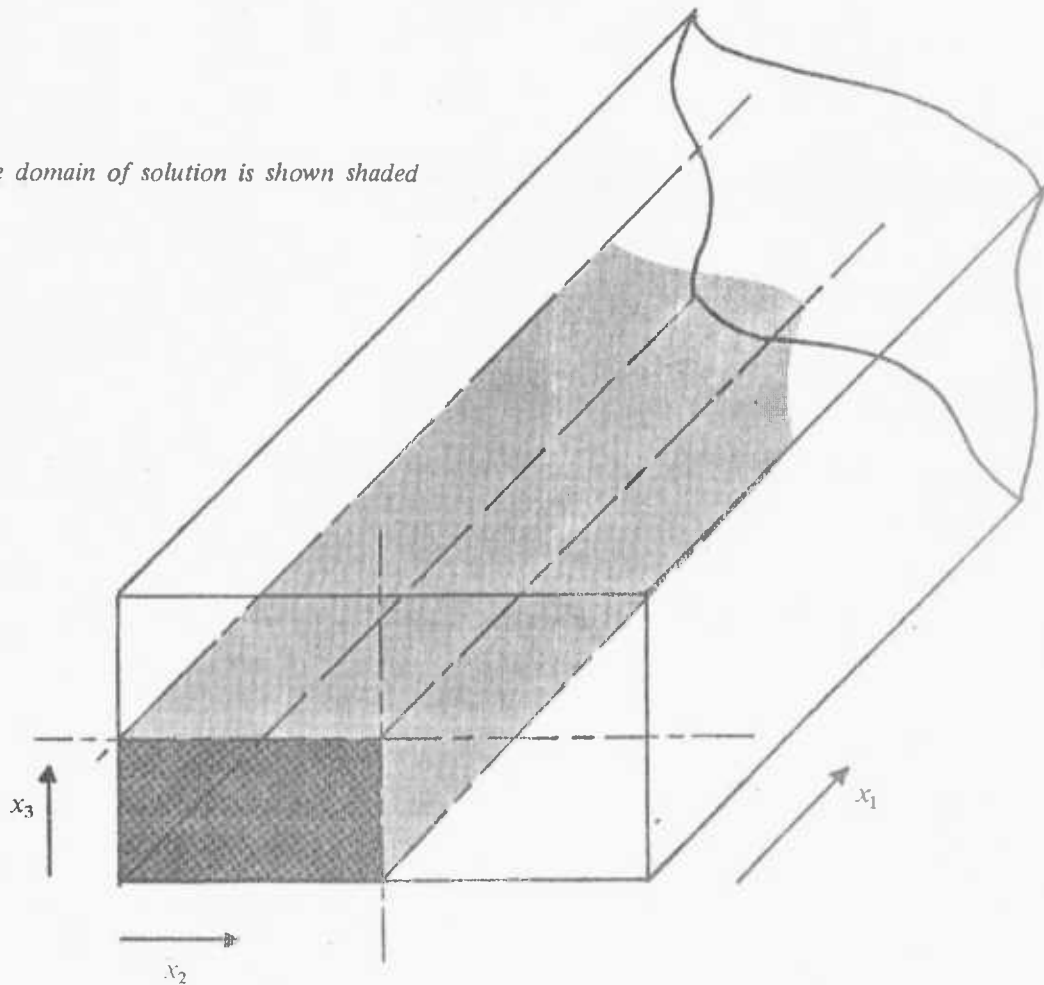


Figure 7.2 The rectangular duct

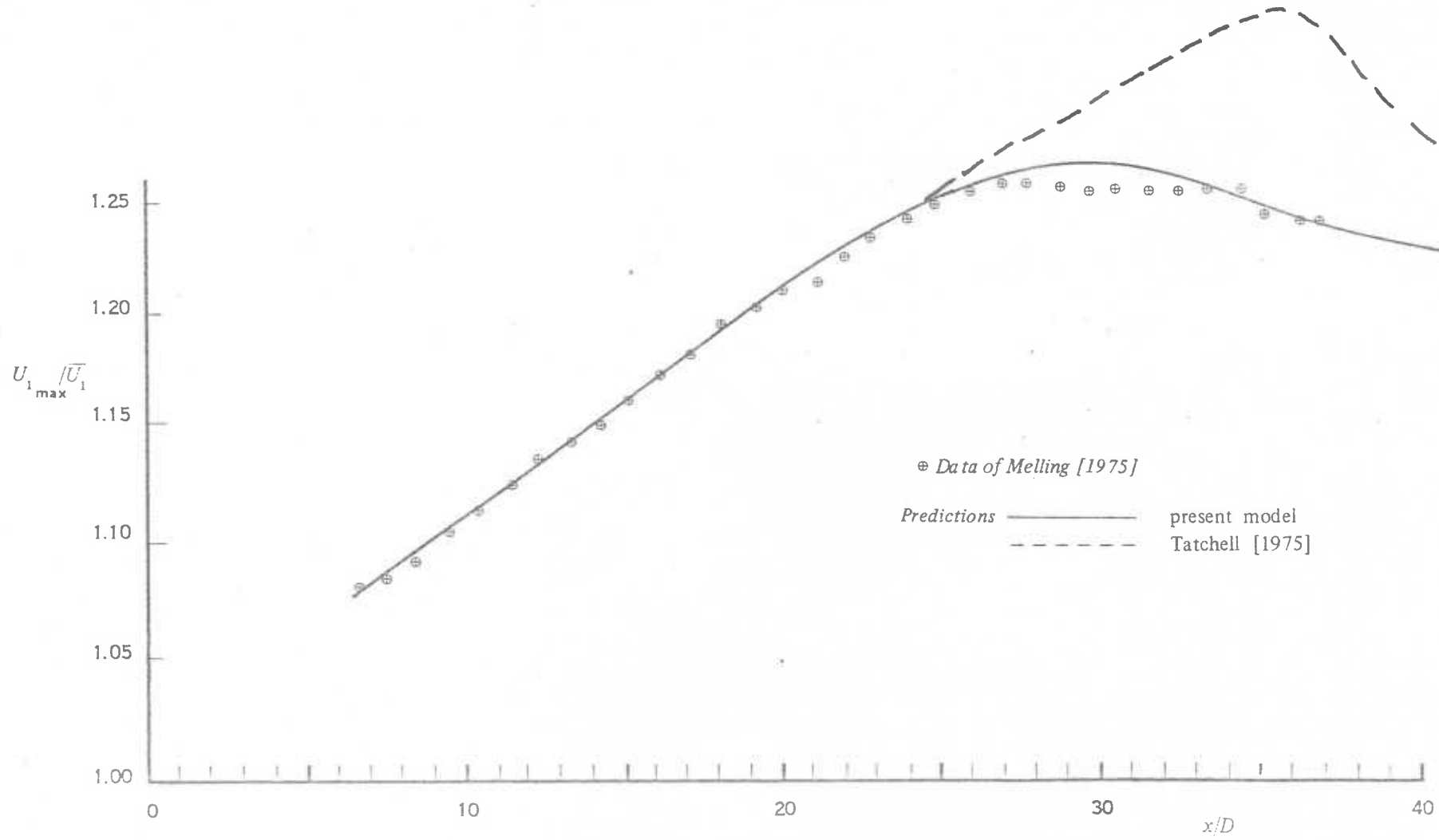
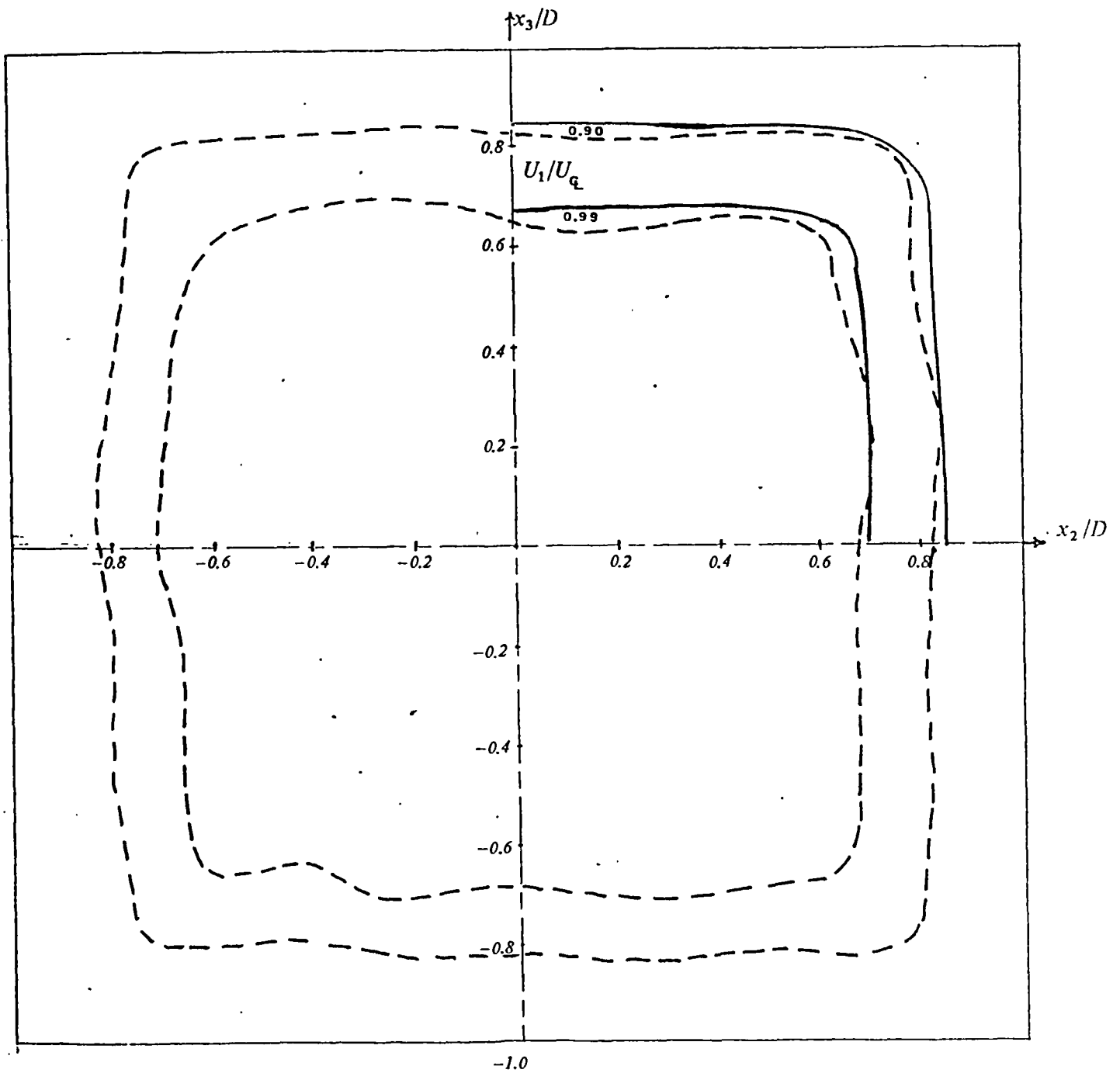
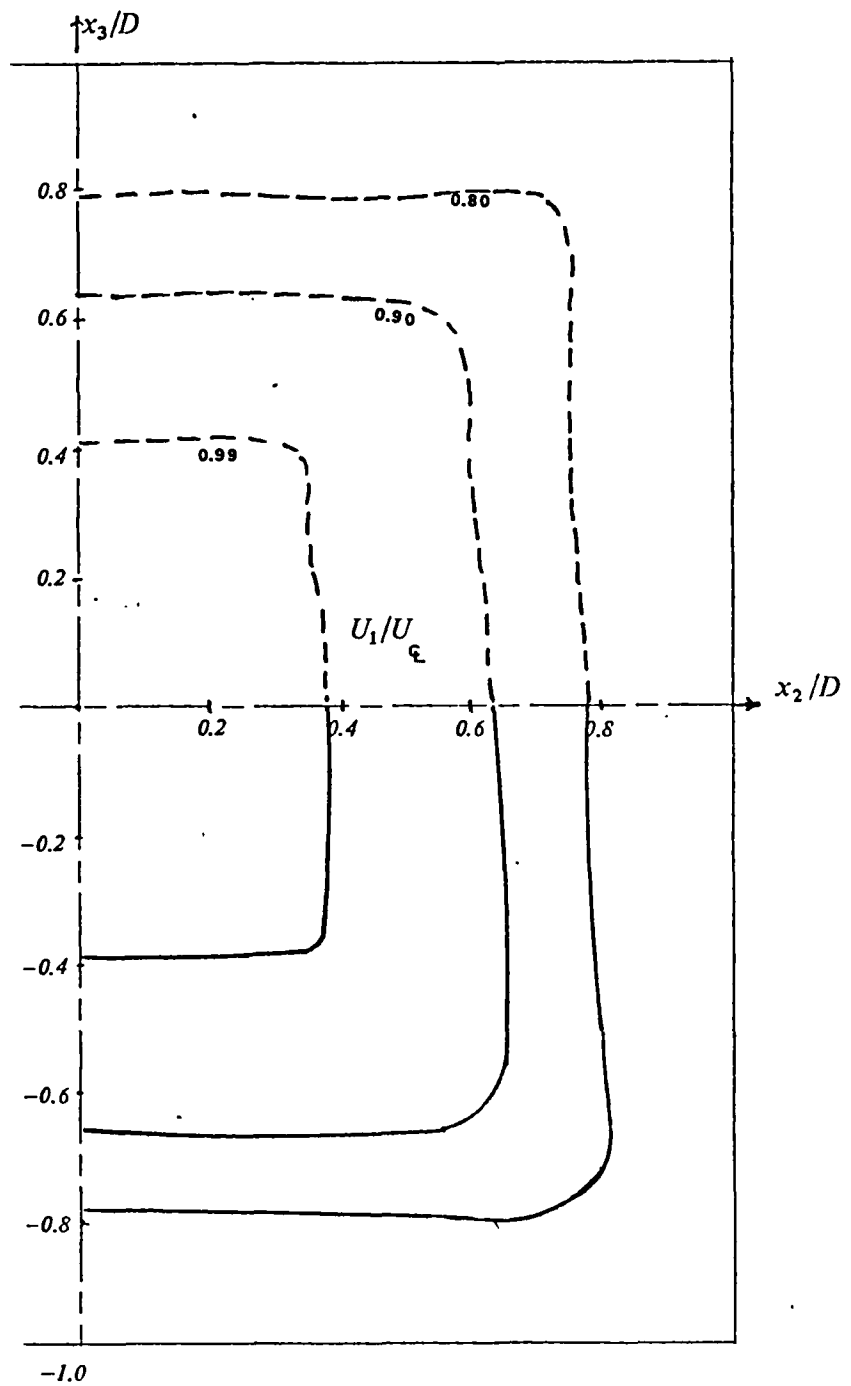


Figure 7.3
 The developing flow in a square-sectioned duct: behaviour of maximum mean velocity



Data of Melling [1975] - - - - -
Predictions of present model ————

Figure 7.4 Mean velocity contours at 5.6 diameters



Data of Melling [1975] - - - - -
 Predictions of present model —————

Figure 7.5 Mean velocity contours at 13.2 diameters

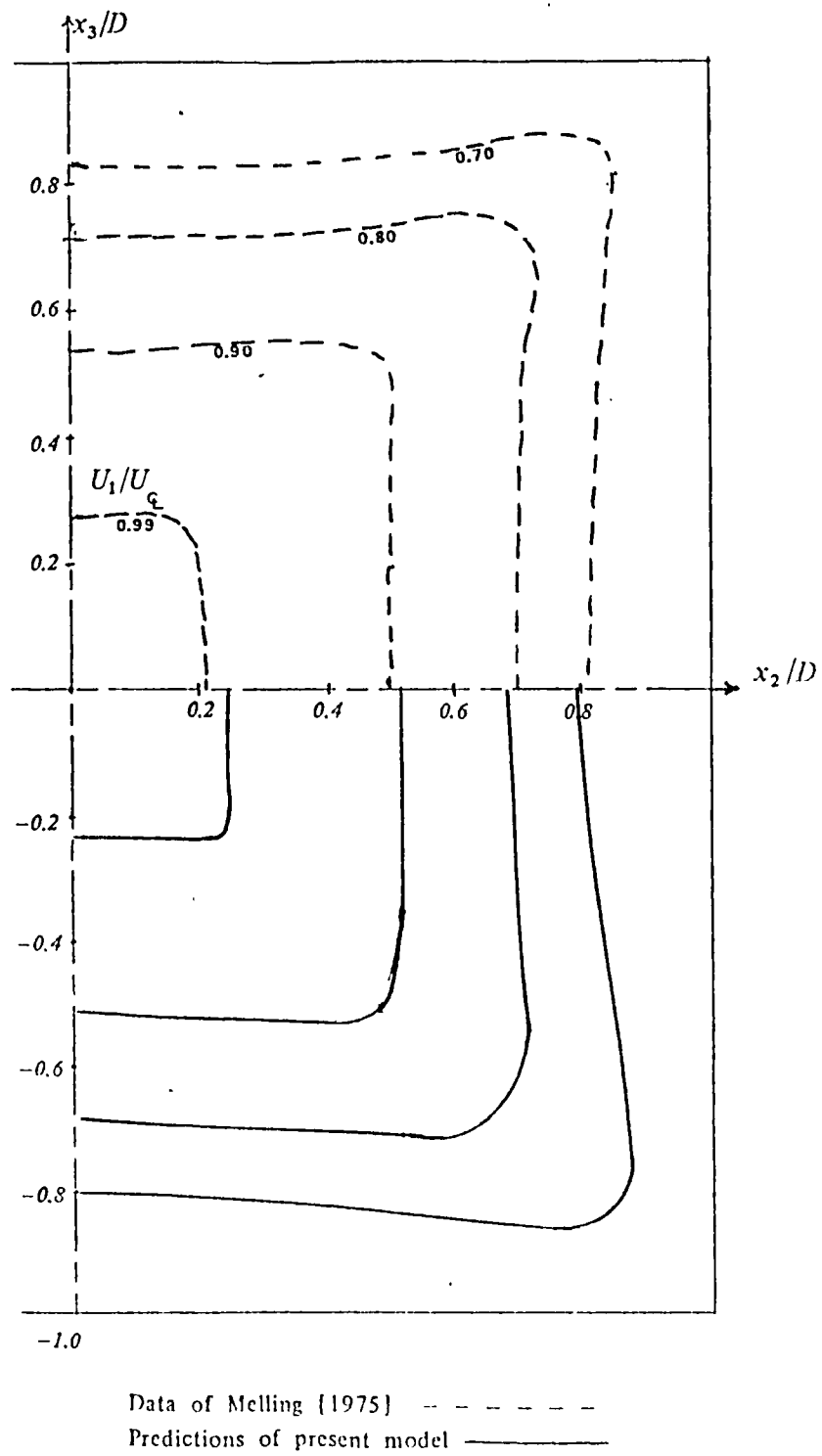


Figure 7.6 Axial mean velocity contours in the square duct at 20.7 diameters

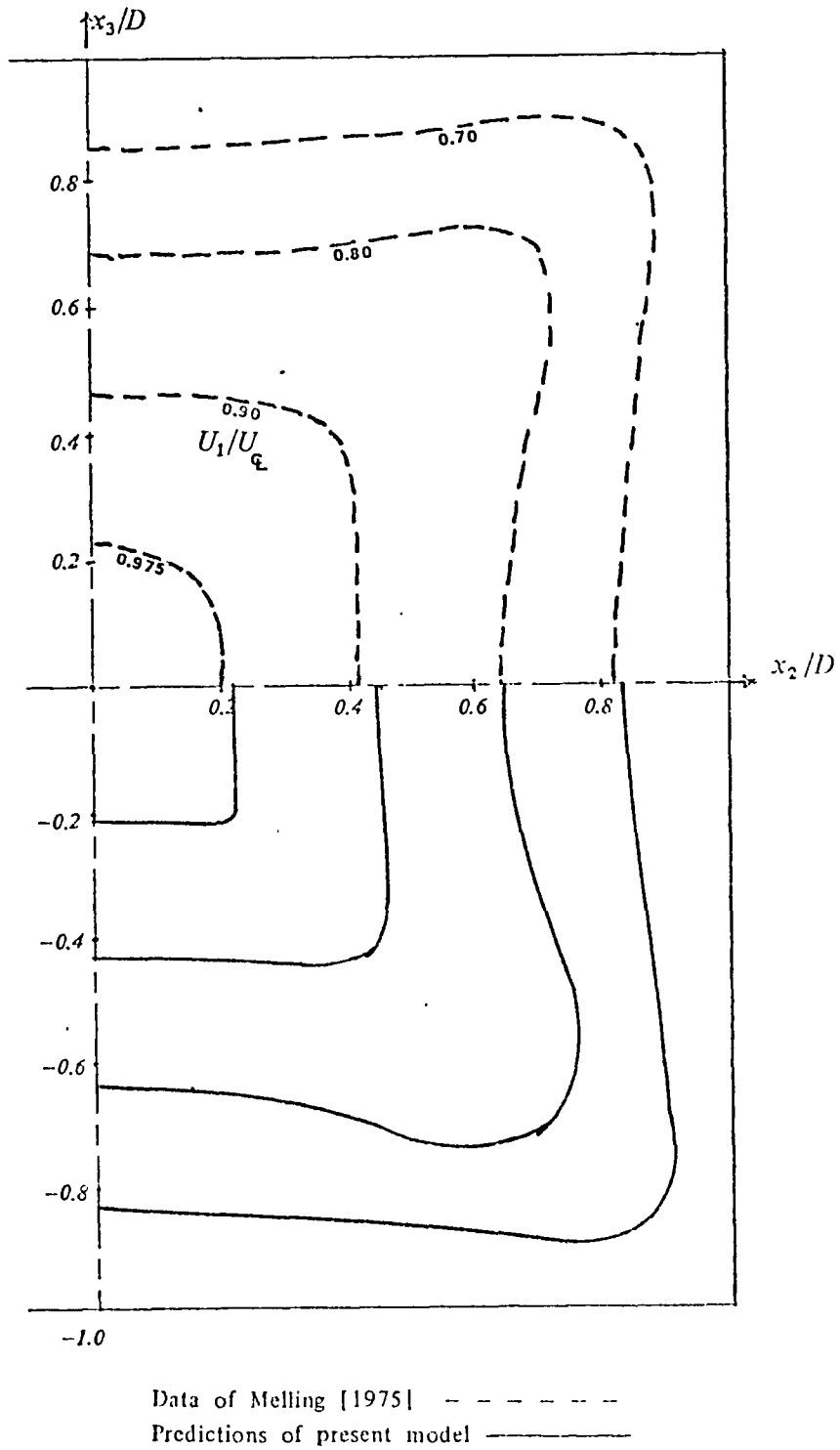
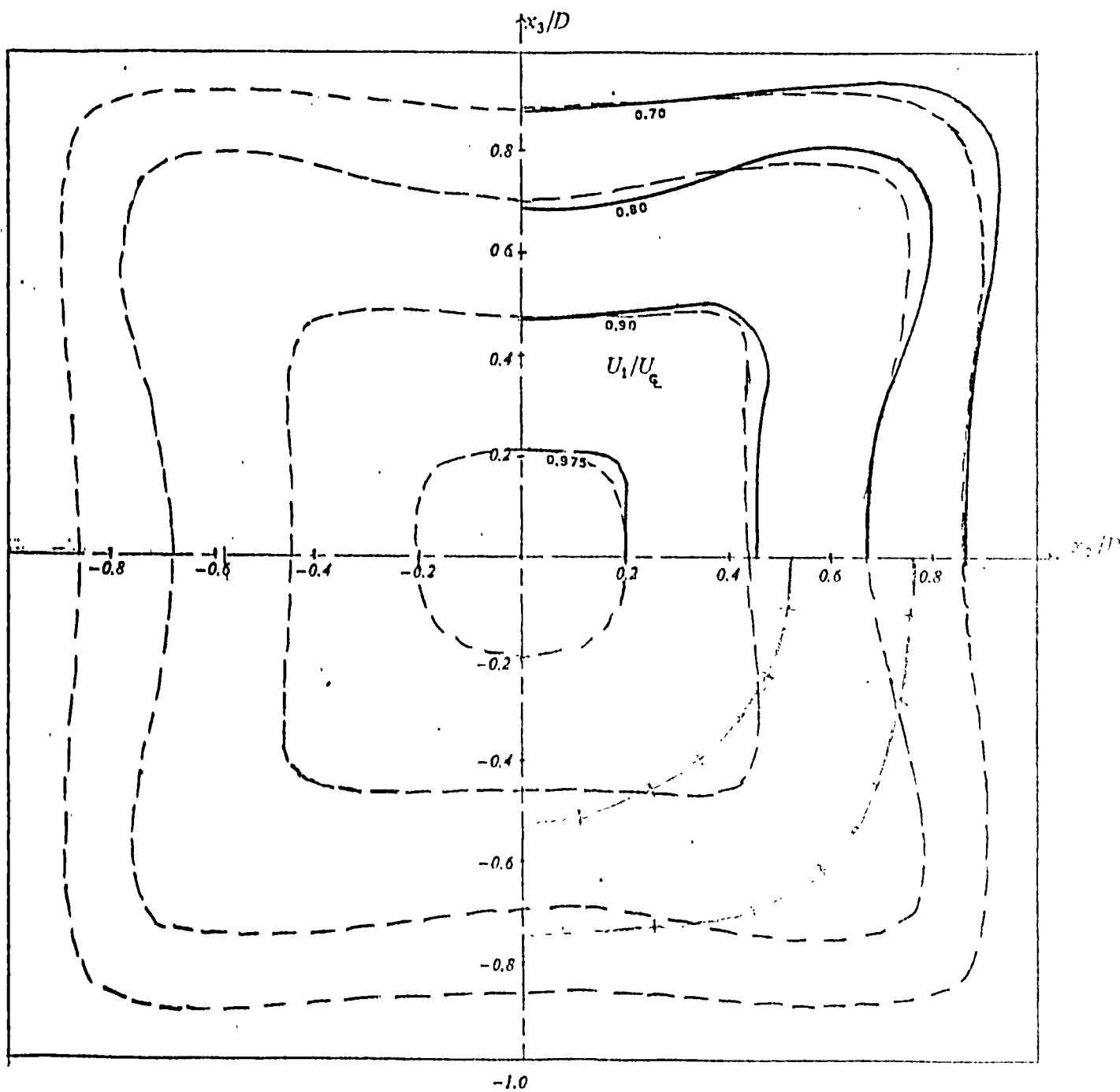
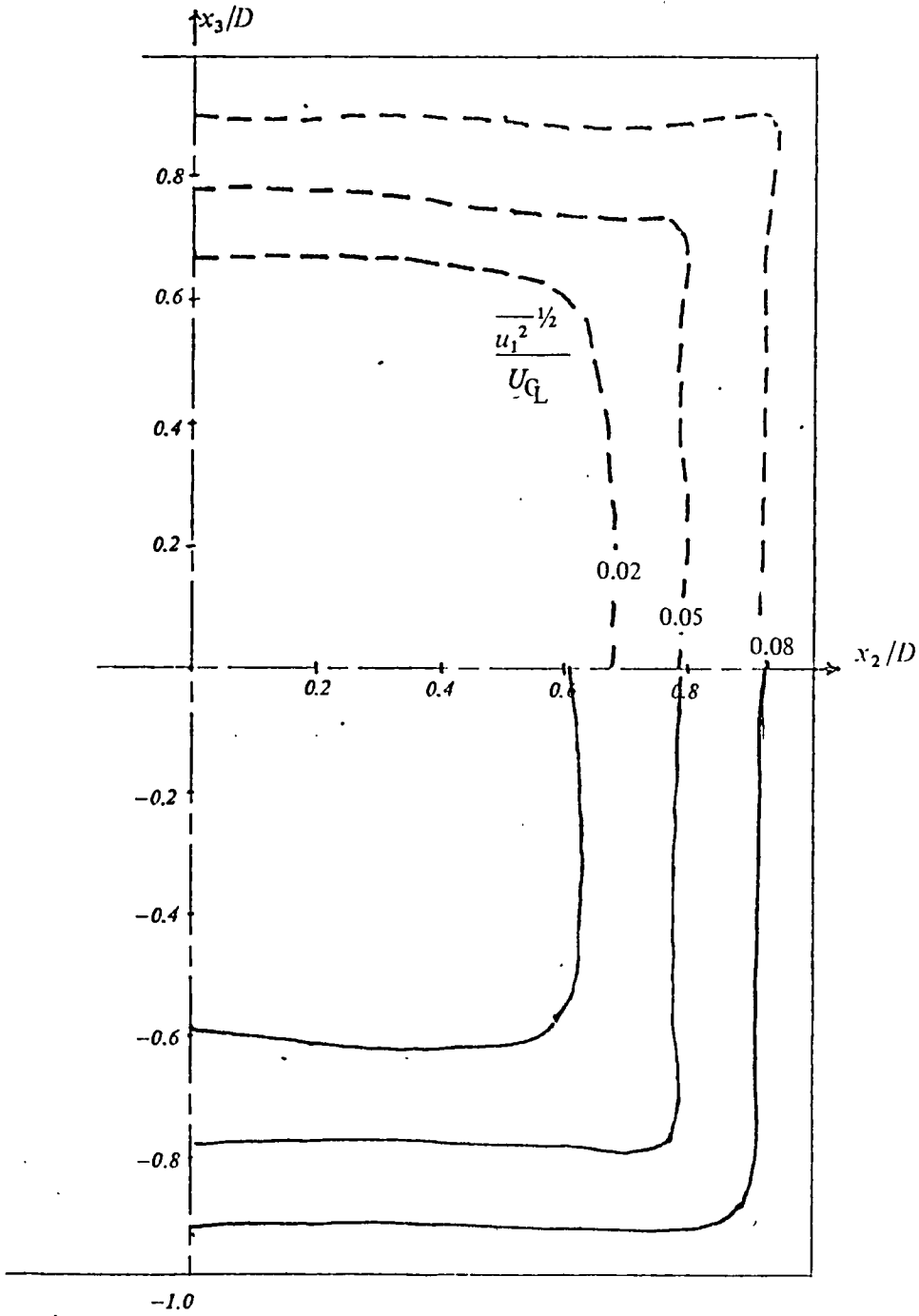


Figure 7.7 Contours of axial mean velocity in the square duct, at 29.0 diameters



Data of Melling [1975] - - - - -
 Predictions of present model - - - - -
 Predictions of Entel [1971] + + + + +

Figure 7.8 Contours of axial mean velocity in the square duct at 36.8 diameters



Data of Melling [1975] - - - - -
Predictions of present model - - - - -

Figure 7.9 Contours of $\overline{u_1^2}^{1/2}$ at station A

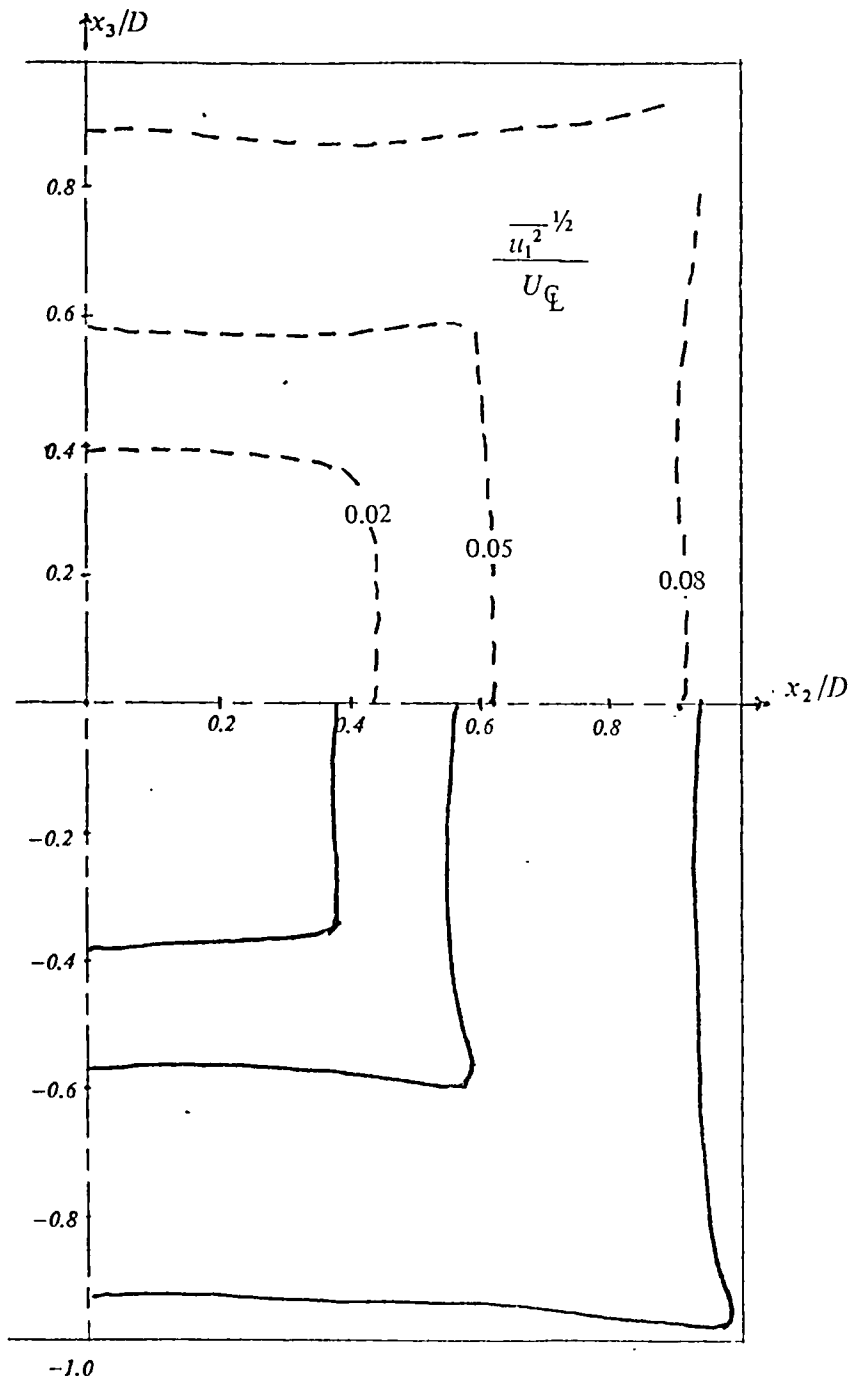
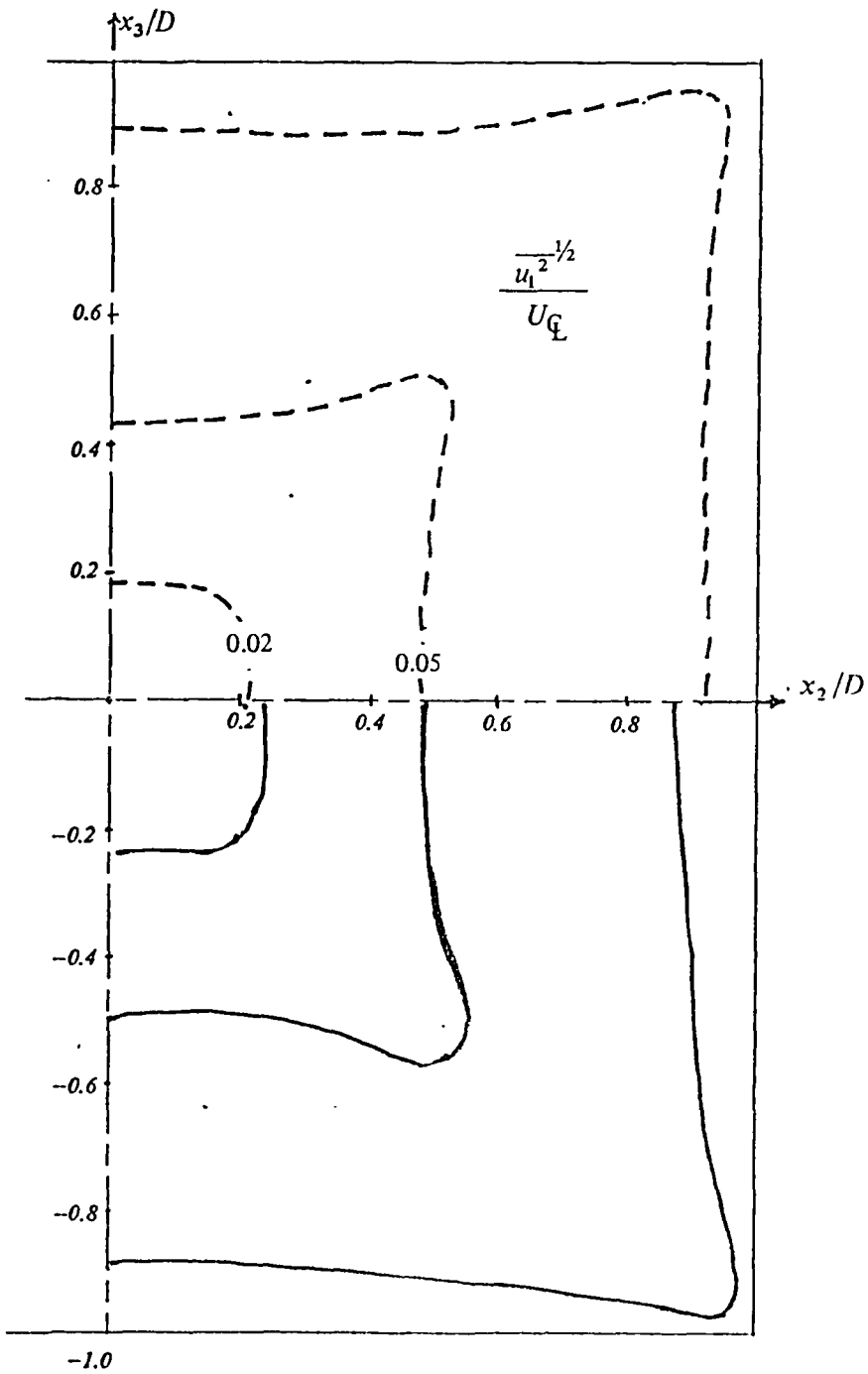
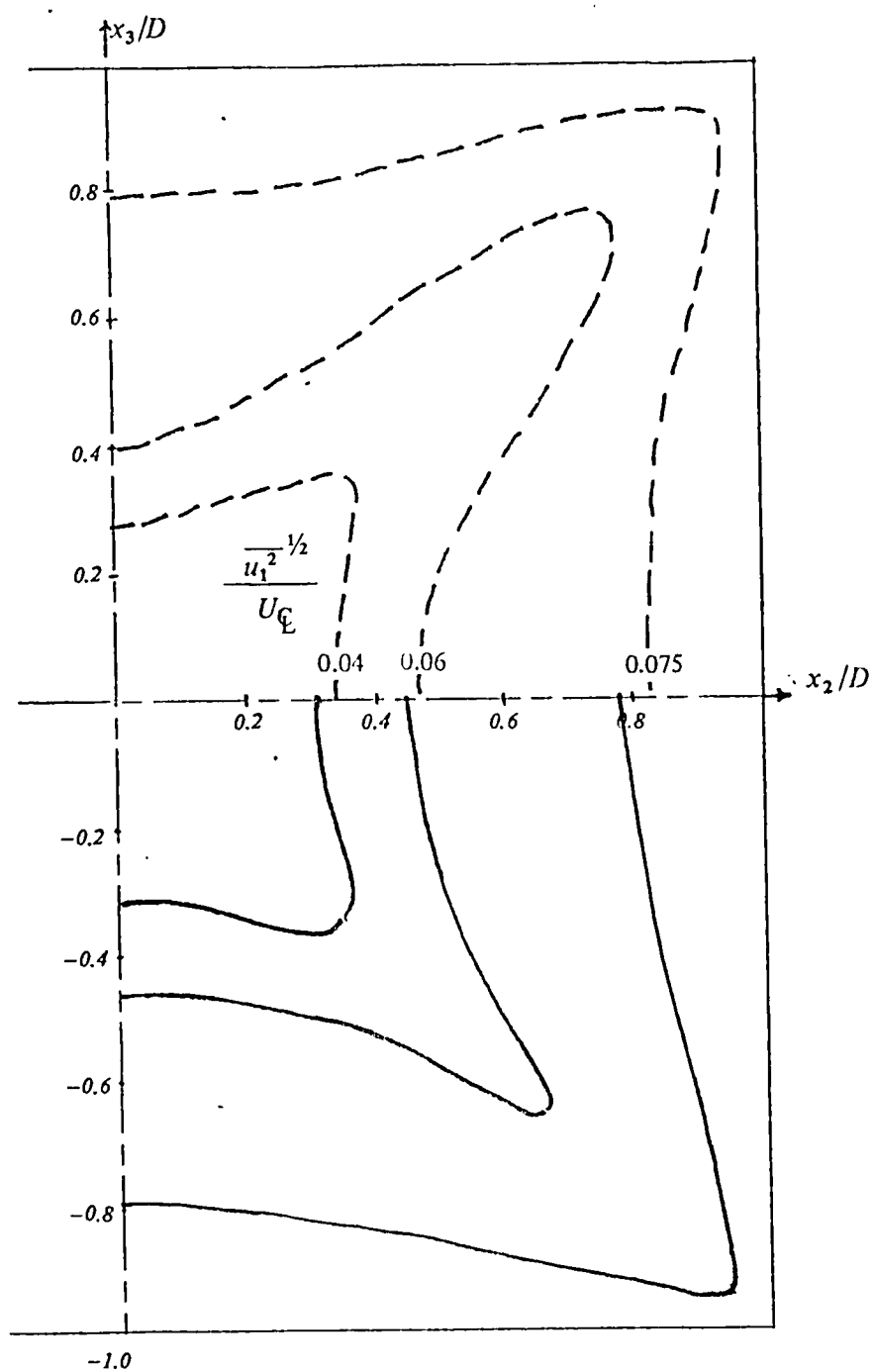


Figure 7.10 Contours of $\overline{u_1^2}^{1/2}$ at station B



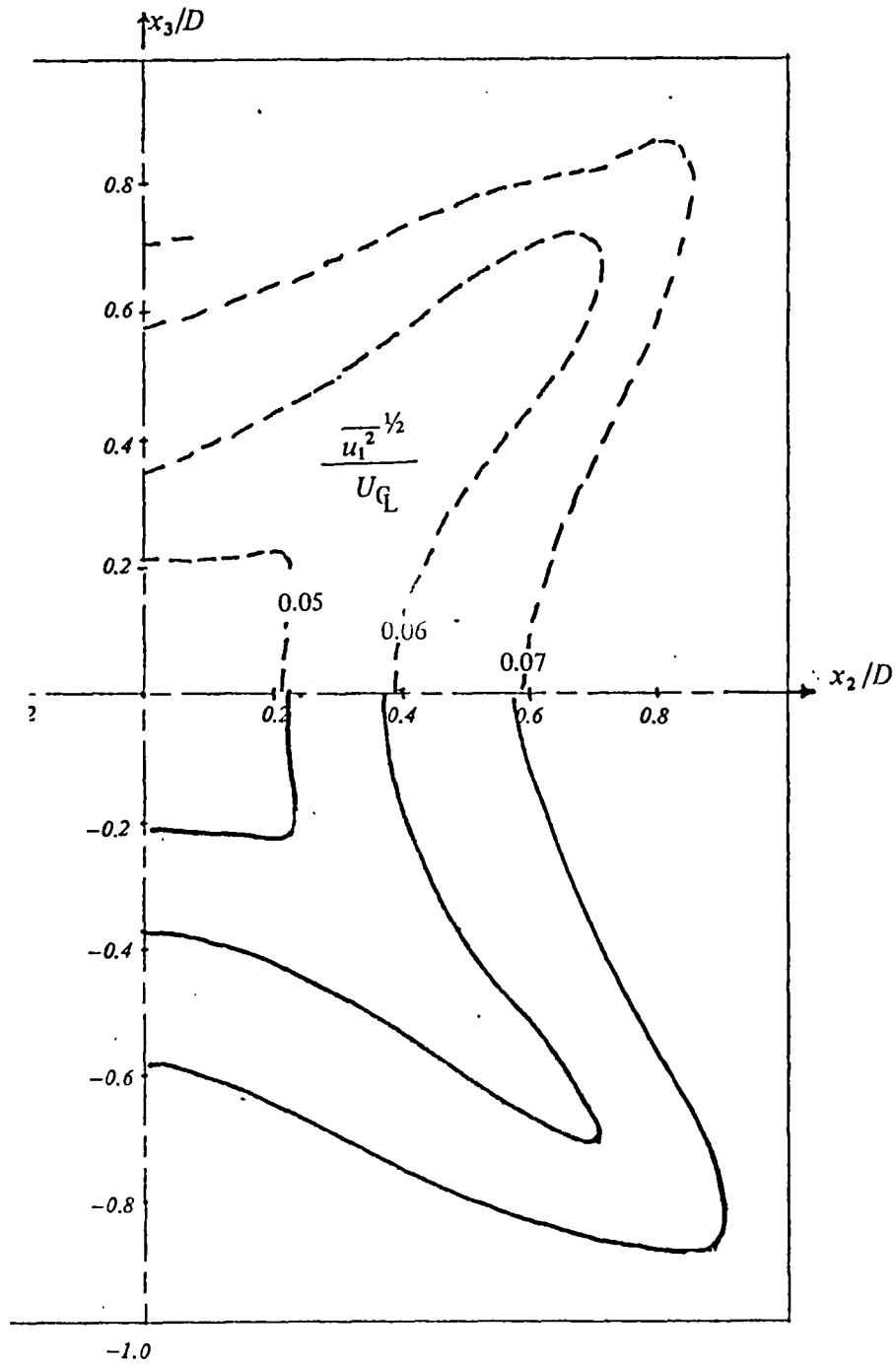
Data of Melling [1975] - - - - -
 Predictions of present model - - - - -

Figure 7.11 Contours of $\overline{u_1^2}^{1/2}$ at station C



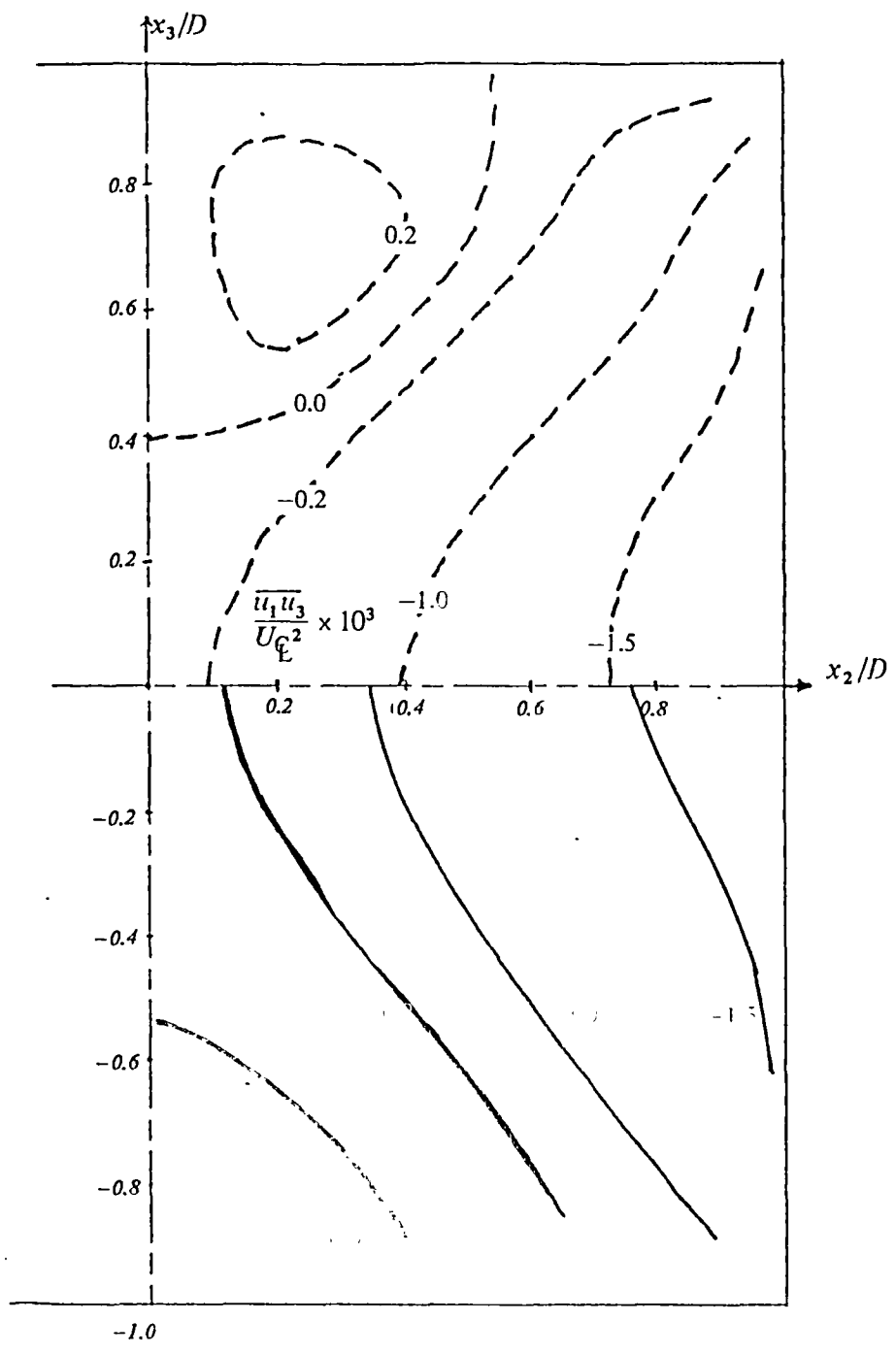
Data of Melling [1975] - - - - -
 Predictions of present model ————

Figure 7.12 Contours of $\overline{u_1^2}^{1/2}$ at station D



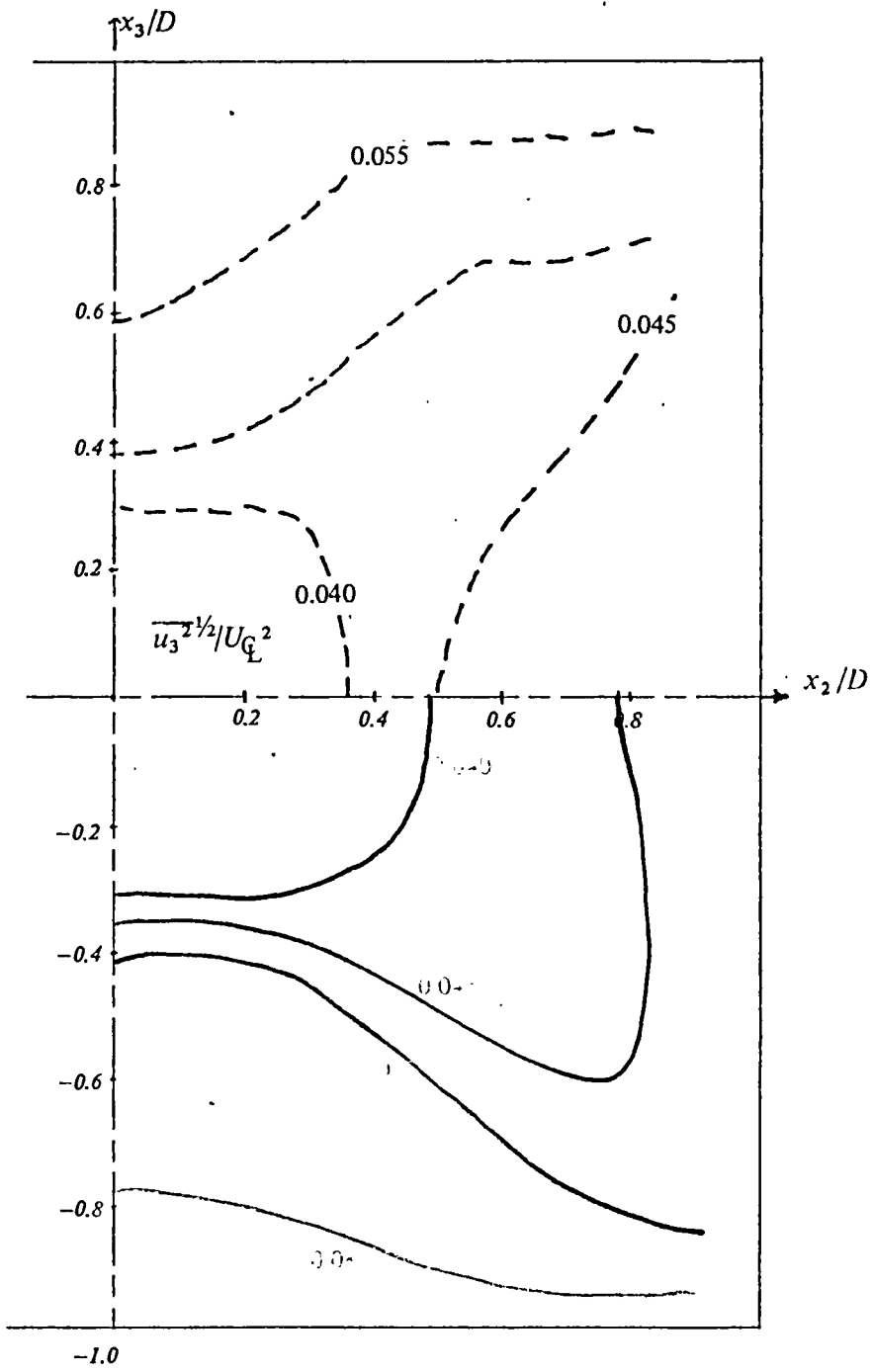
Data of Melling [1975] - - - - -
Predictions of present model - - - - -

Figure 7.3 Contours of $\overline{u_1^2}^{1/2}$ at station E



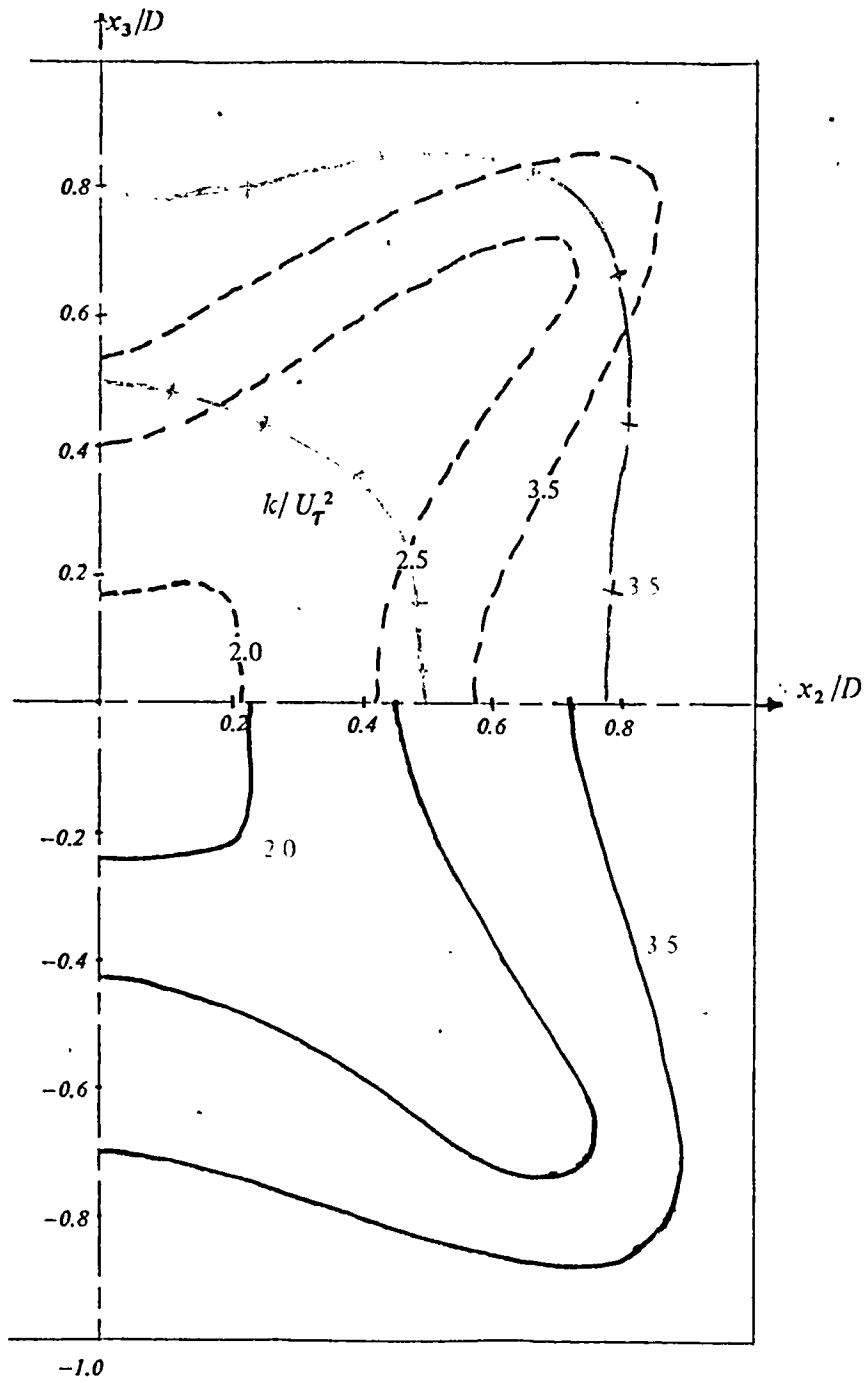
Data of Melling [1975] - - - - -
 Predictions of present model - - - - -

Figure 7.14 Contours of $\overline{u_1 u_3}$ at station E



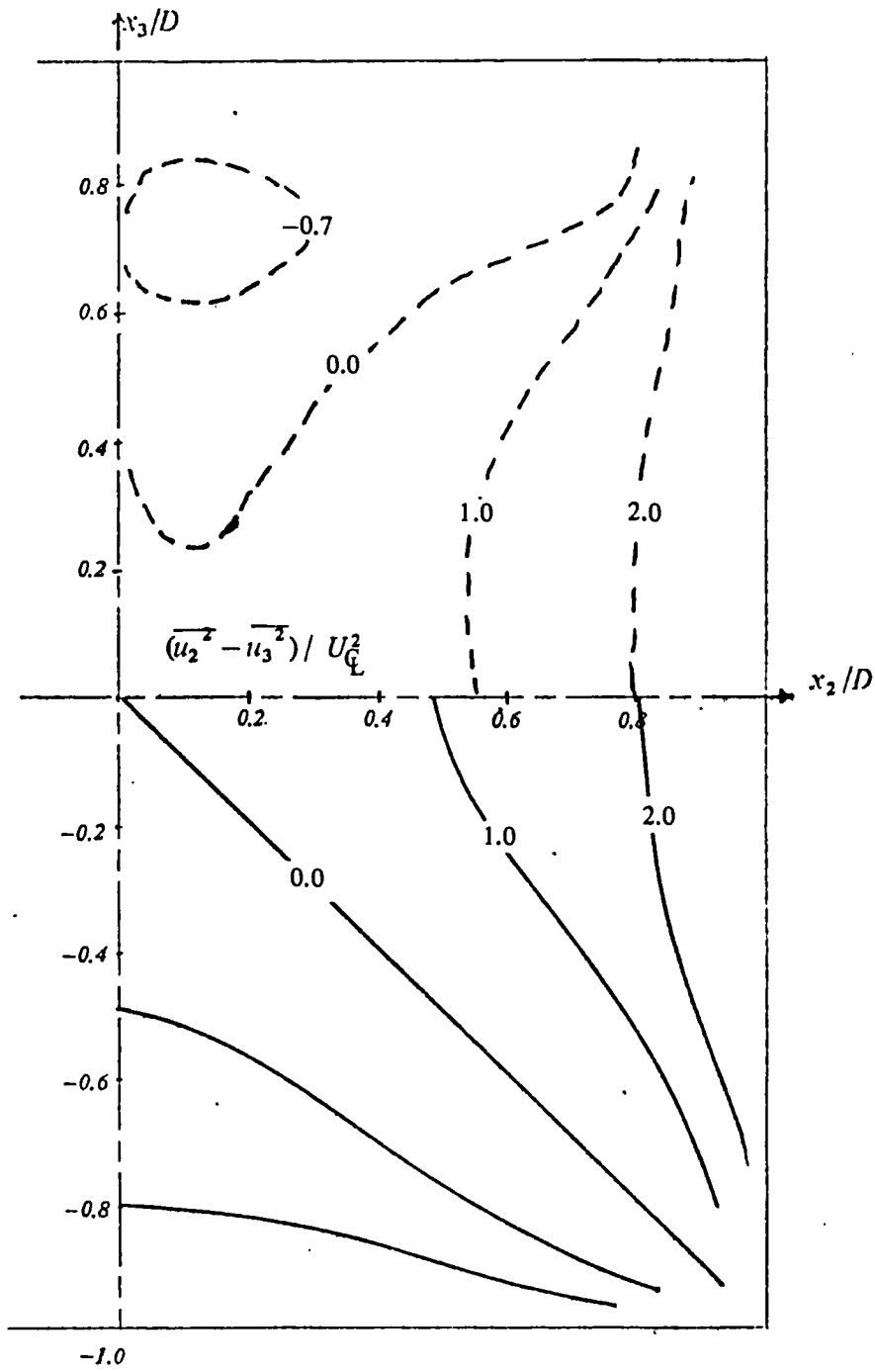
Data of Melling [1975] - - - - -
 Predictions of present model - - - - -

Figure 7.15 Contours of $\overline{u_3^2}/U_G^2$ at station E



Data of Melling [1975] - - - - -
 Predictions of present model ————
 Predictions of Fardet [1971] + + + + +

Figure 7.16 Contours of kinetic energy at station E



Data of Melling [1975] - - - - -
 Predictions of present model - - - - -

Figure 7.17 Contours of $\overline{u_2^2} - \overline{u_3^2}$ at station E

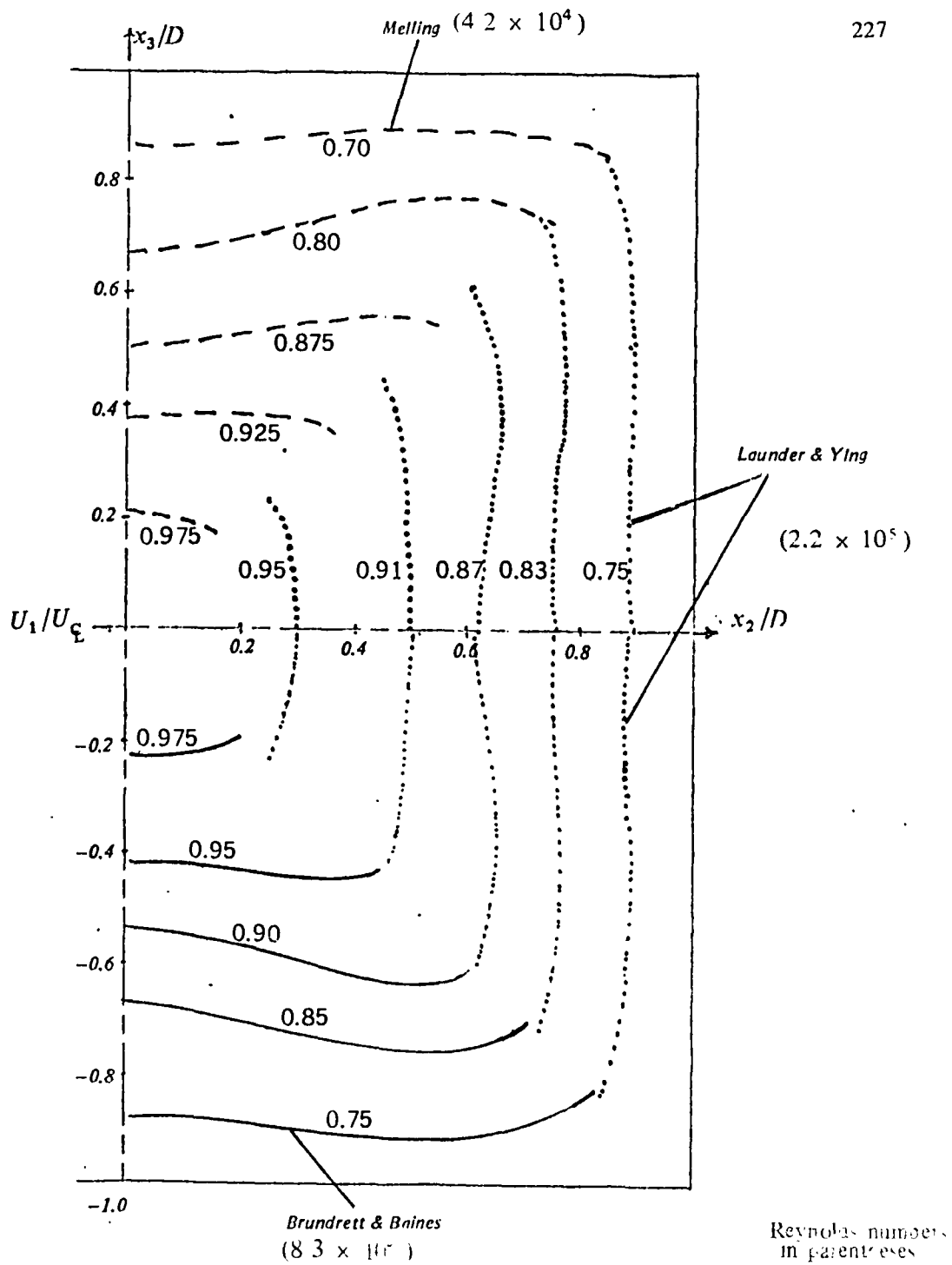


Figure 7.18 Mean velocity contours — data of various workers

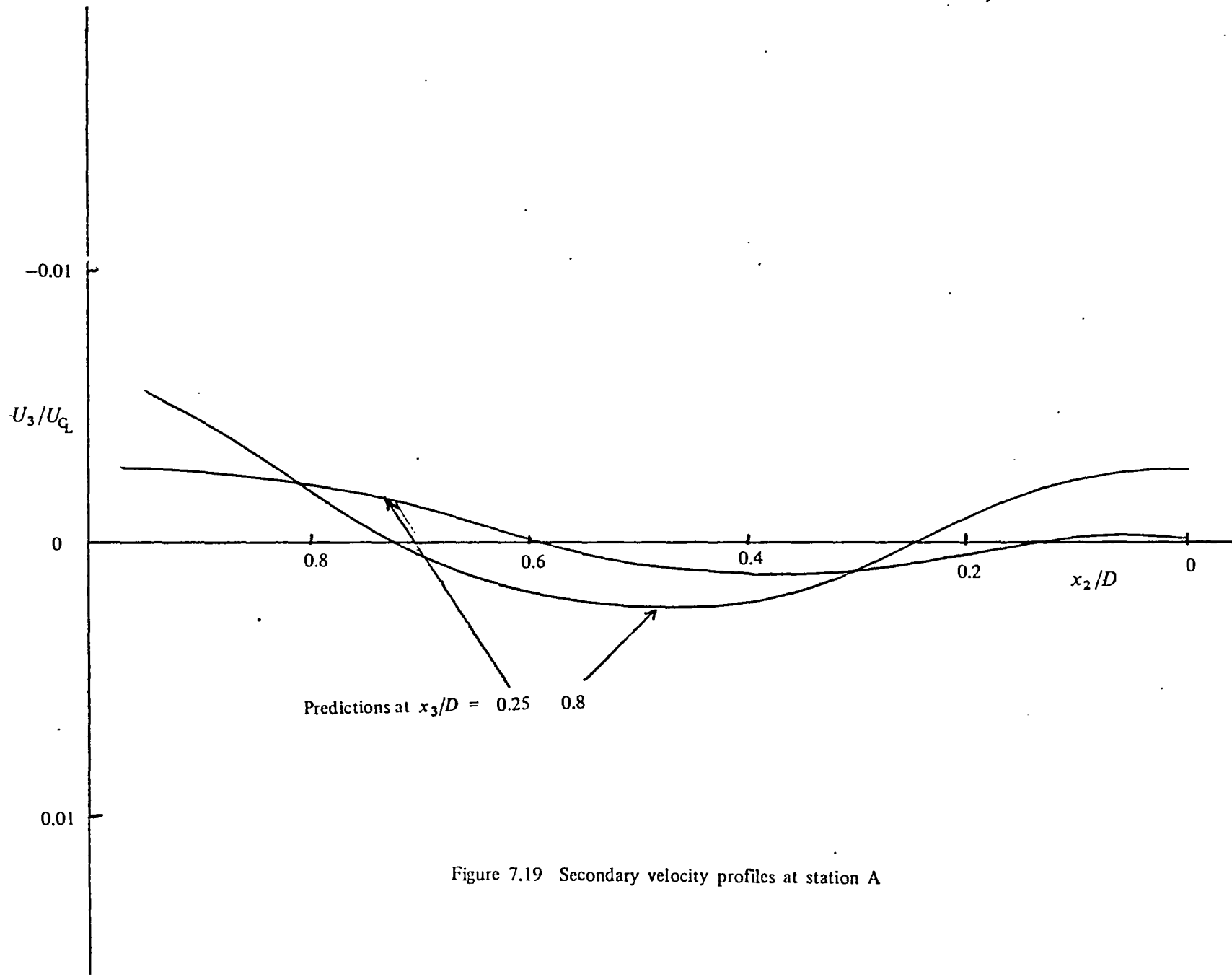


Figure 7.19 Secondary velocity profiles at station A

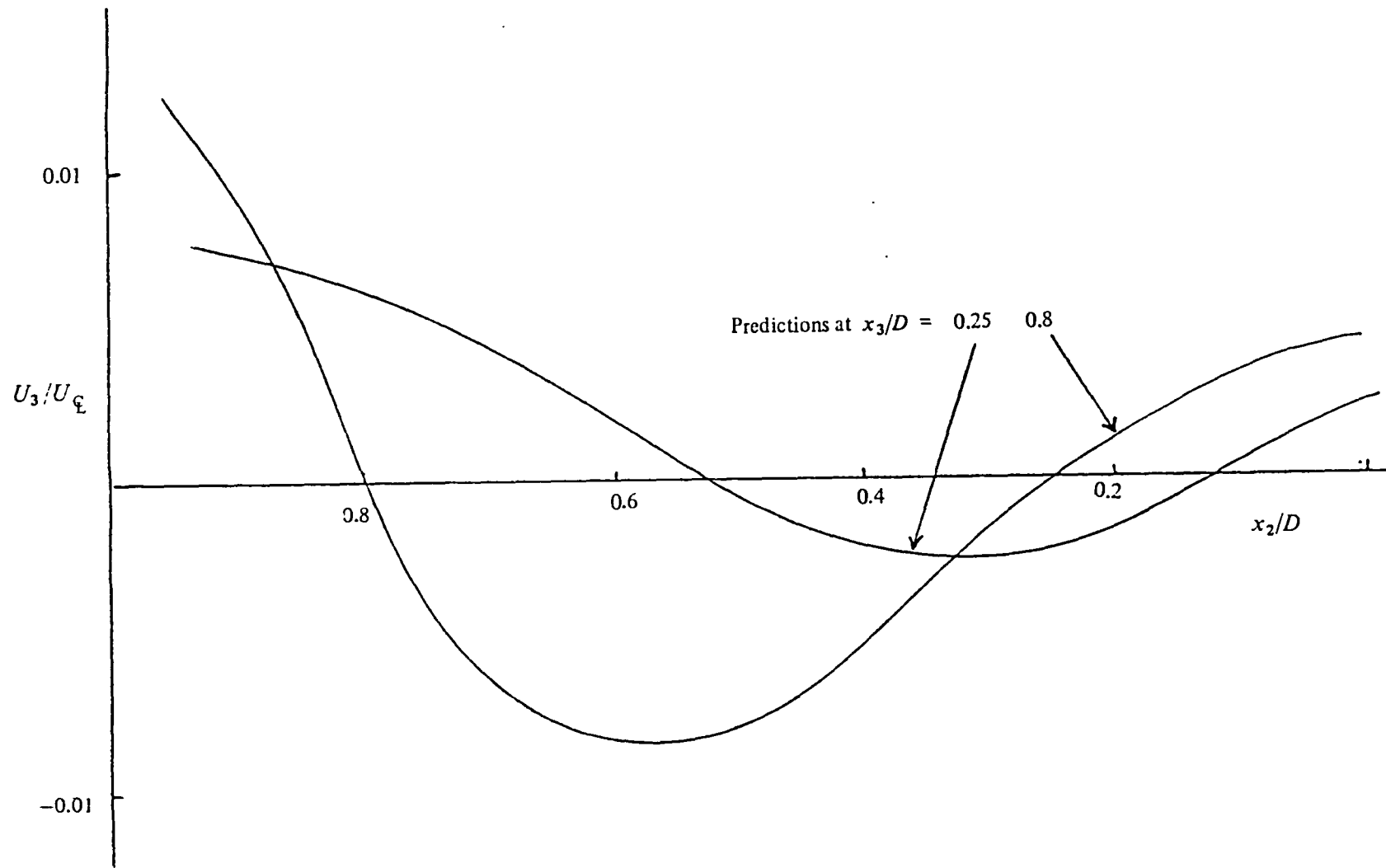


Figure 7.20 Secondary velocity profiles at station C

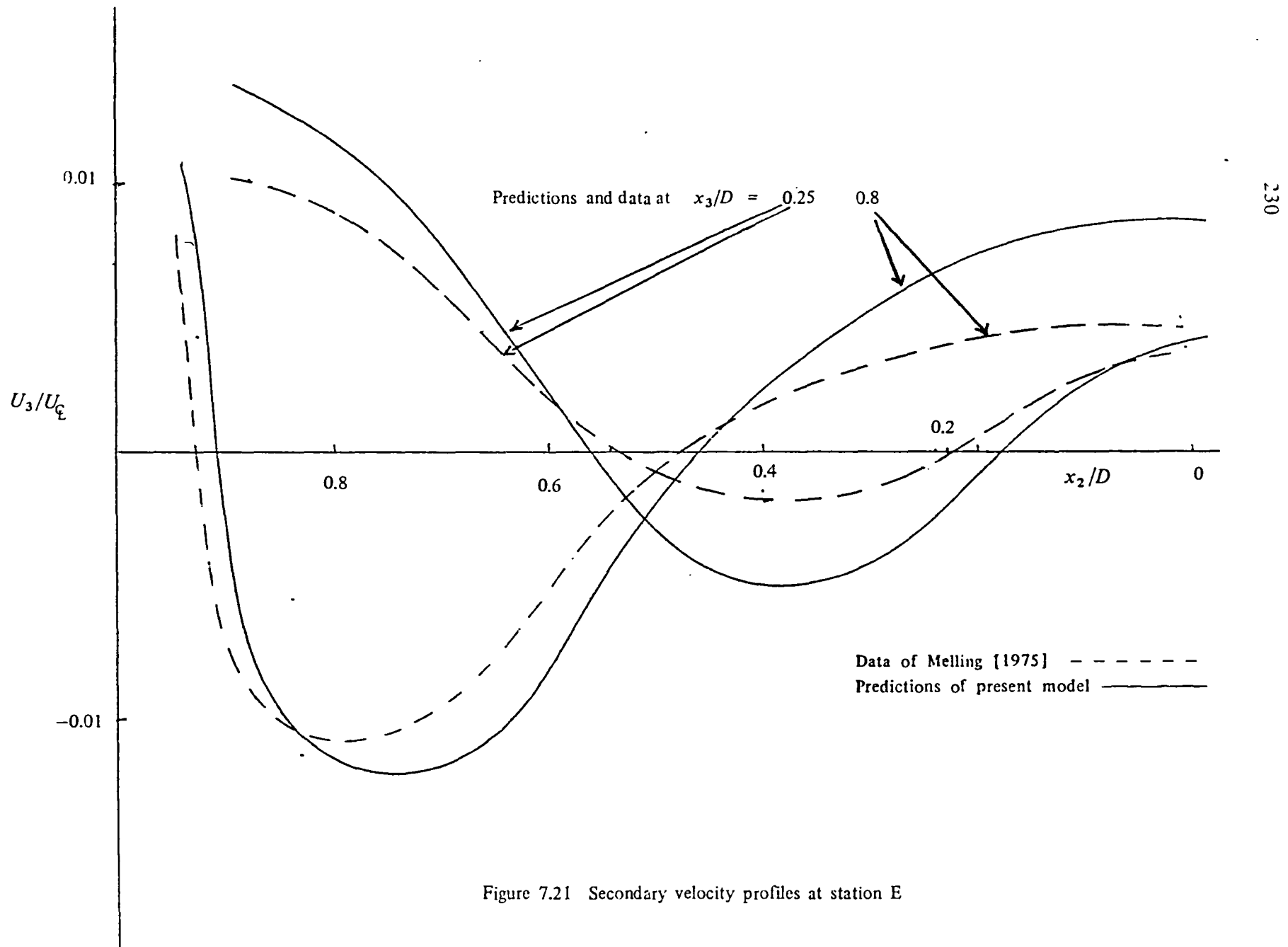


Figure 7.21 Secondary velocity profiles at station E

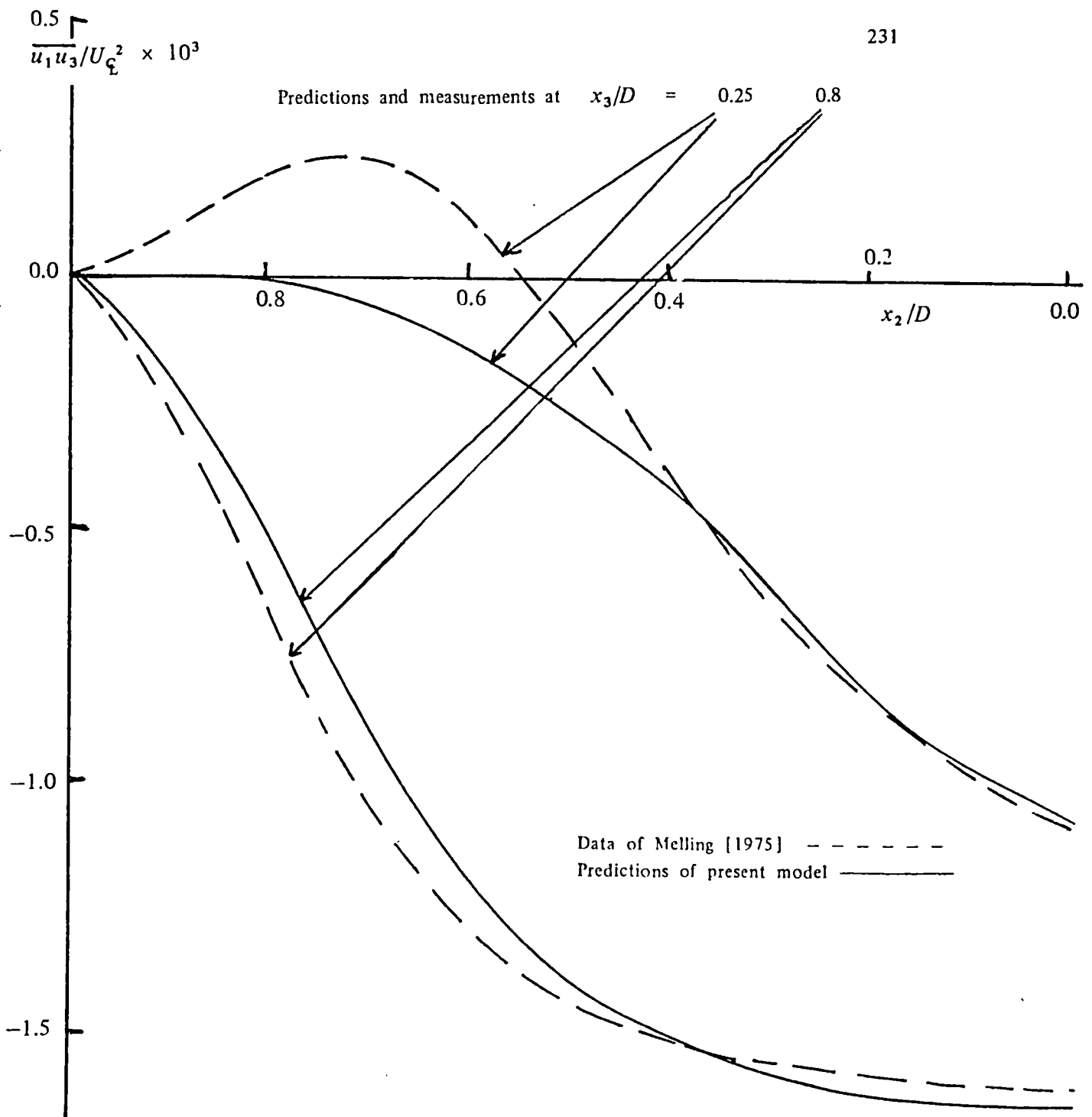


Figure 7.22 Turbulent shear stress profiles at station E

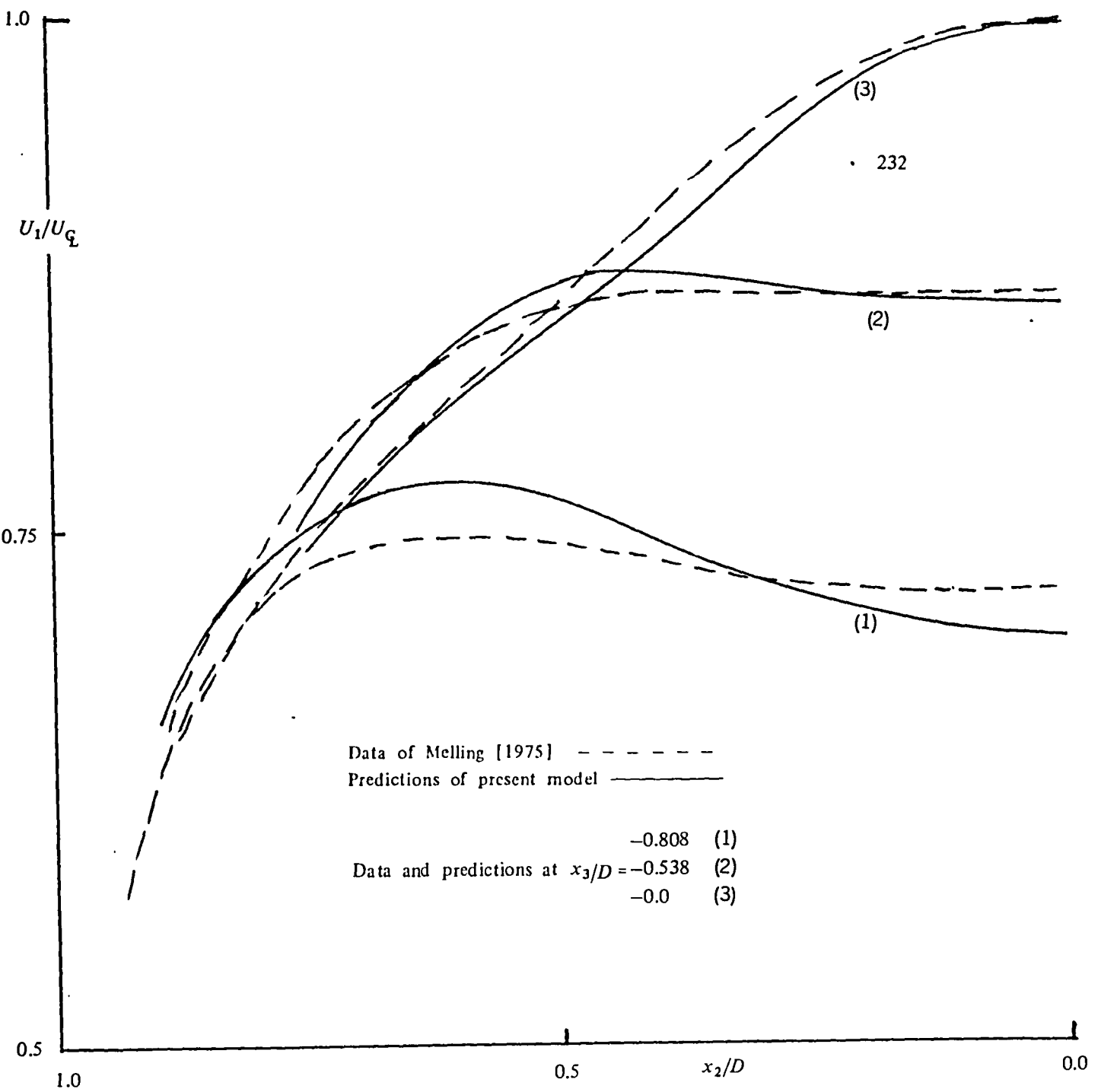


Figure 7.23 Mean velocity profiles at station D

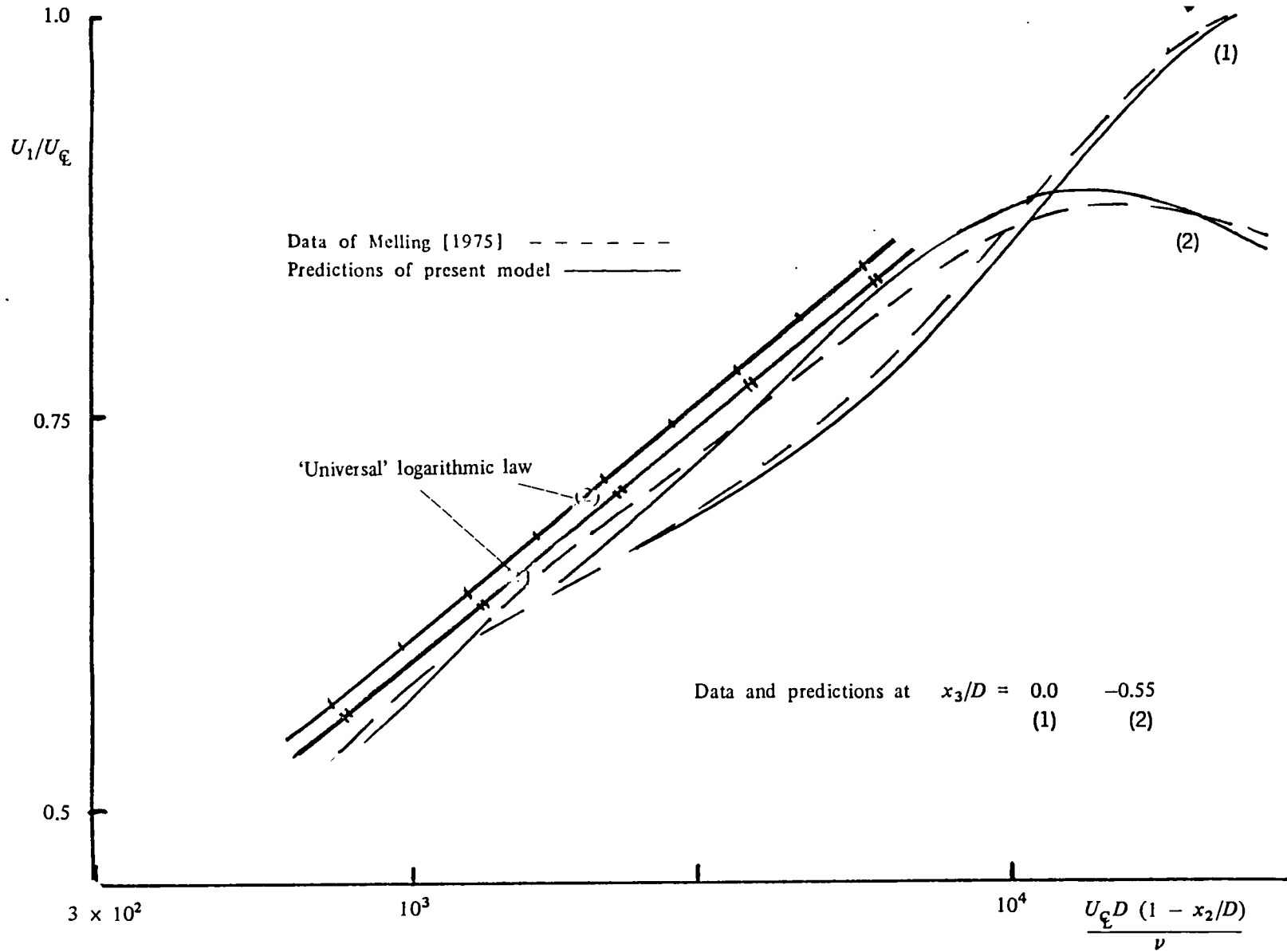


Figure 7.24 Mean velocity profiles at station E

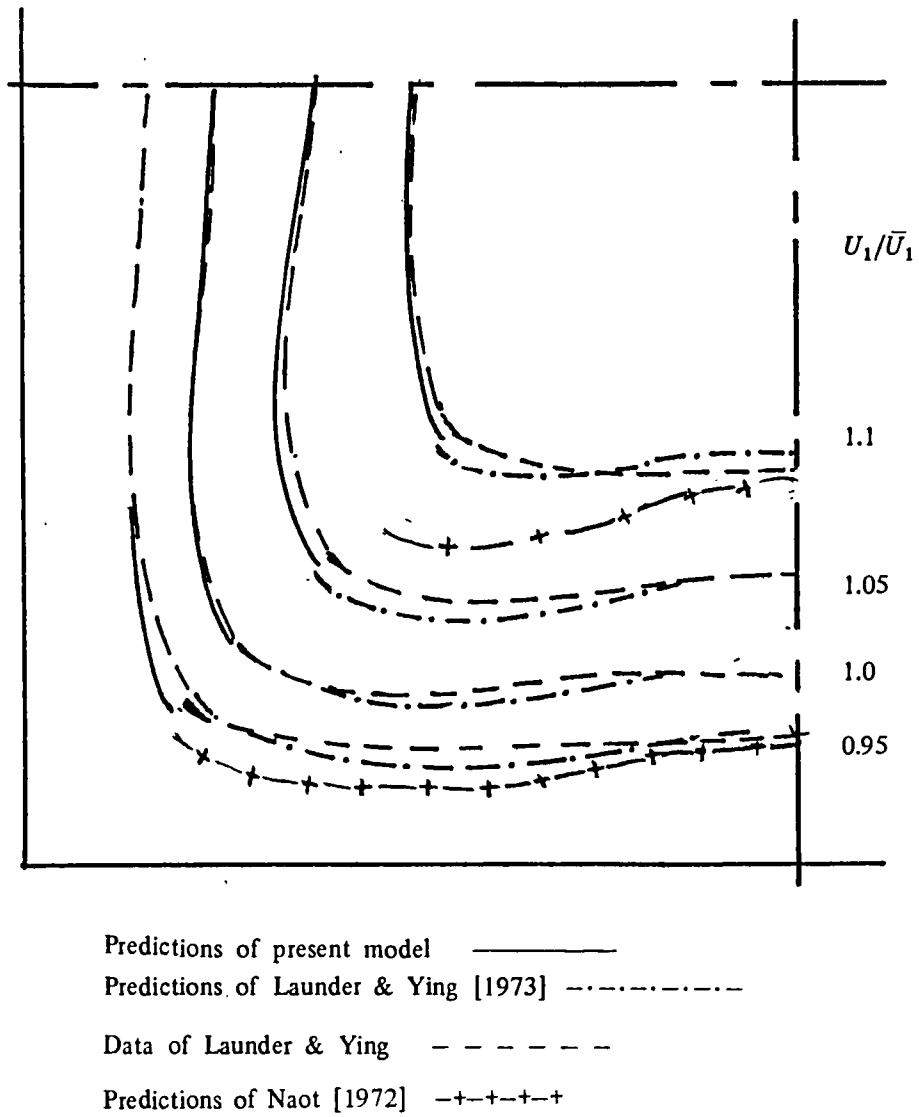


Figure 7.25 Mean velocity contours for fully-developed flow

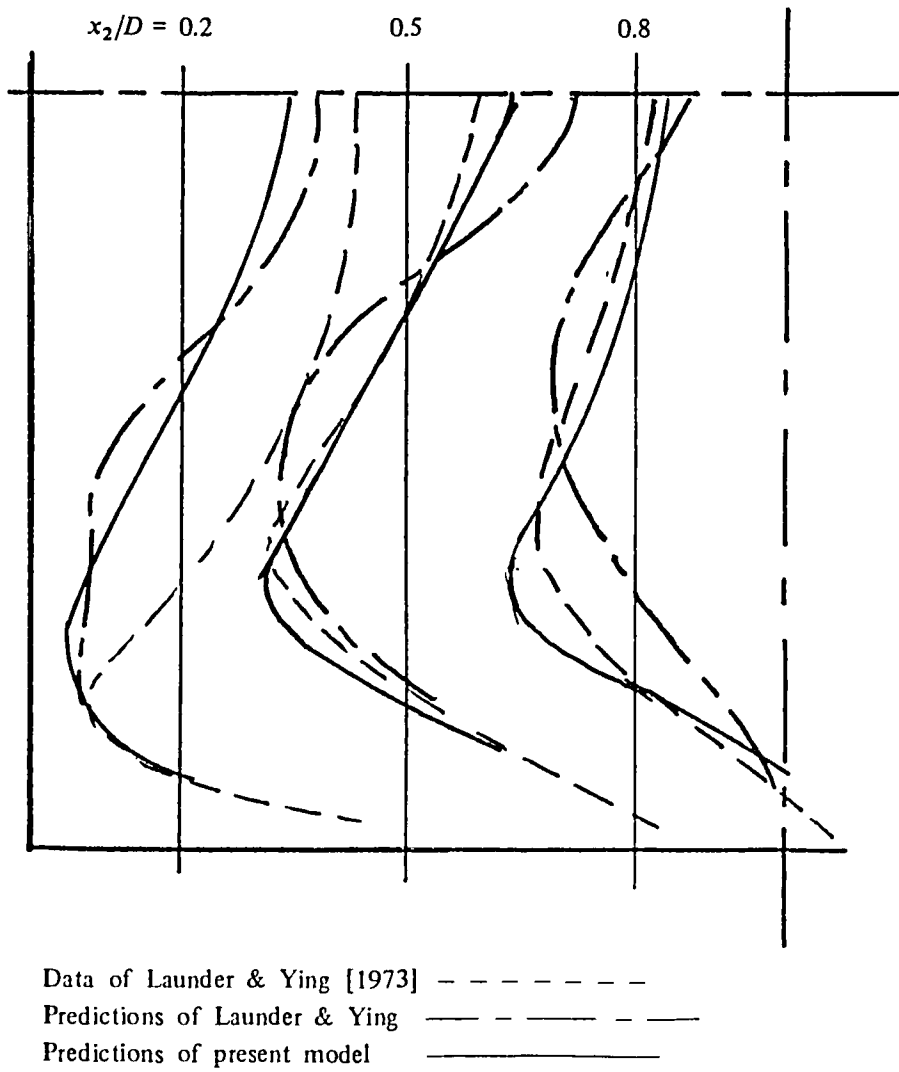


Figure 7.26 Fully-developed secondary velocity profiles

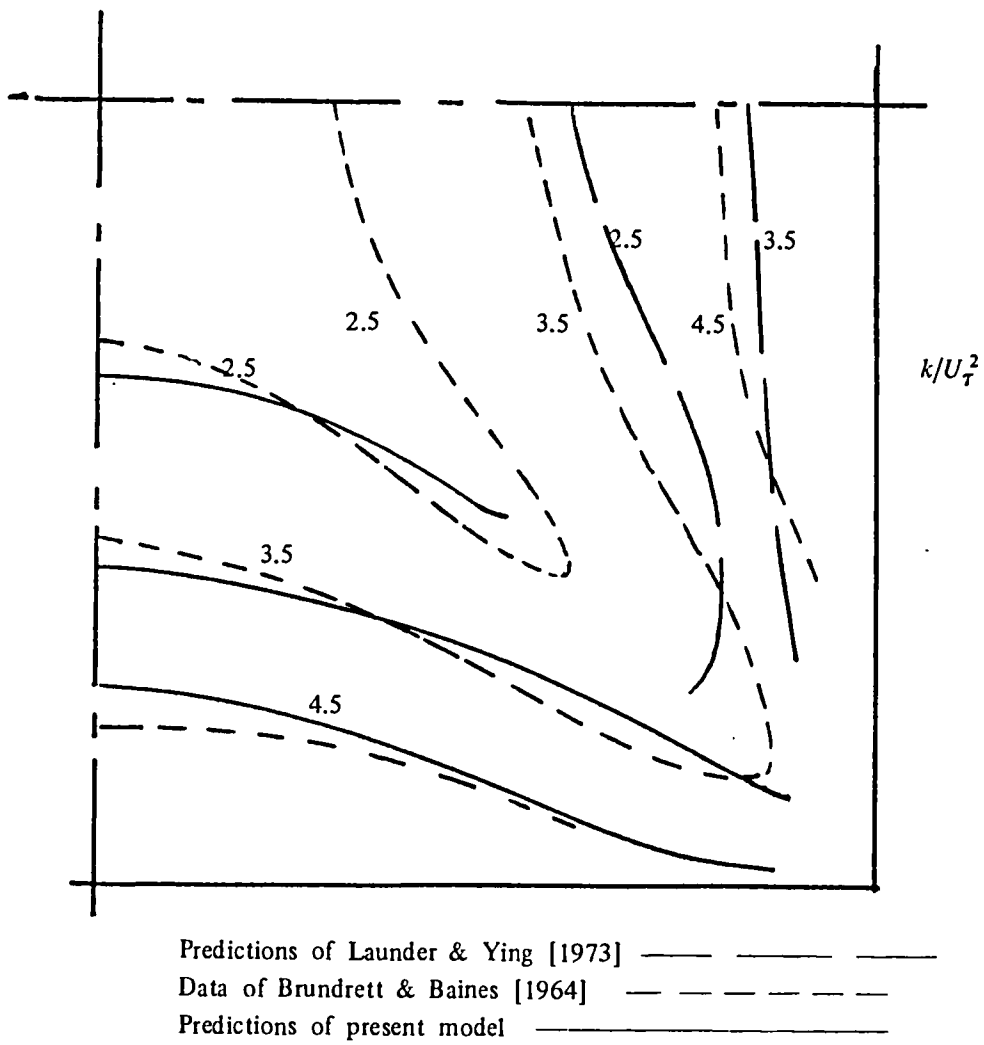


Figure 7.27 Fully-developed kinetic energy profiles

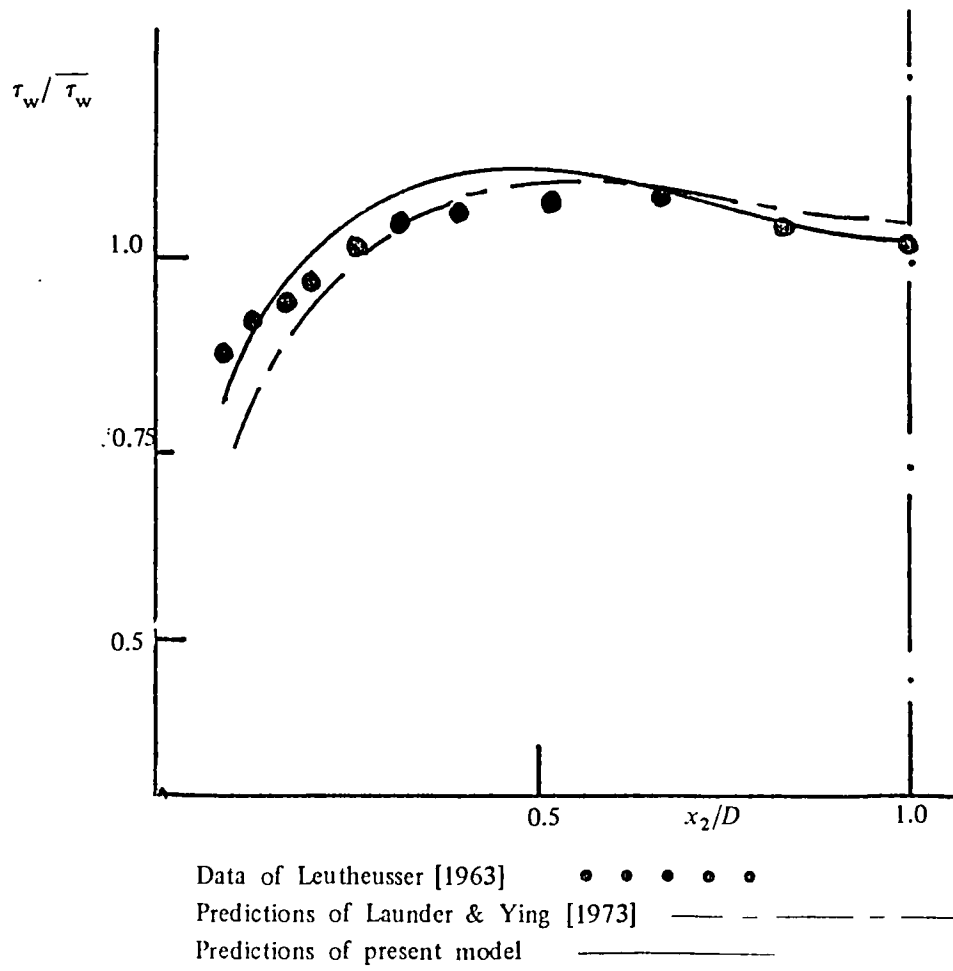


Figure 7.28 Variation of wall shear-stress around duct perimeter for fully-developed flow

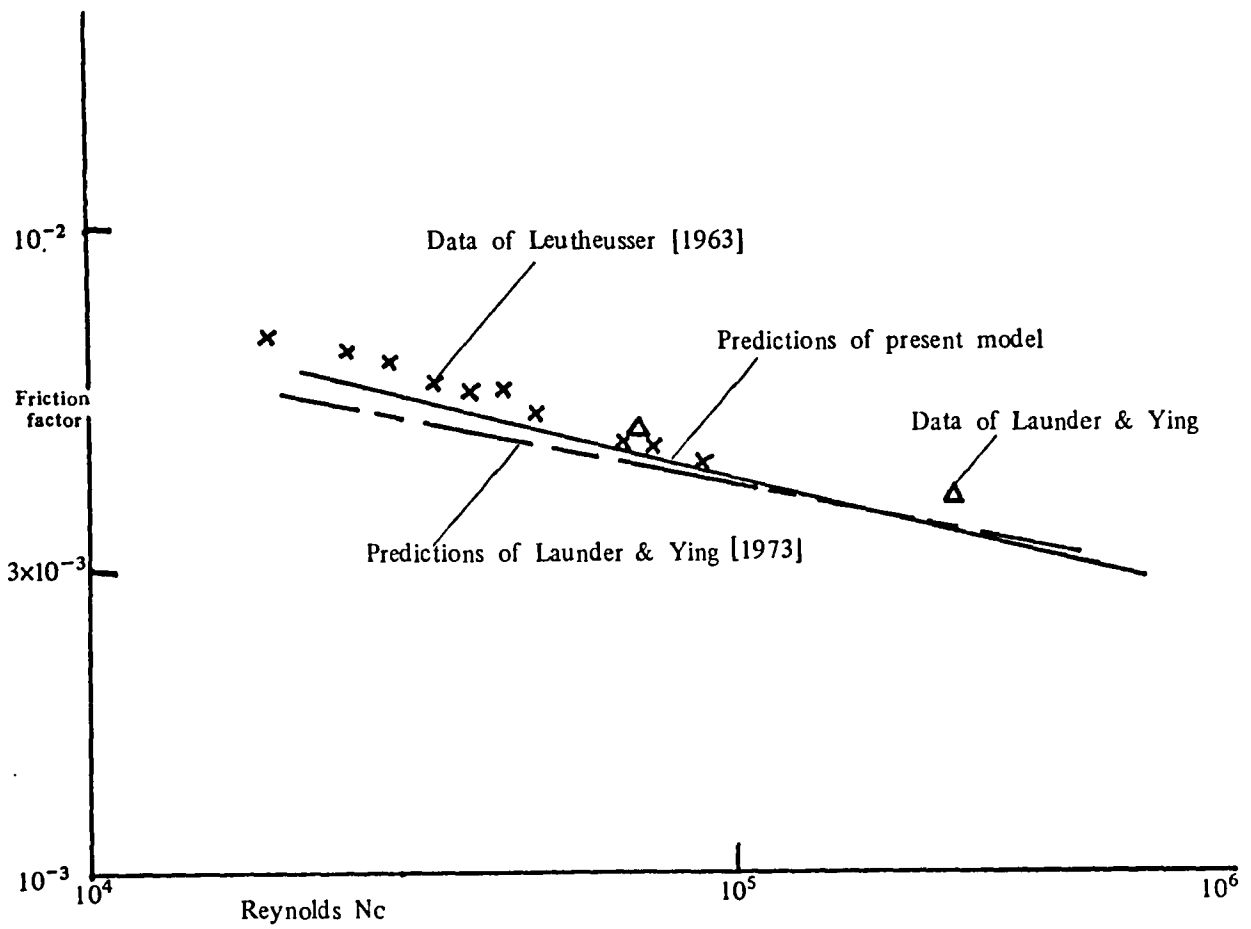


Figure 7.29 Variation of friction factor with Reynolds number

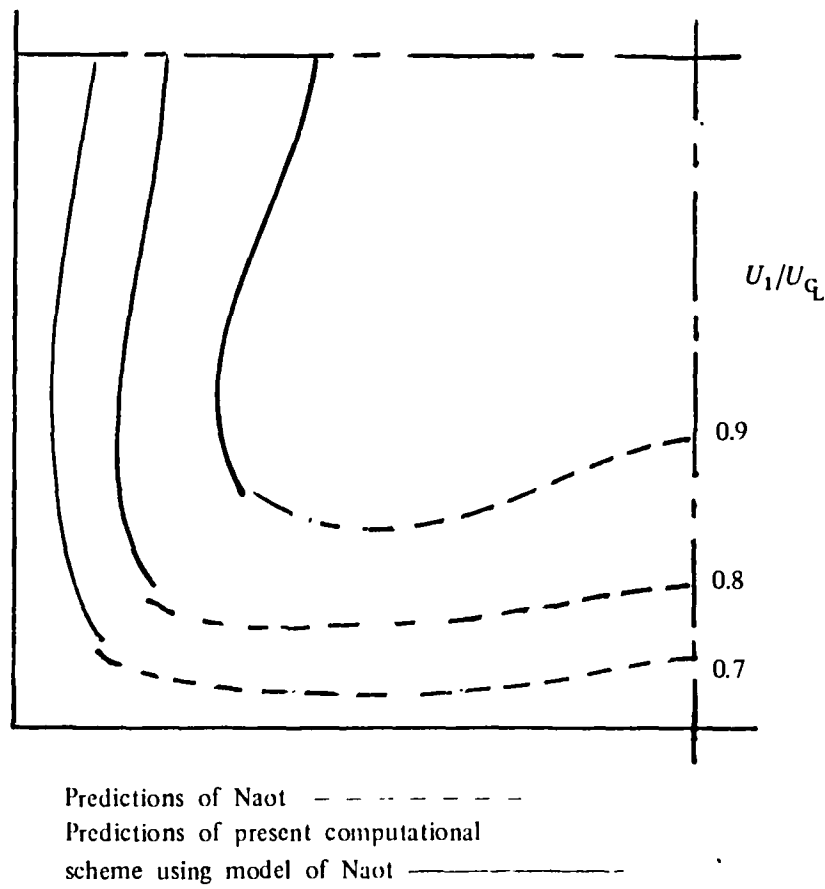
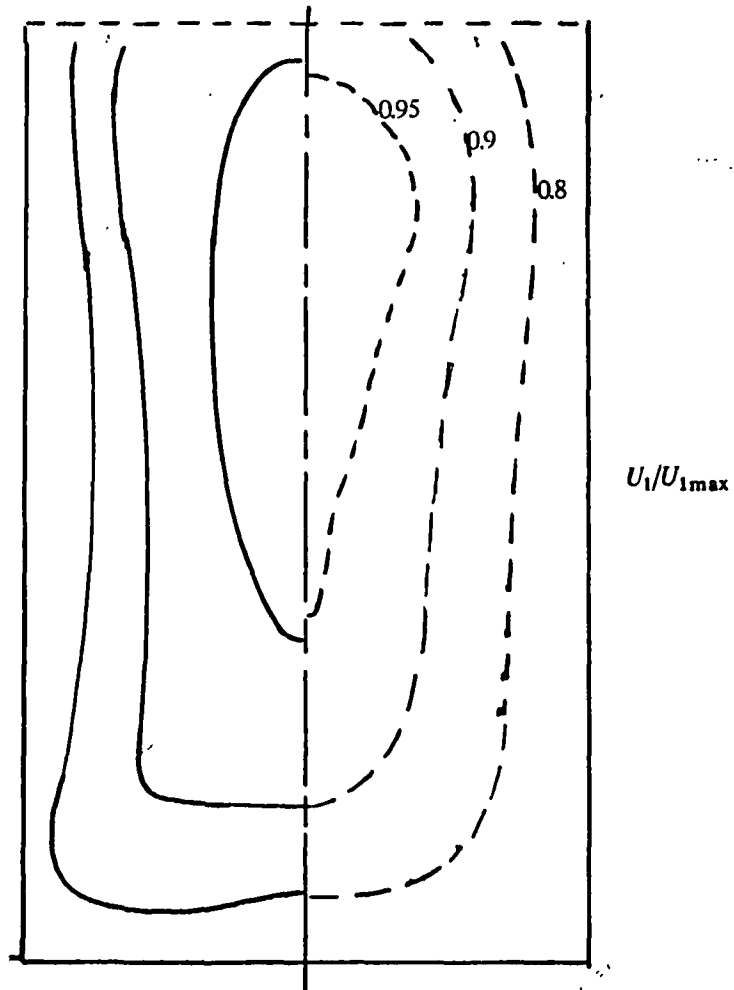


Figure 7.30 Verification of numerical accuracy:
comparison with results of Naot et al.



Data of Nikuradse [1926] - - - - -
Predictions of present model - - - - -

Figure 7.31 Mean velocity contours for open-channel flow

References for Chapters 3–8

1. Batchelor, G.K., & Townsend, A.A., *Decay of isotropic turbulence in the initial period*, Proc. Roy. Soc. A 193 [1948]
2. Boileau, *Traite de la mesure des eaux courantes*, Paris [1854]
3. Boussinesq, J., *Essai sur la theorie des eaux courantes*, Mem. Acad. Sci., 23, 1–680 [1877]
4. Bradshaw, P., *The understanding and prediction of turbulent flow*, Aero. J., 76 [1972]
5. Brundrett, E. & Baines, W.D., *The production and diffusion of vorticity in duct flow*, J.F.M., 19 [1964]
6. Champagne, F.H., Harris, V.G., & Corrsin, S., *Experiments on nearly homogeneous turbulent shear flow*, J.F.M., 41 [1970]
7. Chou, P.Y., *On velocity correlations and the solutions of the equations of turbulent fluctuation*, Quarterly Appl. Math., 3 [1945]
8. Comte-Bellot, G., *Ecoulement turbulent entre deux parois paralleles*, Pub. Sci. Tech. du Min. de l'Air No. 419 [1965]
9. Daly, B.J., & Harlow, F.H., *Transport equations of turbulence*, Phys. Fluids, 13, 2634 [1970]
10. Donaldson, C. duP., *A computer study of an analytical model of boundary-layer transition*, A.I.A.A. Paper No 68–38 [1968]
11. Gessner, F.B., Ph.D. Thesis, Purdue University [1964]
12. Gessner, F.B., & Emery, A.F., *A constitutive model for developing turbulent flow in a rectangular duct*, A.S.M.E. J Fluids Eng [1976]
13. Hadamard, J., *Lectures on Cauchy's problem*, Yale UP. [1923]
14. Hanjalic, K., Ph.D. Thesis, University of London [1970]
15. Hanjalic, K., & Launder, B.E., *Asymmetric flow in a plane channel*, J.F.M., 51, 301 [1972]
16. Hanjalic, K., & Launder, B.E., *A Reynolds stress model of turbulence and its application to thin shear flows*, J.F.M., 52, 609 [1972]
17. Harlow, F.H., & Nakayama, P.I., *Turbulence transport equations*, Phys. Fluids, 10, 2323 [1967]
18. Hegge Zijnen, B.G. van der, Thesis, University of Delft [1924]
19. Hoagland, L.C., Sc.D. Thesis, M.I.T [1960]
20. Irwin, H.P., Ph.D. Thesis, McGill University [1974]
21. Karman, T. von, *Mechanical similarity and turbulence*, Nachr. Ges. Wiss. Goettingen, 58–76 [1930]
22. Karman, T. von, *The fundamentals of the statistical theory of turbulence*, J. Aero. Sci., 4, 131–138 [1937]
23. Karman, T. von, & Howarth, L., *On the statistical theory of isotropic turbulence*, Proc. Roy. Soc. A, 164 [1938]

24. Klebanoff, P.S., *Characteristics of turbulence in a boundary layer with zero pressure gradient*, N.A.C.A. Report no. 1247 [1955]
25. Kolmogorov, A.N., *The local structure of turbulence in an incompressible fluid for very large Reynolds number*, C.R.Acad. Sci. U.R.S.S., 30, 301–5 [1941]
26. Kolmogorov, A.N., *Equations of turbulent motion of an incompressible fluid*, Izvestiya Akad. Nauk S.S.S.R., ser. fiz., 6, 56–8 [1942]
27. Laufer, J., *Investigation of turbulent flow in a two-dimensional channel*, N.A.C.A. report no. 1053 [1951]
28. Launder, B.E., *Private communication*, [1971]
29. Launder, B.E., *Progress in the modeling of turbulent transport*, Supplementary notes for course ME598, Pennsylvania State U [1975]
30. Launder, B.E., Reece, G.J., & Rodi, W., *Progress in the development of a Reynolds-stress turbulence closure*, J.F.M., 68, 537–66 [1975]
31. Launder, B.E., & Spalding, D.B., *Lectures in Mathematical Models of Turbulence*, Academic Press, London [1972]
32. Launder, B.E., & Ying, W.M., *Secondary flows in ducts of square cross-section*, J.F.M., 54, 289–95 [1972]
33. Launder, B.E., & Ying, W.M., *Prediction of flow and heat transfer in ducts of square cross-section*, Proc. I Mech E, 187, 455–461 [1973]
34. Leutheusser, H.J., *Turbulent flow in rectangular ducts*, Proc. A.S.C.E., J. Hyd. Div., 86, 1–19 [1963]
35. Lumley, J.L., & Khajeh-Nouri, B., *Computational modelling of turbulent transport*, Proc. 2nd IUGG–IUTAM Symposium on Atmos. Diffusion in Environmental Pollution [1974]
36. Mathieu, J., & Tailland, A., *Jet parietal*, C.R.Acad.Sci Paris, 261, 2282–2285 [1965]
37. Melling, A., Ph.D. Thesis, University of London [1975]
38. Naot, D., Ph.D. Thesis, Technion, Haifa [1972]
39. Naot, D., Shavit, A., & Wolfshtein, M., *Interactions between components of the turbulent velocity correlation tensor*, Israel J Tech., 8, 259 [1970]
40. Naot, D., Shavit, A., & Wolfshtein, M., *Prediction of flow in square section ducts*, Mech. Eng. Dept., Technion, Haifa, Report 154 [1972]
41. Naot, D., Shavit, A., & Wolfshtein, M., *Two point correlation model and the redistribution of Reynolds stresses*, Phys Fluids, 16, 738 [1973]
42. Nikuradse, J., *Untersuchung ueber die Geschwindigkeitsverteilung in turbulenten Stroemungen*, Forschungsarbeiten auf dem Gebiete des Ingenieurwesens, V D.I. 281 [1926]

43. Patankar, S., & Spalding, D.B., *Heat and Mass Transfer in Boundary Layers*, Intertext Books, London [1969]
44. Prandtl, L., *Ueber Fluessigkeitsbewegung bei sehrn kleiner Reibung*, Proc III Intern. Cong. Math. [1904]
45. Prandtl, L., *Bericht ueber Untersuchungen zur ausgebildeten Turbulenz*, Z.a.M.M., 5, 136–9 [1925]
46. Prandtl, L., & Wieghardt, K., *Ueber ein neues Formelsystem fuer die ausgebildete Turbulenz*, Abh. Akad. d. Wiss., Goettingen, 6–19 [1945]
47. Rodi, W., Ph D. Thesis, University of London [1972]
48. Rotta, J.C., *Statistische Theorie nichthomogener Turbulenz*, Z. Phys., 129, 547 [1951]
49. Rotta, J.C., *Turbulent boundary layers in incompressible flow*, Prog Aero Sci., 2, 1 [1962]
50. Schlichting, H., *Boundary Layer Theory*, McGraw Hill [1975]
51. Shir, C.C., *Turbulence transport model*, IBM Research Report RJ1119 [1972]
52. Stanton, T.E., *The mechanical viscosity of fluids*, Proc. Roy. Soc. A, 85, 366–76 [1911]
53. Tennekes, H., & Lumley, J.L., *A First Course in Turbulence*, MIT Press [1972]
54. Thomson, J. *On the flow of water in uniform regime in rivers and other open channels*, Proc Roy. Soc., 191 [1878]
55. Thomson, J. *On the flow of water round river bends*, Proc. I Mech Eng. [1879]

References for Appendices

1. Temam, R., *The Navier-Stokes equations*, North Holland, Amsterdam [1977]
2. Thom, R., *Modeles Mathematiques de la Morphogenese*, Union Generale d'Editions, Paris [1974]

Nomenclature

a, b, c	tensors defined in (4.27), page 75
c_i	constants, for various λ , defined in Table 6-3, p. 110
c_f	friction factor
f	decay function, defined on page 101
k	turbulent kinetic energy
l	mixing length
l_ϵ	dissipation length-scale
p	fluctuating pressure
t	time
u_1, u_2, u_3	fluctuating component of velocity
u, v, w	fluctuating component of velocity
w	subscript denoting wall-value
x_1, x_2, x_3	distance co-ordinates
x, y, z	distance co-ordinates
A, B, C, ...	labels used to distinguish similar terms (e.g. terms of (4.8))
\mathcal{C}	subscript denoting centre-line value
D	diffusion
D	duct diameter
D_{ij}	see (4.38), page 77
P	pressure
P, P_{ij}	production of k , Reynolds stresses
R	Reynolds number
R_M	Reynolds number based on maximum velocity
U	velocity
V	volume
α_i	coefficients defined in (4.35), page 77
$\alpha \beta \gamma \dots$	coefficients defined in (4.36), page 77
$\alpha' \dots$	coefficients defined on page 98
ϵ	dissipation
κ	von Karman constant (taken as 0.41)
μ	absolute viscosity
ν	dynamic viscosity
ρ	density
τ	shear stress
ω	vorticity
Σ	solid angle